Colour Constancy: Human Mechanisms and Machine Algorithms

by

Cristyn Barry Williams

A Thesis submitted for the degree of Doctor of Philosophy.

The City University,
London, U.K.

Department of Optometry
and Visual Science,
The City University
London U.K.

October, 1995

Contents

List of Figures Preceding Page

Chapter 5.

List of Tables Page

Acknowledgements

This thesis is dedicated to my father, who instilled in me a sense of honour. More than anything I would wish he had lived to see its completion.

There are of course too many people to thank in such a short space. I shall not try to mention everyone, but (in no particular order) special thanks are due:

To my supervisor Professor John Barbur, for teaching me much and for his patience and perseverance.

To Dr. Patrick Forsyth, for his enthusiasm and insight.

To Dr. David Wooding, for much needed encouragement and much heeded wise words.

To Dr. Ian Moorhead, for his considerate sponsorship.

To Gine Craven, for arduous typing beyond the call of friendship and ever warm welcomes.

To Peter Kerr for printing facilities and letting me steal his paper.

To my brother Rhidian and to Claire for putting me up, but mainly for putting up with me.

And to my mother for her eternal faith.

Declaration

I grant powers of discretion to the University Librarian to allow this thesis to be copied in whole or in part, without further reference to me. This permission covers only single copies made for study purposes, subject to normal conditions of acknowledgement.

Abstract

This thesis describes a quantitative experimental investigation into instantaneous colour constancy in humans. Colour constancy may be defined as the ability of the visual system to maintain a constant colour percept of a surface despite varying conditions of illumination. Instantaneous, in this context, refers to effects which happen very rapidly with the change of illumination, rather than those which may be due to long term adaptation of the photoreceptors. The results of experiments are discussed in the context of current computational models of colour constancy. Experiments on subjects with damage to the cerebral cortex are described. These highlight the different uses of chromatic signals within the cerebral cortex and provide evidence for location of the neural substrates which mediate instantaneous colour constancy.

The introductory chapter describes briefly the visual system, in the first section, with particular reference to the processing of colour. The second section discusses the psychophysics of human colour vision and the third presents a summary of computational models of colour constancy described in the literature.

Chapter two describes the dynamic colour matching technique developed for this investigation. This technique has the advantage of quantifying the level of constancy achieved, whilst maintaining a constant state of adaptation. The **C** index is defined as a measure of constancy, with 0 representing no constancy and 1 perfect constancy. Calibration procedures for the computer monitor and the necessary transformations to accurately simulate illuminant reflectance combinations are also described. Light scattered within the eye and its effect on colour constancy are discussed.

Chapter three is concerned with the effects of altering the illuminant conditions on instantaneous colour constancy. The size of the illuminant shift is varied. Artificial illuminants are compared with those of the Plankian locus. The effects of overall illuminance and the luminance contrast between target and surround are investigated.

Chapter four considers the spatial structure of the visual scene. Simple uniform surrounds are compared with those which have a more complex spatiochromatic structure (Mondrians). The effects of varying the test target size and shape are investigated. The decrease in constancy as a black border is placed between test target and surround is measured.

Chapter five describes experiments on four subjects with damage to the cerebral cortex. Chromatic discrimination thresholds are investigated for three subjects with achromatopsia as are the contribution of both sighted and blind hemifields to constancy for a subject with hemianopia.

Contrary to the predictions of many of the current computational models, using unnatural illuminants has no substantial effect on the **C** index, nor does the size of the illuminant shift or the luminance contrast between experimental target and surround. The complexity of the surrounding field does not effect constancy. These findings are similar to those from chromatic induction experiments reported in the literature. However, the effect of a black annulus is found to have different spatial parameters that those reported from experiments on chromatic induction, suggesting that a different mechanism may be involved. The three achromatopsics can be shown to exhibit instantaneous colour constancy. However the blind hemifield of the hemianope does not contribute. This suggests that the fusiform gyrus is not the human homologue of V4 and that the primary visual cortex is necessary for instantaneous colour constancy.

Chapter 1. Introduction

Chapter 1. Introduction

1.1 Morphology and Neurophysiology of the Visual System

1.1.1 Overview

Humans obtain the majority of their information about the outside world from visual stimulation and much of the human cortex is devoted to interpreting this information. The first component in the visual system is, of course, the eye. The eye serves two functions in the process of vision: the first is to form an optical image of the external field on the retina, the second is to convert that image into nervous signals to be interpreted by the brain. After initial processing at the level of the neurons of the retina, the signals are passed in parallel pathways to various midbrain centres and from these on to the visual cortex (figure 1.1.1). Schneider (1969) distinguished pathways which carried *where* information from *what* information. The major (what) pathway proceeds from the retina to a midbrain relay station, the lateral geniculate nucleus. From it here travels to the striate cortex of the occipital lobe (Brodmann's area 17) before turning anteriorly to the visual areas of the prestriate cortex (Brodmann's areas 18 & 19). The second (where) pathway reaches the cortex via the superior colliculus and pulvinar, without going through area 17. More recently there has been shown to be a further division (for primates) within Schneider's what pathway, distinguishing object and spatial vision (Mishkin et al., 1983).

The processing of information at the retinal level for the functional segregation of information is maintained at the lateral geniculate nucleus. A case has been made for perceptual input modules in the main retinogeniculostriate cortex pathway (Zeki, 1974, 1978; Cowey, 1985; Livingstone and Hubel, 1987a), separating the processing of form, motion, stereopsis and colour.

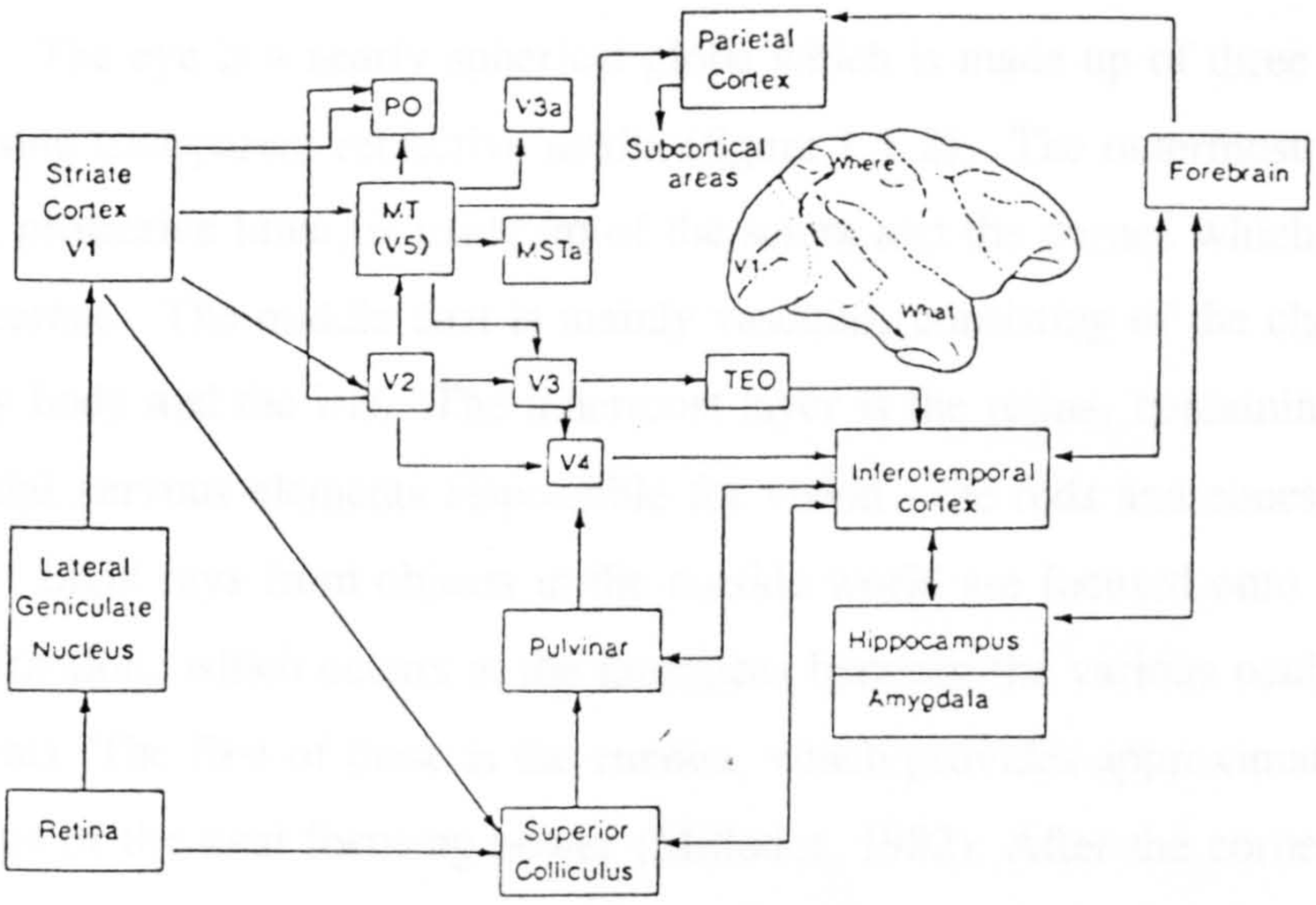

Figure 1.1.1 *The major cortical areas concerned with vision and the principal connections between them. The what and where streams ending at the temporal and parietal cortices are inset on a monkey brain. The Livingstone and Hubel streams are within Schneider's what pathway. (reproduced from Davidoff, 1991).*

The structure and function of these visual pathways are discussed in this chapter, with particular reference to colour perception.

1.1.2 The Eye

The eye is a nearly spherical globe which is made up of three layers enclosing transparent refractive media (figure 1.1.2). The outermost layer, a tough protective tunic, is made up of the sclera and the cornea which is transparent. The middle coat is mainly vascular, consisting of the choroid, ciliary body and the iris. The innermost layer is the retina, containing the essential nervous elements responsible for vision - the rods and cones.

Light rays from objects in the outside world are focused onto the retina by refraction, which occurs at the interfaces between the various ocular elements. The first of these is the **cornea**, which provides approximately 45 dioptres of the total focusing power (Millodot, 1982). After the cornea the light traverses the **aqueous humour** and the aperture of the **pupil**, before reaching the **lens**.

The **iris** is a variable diaphragm, whose aperture is the pupil and which dilates in dim light and contracts in bright light. Typical extreme limits for pupil diameter are eight and two millimetres, which allows a sixteen fold change in retinal illumination. This does not account for the eye's ability to cope with a 10^{10} fold range in illumination, but it has been shown that the rapid pupillary response improves visual sensitivity during the early stages of dark adaptation. A second advantage of a variable pupil is that it can act to minimise the effect of optical aberrations and improve spatial resolution.

The lens provides the remaining fifteen dioptres of focusing power and allows the variation of focal length. The lens is held under tension in a hammock of fibres and this tension may be reduced by the contraction of the **ciliary** muscles, allowing the elasticity of the lens to shorten it's focal length. This elasticity decreases with age and while a child may expect up to sixteen dioptres range of accommodation, this decreases to about nine dioptres in a young adult and to one in later life. The lens can suffer from refractive errors,

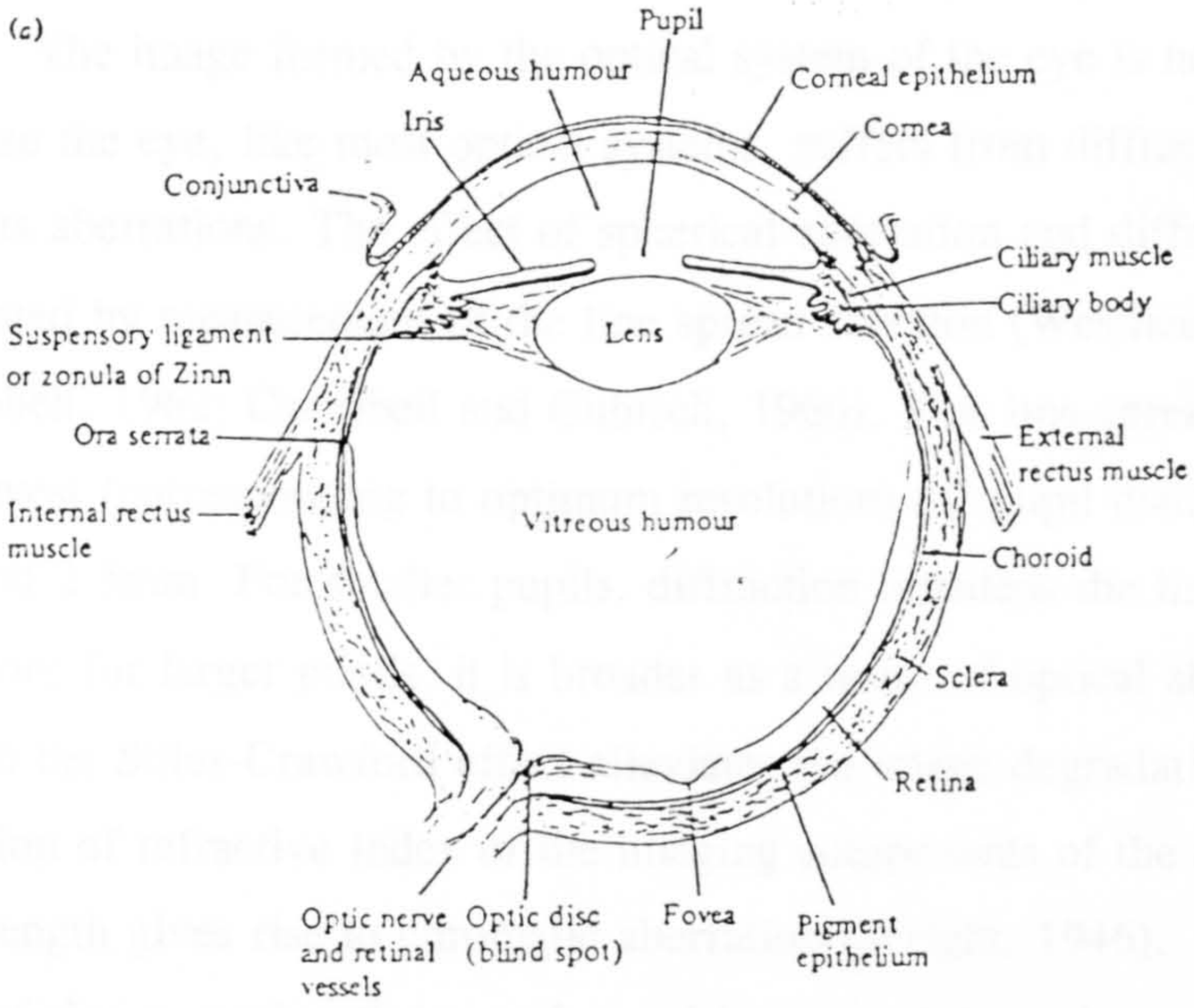

Figure 1.1.2 *Equatorial section through the eye, in diagrammatic form to illustrate main features (reproduced from Barlow and Mollon, 1982).*

such as having different converging power in different meridians (astigmatism) or a range of accommodation which is too weak to focus near objects (hypermetropia) or too strong to focus near objects (myopia). The light focused by the lens travels through the **vitreous humour** and an image is formed on the layer of light sensitive cells on the inner surface of the eye, the **retina.**

The image formed by the optical system of the eye is not perfect because the eye, like most optical systems, suffers from diffraction and various aberrations. The effect of spherical aberration and diffraction has been estimated by measurement of the line spread function (Westheimer and Campbell, 1962; Campbell and Gubisch, 1966). This line spread function is narrowest (corresponding to optimum resolution) for pupil diameters between 1.5 and 2.5mm. For smaller pupils, diffraction broadens the line spread function; for larger pupils, it is broader as a result of optical aberrations, though the Stiles-Crawford effect alleviates the image degradation. The variation of refractive index of the imaging components of the eye with wavelength gives rise to chromatic aberration (Wright, 1946). This results in light of short wavelength being focused in front of the retina and any image is thus surrounded by a de-focused blue penumbra. The macula pigment, which has strong absorption characteristics in the short wavelength, acts as a filter to reduce this blue penumbra (Reading & Weal, 1974, see section 1.2.3). Light is also subject to absorption by the various optical media, predominantly the lens. The absorption of the lens is characteristically high in the short wavelengths (peaking at 365-368nm) and the optical density tends to increase with age (Said & Weal 1959, Norran & Vos 1974).

The quality of the optical image is further degraded by the scattering of light. The atmospheric scattering of light, described by Rayleigh (1912) occurs with randomly distributed, very small particles; the distribution of scattered light increases rapidly towards the blue end of the visible spectrum and bears little relation to the direction of the incident beam. However scattering in the eye occurs due to imperfections in the cornea and the lens, due to light which

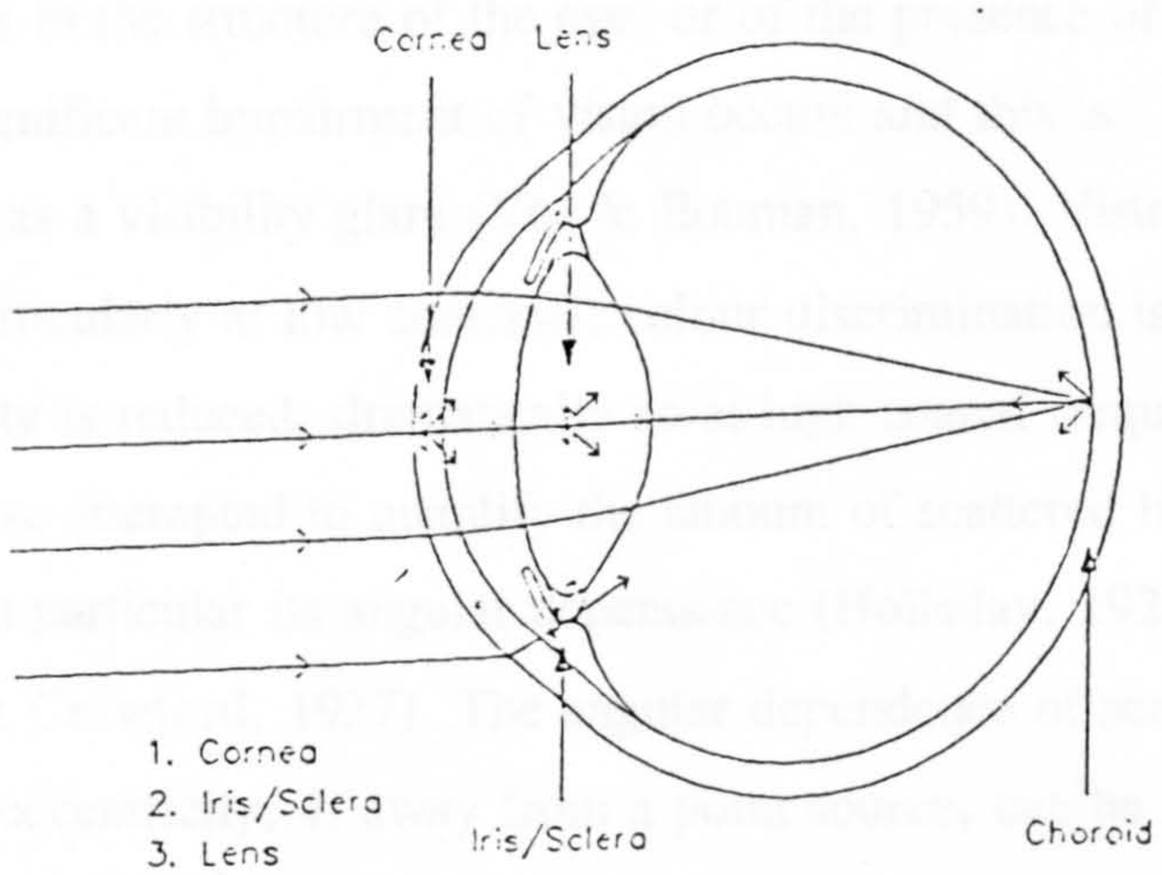

Figure 1.1.3 *Schematic diagram showing sources of forward scatter in the human eye.*

penetrates the iris or sclera and due to back-scattering from the choroid, that is light which is not absorbed by the pigment epithelium (figure 1.1.3). When the scattering centres are of equal or larger dimension than the wavelength of incident light, the angular distribution depends markedly on the direction of the incident beam. In a typical young adult eye only 3-4% of the incident light is scattered, but when the amount of scattered light in the eye is large (either as a result of changes in the structure of the eye, or of the presence of intense sources of light) a significant impairment of vision occurs and this is sometimes described as a visibility glare (Vos & Bouman, 1959). Visual acuity is reduced (particularly at low contrast), colour discrimination is poorer and contrast sensitivity is reduced, dramatically so at high spatial frequencies. Numerous studies have attempted to quantify the amount of scattered light in the human eye and in particular its angular dependence (Holladay, 1926; Stiles, 1929; Stiles & Crawford, 1937). The angular dependence of scattered light at a reasonable eccentricity, θ, away from a point source, can be described by a power law of the form

$$L_s(\theta) = Ek\theta^{-n} \qquad (1.1.1)$$

where E represents the illuminance level generated by the scattering source in the plane of the pupil and **k** and **n** are constants for a given eye (Stiles, 1929). These constants carry useful information regarding the **amount** (parameter **k** or *straylight parameter*) and the **angular dependence** (parameter **n** or *scatter index*) of the scattered light and relate to the number and size of particles causing the scatter respectively. The amount of scattered light and hence the straylight parameter, **k**, increases as a result of increasing the density of the scattering particles, provided the absorbtion of light is either negligible or remains constant. The constant **k** therefore takes into account the number of particles involved as well as their absorbtion properties. Large **k** values and/or small **n** values can result in degraded visual performance.

1.1.3 The Retina - The Photoreceptors

The retina is the innermost of the three layers of the eye and itself has a sharply defined layered structure (figure 1.1.4). It serves the function of converting light energy falling onto it into nervous signals and carrying out the initial stages of neuronal processing.

The pigment epithelium consists of a layer of single cells which are attached to the choroid. These cells are tightly packed together and their function is the absorption of light that has failed to bleach the receptors, thus preventing (reducing) its back-scatter, and hence the degradation of the retinal image. Only a small proportion (around 10% at 500nm) of the light incident on the cornea is absorbed by the photoreceptors, the rest being lost by scattering or absorbtion or by passing through the receptor layer (figure 1.1.5).

The function of the photoreceptors is to convert incident light radiation into an electric signal, a process known as photo-transduction. In humans, there are two types of photoreceptor, the rods and the cones, which are distinguished morphologically and are named after their different appearances (Schultze, 1866). The rod inner segment is cylindrical and maintains the same width throughout its length from the external limiting membrane to the connecting stalk (figure 1.1.6) The outer segment is also cylindrical, about 1.4 microns wide and just noticeably thinner than the inner segment. The cone inner segment departs slightly from the shape of a cylinder, because its width increases from the outer limiting membrane to a maximum of 5 or 6 microns near its centre and then tapers as it approaches the connecting stalk. At the stalk, the inner and outer segment have the same width, but the outer segment continues to taper to give the cone its characteristic shape (Rodieck 1973). Cones display some variation in shape, and in man they display a similar appearance to that of rods in the **fovea**, with a maximum width of 2.5 microns. The fovea is a slight depression in the central retina caused by the lateral displacement of neural tissue. There is a greater density of

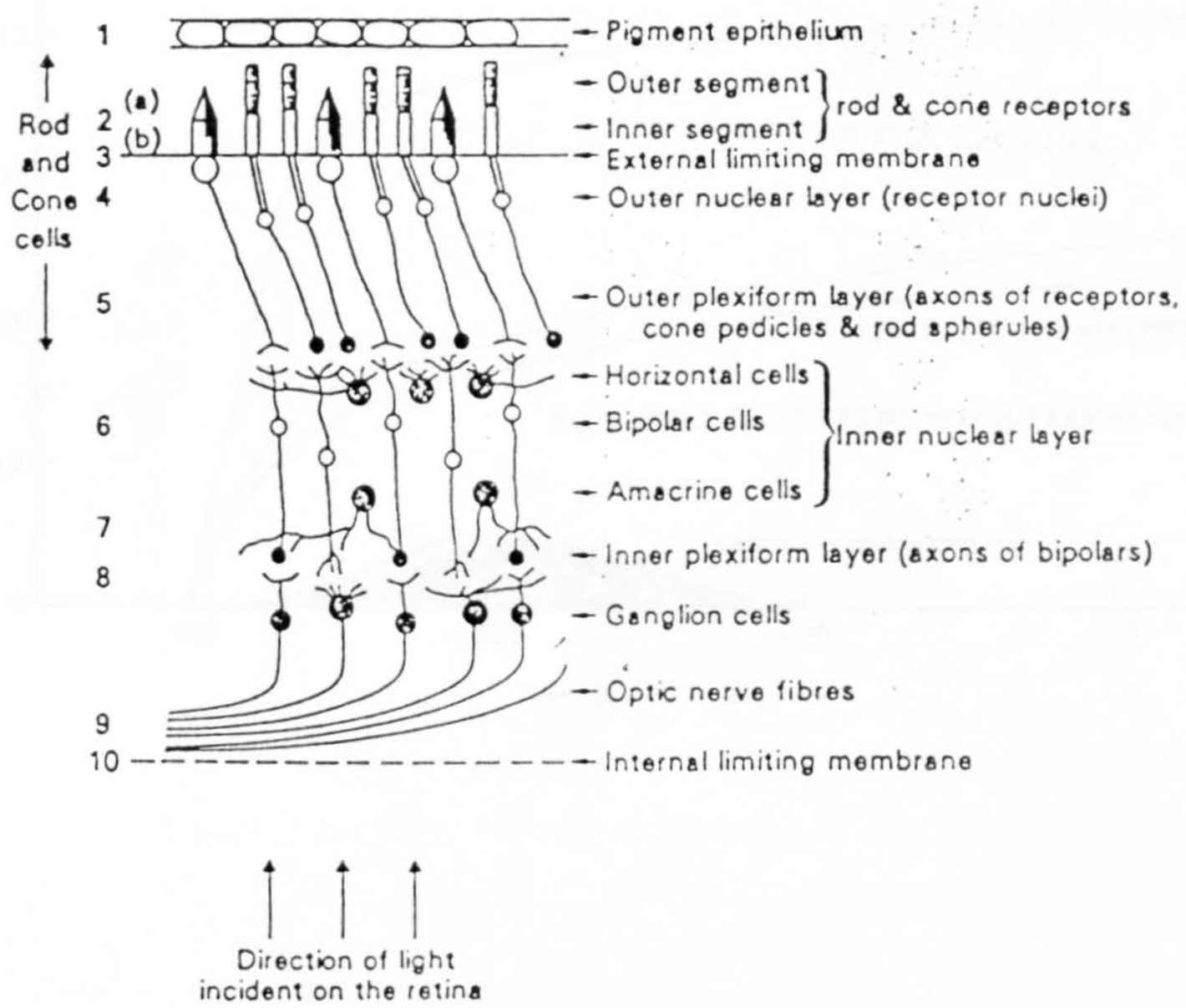

Figure 1.1.4 *A schematic diagram of a transverse section of the retina showing the ten layers (reproduced from Padgham and Saunders, 1975).*

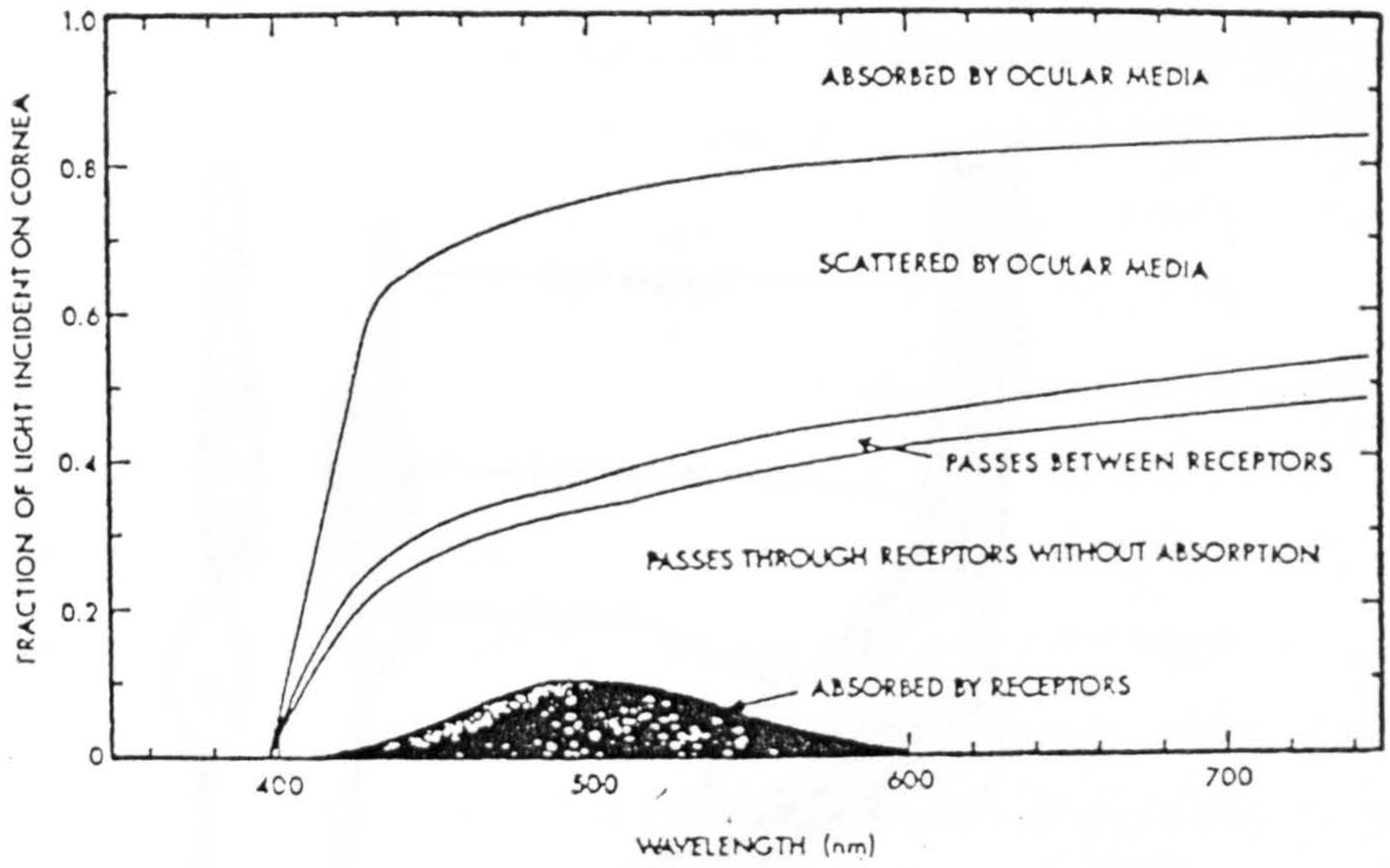

Figure 1.1.5 *The fate of light entering the human eye. Based on transmission data of Boettner (1967) and the assumption that 10% of the 500nm photons incident on the corneal surface are absorbed by the visual pigment.*

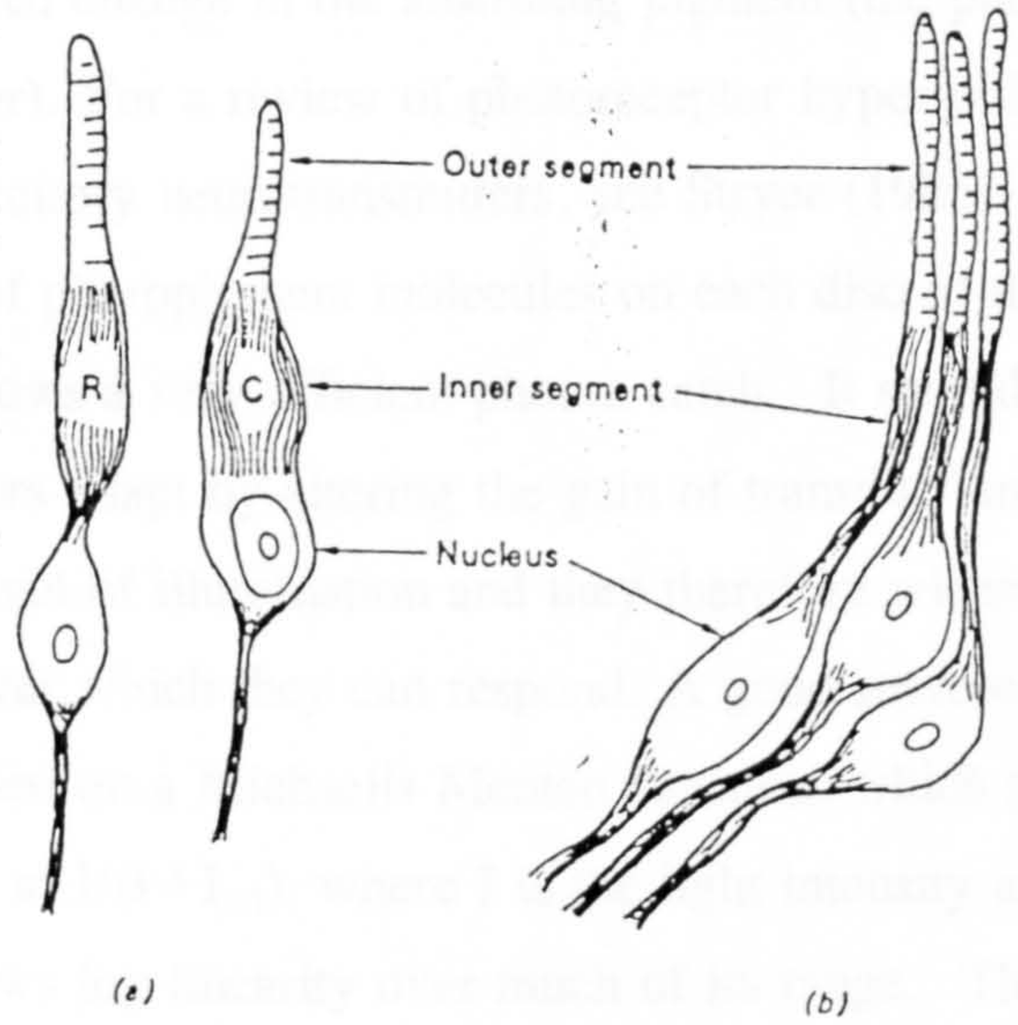

Figure 1.1.6 *Schematic diagram of (a) peripheral rods (R) and Cones (C) and (b) foveal cones (reproduced from Padgham and Saunders, 1975).*

photoreceptor cells giving higher spatial resolution. The receptor cell outer segments consist of a dense stack of 700 to 1,200 disc-shaped double membranes enclosed by the cell membrane. It is here that incident light radiation is converted into a nervous signal. An incident photon causes a conformational change in the absorbing pigment (the photo-pigment of the photoreceptor). For a review of photoreceptor hyper-polarisation and the release of excitory neurotransmitters, see Stryer (1986). The regular disposition of photopigment molecules on each disc of the photoreceptor outer segments allows a very efficient photon catch. It should be noted that photoreceptors adapt by altering the gain of transduction according with the prevailing level of illumination and they therefore widen the range of light intensities over which they can respond. A good representation of receptor output is based on a Michaelis Menten function, which predicts that output is proportional to $I/(I+I_{1/2})$, where I is the light intensity and $I_{1/2}$ a constant. This function shows log linearity over much of its range. The output of a photoreceptor is dependent on the interaction between the spectral distribution of the light radiation and the light absorption characteristic of the photopigment. A single photoreceptor is blind to wavelength; that is, the same photoreceptor output can be achieved by different spectral lights if the power of these lights can be varied, such that the product of the absorption by the photopigment and the power is equal for all of them. This is known as the principle of univariance (Rushton, 1972). Evidence of this principle is shown by the lack of ability to detect colour with rod mediated vision demonstrated by normals in scotopic conditions and by rod and cone monochromats (see section 1.2.2). Osterberg (1935) estimated the total number of rods in the human retina to be between 110 and 125 million and the total number of cones to be between 6 and 8 million. The cones are concentrated in the **fovea** and become more sparsely distributed with increase in eccentricity (figure 1.1.7). There are no rods at the fovea and few surrounding, and the maximum density appears to be at 10 to 15 degrees off axis.

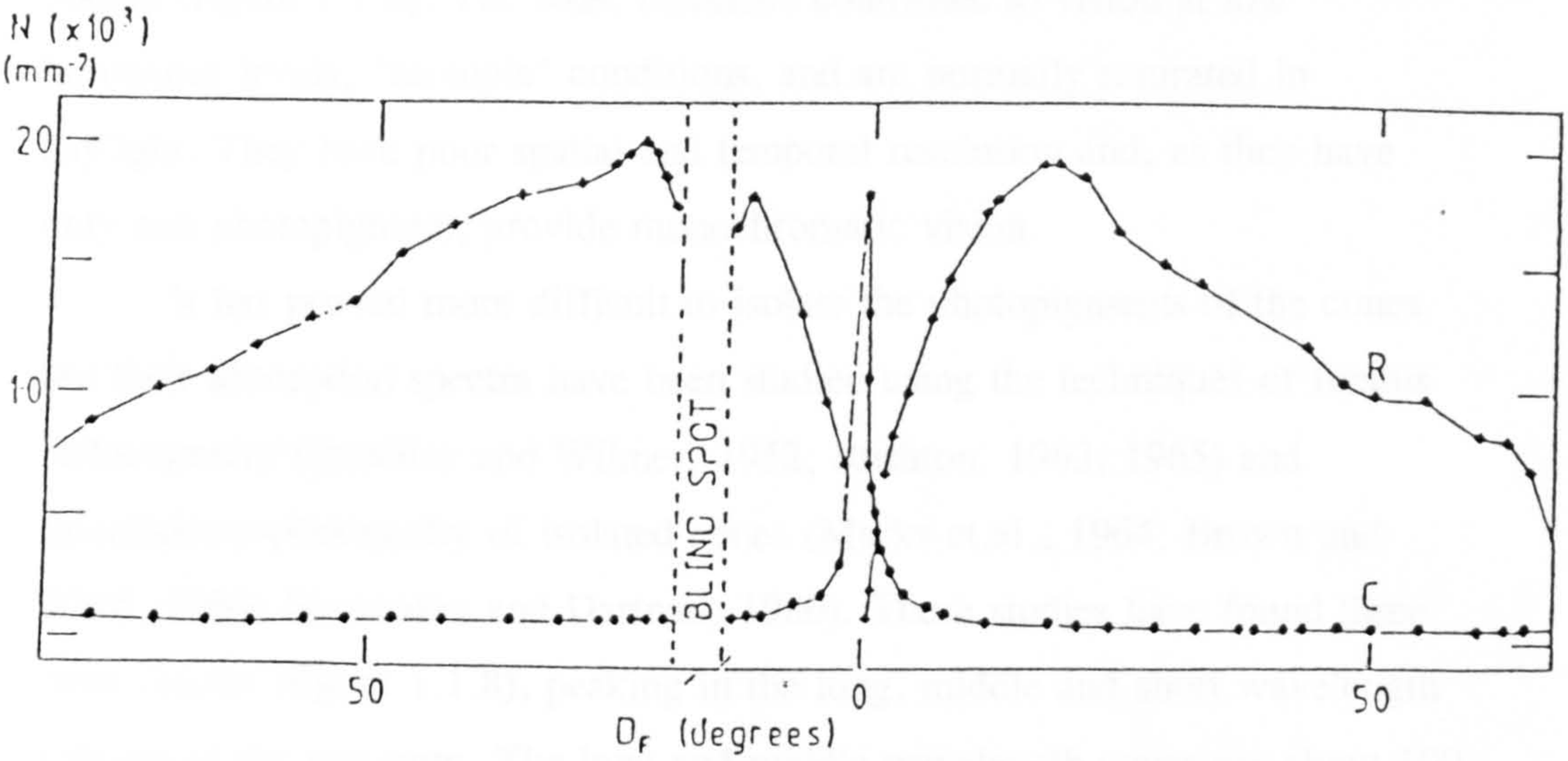

Figure 1.1.7 *Surface density of the rod (R) and cone (C) photoreceptors on the human retina (Oesterberg, 1935).*

In rods the photopigment has been extracted and its absorption spectrum investigated (Dartnall, 1957). It is known as rhodopsin. This absorption spectrum has a high luminance sensitivity, which peaks around 500nm (figure 1.1.8). The rods, therefore contribute to vision at low luminance levels, "scotopic" conditions, and are normally saturated in daylight. They have poor spatial and temporal resolution and, as they have only one photopigment, provide monochromatic vision.

It has proved more difficult to isolate the photopigments of the cones, but their absorption spectra have been studied using the techniques of fundus reflectometry (Brindley and Wilmer, 1952; Rushton, 1963, 1965) and microspectrophotometry of isolated cones (Marks et.al., 1964; Brown and Wald, 1964; Bowmaker and Dartnall, 1980). These studies have found three cone classes (figure 1.1.8), peaking in the long, middle and short wavelength regions of the spectrum. The long and middle wavelength cones are about 100 times as common as the short. Photoreceptor cells project through the external limiting membrane into the outer nuclear layer, where the cell nuclei are found. They terminate in the outer plexiform layer, which consists of the axons of the receptors, cone pedicles and rod spherules (figure 1.1.4). Here they synapse with bipolar and horizontal cells (Dowling and Boycott, 1966; Boycott and Dowling, 1969).

1.1.4 The Retina - Neural Connectivity

The neural connectivity in the inner and outer plexiform layers of the retina is complex and not completely understood. It serves the purpose of the initial neural processing of the visual system, which spreads extensively across the retina via lateral synapses between receptors, bipolar and horizontal cells. This processing involves neural summation (there are far fewer ganglion axons leaving the eye than there are photoreceptor cells) which enhances sensitivity to certain stimuli, and lateral inhibition which serves to emphasise discontinuity in the visual scene.

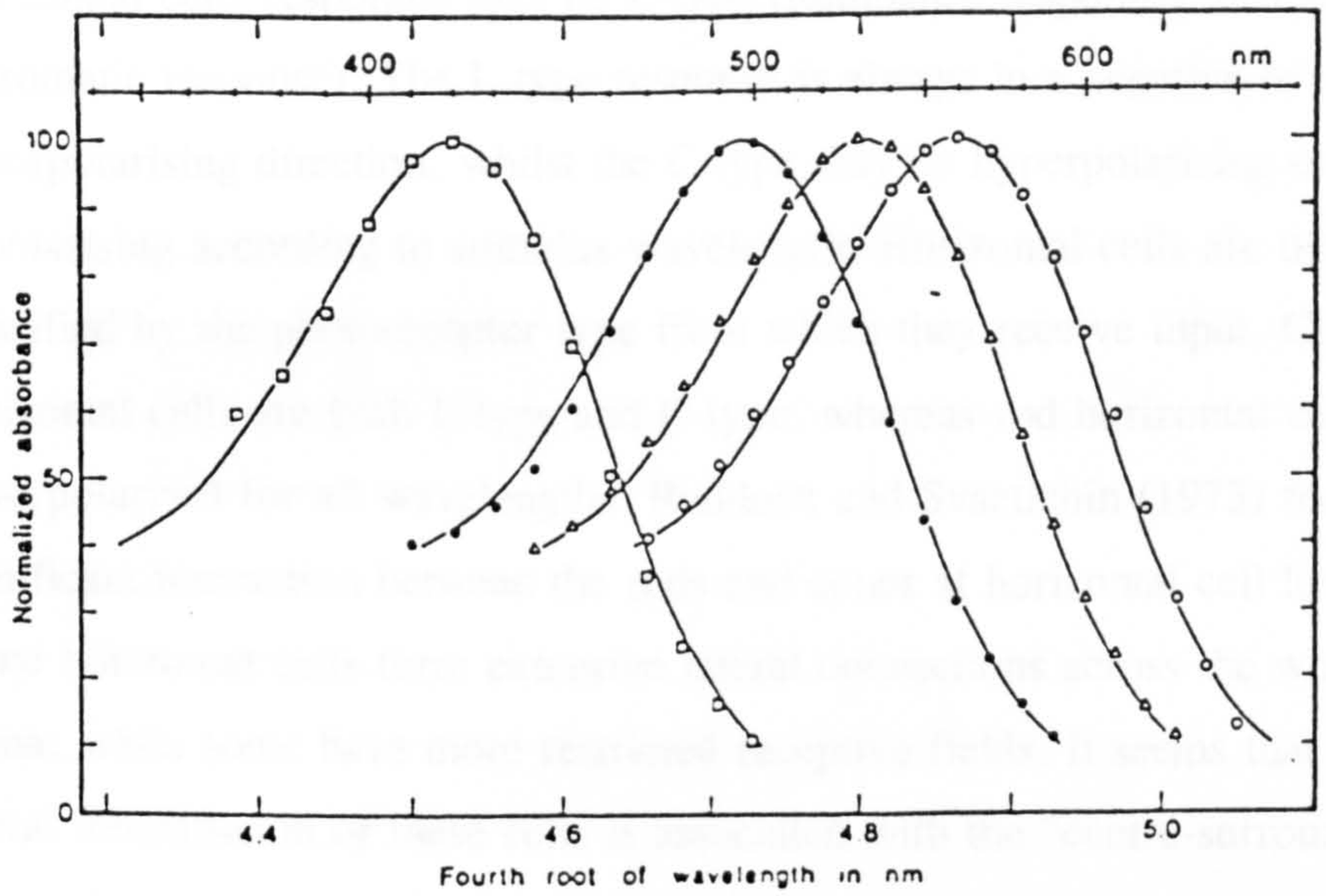

Figure 1.1.8 *The mean absorbance spectrum of human rods and cones. Filled circles, the rods (λ_{max} 496.3±2.3nm, mean of 39); squares, the "blue" cones (λ_{max} 419.3±3.6nm, mean of 5); triangles, the "green" cones (λ_{max} 530.8±3.5nm, mean of 45);plain circles, the "red" cones (λ_{max} 558.4±5.2nm, mean of 58). (From Bowmaker and Dartnell, 1980).*

The **horizontal** cells, as their name suggests, connect across the receptor synapses in the outer plexiform layer, with each cell connecting 6 to 12 cones centrally and 30 to 50 cones peripherally. They have extremely fine cell axons, are up to 1 millimetre long and may contact 80 to 150 rods. Horizontal cells responses may be L-type (luminance response), or C-type (chromatic response). The L-type response is always in a negative or hyperpolarising direction, whilst the C-type may be hyperpolarising or depolarising according to stimulus wavelength. Horizontal cells are usually classified by the photoreceptor type from which they receive input. Cone horizontal cells are both L-type and C-type, whereas rod horizontal cells are hyperpolarised for all wavelengths. Ruddock and Svaetichin (1973) found no significant interaction between the rods and cones at horizontal cell level. Some horizontal cells form extensive lateral connections across the whole retina, while some have more restricted receptive fields. It seems that the lateral transmission of these cells is associated with the "centre-surround" antagonistic response organisation of bipolar cells.

The receptors also synapse the **bipolar** cells in the outer plexiform layer. The rods and cones have separate bipolar pathways. The terminal spherule of each rod is invaginated by the dendrites of up to 45 rod bipolars, whereas the terminal pedicle of the cone synapses with clusters of three dendrites. Dowling and Boycott (1966) suggested that the middle one originates in a midget bipolar cell and the others are from flat bipolar cells. The receptive fields of these bipolars, receiving input from both horizontal cells and photoreceptors, have been found to consist of two spatially concentric and antagonistic regions (Werblin and Dowling, 1969). Stimulation of the surround of the receptive field produces a response of the opposite polarity to that induced by stimulating the centre, or in some cases surround stimulation has an inhibitory effect on the response from the centre (Werblin, 1970).

The **amacrine** cells serve a similar function to the horizontal cells, but lying at the level of the bipolar-ganglion cell synapses at the inner plexiform

layer (Dowling and Werblin, 1969). Amacrine cells, as well as having dendritic communications with other amacrines, can synapse both pre and post synaptically to bipolar cell axon terminals to provide a reciprocal feedback between the two cell types (Werblin, 1973). Chan and Naka (1976), proposed that there were two types of amacrine cell, one which communicated with X-type ganglion cells and the other which communicated with the Y-type ganglion.

Retinal neurones, which have an axon that joins the optic nerve are called retinal **ganglion** cells. There are approximately 1.2 million ganglion cells in the human retina (Oppel, 1967). Their greatest density is at the macular region and the density falls to a minimum in the periphery. A great variety of ganglion cells have been described.

Each ganglion cell, like other visually responsive cells, has what is termed a receptive field, that is an area of the visual field which is able to stimulate the cell. Kufela (1953) found that the receptive fields of ganglion cells are not uniformly responsive to light. Some ganglion cells have an 'on' centre, i.e. stimulation of the cell raises the output from the cell above its resting level. Others have an 'off' centre, i.e. similar stimulation reduces the cell's output below that of the resting level. These cells are surrounded by an annulus of the opposite polarity (figure 1.1.9). The function of the on/off centre surround system is to detect increments and decrements in brightness, and thus to detect contrast.

Cells with this concentric antagonistic field arrangement can further be classified into two groups: 'X' type and 'Y' type (Enroth-Cugell & Robson, 1966). The X and Y type cells may be distinguished by their spatial resolution. A position can be found for a grating stimulus presented to an X type cell which will elicit the same response from the cell as that of a spatially uniform stimulus of the same luminance. This is not true for the Y type of cell. These types of ganglion cell might also be categorised by their temporal properties. An X type cell will give a sustained response to stimulus presentation, whereas a Y type cell will only fire at stimulus on-set and off-set

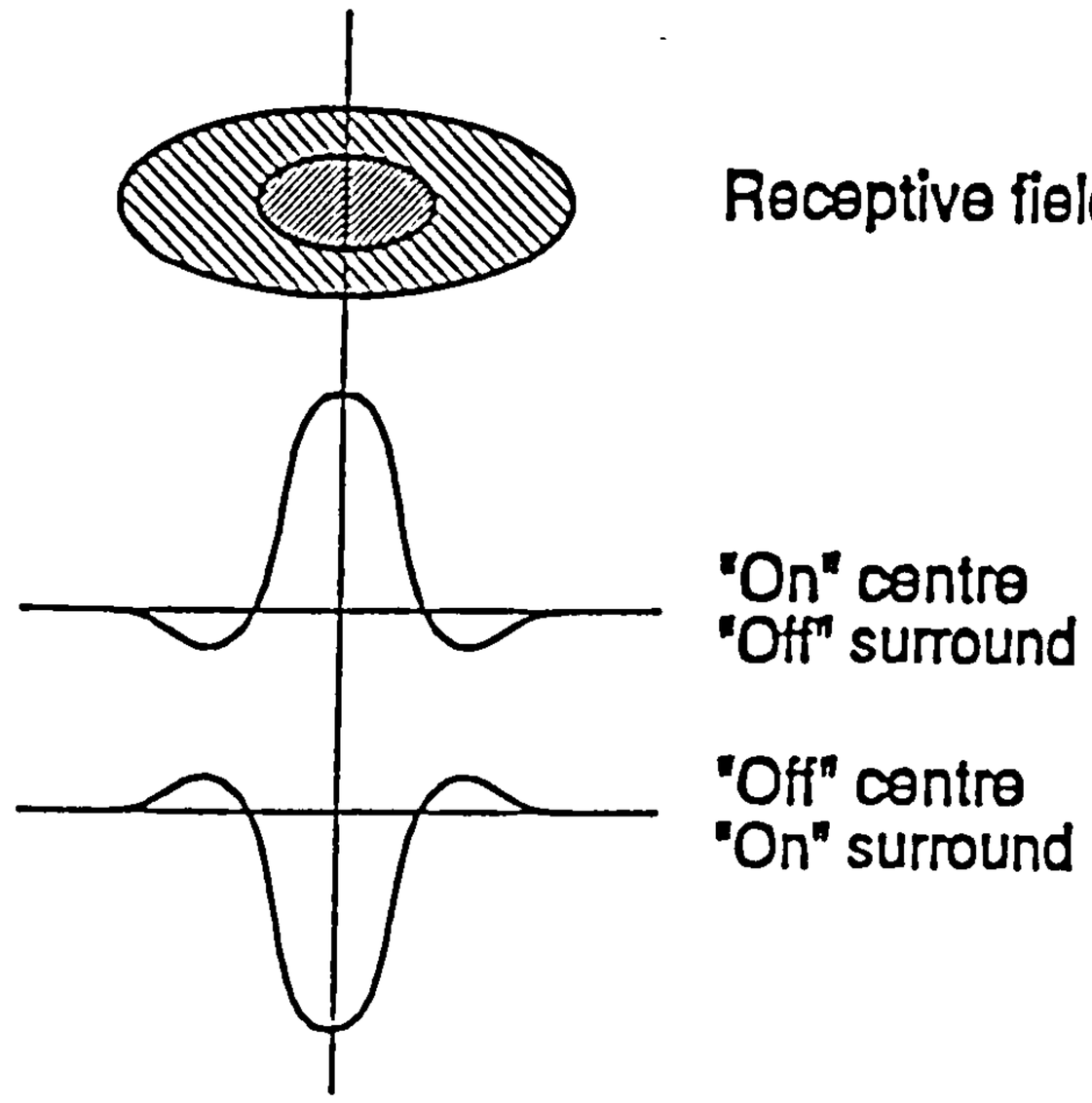

Figure 1.1.9 *Representation of the receptive field organisation of an "on" centre, "off" surround and an "off" centre, "on" surround ganglion cell.*

(Gouras 1968). This has led to them being classified as sustained or tonic respectively. Gouras also showed that the conduction speeds along the ganglion axon are higher for the Y type cells than for the X type. Another type of ganglion cell, named the W cell has also been described (de Monasterio 1978 a & b). These have small receptive fields and the slowest conduction rate. Ingling and Drum (1972) described the X cells as chromatic units and the Y type cells as achromatic units, because of different cone receptor class inputs into the centre and surrounds of the cell receptive fields. The X type cells, or chromatic units, receive input into their receptive field centres from a different class of cones than into their surrounds. This is known as colour opponency (figure 1.1.10) and has been well characterised by electrophysiological studies (De Monasterio, 1978 a & b) and more recently by psychophysical methods (Brent and Ruddock, 1990).

This colour opponency is created by the centre of a ganglion's receptive field taking the output of bipolar cells of a different spectral class from that of the surround (figure 1.1.11). In the central 5 to 10 degrees of the retina, midget bipolar cells contact just a single cone (Wassle, Grunert, Rohrenbeck & Boycott 1989; Curcio & Allen 1990). These in turn feed the ganglion cells in such a manner that one bipolar will drive the centre of the ganglion's receptive field and a number of surrounding bipolars the surround of the field. It is not clear whether these surround fields take input from a single spectral class or whether there is random retinal connectivity (Young & Marrocco, 1989; Lennie Haake & Williams, 1991). Nevertheless, we may distinguish 4 types of red/green opponent cell with both on-and off-centre cells, taking their central field input from red or green cones. In the periphery, there is anatomical evidence to suggest that the red and green midget bipolars pick up from more than one cone and do not appear to distinguish cone types (Mariani 1984a). The bipolar cells driven by inputs from the blue sensitive cones also input to ganglion cells in an opponent manner, the antagonistic field having input from both red and green cone driven bipolar cells. This gives rise to a blue/yellow colour opponent

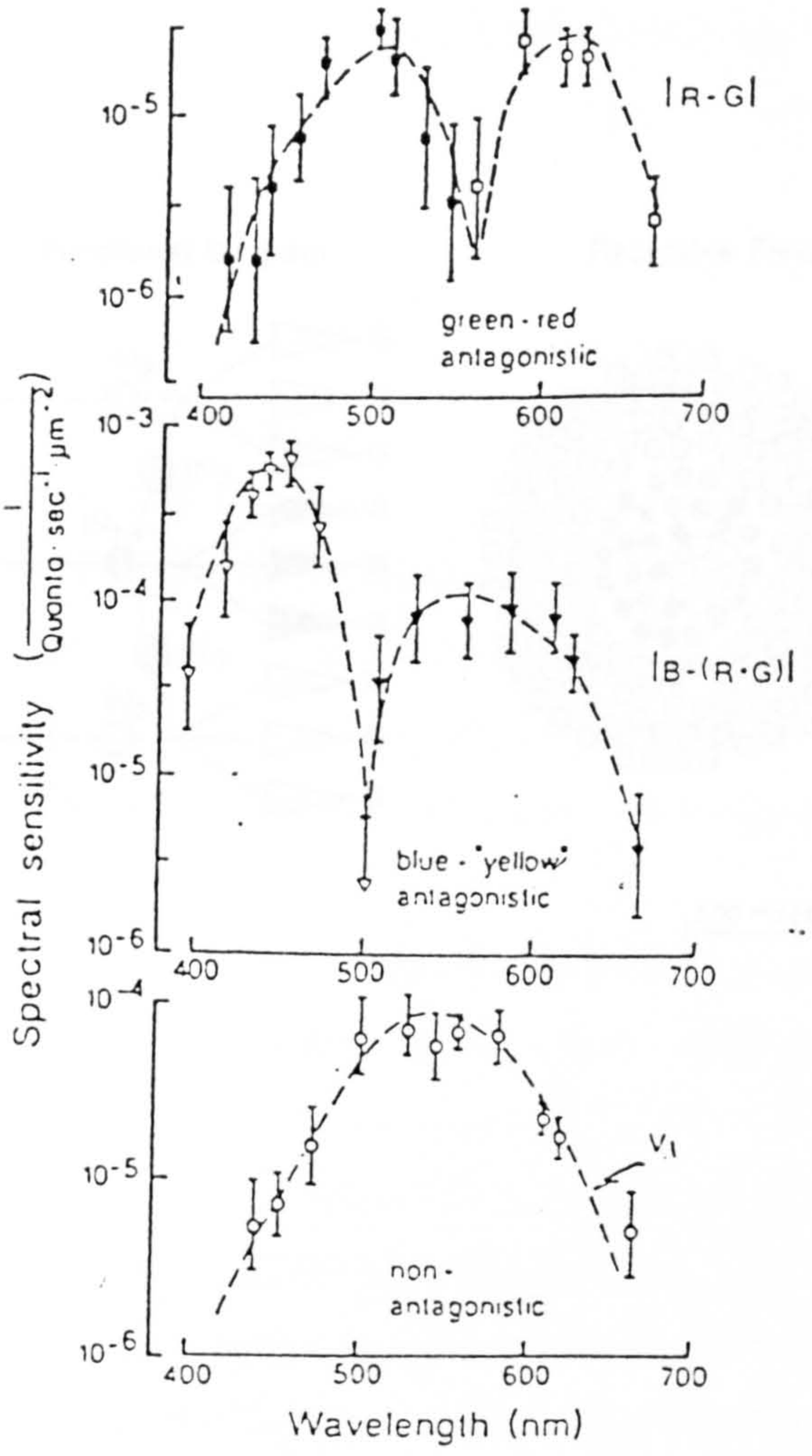

Figure 1.1.10 *Spectral sensitivity functions of primate ganglion cells, showing (a) red-green antagonism, (b) blue-yellow antagonism. Open symbols represent excitatory responses and filled symbols inhibitory responses. (c) A non-antagonistic ganglion cell response fitted by the photopic luminosity function* V_λ *(Zrenner, 1983).*

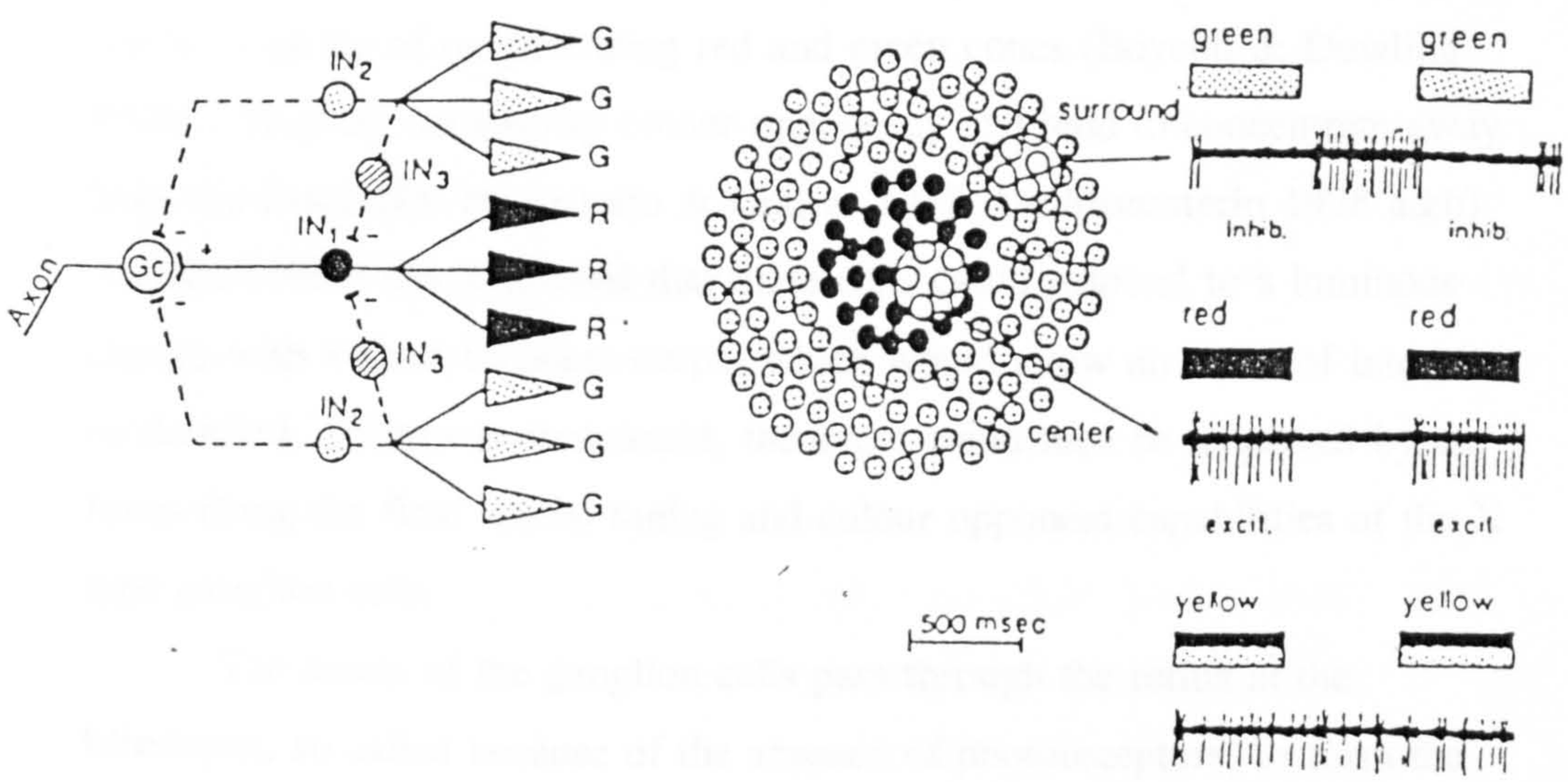

Figure 1.1.11 *A schematic representation of neuronal connections to a colour opponent ganglion cell with the receptive field and response characteristic (Zrenner, 1983).*

ganglion cell. The blue or S cone bipolar, described by Mariani (1984b) has been found to output only to the centre of the blue/yellow ganglion cell. Thus there are only 2 types of blue/yellow opponent cells with on- or off-centre blue central inputs.

The Y type ganglion cells receive input from diffuse bipolars which contact a group of neighbouring red and green cones (Boycott & Dowling 1969). They do not display colour opponency and tend to concentrate away from the fovea (De Monasterio & Gouras 1975, De Monasterio 1978 a&b). Zrenner (1983) has suggested that these cells could respond to a luminous change with a short transient output which would allow an event of interest to be detected. After eye movement, the event could then be inspected by the fovea using the final spatial tuning and colour opponent capabilities of the X type ganglion cells.

The axons of the ganglion cells pass through the retina at the **blindspot**, so called because of the absence of photoreceptors, to form the **optic nerve.**

1.1.5 Optic Nerve, Tract and Chiasm

There are about one million optic nerve fibres, which pass from the retina to the **optic chiasm**, which is a mid-line structure beneath the hypothalamus, formed by the junction of the two optic nerves. At the optic chiasm, the fibres of the optic nerve separate, with those of the nasal retinae cross to join those of the temporal retinae of the other eye and form the optic tracts. This process is known as decussation. Thus the left visual field is mapped to the right side of the brain and vice versa, although a central strip of 1 to 2 degrees may be represented in both brain hemispheres (Bunt and Minkler, 1977). The majority of optic tract fibres terminate on the lateral geniculate body. X type ganglion cell axons project to the parvocellular layers of the lateral geniculate nucleus, whereas the Y type cells project to the magnocellular layers. Some Y type and all of the W type of ganglion cells project to the superior colliculus. There are also projections to the

pregeniculate nucleus, the pretectal nuclei, superior colliculus, the pulvinar and the accessory optic nuclei. The projections of ganglion cells are summarised by Perry et al. (1984) and Perry & Cowey (1984).

1.1.6 Lateral Geniculate Nucleus

In primates the lateral geniculate nucleus of the main retino-cortical pathway divides into two anatomically distinct sections. These in turn are subdivided by function. The parvocellular (four dorsal) and magnocellular (two ventral) layers receive input from different types of retinal ganglion cells, maintaining the on/off centre distinction by layers. The nasal fibres of the optic tract (from the contralateral eye) terminate on layers 1, 4, and 6 and the temporal fibres on layers 2, 3 and 5. Within each layer there is a topographical map of the contralateral visual hemifield (Hubel, 1988). The physiological characteristics of retinal neurons are duplicated in the LGN with alpha or Y neurons confined to the magnocellular and beta or X neurons to the parvocellular layers. Schiller and Malpeli (1978) found that in the macaque, "on" centre, colour-opponent ganglion cells projected to layers 5 and 6, whereas "off" centre cells projected to layers 3 and 4. The transient broad-band ganglion cells project to layers 1 and 2. The differences in functions of the magnocellular and parvocellular layers have been documented by Livingstone and Hubel (1984, 1987) from their own and others' work. They propose differences in colour, contrast sensitivity, spatial resolution and temporal resolution between the parvocellular and magnocellular layers (table 1.1.1).

The most common type of receptive field organisation in the parvocellular layers are colour-opponent centre-surround (type I, see figure 1.1.12). These account for about 80 percent of the neurons examined in the parvocellular layers, but have not been found in the magnocellular. Their small "on" or "off" centres receive input from one cone type and are surrounded by an antagonistic annulus of a different spectral sensitivity. It is not clear if these surrounds are all fed by one cone type alone (DeValois and

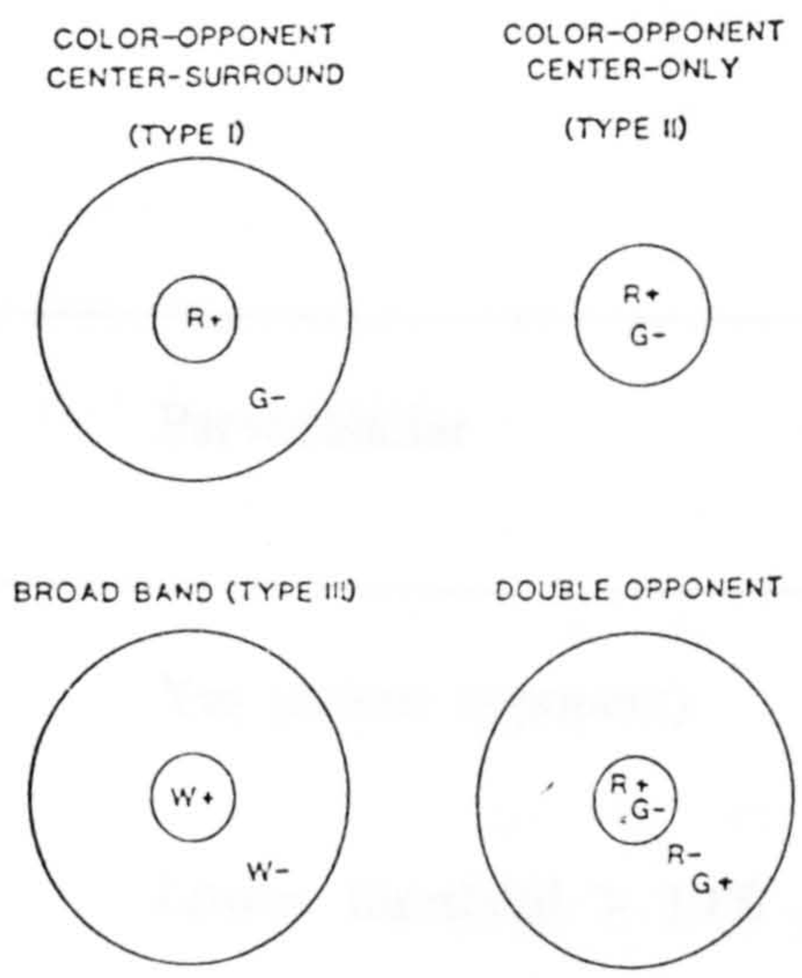

Figure 1.1.12 *Types of cell in the primate visual system that have radially symmetrical receptive fields. The double opponent cells are the outstanding characteristic of the blobs in V1 (Livingstone and Hubel, 1984; reproduced from Davidoff, 1991).*

	Parvocellular	Magnocellular
Colour	Yes (colour opponent)	No (Broad band)
Contrast sensitivity	Lower: threshold > 10%	Higher:threshold < 2%
Spatial resolution	Higher	Lower
Temporal resolution	Slow (sustained responses, low conduction velocity)	Fast (transient responses, high conduction velocity)

Table 1.1.1 *Parvocellular and Magnocellular differences.*

DeValois, 1993). Type I cells are mostly red versus green (56%), or blue versus red plus green (blue v. yellow, 18%), with 3 to 4 % each of green versus blue plus red and red versus blue plus green. Type II cells are colour-opponent centre-only cells (figure 1.1.12). They make up a further 10% of the parvocellular neurons and are not found in the magnocellular layers. They consist of a centre-only receptive field fed by two antagonistic sets of cones, either red versus green or blue versus yellow. Thus the neuronal organisation with respect to colour is no longer the trichromatic system (Young-Helmholtz) of the retina. It is now a (Hering) opponent system (Hurvich, 1981; Derrington, Krauskopf and Lennie, 1984).

The remaining 10 % of parvocellular cells appear to be exclusively for signalling luminance (although to some extent all parvocellular are capable of this). These are the broad-band or type III cells. They have a centre surround receptive field organisation, but the spectral sensitivities of the each are the same. Adapting these cells to particular colours suggests that they receive input from more than one cone type, possibly just red and green (De Monasterio and Gouras, 1975) or all three (Wiesel and Hubel, 1966).

Magnocellular neurons are of the broad band type and as such cannot signal colour differences within their receptive fields. However, there is a variety of spectral tunings of cells within the magnocellular system, so they might be able to play a part in colour vision when larger stimuli are involved. Livingstone and Hubel (1987) say that they show selectivity of receptive field surround which is indicative of red cone input. They are tonically suppressed by diffuse red light, but not by diffuse white light.

There are other differences between the magnocellular and parvocellular systems. Magnocellular neurons are about ten times more sensitive to luminance contrast than parvocellular, the parvocellular neurons do not respond to borders with less than 10% contrast. The magnocellular neurons have receptive field sizes two to three times those of the parvocellular, giving much poorer spatial resolution. Parvocellular cells have a

slower response than magnocellular, and produce a sustained output, which suggests they are less sensitive to temporally varying stimulation.

1.1.7 The Primary Visual Cortex (V1)

The nerve fibres leaving the lateral geniculate nucleus dorsolaterally are termed the optic radiations. The great majority of the fibres of the optic radiations terminate on the primary visual area, V1, which is equivalent to Brodmann's Area 17 (Brodmann, 1909). This area is distinguished from other cortical areas in that it possesses a thin band of medullated nerve fibres running parallel to the cortical surface, hence it is also known as the striate cortex.

V1, as identified in monkeys, is located on both sides of the Calcarine Fissure on the medial aspect of the occipital lobe, extending for a short distance onto the occipital pole (Pearlman, 1987; see figure 1.1.13 for human equivalent). It is bordered anteriorly by an approximately 1 centimetre wide rim of cortex called prestriate cortex, or Area 18 of Brodmann, which lacks the stria of Area 17 and is considerably thinner.

Practically all of the remainder of the occipital lobe is occupied by Area 19. The cytoarchitectonic differences between Areas 18 and 19 are not easily recognised. These areas are concerned exclusively with vision and may be described collectively as the prestriate visual areas (Ruskell, 1993).

Like all sensory cortex, the primary visual cortex is divided into 6 layers. A section of layer 4 called 4C, is the arrival area for the main projections from the lateral geniculate nucleus (figure 1.1.14). Projections from the magnocellular layers of the lateral geniculate nucleus arrive in Layer 4Cα. The neuronal projections from Layer 4Cα are predominantly to Layer 4B. The main projection from the parvocellular layers of the lateral geniculate nucleus arrive at Area 17 in a physiologically distinct section of Layer 4C called 4Cβ, and at Layer 4A.

The important characteristics of LGN magnocellular cells are carried forward to Layers 4Cα and 4B, although there are some differences (Malpeli,

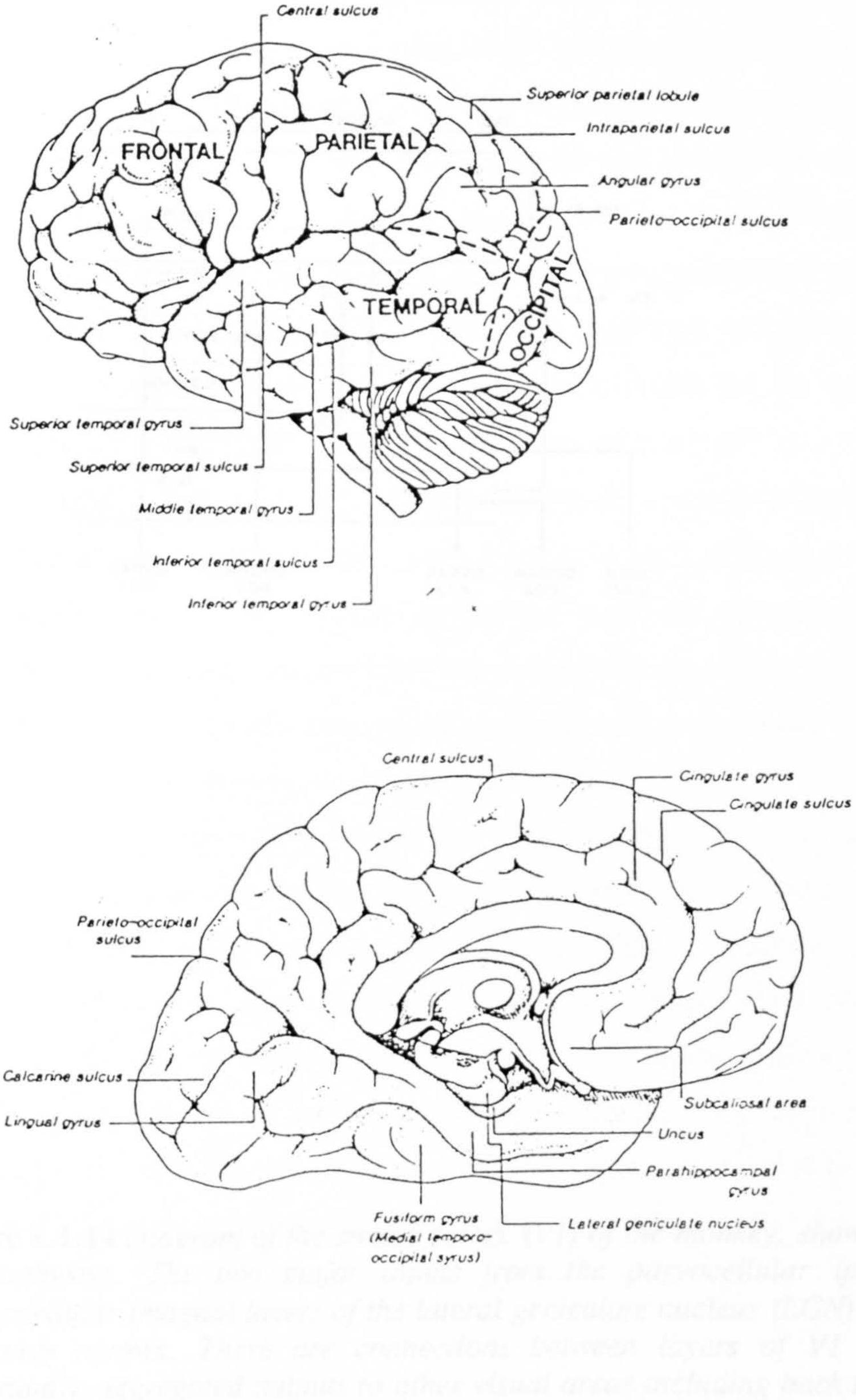

Figure 1.1.13 *Lateral surface of the left hemisphere of a human brain (top). Medial view of an isolated left hemisphere with brain stem removed to show the medial surface of the temporal lobe (bottom) (reproduced from Davidoff, 1991).*

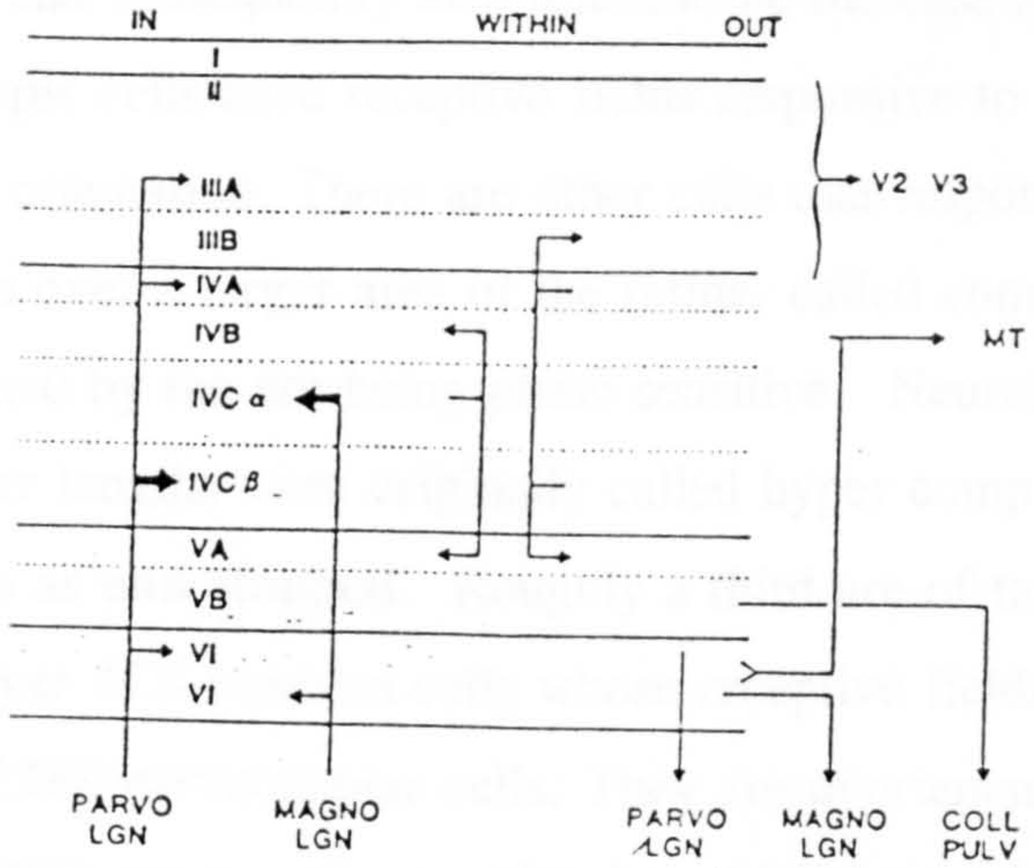

Figure 1.1.14 *Diagram of the striate cortex (V1) of the monkey, showing in and out pathways. The two major inputs from the parvocellular (parvo) and magnocellular (magno) layers of the lateral geniculate nucleus (LGN) are shown by heavy arrows. There are connections between layers of V1 and, most importantly, segregated outputs to other visual areas including back to the LGN (not marked) and to the superior colliculus (COLL) and Pulvinar (PULV) (Cowey, 1985; reproduced from Davidoff, 1991).*

Schiller & Colby 1981). The most important, as discovered by Hubel & Wiesel (1965), is that the receptive fields of Layer 4B neurons are of remarkably different shapes from those of the lateral geniculate nucleus. At Layer 4B and subsequently also found to be the case at Layer 4Cα, the so called **simple cells** have receptive fields responsive to a bar or an edge of a particular orientation. There are other cells that respond to the same orientation over a larger area of the retina, called **complex cells**, further distinguished by the not being phase sensitive. Neurons that respond to more specific bar lengths were originally called hyper complex, but are now referred to as **end stopped**. Roughly a third are of this type.

Layer 4Cβ contains cells whose receptive fields are indistinguishable from the LGN parvocellular cells. They are unorientated in the Hubel & Wiesel (1965) sense, and are either broad band or colour opponent centre surround. In one typical microelectrode penetration from which recordings were taken from 124 cells, Livingstone & Hubel (1984) found that 46 were broad band and 78 were colour opponent centre surround.

Hubel & Wiesel (1965) made the important observation that neurons in the striate cortex are anatomically organised according to the visual characteristics to which they best respond. For example, penetrations with their microelectrodes perpendicular to the surface of Area 17 provided evidence for columns of cells with a systematic organisation. These columns of cells are driven by one eye and are known as ocular dominance columns. Cells of a similar orientation were found to be close to each other in the columns. Thus the neurophysiological foundations of a modular structure for orientation and stereopsis is well established by Area 17.

Blobs - Neurons involved in the transmission of visual information may be distinguished by staining the cells for the presence of an enzyme that results from neuronal activity. Wong-Riley (1978), using this technique, reported that visual input seemed to be having an effect on other parts of Area 17 besides Layer 4. Houghton & Hubel (1981) followed up the observation and

confirmed that there was a pattern of regularly repeating structures in Area 17, with the most conspicuous staining for a particular enzyme (cytochrome oxidase) in layers 2 and 3 (figure 1.1.14). These structures were called 'blobs' by Hubel & Livingstone (1987) from their appearance in tangential section. They have been found in all primates studied, but not in any non primates. Blobs extend throughout the full thickness of Layers 2 and 3 in Area 17 and may be seen more faintly in Areas 4B, 5 and 6, where they lie exactly underneath the overlying upper layer blobs. No blobs have been found in Layers 4A and 4C.

Livingstone & Hubel (1984) found that the outstanding feature of these blobs was the abundance of double opponent cells (figure 1.1.12). Cells of this type, originally described by Daw (1968) in the goldfish retina, were absent in the lateral geniculate nucleus and in Layer 4Cβ of the striate cortex, although the latter is disputed by Michael (1988). According to Livingstone & Hubel, primate double opponent cells are organised like those found in the goldfish. Such cells tend to respond poorly or not at all to white light spots of any size or shape, or to diffuse light of any spectral composition. Double opponent cells were the most common class of blob cell. There was a preponderance of R+G- cells over all other types, with B-Y+ cells being rare. Livingstone & Hubel also found what they called three quarter double opponent cells, which resembled double opponent cells, except for an absence or weakness of one of the two surround systems. Although not rare, they were less common than proper double opponent cells. The blobs apparently lack colour opponent centre surround cells, which were the most common type found in the lateral geniculate nucleus. There were also relatively few (13%) centre-only colour opponent cells. Next only to the double opponent cells, broad band cells were the most important class. The broad band cells had relatively strong surround antagonism. On centre cells outnumber off centre cells by more than 2:1. Most of these cells give vigorous responses at all wavelengths from 440 nanometres to 680 nanometres, thus they probably

receive input from all 3 cone types. Hubel & Livingstone (1987) have speculated that any individual blob contains only one of these cell types.

Hubel & Livingstone (1987) maintained that it is extremely difficult to conceive of a way in which a double opponent cell could be generated from any straightforward combination of colour opponent centre surround cells, because the surrounds would have the wrong polarity. Projections from Layer 4Cβ to the blobs seems unlikely therefore, because of the profound differences between the colour opponent centre surround cells of Layer 4Cβ and the double opponent cells in the blobs. So, at the moment, any connection between Layer 4Cβ and the blobs is based solely on anatomical proximity. It is possible that the blobs may also receive input directly from the lateral geniculate nucleus.

A particularly striking aspect of the blob cells is their lack of orientation specificity. Cells close to the blobs are orientation specific. On approaching a blob with their microelectrodes, Livingstone & Hubel (1984) found that cells show a sudden decline in orientation selectivity. Within the blob itself there was a complete absence of cells with orientation selectivity, thus producing the same effect as if the electrode had entered a lateral geniculate nucleus or Layer 4Cβ of Area 17. A lack of orientation selectivity in the blob cells could be due to their receiving input from neurons with centre surround receptive fields like those of Layer 4Cβ, or the lateral geniculate nucleus, but the connections are not proven. Hubel & Livingstone (1987) argue that it cannot be due to the blob cells pooling the inputs of the neighbouring orientation specific cells and consequently responding to line segments in all orientations.

Interblobs - Each of the blobs described above consists of a core of unorientated cells 100 -150 nanometres in width surrounded by a shell of poorly orientated cells (Livingstone & Hubel, 1987a). Away from this shell is the interblob region (i.e. surrounding and between the blobs), where cells show an orientation specificity even greater than the cells of Layer 4Cα.

In Layers 2 and 3, cells outside the blobs are mostly complex. They are precisely tuned for orientation and have relatively small receptive fields, but are not obviously selective to direction of motion or wavelength. Only a quarter are end stopped. Some interblob cells respond poorly or not at all to white light, but vigorously to coloured light regardless of the stimulus intensities. These orientation colour coded cells (including cells responding to dark bars) make up 17% of the interblob population receiving input from 6 to 8 degrees from the fovea. At 0 to 2 degrees, there is a higher proportion (38%). Interblob neurons have smaller field centres than those of the blobs. The interblob cells receive projections from Layer 4Cβ, but their properties are clearly different.

1.1.8 The Prestriate Cortex

Area 18 contains the visually responsive prestriate regions known as V2, V3, V3a and V4 (Zeki, 1971) in the rhesus monkey, each of which contains a separate map of the visual field. Circumstantial evidence for a separate V2 area in humans (Cowey, 1979) has been backed by more recent functional imaging studies (Clark, 1992). V2 receives a topographically organised input from Area 17 (V1). Cytochrome oxidase staining reveals alternating dark and light stripes about one millimetre wide, running perpendicular to the Area 17/18 border (Tootell et al., 1983). The dark stripes are of 2 sorts (thick and thin) which are much harder to tell apart in the macaque than in the squirrel monkey. Livingstone & Hubel suspected that blobs in Area 17 projected to the stripes in Area 18.

Thin Stripes - The thin stripes cells are like cells in the blobs of Area 17 to which they are connected, they are not orientation specific and many of them are colour coded. Thin stripe neurons of Area 18 show less specialisation with a respect to spatial localisation, although the optimum stimulus size to make the neurone respond is the same as in Area 17. The cells in the thin stripes work like those of Area 17, mostly double opponent. Hubel &

Livingstone (1987) concluded that over half the unorientated cells in the Area 18 were similar in every way to the blob cells of Area 17. However, they regarded their subgrouping of colour responsive cells for Area 18 as uncertain, because they did not carry out the time consuming chromatic adaptation or other procedures (Derrington et al., 1984) necessary to distinguish red/green from yellow/blue neurons. The interactions between centre and surround of thin stripe neurons were found to be complex with respect to colour. The response to a red spot and a green annulus was not necessarily stronger than the response to a red spot alone. Indeed, it was sometimes weaker. There were also colour opponent cells comprising 10% of the thin stripe neurons with very odd properties. For example, neurons were found that were red on/green off in one eye and the reverse in the other. These cells would, with both the animal's eyes open respond only to out of focus coloured objects, and not to large coloured objects at all distances. There were also complex unorientated cells that responded to the optimum spot size (1/4 to 1/2 a degree) up to 4 degrees from the centre of the receptive field. Twelve percent of the cells were unorientated, in sharp contrast to cells found in other stripes, where they were orientation tuned and responded poorly, if at all, to stationary stimuli.

Pale Stripes - The pale stripes of Area 18 receive their input from the interblob regions of Area 17 and exhibit similar properties. However, in Area 18 a higher proportion of cells are end stopped, that is they respond to short, but not to long lines or edges. The pale stripes also contain many complex, orientation specific cells.

Thick Stripes - Large injections of label into Area 17 do not spread uniformly to Area 18, little goes to the thick stripes (Livingstone & Hubel, 1987b). They appear to be connected to Layer 4B of Area 17, but also probably receive input from elsewhere, for example the pulvinar. It appears that the thick stripes respond only to moving stimuli. They contain neurons tuned for

binocular disparity, but they have rather less directional specificity than those at Layer 4B. The thick stripes also have orientation specific neurons of the complex type.

Beyond V2 - The anterior projections from V2 to the multiplicity of visual areas in the cortex are not yet fully known. Area V4 in the Macaque has been reported to have a high proportion of cells that are selective for chromatic information (Zeki, 1980, 1983). This is in contrast with V3, which has a great number of cells tuned to stimulus orientation, and area V5, which is dominated by cells selective for the direction of motion (Zeki, 1978a&b). Thin stripes of V2 certainly project to Area V4, which has been shown to have interesting properties with respect to colour. Pale stripes may also project to V4 and to the little investigated area, V3. Thick stripes show connections with the superior temporal sulcus in the macaque, this area is often referred to as MT (middle temporal), from the anatomy of the Owl monkey (Allman and Kass, 1971) or as V5 (from electrophysiology). MT also has connections with Layer 4B of Area 17 and contains cells with a similar directional selectivity. It might even be considered as part of a movement pathway separate from the 'where' and 'what' pathways.

Neurons in V4 have interesting properties with respect to colour (Schein, Marrocco and De Monasterio, 1982). V4 neurons have large receptive fields, even extending into the ipsilateral visual field, suitable for carrying out the summation of thousands of LGN afferents covering a large area of retinotopic space. V4 cells can be suppressed by a stimulus as much as 30 degrees outside their receptive fields. Such stimuli are silent, that is they have no effect unless the cell's receptive field is stimulated. The suppression is wavelength dependent. Zeki also suggested that V4 cells have the property of colour constancy. They respond to a particular colour independent of the wavelength of incident light. V4 neurons are not the only cells that have been accredited with colour constancy, but their large receptive field sizes suggest them as more suitable than any other candidates, for example the retinal cells

(Pöppel, 1986) or the double opponent cells of Area 17 (Hubel & Livingstone 1987). Recent work with rhesus monkeys who have V4 ablations (Wild et al., 1985; Walsh et al. 1992, 1993) has indeed found that colour categorisation and hue discrimination are little affected, whilst colour constancy is impaired. Heywood and Cowey (1987) found that V4 ablations did effect hue discrimination, but Walsh et al. (1993) claim that this is comparatively mild. The function of V4 with respect to colour is more complicated as suggested by the correlation of V4 neuronal activity with attentive selection (Motter, 1994a) and feature selection (Motter, 1994b).

1.1.9 High Level Disorders

The particular claim for independent streams of information in the visual system has gained further support from studies of vision in patients with brain damage. Such phenomena as akinetopsia and achromatopsia (see reviews by Zeki, 1990, 1991) provide evidence for a modular processing of visual information and the blindsight phenomenon (see reviews by Weiskranz, 1986, 1990) indicates that some visual function can be mediated by the subcortical pathways.

The retina connects with the primary visual cortex (V1) which, in humans, lies buried within the calcarine sulcus (figure 1.1.13). The connections between cortex and retina are topographical, thus reproducing a map of the retina (and hence of the contralateral field of view) in each V1. The lower part of the field of view is represented in the upper calcarine cortex and the upper part in the lower calcarine cortex, while central vision is represented at the occipital pole. Lesions to the striate cortex may thus cause a scotoma or area of blindness in the visual field, the size and location of which depend precisely on the location and size of the lesioned area (figure 1.1.15) (Holmes, 1918). These subjects often lack the conscious percept of stimuli when presented in the 'blind' field, however various studies have demonstrated the ability to detect stimuli and even discriminate orientation and direction of motion (Weiskrantz et al., 1974; Weiskrantz 1986, 1990; Barbur

(a) HEMIANOPIA

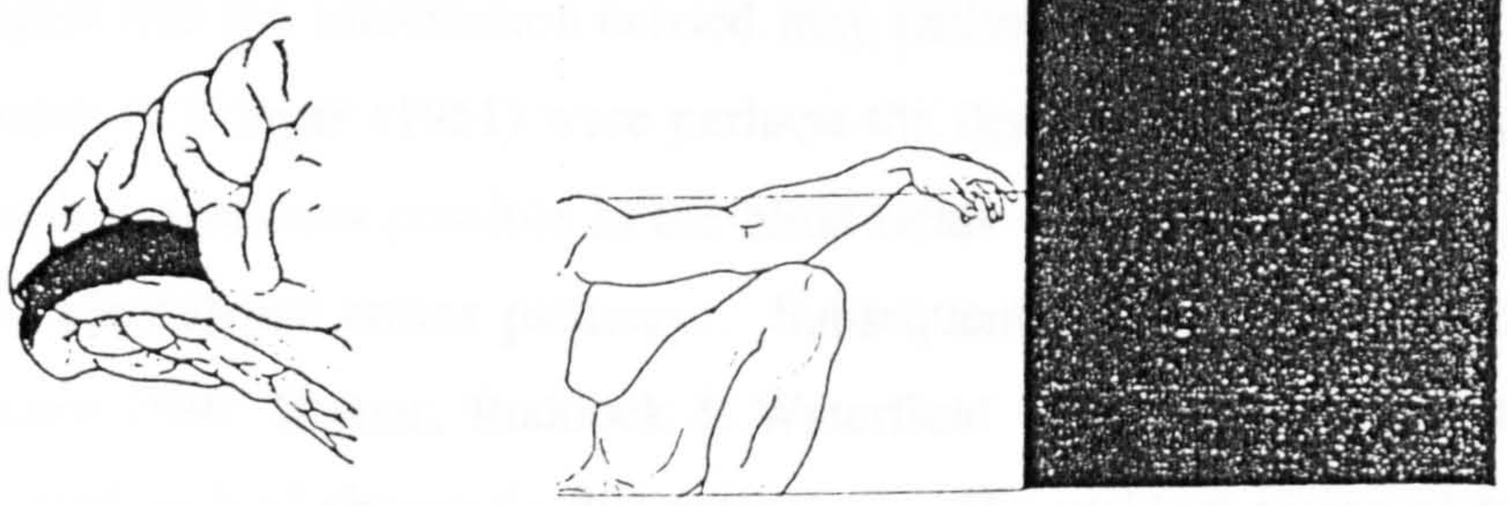

(b) SCOTOMA

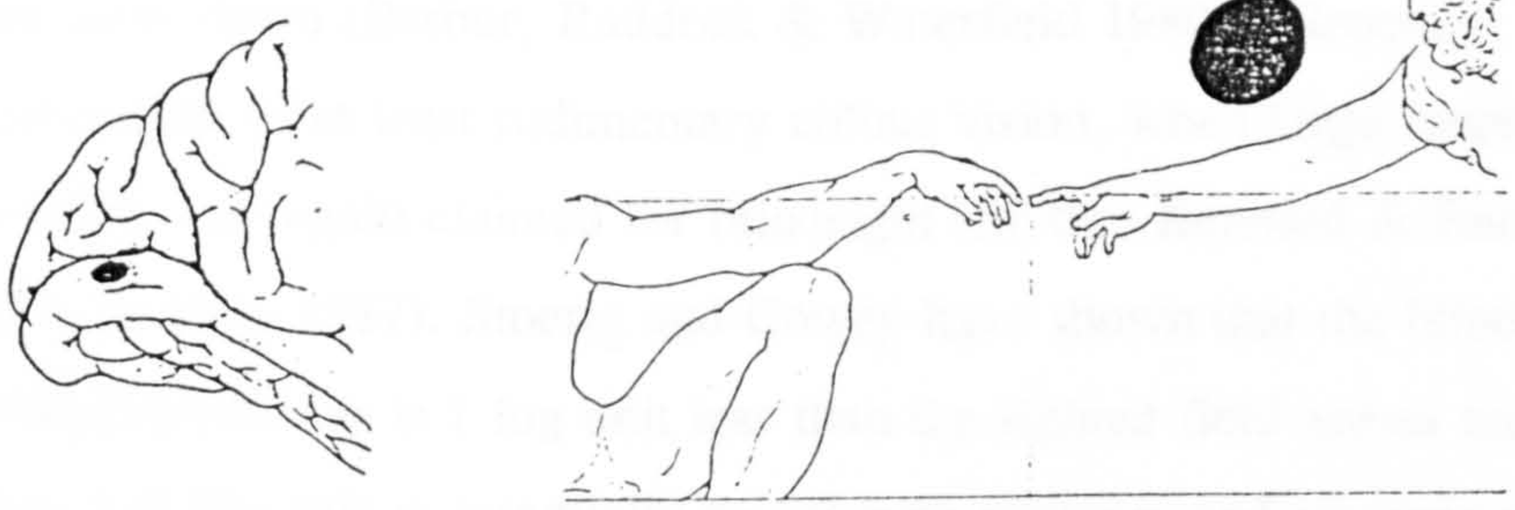

(c) QUADRANTANOPIA

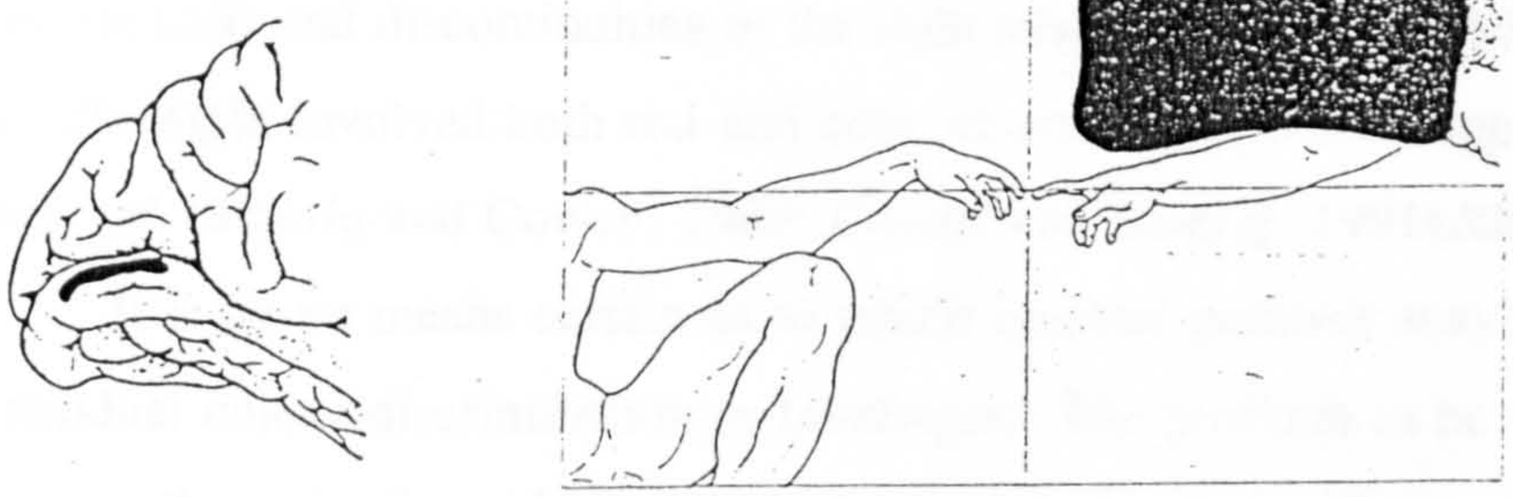

Figure 1.1.15 *The consequences of lesions in the striate cortex (area V1). (a) A total lesion affecting the whole of left hemisphere V1; the result is a hemianopia affecting the right field of view. (b) A small lesion in the lower lip of the area V1; the result is a scotoma in the upper quadrant of the right field of view. (c) A larger lesion affecting the lower lip of the left area V1; the result is quadrantanopia restricted to the contralateral upper quadrant of the field of view. (reproduced from Zeki, 1994).*

et al. 1980, 1988, 1993). The existence of blindsight implies that the pathways from subcortical areas to Area 18 and other parts of the prestriate cortex are capable of carrying considerable amounts of information. Recent studies suggest that the information carried may include colour.

Bender & Krieger (1951) were perhaps the first to report that wavelength discrimination was possible in the blind fields of patients with lesions to the geniculate striate cortex pathways. Subsequent studies (Perenin, Ruel & Hecaen 1980; Barbur, Ruddock & Waterfield 1980; Weiskrantz 1987) reported lack of chromatic discrimination. The residual vision of blindsight patients under most conditions shows the spectral characteristics of rod, rather than cone vision (Barbur, Ruddock & Waterfield 1980). Recently, the preservation of at least rudimentary colour vision, when large targets are involved, was again claimed for blindsight (Blythe, Kennard & Ruddock, 1987; Stoerig, 1987). Stoerig and Cowey have shown that the blind field spectral sensitivity is 1 log unit less than the sighted field across the visible range and that this is essentially so for both photopic and scotopic conditions with stimuli located in the near periphery. They found the presence of the Purkinje shift and discontinuities in the light adaptation curve which indicated that blindsight involved both rod and cone vision. Some colour opponency was preserved (Stoerig and Cowey, 1989; Cowey and Stoerig, 1991a&b).

It is by no means certain as to which residual pathway may be involved in residual colour discrimination in blindsight. The problem to be resolved concerns the route from the retina to the pre-striate cortex after loss of Area 17. Intact retinal ganglion cells would still allow processing of chromatic information. Indeed, it is known that some of these cells survive after the removal of the striate cortex of monkeys (Cowey, Stoerig & Perry, 1989). However, the route cannot use the mid-brain (collicular) pathway that allows achromatic blindsight, because this is not colour coded (Wolin, Massopust & Meder 1966; Perry, Oehler & Cowey, 1984). If there is residual processing, it must occur in the retinothalamic pathway, but it is not yet clear how. Some less well known pathways must be involved. It was shown previously that the

main pathway for colour information begins at the retina (Kaplan & Shapley, 1986) and can be argued to remain separate in the geniculostriate pathway to V4. This pathway will be unavailable. As well as the parvocellular layers of the lateral geniculate nucleus, colour specific ganglion cells also project to the lateral pulvinar nucleus where a small proportion of colour opponent cells have been found (Falsten, Benevento & Birman, 1983). Thus, from the monkey research, it would have to be the pulvinar extrastriate pathway, or perhaps the sparse, but direct projection from the lateral geniculate nucleus to Area 18 (Yukie & Iwai 1981) that is responsible for colour blind sight.

Achromatopsia is obviously of great interest to any study of cortical function and colour vision. The history of the clinical evidence has been reported in an epic review paper by Zeki (1990). Central achromatopsia may be described as the inability to perceive colours due to cortical damage. It should be distinguished from monochromacy (described in section 1.2.3) and a number of medical conditions which by injuring the optic nerve or retina can preferentially impair colour vision (Mullen and Plant, 1986). Neither Holmes (1918) nor Teuber, Battersby and Bender (1960), in their large scale studies of patients with missile wounds to the brain, observed any cases of achromatopsia. It seems that this is due to the location of the brain area of interest is such that a traumatic injury reaching it would be likely to cause death. The most common manner of acquiring achromatopsia is from stroke damage. The extent of this damage must be fairly specific to avoid impairing other visual function, consequently the reported cases are rare and there is considerable variation in accompanying symptoms. Strictly speaking, the true achromatopsic should see the world in shades of grey and those patients who report surface colours as "washed out" be termed incomplete achromatopsics, but these terms are not used consistently throughout the literature.

The anatomical evidence for the site of a lesion causing achromatopsia (Damasio and Damasio, 1980; Verrey, 1888 cited in Damasio and Damasio, 1986 and Zeki, 1990) points to the infracalcarine region of the lingual and fusiform gyri as the crucial area (in particular Brodmann's area 37). Damage

may often extend to the inferior lip of the calcarine cortex or part of the inferior contingent of the optic radiation. This results in visual field loss in the upper quadrants, which is a very common accompanying symptom, as is prosopagnosia (Meadows, 1974). The case of Damasio et al. (1980) was particularly interesting in that the subject showed achromatopsia (and the associated upper quadrant scotoma) for only one hemifield. All other visual functions were reported to be normal, including unfamiliar face recognition (although Heywood et al. (1987), point out that normal grey level discrimination was not investigated).

Meadows (1974) and Damasio et al. (1980) suggest that achromatopsia provides evidence for a human homologue of macaque V4, a colour centre. It should be noted that V4 is on the lateral surface of the hemisphere, whereas the critical damage in humans is ventromedial (area 37 rather than 18). According to Heywood et al. (1987) this conclusion would require loss of human V4 to bring about impaired colour constancy, while preserving wavelength discrimination.

1.2 Psychophysical Studies of Colour Vision

1.2.1 Introduction

A system based on a single spectral response mechanism cannot distinguish between two wavelengths, because if the product of sensitivity, S_λ, and light flux, E_λ, at one wavelength equals that at another, both stimuli will produce the same effect on the mechanism. It was Thomas Young (1802) who first realised that the eye could not contain a multiplicity of receptors and pathways, each sensitive to one particular colour.

> *"As it is almost impossible to conceive each sensitive point of the retina to contain an infinite number of particles, each capable of vibrating in perfect unison with every possible undulation, it becomes necessary to suppose the number limited; for instance to the three principal colours, red, yellow, and blue, and that each of the particles is capable of being put in motion more or less forcibly by undulations differing less or more from perfect unison. Each sensitive filament of the nerve may consist of three portions, one for each principal colour."*
> Young (1802)

He proposed that since three primaries could be used to match any colour, the eye could be arranged on the basis of three types of colour mechanisms, sensitive to three different parts of the spectrum. If these are chosen as red, green and blue light, any colour would excite each of these three types to varying degrees, and elicit the perception of that colour. This idea was initially rejected by von Helmholtz (1866), due to the discovery of colours which could not be satisfactorily matched with only three primaries, but he later realised that it was possible if the spectral sensitivities of the mechanisms were sufficiently broad-band, i.e. overlapping, and this became

the **Young-Helmholtz theory of Trichromacy**. The experimental measurements of Maxwell towards the end of the last century established that human colour vision is trivariant, i.e. it involves three independent mechanisms, and these are now identified as the three classes of cone photoreceptors (Wright, 1926-27). Variations in this trivariance principle exist: for very small central fields (i.e. less than 15 minutes in diameter), colour vision is divariant, relying on only the red and green sensitive mechanisms because blue sensitive cones are absent from the central fovea. For non-foveal vision, the contribution of the rods causes colours to appear desaturated at low light levels.

Hering (1870) noted the existence of four different colour sensations, red, yellow, green and blue, together with white, and observed that while colours such as bluish-green or reddish-yellow exist, there is no reddish-green or yellowish-blue. He proposed in his **Opponent Colour Theory** that these psychological primaries acted in two pairs, red and green, and blue and yellow, with the constituent colours in each pair opposing one another. He also suggested the existence of a third, black-white mechanism. The observations of Hering are now attributed to the colour opponent neural channels beginning with the retinal ganglion cells described earlier (section 1.1.1.4), and this colour-difference encoding of colour information has been shown to be an extremely efficient solution (Buchsbaum and Gottschalk, 1983).

1.2.2 Colour Discrimination and Matching

Trichromatic colorimeters allow a test field of any spectral characteristic and a matching field consisting of 3 primaries to be presented to an observer. It is usually most informative if both the test and each of the 3 primaries are near monochromatic. In the definitive study, Wright (1927, 1928 & 1946) detailed the design of a trichromatic colorimeter, and many

results derived from it. He was able to derive normalised colour matching functions (figure 1.2.1) by measuring the ratios of 3 primary stimuli required to match test pseudo-monochromatic wavelengths.

These colour matching functions must be linear combinations of the absorption spectra of the human photopigments, once prereceptoral absorption has been accounted for. It is not, however, possible to derive the individual spectral responses of the cone mechanisms using colour matching data from a normal human trichromat.

By measuring the ratios of spectral stimuli of wavelength 650, 530 and 460nm required to match test wavelengths, Wright (1928) determined the chromaticity coordinates of monochromatic (spectral) stimuli. Averaged with the data of Guild (1931), these were accepted by the Commission Internationale de l'Eclairage (CIE) in 1931 as defining the colour matching characteristics of the standard observer for a 2 degree field. Wyszecki & Stiles (1982) give a detailed discussion of the principle of trichromatic colorimetry.

If a coloured field is varied in hue, saturation or luminosity until a just noticeable difference (or jnd) in perception occurs, the corresponding change in the psychophysical variable is termed the difference threshold. The first measurement of this kind involved wavelength differences, which were determined by presentation of a bipartite visual field, with both halves matched for brightness and initially at the same reference wavelength, λ_0. The wavelength of one half-field is then changed, whilst maintaining brightness equality, until at wavelength $\lambda_0+\Delta\lambda$, a difference in colour is perceived; $\Delta\lambda$ constitutes the just noticeable wavelength step. Determination of $\Delta\lambda$ for a range of values of λ_0 gives rise to the characteristic discrimination response (figure 1.2.2), with three minima at around 590, 490 and 440nm. Wright (1941) measured approximate values for jnds not just along the spectrum locus, but also just noticeable differences in colours across the CIE diagram (figure 1.2.3).

(b)

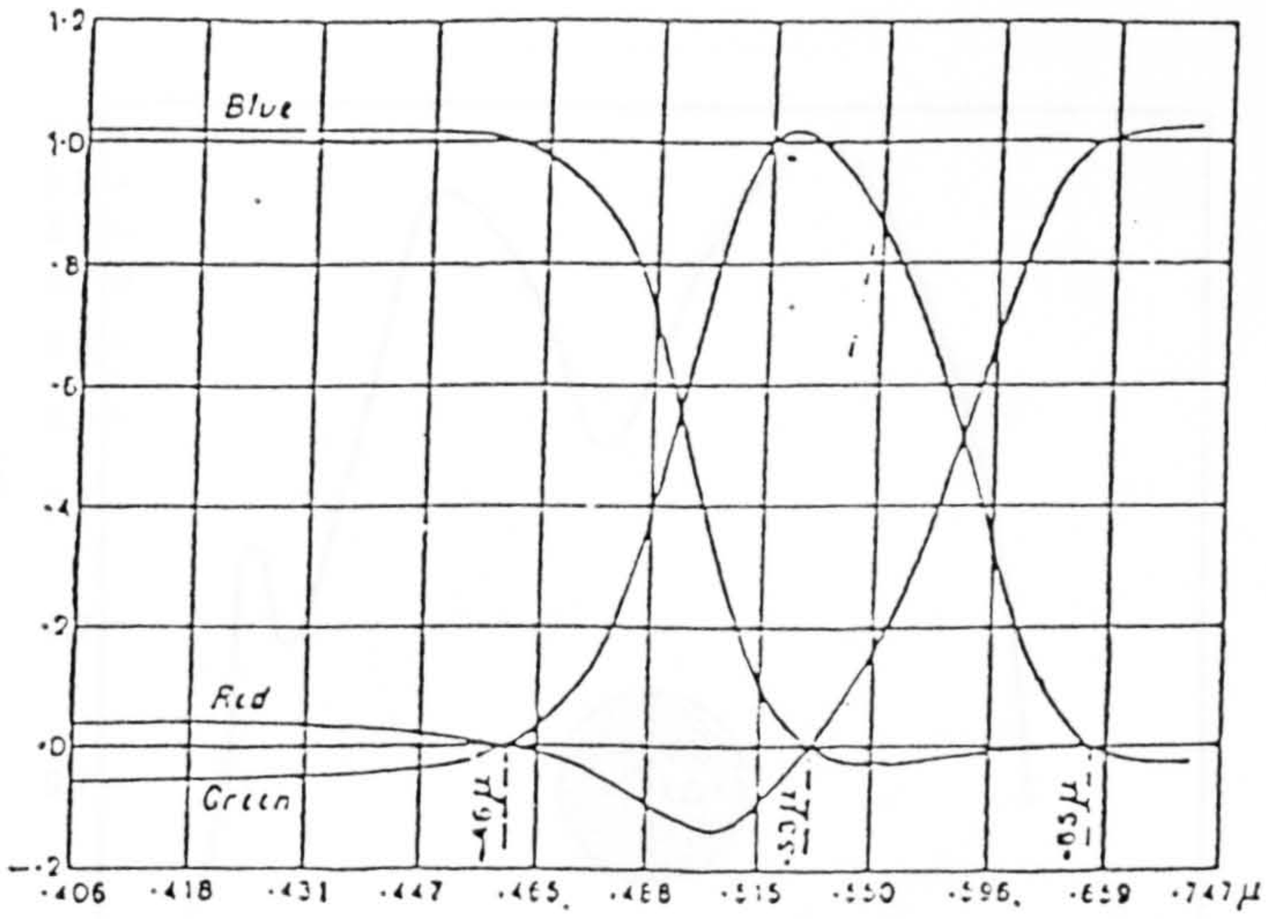

Figure 1.2.1 *Spectral colour matching functions for an average of 10 normal trichromats (Wright, 1946).*

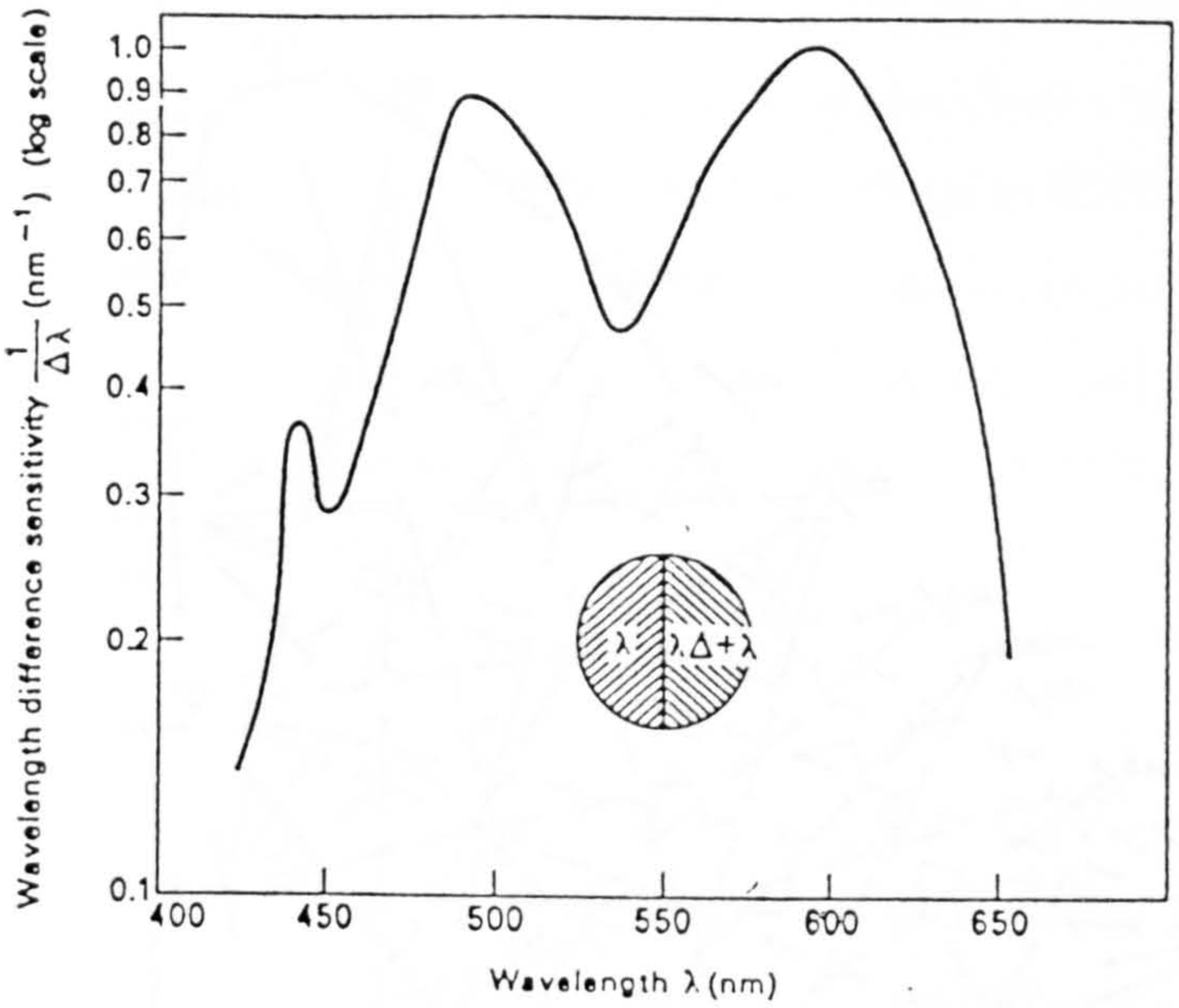

Figure 1.2.2 *Wavelength difference sensitivity function measured at threshold with monochromatic fields (after Padgham and Saunders, 1975).*

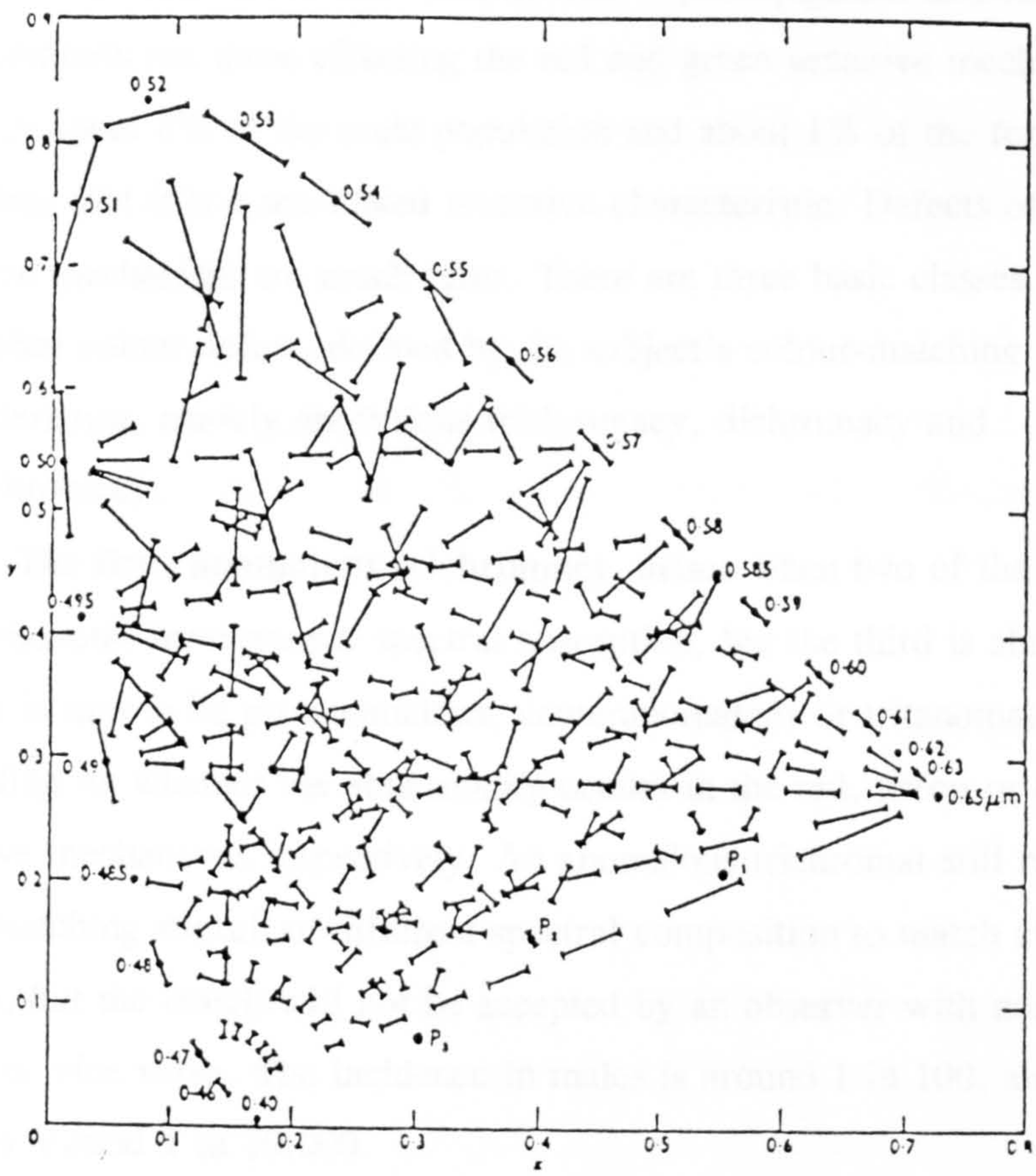

Figure 1.2.3 *Subjectively equal colour steps plotted on the CIE 2° chromaticity chart. The lines represent a colour difference about three times the size of the just noticeable difference for a 2° field (Wright, 1941).*

1.2.4 Congenital Colour Deficiencies

Congenital colour defects arise due to photopigment abnormalities. The most common are those affecting the red and green sensitive mechanisms, found in about 8% of the male population and about 1% of the female, indicating that it is a sex-linked recessive characteristic. Defects of the blue sensitive mechanism are much rarer. There are three basic classes of congenital colour defect, defined by the subject's colour-matching characteristics, namely anomalous trichromacy, dichromacy and monochromacy.

The first, **anomalous trichromacy**, arises when two of the photopigments have normal spectral absorption, but the third is abnormal. A subject is said to be protanomalous, deuteranomalous or tritanomalous, depending on whether the abnormality occurs in the red, green or blue sensitive mechanisms respectively. An anomalous trichromat still requires three matching stimuli of different spectral composition to match all test stimuli, but the match will not be accepted by an observer with normal colour vision or vice versa. The incidence in males is around 1 in 100, and for females around 1 in 10,000.

Dichromacy refers to the condition where one of the receptoral mechanisms is either absent or dysfunctional, enabling the dichromat to match all test colours with only two matching stimuli. The three types of dichromacy are protanopia, deuteranopia and tritanopia, which occur when the red, green or blue sensitive mechanisms respectively are absent. True protanopia and deuteranopia each affect approximately 1 in 100 males and 1 in 10,000 females, but tritanopia is more rare, affecting about 1 in 100,000. Some studies have suggested that when using large field colour-matching, some dichromats exhibit anomalous trichromacy (Ruddock, 1971; Smith and Pokorny, 1977; Jaeger and Kroker, 1952) and the existence of a third weak cone system has been identified as a possible cause (Nagy, 1980).

Complete lack of colour vision, **monochromacy**, occurs in patients who have only one functional cone system (cone monochromacy) or no

functional cone mechanisms leaving only the rod vision (rod monochromacy). Rod monochromats (with an incidence of about 1 in 10,000 people) are photophobic, have poor visual acuity and may also suffer from poor fixation and nystagmus. The rarer condition of cone monochromacy (affecting around 1 in 100,000 of the population), is not associated with reduced visual acuity or photophobia under photopic conditions.

The most accurate method for the diagnosis of colour vision defects is colour matching. To identify red-green defects, a Rayleigh or yellow colour match is used, but the identification of tritanopia is more difficult due to the great variability in matches for blue-green stimuli caused by light losses associated with lens aging and the macular pigment.

1.2.4 Variability in Normal Colour Matches

Prereceptoral Absorption

Before reaching the cone photoreceptors, the incident light is modified by selective absorption at a prereceptoral level. This is due to a number of causes. Ignoring the smaller effects of selective reflection from the surface of the cornea and absorption by the intraocular media, the two main sources of spectral modification are the lens, which, as has already been stated, absorbs strongly in the near ultraviolet, and the macular pigment, concentrated around the fovea and extending up to 8 degrees from it.

The lens sets the short-wavelength limit of visual sensitivity at around 380nm; aphakic subjects (i.e. those who have had the lens removed) have a sensitivity which extends down to around 310nm.

The optical density of the lens increases with observer age (Said and Weale, 1959), thus normal controls for colour vision studies should be age-matched to the group under study.

The effect of absorption by the macular pigment is the source of much debate concerning its absorption spectrum, inter subject variability in optical density and the average density in the population. The effect of the macular

pigment is, however, quite noticeable, and can be illustrated *in vivo* by presenting a subject with a large uniform blue field. The selective absorption of the yellowish macular pigment is then apparent to around 80% of subjects as a dark area around the fixation point or fovea (Viénot, 1983). Ruddock (1963) used a small field colour matching technique for two positions, on and off axis, and was able to isolate the effect of the macular absorption and produce an absorption spectrum for it. This showed a peak absorption at 560nm, but argument continues about the extent to which the tail extends into the middle wavelength region. Wyszecki and Stiles (1982) use a wavelength of around 540nm, while Pease et al. (1987) suggest a value which is nearer Ruddock's at around 560 to 590nm.

A survey of previous studies by Pease et al. (1987) resulted in an average pigment optical density of between 0.45 and 0.65 log units for most studies, with a range in most of over 1 log unit, though some methods give consistently different results, such as fundus reflectometry which produced an average of around 0.12 log units (Kilbride et al., 1989).

Calculations on the data of Ruddock (1963), Stabell and Stabell (1980) and Viénot (1983) by Moreland and Bhatt (1984) agree with their own findings and those of Kilbride et al. (1989) that the decadic angle (i.e. the angular distance from the fovea at which the density of pigment had fallen by an order of magnitude) varies from 1.8 to 5.0 degrees.

Though the macular pigment still fuels debate and disagreement, it is clear that its contribution cannot be ignored in studies of foveal colour vision (Morland and Ruddock, 1993), nor can it be simply corrected for by taking an average for the population as a whole.

Photopigment Variations

Alpern & Pugh (1977) applied a colour matching technique for dichromatic subjects to deuteranopes and derived successfully spectral responses which, after correction for preretinal absorption are the absorption spectra of the long wavelength and short wavelength sensitive photopigments. The authors

suggested that significant variation in the response of the long wavelength sensitive pigment existed for the group of 8 subjects. In addition, only one of the 8 deuteranopes accepted a normal trichromatic colour match. In further work on dichromats, Alpern (1979) found a lack of uniformity in colour matching of normal subjects under different light intensities, which led him to suggest a variation in the absorption spectrum of the long wavelength absorbing pigment amongst his normal subjects which could not be explained by density differences of cone photopigments.

Nietz & Jacobs (1986) obtained Rayleigh matches for 100 male and 100 female normal trichromatic observers using a large annular field. For the male subjects, the ratios of primary stimuli show a clear bimodal distribution. However, for the female subjects the distribution was found to be trimodal (figure 1.2.4). The author's reason that the long wavelength sensitive photopigment was expressed in 2 different forms which had wavelengths of peak absorption differing by 3 nanometres. The gene for the long wavelength sensitive photopigment is located on the X-chromosome, and therefore the male subjects could be expected to have either one or other of the photopigments alone, whereas the females could have either one alone or both, thus explaining the bimodal and trimodal distribution discrepancy. A theoretical analysis of variations in normal colour matching data was also made by Smith et al. (1976) who concluded that the variations could not be reconciled with the model of 3 photopigments (expressed identically in each observer and varying absorption of the prereceptoral filtering characteristics of the eye).

Direct measurements on the extracted pigments of the human retina have determined the absorption spectrum of the rod photopigment rhodopsin (Crescitelli & Dartnell, 1953). The form of the spectrum was supported by comparisons with the scotopic luminosity function and data from fundus reflectometry (Campbell & Rushton, 1955). Dartnell (1953) later suggested that all visual pigments would possess an absorption spectrum with the same shape as rhodopsin, but simply shifted on a reciprocal wavelength scale. This

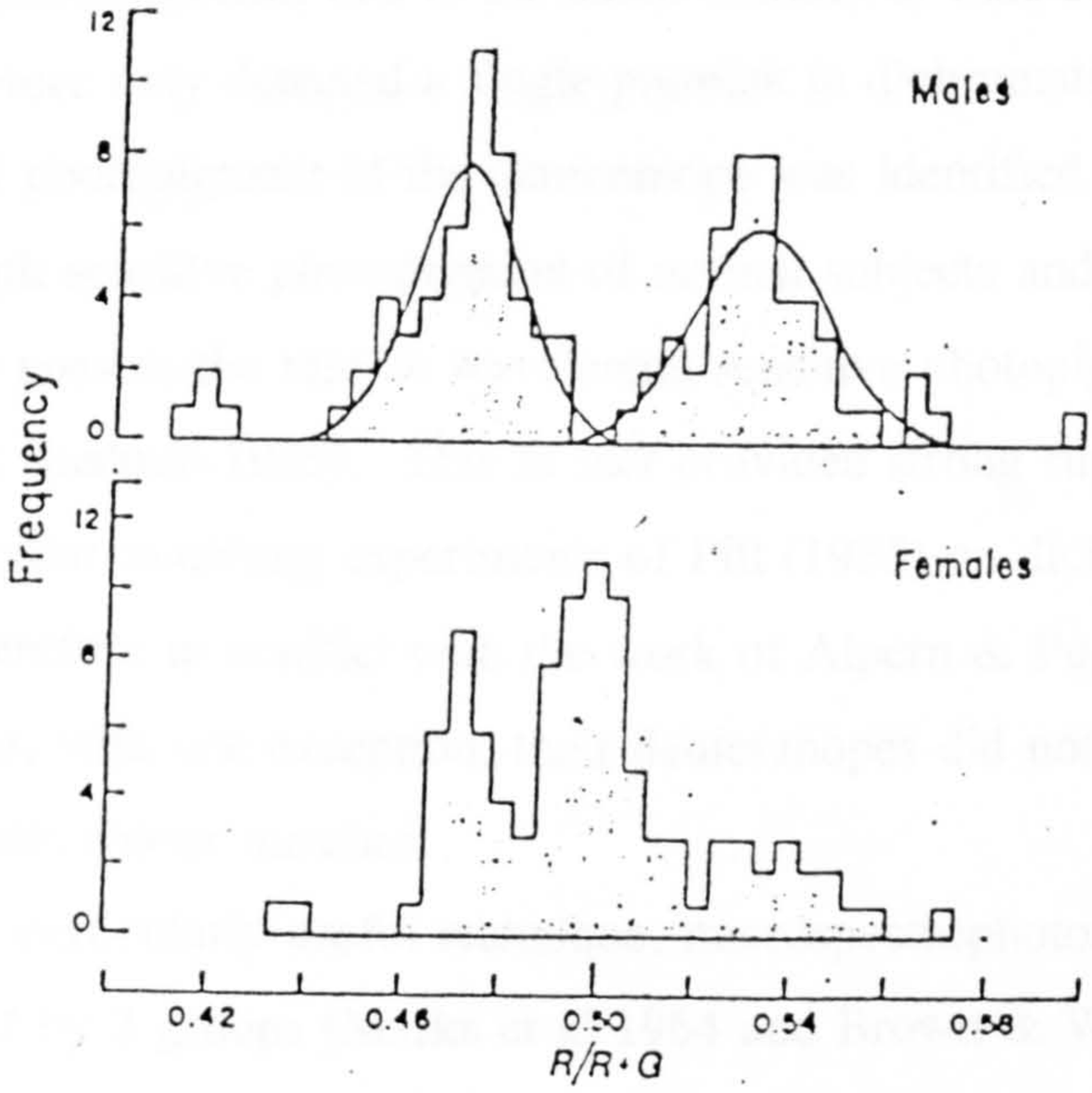

Figure 1.2.4 *The colour matching ratio R/R+G for a test stimulus of wavelength 590nm and matching wavelengths R=690nm and G=546nm. Frequency distributions are plotted for 100 males and 100 females as indicated (Neitz and Jacobs, 1986).*

position was not supported by analytical treatment of colour matching data in which 3 rhodopsin like absorption spectra were substituted for the cone spectral sensitivities (Brindley, 1960). By developing the method of fundus reflectometry and applying it to dichromatic subjects, Rushton (1963, 1965) showed that red/green dichromats only possess a single photopigment in the yellow region of the spectrum. The method is insensitive to the presence of the blue photopigment, due to the small number of blue cones in the retina and therefore only detected a single pigment in dichromats. Furthermore, the measured photopigment of the deuteranope was identified as the long wavelength sensitive photopigment of normal subjects and the protanope was shown to possess the middle wavelength sensitive photopigment of the normal (Baker & Rushton 1965). This in fact provided strong supporting evidence for the colour matching experiments of Pitt (1935) on dichromatic subjects, and is therefore in conflict with the work of Alpern & Pugh (1977), who found that, with one exception, their deuteranopes did not accept normal trichromatic colour matches.

A particularly useful technique, microspectrophotometry, was developed by 2 groups (Marks et al 1964 and Brown & Wald 1964). This method allowed the different spectrum of the photopigments to be measured while in the cone receptors in vitro. The initial results gave rise to the conclusion that the cone receptors only contained one of the 3 photopigments. Later, the method was applied by Dartnall et al. (1980), who considered the technique sensitive enough to detect variations in the photopigment absorption spectra of a single class of cones. The conclusion they reached was that the photopigments of long wavelength and middle wavelength sensitivity were expressed in two discrete sub-populations and an individual could possess both, in different quantities, which would explain variations in colour matching for normal subjects. The authors identified the wavelengths of maximum absorption (λ_{max} of the 2 green pigments as 533.7 +/- 2.1 nm and 527.8 +/- 1.8 nm for the 2 red pigments and as 563.2 +/- 3.1 nm and 554.2 +/- 2.3 nm, figure 1.2.5).

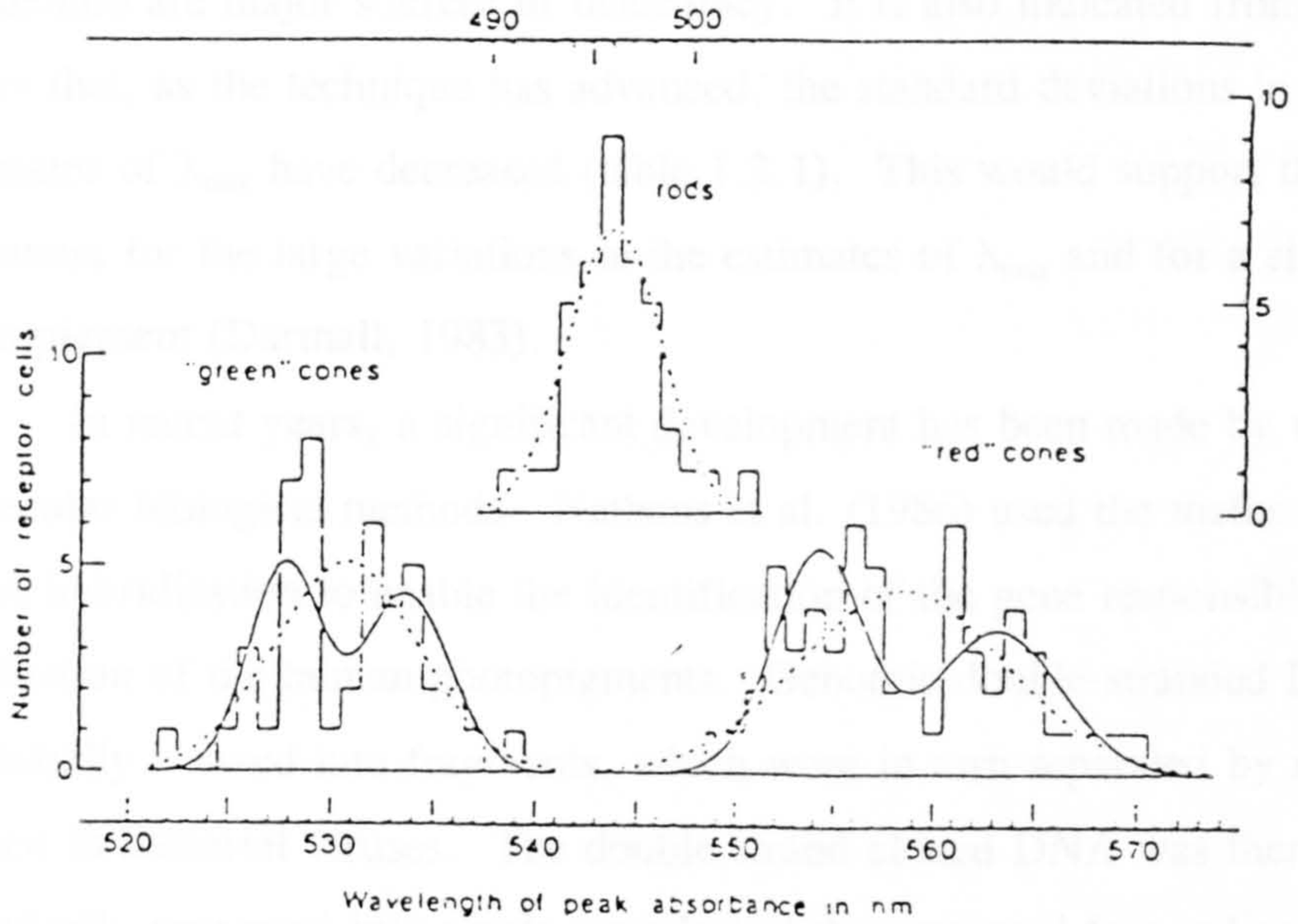

Figure 1.2.5 *Distributions of λ_{max} for the rods, middle wavelength and long wavelength sensitive cones. The dashed lines give the normal distributions expected from the relevant means and standard deviations. The double hump continuous curves drawn through the middle and long wavelength sensitive cone data give the expectations if the respective populations are regarded as containing two subpopulations (Dartnall et al., 1983).*

MacNichol et al. (1983) have pointed out that there are many problems associated with the technique. Partial bleaching of the pigment during measurement and therefore the necessity to use very low light intensities in the measuring beam, and contamination of measuring light path by pigment epithelium are major sources of inaccuracy. It is also indicated from their paper that, as the technique has advanced, the standard deviations in the estimates of λ_{max} have decreased (table 1.2.1). This would support the argument for the large variations in the estimates of λ_{max} and for a single photopigment (Dartnall, 1983).

In recent years, a significant development has been made by the use of molecular biological methods. Nathans et al. (1986) used the method of a DNA hybridisation to enable the identification of the gene responsible for the production of the human photopigments. Genomic double-stranded DNA was chemically cleaved into fragments, which were in turn separated by size and cloned in bacterial viruses. The double strand cloned DNA was then chemically separated into single strands and then exposed to a radioactive labelled probe (a single strand DNA from the bovine rhodopsin gene).

If the probe was similar to the sample of human DNA, as would be expected for the human photopigment genes, the probe hybridised with (bound to) the human DNA. To confirm whether hybridisation had occurred, the sample was washed in order to remove unbound probe and then exposed to photographic film. Dark spots appear on the film for the samples for which the hybridisation had occurred.

Nathans successfully identified 2 genes for human rhodopsin, which are bound very strongly to the bovine equivalent probe. In addition, 3 other gene sequences bound to the probe, but less strongly than for rhodopsin.

Analysis of the amino acid sequences of the encoded proteins showed the molecules were similar. 40% of each protein chain was identical with the sequence of rhodopsin. These 3 DNA sequences were assumed to be the genes for the 3 cone photopigments. Evidence confirming this hypothesis was provided by the finding of messenger RNA corresponding to the probe bound

Method	Species	Rod	Red cone	Green cone	Blue cone	Reference
Axial	human and		565	535		Brown and Wald (1963)
(patch)	rhesus		565	527		
Axial	human and		570	535	445	Marks, Dobelle and MacNichol (1964)
(single)	rhesus					
Axial	human and		577	540	450	MacNichol (1964)
(single)	rhesus					
Axial	human	505	555	525	450	Brown and Wald (1964)
(single)						
Axial	human		565	529	440	Wald and Brown (1965)
(single)						
Sonicated foveal suspension	rhesus		573	526		Murray (1968)
Axial and transverse	human and rhesus	498	575-580	535	440	Liebman (1972)
Transverse (single)	rhesus	502 ± 2.5	565 ± 2.5	536 ± 3 5		Bowmaker, Dartnall, Lythgoe and Mollon (1978)
Transverse (single)	cynomolgus	500 ± 1.6	567 ± 6.1	533 ± 3 9	415	Bowmaker, Dartnall and Mollon (1980)
Transverse (single)	human	498 ± 3.3	563 ± 4.7	534 ± 3 7	420 ± 4.7	Bowmaker and Dartnall (1980)
Transverse (single)	cynomolgus	502.5 ± 2	567.5 ± 2	531.8 ± 2 (543 ± 4)[a]	429 ± 3.5	Present study
Transverse (single)	rhesus	503.4 ± 2	564.4 ± 3			Present study

a Anomalous green cones.

Table 1.2.1 *A summary of the determinations of* λ_{max} *using the method of microspectrophotometry for primate rods and cones (MacNichol et al., 1983).*

DNA in the eye (messenger RNA being a single-stranded molecule involved in the production of the protein encoded by the gene). An additional finding consistent with the cone photopigment genes was that 2 of the 3 pigments were found to be on the X-chromosome which had already been put forward as the site for the red and green photopigment encoding genes, due to the sex linked nature of red/green colour deficiencies. Similarly, the third gene was found to come from chromosome 7, again consistent with findings that colour vision deficiencies associated with the blue sensitive photopigment are not sex linked.

Further work on the red and green photopigment genes showed that the genes were immediately adjacent on the X-chromosome and were 98% homologous (figure 1.2.6). Also, when the authors studied visual pigment genes from 17 male human subjects with normal colour vision, they found that although the gene for the red photopigment was expressed once, the gene for the green photopigment was expressed in either 1, 2 or 3 copies. This was explained by the tendency of similar adjacent genes to undergo changes in copy number during meiosis, the process of cell division that gives rise to sperm and eggs. The modifications made under this process, known as unequal homologous recombination was used as an explanation of red/green colour defects (see previous section). The authors concluded that hybrid genes could be created, which in the most extreme case, could have genetic code which would select, for example, the green cones for the site of production of the red photopigment. In less severe cases, the pigment produced would have a degree of greenness. The extent of the colour defect therefore depends on the position of the gene where the code changes from one pigment to the other. The results they found were that for deuteranopes the green pigment gene was either absent or hybridised in the most severe case outlined above. For protanopes, hybrid red pigment genes were found. For deuteranomaly and protanomaly, hybrid green genes and red of less severe form were found respectively in addition to some or all of the normal genes. In work on variations in colour matching in the normal population,

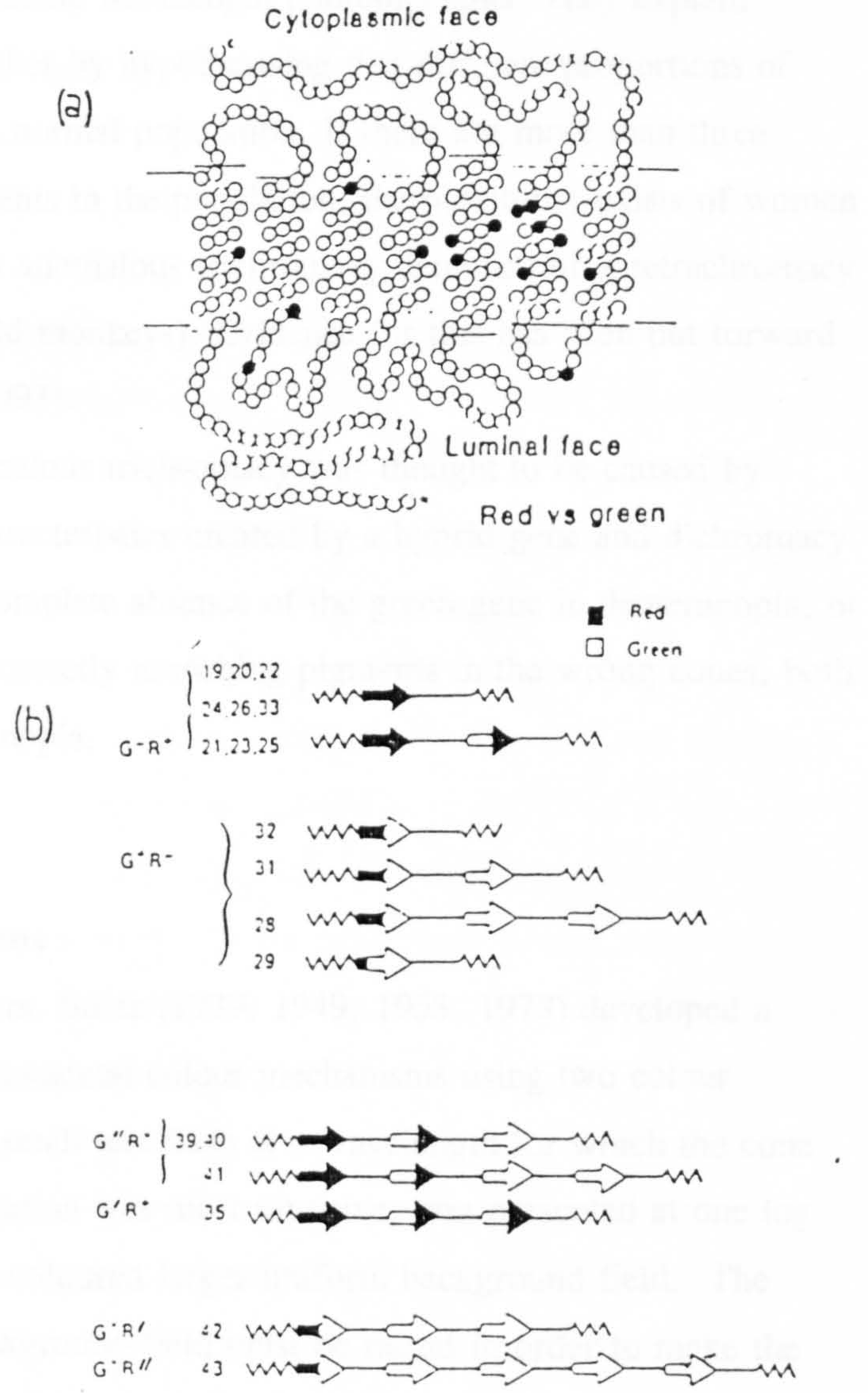

Figure 1.2.6 *(a) A comparison of the long and middle wavelength sensitive photopigments. The filled circles represent amino acid substitutions between these two molecules; open circles represent identical amino acids (Nathans et al., 1986). (b) Genotypes of colour deficient males: G+R-, protanopes: G-R+, deuteranopes; G'R+, simple deuteranomalous; G''R+, extreme deuteranomalous; G+R', simple protanomalous; G+R'', extreme protanomalous. Each arrow represents one cone-opsin gene. Filled portions of the arrow represent nucleotide sequence derived from the long wavelength sensitive gene and unfilled portions represent sequences from the middle wavelength sensitive gene.*

Neitz, Neitz and Jacobs (1990, 1991, 1992) suggest that a serine or alanine substitution at position 180 causes a 5-7nm shift towards longer wavelengths in the λ_{max} of a long or middle wavelength photopigments. They explain variations in normal matches by hypothesising that different proportions of each pair exist within the normal population. If there are more than three different cone photopigments in the population, the possibility exists of women who are heterozygous for anomalous trichromacy demonstrating tetrachromacy (by analogy to New World monkeys). Evidence for this has been put forward by Jordan and Mollon (1993).

In summary, anomalous trichromacy was thought to be caused by anomalous absorption characteristics created by a hybrid gene and dichromacy was either a result of a complete absence of the green gene in deuteranopia, or hybrid genes producing correctly absorbing pigments in the wrong cones, both in deuteranopia and protanopia.

1.2.5 Stiles' π Mechanisms

In a series of papers, Stiles (1939, 1949, 1953, 1978) developed a technique to measure fundamental colour mechanisms using two colour increment thresholds. A small test flash at a wavelength for which the cone mechanism under investigation was most sensitive, was presented at one log unit above threshold on a coloured larger uniform background field. The radiance to which the background field must be raised in order to make the test flash just disappear, defines the reciprocal of the sensitivity of the cone mechanism at the wavelength of the background field. The spectral sensitivity of the colour mechanism can therefore be determined by using a number of background fields at different wavelengths.

Stiles proposed that the spectral sensitivity curves obtained from the detection threshold for a range of stimulus wavelengths on a uniform background is determined by the properties of several component mechanisms operating in the retinal area to which the test of stimulus applied.

Corresponding curves of the individual components may only be obtained if they are the only mechanisms contributing to the detection of the stimulus under the given experimental conditions. Symbols $\pi 0$, $\pi 1$, $\pi 2$ etc were then used to denote the component mechanisms inferred in applications of the 2 colour incremental technique when the field and test colours were varied independently. These functions, called $\pi 3$ for the blue, $\pi 4$ for the green and $\pi 5$ for the red sensitive mechanisms, are illustrated in figure 1.2.7. Although receptoral in origin, $\pi 3$, $\pi 4$ and $\pi 5$ have respective peaks at 440 nanometres, 560 nanometres and 580 nanometres, which are not consistent with estimates of cone photopigment absorption.

Stiles emphasises that other contributing factors could not be excluded from the responses he isolated. Other spectral functions have also been isolated under different conditions. The red sensitive and green sensitive mechanisms are modified under high background field energies and become narrower. Two other blue sensitive mechanisms have also been isolated. $\pi 1$ is very similar to $\pi 3$, but has a secondary lobe at longer wavelengths. Explanations of this difference vary, but the most likely reason is that either $\pi 4$ or $\pi 5$ contaminate the $\pi 3$ function. $\pi 2$ is not found in all subjects and can only be measured over a very small range of short wavelengths. The relationship between the 3 blue sensitive mechanisms is still not completely understood. An explanation involving each mechanism taking signals from different stages of processing has been proposed by Pugh & Mollon (1979). Colour matching functions have been fitted with linear combinations of π mechanisms (Estevez & Cavonius, 1977) with a reasonable degree of success, but discrepancies are significant in some regions of the spectrum.

1.2.6 After Images

After-images are the phenomena of persistence of vision from a stimulus which has changed in retinal position or nature. If the eye is dark adapted and the stimulus is a bright flashed light, the result is an after-image which can last several minutes, particularly if the subject remains in the dark.

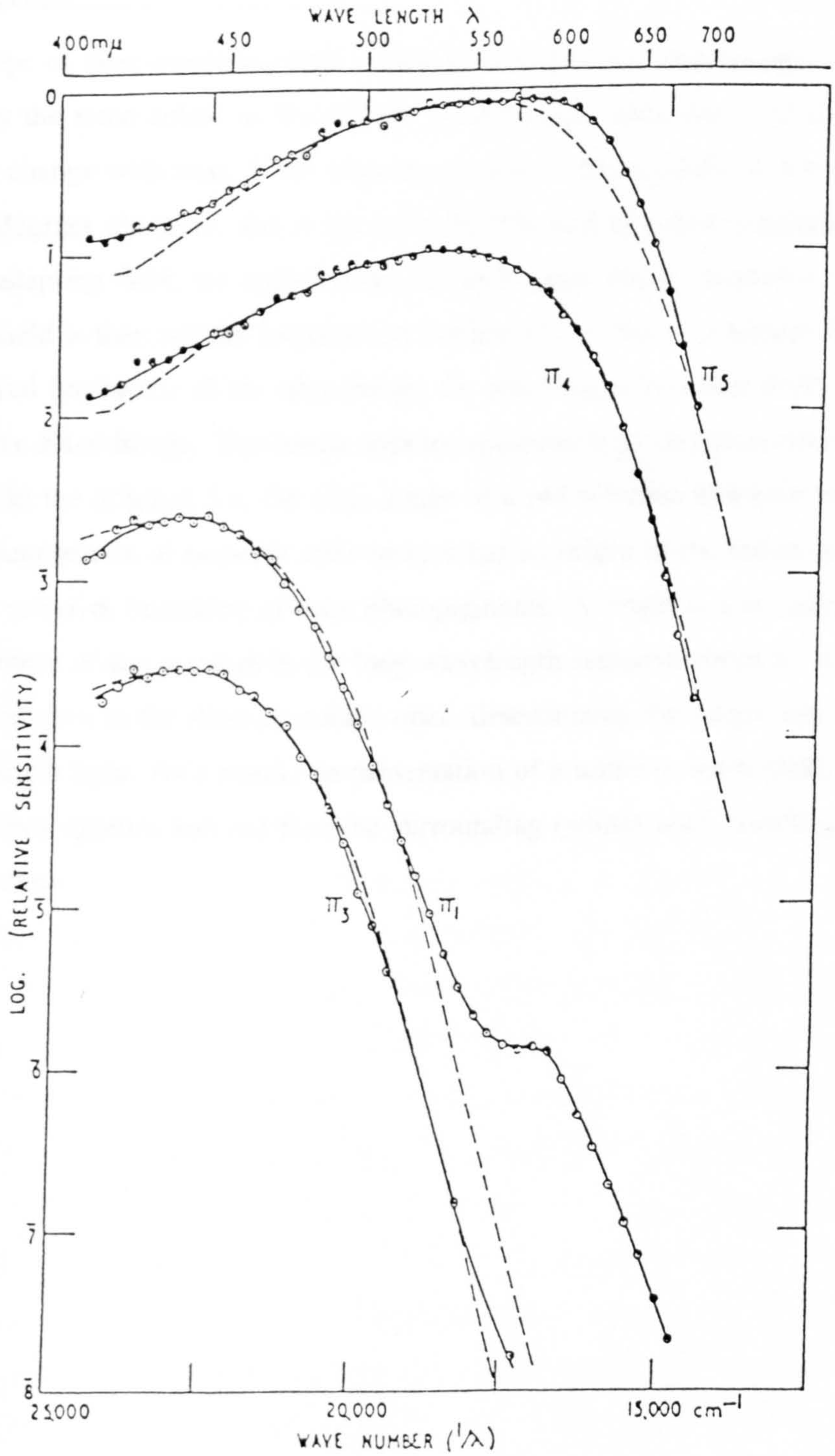

Figure 1.2.7 *The receptoral π mechanisms derived by Stiles plotted on a linear wavenumber (1/λ) scale. π_5 corresponds to the red sensitive mechanism, π_4 to the green sensitive and π_3 to the blue mechanism. π_1 is similar to the blue sensitive mechanism, but suffers from 'contamination' at long wavelengths (Stiles, 1978).*

This type of after-image is called a **long period positive after-image**, and is initially the same colour as the original stimulus, but undergoes a gradual colour change with time. If the stimulus is again a flashed light of the order of a few degrees diameter, and is immediately followed by a low luminance white adapting field, we again obtain a positive after-image. However, if the white field is then rapidly increased in luminance, so that it is greater than the perceived luminance of the after-image, the after-image becomes dark, the **negative after-image**. The image appears approximately complementary in colour to the original, i.e. the after image of a red stimulus is a cyan colour. The phenomenon of negative after-images has its origin in the retina, and is due to selective bleaching of cone photopigments. A bright red stimulus will cause more of the pigment in the long wavelength sensitive cones to be bleached than in the short or middle ones, desensitizing the target area to long wavelength light. As a result, on presentation of a uniform white field, the target area appears less red than the surrounding (white) area, resulting in a cyan colour.

1.3 Colour Constancy

1.3.1 Background

"The approximate constancy of the colour of objects in spite of large quantitative and qualitative changes in general illumination of the visual field is one of the most striking and important facts in the domain of physiological optics" (Hering, 1920 cited in Hurvich and Jameson, 1989). This phenomenon of colour constancy has been known at least since Helmholtz (1866), who described the visual system as able to "discount the illuminant". More recently, several authors have reviewed the subject of colour vision (Lennie, 1984; Daw, 1984; Maunsell and Newcombe, 1987; Boynton, 1988) and all have discussed the importance of colour constancy. Hurvich and Jameson (1989) in an essay devoted to colour constancy paid particular attention to the neural mechanisms involved (as did Daw, 1984).

Colour vision has two evolutionary benefits: it aids in the segmentation of an image and in the identification of objects within that image (Hurlbert, 1990). For object colour to be useful in object recognition, it must remain constant or vary in a predictable manner with different viewing conditions (different illumination). As might be expected, a wide variety of animals have been shown to operate a colour constancy mechanism, including monkeys (Zeki, 1983; Wild et al., 1984), goldfish (Ingle, 1985) and honey-bees (Werner et al., 1988).

Early attempts to explain this phenomenon relied on reweighting the photoreceptor sensitivities in inverse relationship to the level of stimulation they receive from the scene (Von Kries, 1905; Ives, 1912; cited in Worthey, 1985). Symbolically,

$$\alpha' = k_1\alpha, \qquad 1.3.1$$

$$\beta' = k_2\beta, \qquad 1.3.2$$

$$\gamma' = k_3\gamma, \qquad 1.3.3$$

Where α, β and γ are the photoreceptor sensitivities before a change in the adapting light and α', β' and γ' are the sensitivities after in the change. This type of approach has come to be known as the von Kries coefficient law or von Kries adaptation (Jameson and Hurvich, 1972). It should be emphasised that the general principle of the coefficient law does not constitute a theory of colour constancy; this would require detailed rules for the calculation of the coefficients k_1, k_2 and k_3 (Worthey, 1985). Helson and Judd (Helson, 1938; Judd, 1940) studied the ability of observers to achieve colour constancy and formally modeled it using a von Kries type coefficient law (this is discussed in more detail in the next section). They found that "there is general agreement between observation and theory, but in isolated cases the hue changes are very different in amount and sometimes in direction from those predicted." (Helson, Judd and Warren, 1952). These experiment were carried out using a paradigm in which the observer memorised a colour system and then reported colour appearance according to this system.

In the late 1950's Edwin Land made a series of demonstrations of his two colour projection experiments (Land, 1959 a&b). He used two black and white slides taken through coloured filters and then projected them through (not necessarily the same) coloured filters. He claimed that almost a full colour gamut was recreated using only these two primaries and even using narrow band filters gave a wide range of perceived colours. This led him to conclude that "two packages of information are sufficient for colour vision. The significance of the third is far from obvious" (Land, 1959c) and that "colour in images cannot be described by wavelength" (Land, 1959a). Judd (1960) reviewed the Land demonstrations and summarised the comments of several other authors (mainly critical); he was able to account for all of the colours perceived.

Land (1964; 1974) extended his ideas on the perception of colours in a complex scene with experiments using his "triple-image illuminating monochromator". A large number of coloured matt papers were arranged, overlapping arbitrarily, so that no paper was surrounded by a single colour.

This was to eliminate the effects of simultaneous contrast, a white background and specular reflections. These arrangements were illuminated by three projectors with a red, a green or a blue narrow band filter being placed over each lens. The amount of light from each projector was variable and the light reflected from each patch could be measured with telescopic photometer. Thus the illumination could be changed so that any patch reflected the same light as a white area under a reference illuminant. It was found that the appearance of the collection of coloured patches did not vary with the illuminant. Rapid presentations (0.1s) were used to eliminate the effects of photoreceptor adaptation, but later experiments found insignificant changes in colour during extended observation. Land (1964) postulated that his results could be explained if the colour perceived was not determined by the amounts of red, green and blue light entering the eye from the area in question, but by the lightness of the area in relation to all other areas in the field of view, separately for each of the red, green and blue channels. He further postulated an algorithm (Land and McCann, 1971) to carry out to evaluate these relationships and as it was not clear where in the visual system these evaluations might take place, the retina or the cortex, he coined the term retinex to account for both possibilities. This algorithm is discussed in more detail in section 1.3.2. In order to determine the site of the postulated retinex computations, Land et al. (1983) carried out experiments using an observer whose *Corpus Callosum* had been severed to cure intractable epileptic seizures. This operation prevents the two hemispheres of the brain from communicating with each other, the right visual hemifield is projected to the left brain hemisphere and vice versa. Each half operates independently. The experimental procedure involved the subject viewing a scene, half of which was covered with coloured patches (a Mondrian) and the other half covered velvet. In the middle of and just to the velvet side of the vertical line was placed a target area with a fixation point within it. The light flux from the target was kept constant while the illumination on the background was altered. For the normal observer, this procedure altered the colour of the target area

from purple to white. However, when the subject with the severed *Corpus Callosum* performed this experiment he gave reported different target colours when the Mondrian half of the background was in each of the visual hemifields. The speech centre is in the left brain hemisphere. When the "verbal" half of the brain was dealing with Mondrian plus target (Mondrian presented in right hemifield) the subject reported the target change from purple, as for a normal observer. When the Mondrian was presented in the left hemifield and the "verbal" half of the brain was dealing with black velvet plus target the subject reported that the target remained white. If the computation of colour constancy are carried out entirely within the retina the results of the computation for any part of the field of view would be independent of which part of the brain was used to read the results. This was emphatically not the case. The experiment establishes that the computations are long range and require the cortex.

Edwin Land thus sparked off considerable debate on the subject of colour constancy and in recent years there has been considerable work on the subject. He was the first to try to develop a computational model of how human colour constancy is achieved (Marr, 1982; Brainard and Wandell, 1986) and the first to examine its site in the visual system. He also popularised the use of visual scenes containing many coloured patches. These are usually called "Mondrians" because of there resemblance to the paintings of Piet Mondrian, although in fact they more closely resemble those of Van Doesburg as Mondrian separated his coloured areas with black lines.

Recent experiments have investigated colour constancy and attempted to quantify it. This is usually done using some sort of colour matching paradigm. McCann, McKee and Taylor (1976) used a set up where the right eye viewed a Mondrian display whilst the left viewed one Munsell chip at a time against a neutral surround. The scenes in the two eyes were illuminated separately and the subject had to chose a Munsell chip in the left eye's view to match each of the patches in the Mondrian display. They compared the results with the output of an implementation of the retinex algorithm and found good

agreement between experimental findings and theoretical predictions. It should be noted that dichoptic matching experiments of this type do not distinguish between the effects of long term photoreceptor adaptation and more instantaneous effects. Valberg and Lange-Malecki (1990) employed a similar approach, but allowed infinite variation of the left eye scene (rather than restricting it to the available Munsell papers) by adjusting the illumination on a neutral paper in the left eye view, maintaining constant illumination on its surround, to obtain a perfect match. They found that contrary to the predictions of the Retinex theory, the complexity of the Mondrian surround did not affect the results and that moving the test patch within the Mondrian produced different results. They suggest that local contrast effects are required to account for these results.

Tiplitz Blackwell and Buchsbaum (1988 a&b) simulated the appearance of Munsell chips under various illuminants on a computer monitor. They used a centre surround paradigm where a target patch was surrounded by a neutral frame (directly abutting or with a dark border between target and frame). The simulated illuminant on the target and frame was varied and the subject had to make a match by selecting from a series of matching patches arranged around the outside of the display. They found that simultaneous mechanisms contributed to colour constancy and that "an association between colour constancy and chromatic induction was shown". Many studies of this type, to investigate spatial and chromatic parameters, have been carried out under the rubrics of "chromatic induction" or "simultaneous contrast" (see Worthey, 1985; Walraven et al., 1987) rather than "colour constancy". These often employ the setting of a pure grey (Jameson and Hurvich, 1961; Kinney, 1962; Valberg, 1974) or a unique hue, usually yellow (Walraven, 1976; Shevell, 1978). In general the findings were that purer chromatic surrounds produced a larger effect, increasing the size of the surround decreased the effect and the effect decreased with the increase in size of a black border between the target and surround. This decay was found to be exponential by Tiplitz Blackwell and Buchsbaum (1988b) and Brenner et al. (1989). However, Uchikawa et al.

(1989) found that a tiny white surround (less then 0.4 degrees) placed around a test stimulus was sufficient to yield substantial effects on the categorical perception of colours.

Arend and Reeves (Arend and Reeves, 1986; Arend et al., 1991) distinguished between two types of matches, the "hue, saturation" match and the "paper" match. Subjects were presented with a simulated display of a Mondrian under each of two illuminants. The two Mondrians were separated, but simultaneously visible on the computer screen. One of the Mondrians was designated the reference and the other the test. The subject had control of one of the patches in the test Mondrian and was asked to match it to the patch in the same position in the reference Mondrian. Two sets of matching instructions were used. In the "hue, saturation" match, subjects were instructed to match the hue and saturation of the test patch to the reference patch and disregard, as much as possible, the other areas of the screen. In the "paper" match, subjects were told that the two displays were identical paper arrays, differently illuminated; They were instructed to make the test patch "look as if it were cut from the same piece of paper" as the corresponding patch of the other Mondrian. They found substantial differences between the two conditions for all observers and concluded that, in contrast to most of the above mentioned work, "mechanisms such as simultaneous contrast,... contribute little to colour constancy" and consider some higher level process to be involved. It should be noted that although the authors dismissed the hue shifts measured in the "hue, saturation" condition, they were significant and further there was a difference in the "paper" match between the results of the experienced and naive subjects. The effect of familiarity with the experimental paradigm on the results is not obvious, although Brenner and Cornelissen (1993) have suggested that it may in part be due to a difference in eye movements and a consequent difference in photoreceptor adaptation between the two subject groups.

Taking up this view of a higher level process, Foster (Foster, Craven and Sale, 1992; Craven and Foster, 1992) has proposed an alternative

property of colour constancy as "the ability of a subject to correctly attribute changes in the colour appearance of a scene either to changes in the spectral composition of the illuminant or to changes in the reflecting properties of that scene." He employed an experimental procedure which involved presenting the simulation of a Mondrian under one of a large number of illuminants followed by another Mondrian, which could either be produced by the same arrangement of reflecting patches, under a different illuminant or could only be produced by a different physical set of reflecting patches. He found that subjects were able to distinguish these cases reliably and rapidly. Troost and De Weert (1991) also argue that colour matching tasks are not appropriate for studying colour constancy as colour serves to identify objects. They compare results of matching and naming experiments and suggest that cognitive explanations are, at least in part responsible for the observed phenomena. A similar conclusion was reported by Hurlbert, from colour matching experiments involving a banana shaped object.

In summary, it seems likely that at least three distinct mechanisms contribute to the phenomenon of colour constancy. Photoreceptor adaptation of the Von Kries type, simultaneous contrast or lateral inhibitive effects and cognitive factors all contribute to colour constancy as we know it. Asymmetric colour matching experiments with the subject viewing a scene under different illumination with each eye (e.g. McCann, McKee and Taylor, 1976) will measure effects due to the first two of these. Experiments which separate two separately illuminated scenes and allow free eye movements between them (e.g. Arend and Reeves, 1986) do not control for adaptation. Experimenters should be careful as to which of these effects are under investigation in their particular choice of experimental paradigm (Brill and West, 1986).

1.3.2 Chromatic Adaptation and Lightness Algorithms

The Von Kries rule states that the eye has three receptor systems with different spectral sensitivity functions; the shapes of these spectral sensitivity are presumed invariant, with all adaptation accounted for by the adjustment of

three scalar coefficients (equations 1.3.1, 1.3.2, 1.3.3). The most popular version of this scalar adjustment is that the coefficients are altered to keep the adapted appearance of a reference white surface constant (Land and McCann, 1971; Ives, 1912 cited in Worthey, 1985). Land and McCann (1971) used the concept of integrated reflectance to compute the response of each receptor type to the light reflected from a given area of the visual scene. The response S_j of the j^{th} photoreceptor type is given by:

$$S_j = \int_{\lambda} \rho(\lambda)\ E(\lambda)\ k_j\ q_j(\lambda)\ d\lambda \qquad (1.3.4)$$

where $\rho(\lambda)$ is the spectral reflectance function of the area in question, $E(\lambda)$ is the illuminant spectral power distribution, $q_j(\lambda)$ is the (normalised) spectral sensitivity of the j^{th} photoreceptor type and k_j is a constant. The integration is over the range of wavelengths to which the photoreceptor is sensitive. To maintain the adapted appearance of the reference white, the constants k_j are set to $1 / S_{j0}$, where S_{j0} is the response of the j^{th} photoreceptor type to that reference white and

$$S_{j0} = \int_{\lambda} \rho(\lambda)\ E(\lambda)\ q_j(\lambda)\ d\lambda \qquad (1.3.5)$$

Several authors have explored the extent to which this von Kries type of chromatic adaptation could account for colour constancy (West and Brill, 1982; Worthey, 1985; Worthey and Brill, 1986; Brill and West, 1986). The overlap of the photoreceptor spectral sensitivities of human eyes and hence object metamerism was held to place a limit on the degree of colour constancy which could be achieved by von Kries adaptation (Worthey, 1985; Worthey and Brill, 1986). Projecting the data of Land and McCann (1971) into an opponent colours system (Guth et al., 1980), Worthey (1985) found that illuminant shifts along the tritanopic confusion line (blue-yellow shifts) were

discounted better than those along the deuteranopic confusion line (red-green shifts). Brill and West (1986) discounted chromatic adaptation as the mechanism of human colour constancy because of the long time required for adaptation compared with the apparently instantaneous effect constancy and the claim that colour constancy is most powerful in complex visual scenes. An obvious shortcoming of the integrated reflectance method is the requirement that the visual system knows which surface, if any, is white. It was addressing this spatial consideration which led to Land's Retinex algorithm (Land and McCann, 1971).

Edwin Land described a number of versions of the Retinex algorithm (Land and McCann, 1971; Land, 1983; Land, 1986) with slight variations between them. The essential features are described here. His work inspired a number of similar algorithms which are derived from the same principles (Horn, 1974; McCann and Houston, 1983; Blake, 1985). These are known as Lightness algorithms as they attempt to recover an approximation to surface reflectance in independent wavelength (or lightness) channels. Brainard and Wandell (1986) have published an analysis of the behaviour of the retinex algorithm. Hurlbert (1986) has demonstrated the formal connections between lightness algorithms in general.

Hurlbert's (1986) analysis expanded on the integrated reflectance model of equation 1.3.4 and approximated the nonlinear response of the signal from human photoreceptors by a logarithm. So that

$$S_j(\boldsymbol{r}) = \log \int_{\lambda} \rho(\lambda,\boldsymbol{r})\ E(\lambda,\boldsymbol{r})\ k_j\ q_j(\lambda)\ d\lambda \qquad (1.3.6)$$

Where **r** is the spatial coordinate in the sensor array (or the two dimensional projection of the surface coordinate). It should be noted that in this statement any effect of viewing geometry is ignored, that is $E(\lambda,\mathbf{r})$ is defined as the effective irradiance for the particular geometry under consideration. Lightness algorithms either include this assumption of the response of the sensors or

explicitly take logarithms. Hurlbert then states that lightness algorithms make three assumptions of the world in which they operate:

1. The scene is a two dimensional flat surface divided into patches of uniform reflectance (a Mondrian);

2. The illumination varies smoothly and slowly across the scene and is independent of viewing geometry;

3. The average surface reflectance of each scene in each lightness channel is the same (grey world assumption).

The problem may then be broken down into two sub problems, which Hurlbert (1986) terms "spatial decomposition" and "spectral normalisation". The logarithmic nature of the sensor signal means it may be expressed as the sum of two terms representing the surface reflectance and the effective irradiance. For the monochromatic case this may be written

$$S_j(\lambda,r) = \log k_j q_j(\lambda) \rho(\lambda,r) + \log E(\lambda,r) \qquad (1.3.7)$$

If the photoreceptor sensitivities overlap, as is the case with humans, this decomposition is not obvious for the integrated signal. However, by using appropriate linear combinations of the photoreceptor sensitivities this problem may be averted (Hurlbert, 1986). The two components are separated by differentiating the intensity signal $S_j(\mathbf{r})$ over space, thresholding the derivative $d[S_j(\mathbf{r})]$ to eliminate small values due to smooth changes in the effective irradiance, but retain large values due to changes in the surface reflectance at borders between patches and integrating the thresholded derivative $Td[S_j(\mathbf{r})]$ over space to recover the surface reflectance. The result of this calculation is (approximately) proportional to the surface reflectance.

$$L_j(r) = [k_j]^{-1}[TS(r)]_j \qquad (1.3.8)$$

where L_j is the lightness in the j^{th} channel and $[TS(\mathbf{r})]_j$ is the result of the integration of the thresholded intensity, before the constant of integration, k_j^{-1}

has been set. Spectral normalisation is now required to reset k_j, that is to reset the scale of ρ relative to S. This is commonly achieved using assumption three above.

Land's retinex algorithm assumes that the intensity signal is recorded by a discrete array of sensors indexed by a one dimensional variable, or pixel, x. A lightness value L_{jx} is determined at each pixel, x, for each channel, j. This is done by defining a series of *paths*. Starting at pixel x_1, a neighbouring pixel x_2 is selected randomly. The difference of the logarithms of the sensor responses at the two positions is added to an accumulator register for position x_2 such that

$$A(x_2) \leftarrow A(x_2) + \log S(x_2) - \log S(x_1) \qquad (1.3.9)$$

provided that the difference between the two sensor values is above a predetermined threshold. In addition a counter register $N(x_2)$ is incremented to indicate that a path has crossed this position. All counters and accumulators start at zero. A random neighbour of pixel x_2 is then selected and the calculation repeated. The number of positions traversed by a path is a parameter of the algorithm, as is the total number of paths required for a complete calculation. The lightness value at each pixel, x, is then computed by dividing the accumulated values in A(x) by the corresponding counter register N(x). The lightness triplet at each pixel should depend only on the surface reflectance, not on the effective irradiance.

Brainard and Wandell (1986) have performed an analysis of the statistical effects of the choice of path length on the output of the algorithm. They expressed lightness as

$$L_{jx} = \log[S_{jx} / G_j(x)] \qquad (1.3.10)$$

Where $G_j(x)$ is an average response over the path, the precise form of which depends on the choice of path length and step size. They found that near

neighbours of each pixel contributed more frequently to $G_j(x)$ until path length was much greater than 200 pixels; in which case $G_j(x)$ tended to the geometric mean from all pixels in the image and was independent of x. Further, they found that the dependence of the algorithm on the choice of surfaces in the image was too strong for all path lengths.

Hurlbert (1986) reviewed a number of lightness algorithms from the literature and showed that they were all formally connected. In essence they differ in the way that the differential operator performs the spatial decomposition. In Horn's algorithm, the rotationally symmetric Laplacian operator, ∇^2, is used. The lightness obtained by this method is then a solution of the Poisson equation inside the Mondrian:

$$\nabla^2 L_j(x,y) = T[\nabla^2 S_j(x,y)] \qquad (1.3.11)$$

where T represents the threshold operation that is performed on the output of the Laplacian. The solution of this equation requires that the boundary of the field of view has a constant surface reflectance. To obviate this problem, Blake proposed using the gradient operator ∇ in place of the Laplacian. Lightness must now satisfy the equation

$$\nabla L_j(x,y) = T[\nabla S_j(x,y)] \qquad (1.3.12)$$

and is solved for by the path integral

$$L_j(x,y) = \int_P T[\nabla S_j(x,y)]\,ds \qquad (1.3.13)$$

where P is a path connecting (x_0,y_0), at which the value of L is arbitrarily defined, and (x,y). If curl(T[∇S])=0 as for a Mondrian, then the value of the integral is dependent only on (x_0,y_0) and (x,y) and is independent of path

between them. This method represents a formalisation of Land's algorithm for a Mondrian. However, as Arend and Goldstein (1987) pointed out, gradient illusions require that models of appearance include a spatial integration which fills areas between edges and that for many scenes there are inconsistencies (non zero curl) in threshold derivatives which prevent simple spatial integration. They suggested that the human visual system does encounter curl problems and that it uses two types of perceptual solution: field segmentation and lightness gradient manipulation.

Hurlbert (1986) also expanded on Horn's algorithm, pointing out that the Laplacian of a Gaussian is approximately equal to the difference of two Gaussians of different scales. This multiple scales algorithm therefore filters the intensity signal S(x,y) through $-\nabla^2 G$ (the DoG operator), thresholds the result and sums it over a continuum of scales to recover L(x,y). The sum over multiple scales of DoGs yields the difference between the smallest and largest scale Gaussians. Hurlbert relates this physiologically to a "lightness" neuron with a narrow receptive field centre and a large surround. Hurlbert and Poggio (1988) synthesised an algorithm from examples and derived just such an operator.

1.3.3 Discounting the Illuminant

Several related models have been presented in the literature which attempt to achieve colour constancy by estimating the illuminant and discounting its effect (Sällström, 1973; Buchsbaum, 1980; Wandell and Maloney, 1984; Maloney and Wandell, 1986; D'Zmura and Lennie, 1986; Lennie and D'Zmura, 1988; Dannemiller, 1989; D'Zmura and Iverson, 1993a&b; Iverson and D'Zmura, 1994) or by using illuminant invariant properties to directly estimate reflectances (Brill, 1978; 1979). These all rely on modelling both the illuminant and reflectance spectral distributions by linear combinations of known basis functions so that the illuminant

and at each spatial location, x, the surface reflectance

$$E(\lambda) = \sum_{i=1}^{m} a_i E_i(\lambda) \qquad (1.3.13)$$

$$\rho_x(\lambda) = \sum_{j=1}^{n} b_{jx} \rho_i(\lambda) \qquad (1.3.14)$$

These basis functions are fixed and assumed known so that knowledge of the weights a_i and b_{jx} amounts to a complete description of $E(\lambda)$ and $\rho_x(\lambda)$, respectively. The response of the k^{th} ($k = 1...p$) photoreceptor S_k is then

$$S_{kx} = \int q_k(\lambda) \sum_{i=1}^{m} a_i E_i(\lambda) \sum_{j=1}^{n} b_{jx} \rho_i(\lambda)\, d\lambda \qquad (1.3.15)$$

(from equation 1.3.4)

This may be written

$$S_{kx} = \sum_{i=1}^{m} a_i \sum_{j=1}^{n} b_{jx} \int q_k(\lambda)\, E_i(\lambda)\, \rho_j(\lambda)\, d\lambda \qquad (1.3.16)$$

or in matrix notation

$$S_x = \Lambda_E\, b_x \qquad (1.3.17)$$

where S_x is a (column) vector formed from the responses of the p sensors at location x, b_x is a column vector which specifies the surface reflectance function at location x and the illuminant matrix Λ_E is p by n with kj^{th} entry of the form $\int E(\lambda)\rho_j(\lambda)q_k(\lambda)d\lambda$.

Equation 1.3.17 dictates various limits on the recovery of surface reflectance. If the ambient light is known then so is the lighting matrix Λ_E. To recover the n weights which determine surface reflectance it is necessary to

solve a set of simultaneous linear equations. The problem then becomes that of finding the inverse of the illuminant matrix Λ_E when p=n.

$$\boldsymbol{b}_x = \Lambda_E^{-1} \boldsymbol{S}_x \qquad (1.3.18)$$

If p < n then equation 1.3.17 is undetermined and there is no unique solution. If the ambient light is not known, it is not in general possible to recover the illuminant vector **b** or the spectral reflectances even when p=n (Maloney and Wandell, 1986), additional information is required. Sällström (1973) assumes a known white patch and Buchsbaum (1980) a known space averaged surface reflectance for which the terms of Λ_E are known *a priori* and hence the illuminant weights may be determined. Lee (1986) and Lennie and D'Zmura (1986) say that in principle it is possible to use specular highlights in an image to determine the illuminant chromaticity. Maloney and Wandell (1986) assume two degrees of freedom (n=2) in the surface reflectances. D'Zmura and Iverson (1993a&b) allow the visual system to receive information from two or three lights shone sequentially on the surfaces and further give an exhaustive treatment of the general criteria for these bilinear models to achieve colour constancy (see also Iverson and D'Zmura, 1994).

For the solution of the above models to be tractable the number of basis functions required to model both the reflectances and the illumination must be small. Judd et al. (1964) found that three or four principal components were sufficient to match daylight and point out that the daylight locus is for most practicable purposes equivalent to the Plankian locus, which may be characterised by the colour temperature alone. Dixon (1978) reported similar findings for Australian daylight. The situation for spectral reflectance functions is not quite so clear. Cohen (1964) used a characteristic vector decomposition of the spectral reflectances of 150 Munsell chips . He found that a linear model with as few as three basis reflectances captured 99.2% of the overall variance. Stiles et al. (1977) and Buchsbaum and Gottschalk (1984) report similar results for naturally occurring objects. Maloney (1986) showed

that approximately 99% of the variance in a set of 337 Munsell spectral reflectances, published by Krinov (1947; cited by Maloney, 1986) could be captured using three functions. However, more recently Parkkinen et al. (1989), in a more exhaustive study of all 1257 Munsell chips using a smaller sampling interval, reported that as many as eight characteristics are needed to achieve a good representation for all spectra. Dannemillar (1992) carried out ideal observer analysis on the 337 reflectances of Krinov and found, using daylight illumination that discrimination reached an asymptote when three or four basis functions were used. He makes a valid point that percentage error across the spectrum (Parkkinen et al., 1989) may not be the most appropriate measure for assessing the accuracy of a reconstructed spectrum, but only tests a limited data set.

Dannemillar (1989) discusses the ontogenetic implications of models of this type. There is a requirement of the visual system to know 27 constants of the matrix Λ_E (assuming three basis functions each are sufficient to describe illuminant and reflectance). This suggests a high level process which is plausible, and an innate programming for these constants which is less so. The system would also be highly susceptible to differences in the spectral response functions of the photoreceptors and to changes in the transmissibility of the ocular media.

1.3.4 Other Methods

The computational models of colour constancy discussed above in general assume a single process. Several authors however have argued for a two stage process (e.g. Werner and Walraven, 1982; Worthey, 1985; Shevell et al., 1992). Dannemiller (1989) extends his model to the adaptive requirements of a second stage in the visual system and discusses how this might be accommodated within the scheme of Buchsbaum and Gottschalk (1983) who formulated an opponent colours model on the basis of the most efficient transfer of information from the retina.

Other authors have stressed the importance of higher level, cognitive processes. It has clearly been demonstrated that there is a cognitive input to colour constancy (Hurlbert, 1993), but despite Arend and Reeves (1986) it cannot account for the entire phenomenon. Troost and De Weert (1991) discuss the difficulty of separating what they call sensory and cognitive colour constancy.

In contrast Foster and others (Craven and Foster, 1992; Foster, Craven and Sale, 1992) determine colour constancy to be very rapid and probably preattentive in origin. They suggest that chromatic relationships within a scene, rather than colour percepts are preserved and propose cone contrast as the mechanism by which this is achieved. Lucassen and Walraven (1992) also identify cone contrast as the important variable.

An approach which may prove fruitful is that of network simulation (Courtney et al., 1995). They used a neural network based on biological principles to investigate the contributions of different stages in the visual system. They found that a degree of colour constancy is produced by an adaptation of the simulated photoreceptors and that their "V4" cells were effective at producing colour constancy. Further, these two processes worked in cooperation so that when the conditions were unfavourable for one, the other was able to contribute more. This highlights one of the problems of psychophysical experiments in human colour constancy, that of isolating the mechanism under investigation.

The goal of colour constancy is often stated as the ability of the visual system to maintain an invariant colour percept despite changing conditions of illumination. It may not be possible, nor even desirable to achieve this invariance perfectly. It should also be borne in mind that colour serves to identify and discriminate objects and that it is possible to "discount the illuminant" and be aware of its quality simultaneously (Hurvich and Jameson, 1989).

Chapter 2. Experimental Methods and Equipment

Chapter 2. Experimental Methods and Equipment

2.1 The Use of Computer Controlled VDUs. in experiments on Colour Vision

2.1.1 Introduction

Modern developments of Visual Display Unit (VDU) technology make the use of computer controlled monitors an attractive proposition for psychophysical experiments. It is possible to specify precisely the spatial, temporal and chromatic properties of stimuli presented to an experimental subject. Accurate control of the stimulus is only possible if the relationship between the digital input values to the frame buffer that controls the monitor and the monitor output is known. That is, provided that the chromaticity coordinates of the monitor phosphors are known, along with the luminance output for each of the phosphors at each value of digital input to the electron guns, it is possible to reproduce (within certain limits) a desired set of tristimulus values.

Several authors have recently described methods of calibrating monitors for colour reproduction (Brainard, 1989; Cowan & Rowell, 1986; Lucassen & Walraven, 1990; Post & Calhoun, 1989). Post and Calhoun (1989) compared different models of generating monitor output with specific CIE chromaticity coordinates and luminances. They conclude that a piecewise linear interpolation method is most accurate and found that 16 calibration points per electron gun are sufficient to reconstruct the input output relationship. Lucassen and Walraven (1990) report a method of recalibrating quickly to deal with changes in the input output relationship. The model for generating specified colours (section 2.1.2) and the method of recalibration (section 2.2) used for the experiments in this thesis are described below. They

are more comprehensive than the methods investigated by the above authors, but do not cause inconvenience or loss of generality.

In order to make the problem of calibrating a monitor a tractable one, it is necessary to make certain assumptions of its performance (Brainard, 1989; Cowan & Rowell, 1986). The most important of these are spatial independence, phosphor independence and phosphor constancy. The assumption of spatial independence is that the monitor's output at a location depends only on the input to that location; the assumption of phosphor independence is that the intensity of stimulation of a phosphor is determined by the input value for that phosphor and is independent of the other two; the assumption of phosphor constancy is that the relative spectral power distribution of the phosphor output does not vary with the intensity of stimulation. These assumptions may be compromised if there is an interaction between the screen luminance and the beam current or if there is imperfect shadow masking of the individual phosphor electron guns (this may be caused by magnetic interference). These assumptions are necessary to reduce the problem of calibration to that of measuring the relative spectral power distribution and the digital to analogue input output relationship of each phosphor at a single location. That is the measurement of three spectral power distributions and $2^8 \times 3 = 768$ luminances (for 8 bit resolution on each phosphor electron gun).

Brainard (1989) and Lucassen & Walraven (1990) also discuss the problems of spatial inhomogeneities and temporal stability of the monitor output. In general it is found that the phosphor chromaticity coordinates do not vary with time, but that the luminance input output relationship can vary substantially. Further, the luminance output of the monitor decreases for the same input value away from the centre of the screen. These points are discussed further in section 2.2.

2.1.2 The Generation of Tristimulus Values on a VDU.

In order to simulate the chromaticity of a given reflecting surface under a specified illuminant the XYZ (CIE, 1931) tristimulus values of the combination must first be computed. This requires that the spectral reflection function R(λ) of the surface and the spectral emittance of the illuminant E(λ) are both known. The spectral reflection function R(λ) gives the proportion of the incident light reflected from the surface against wavelength and is measured for the surface in question (see section 2.2.3). The spectral emittance functions for various illuminants are available in the literature (Wysecki and Stiles, 1982) and can be computed for Planckian radiators. Thus the tristimulus values are given by:-

$$X = K\int R(\lambda)\ E(\lambda)\ \bar{x}(\lambda)d\lambda \qquad (2.1.1)$$

$$Y = K\int R(\lambda)\ E(\lambda)\ \bar{y}(\lambda)d\lambda \qquad (2.1.2)$$

$$Z = K\int R(\lambda)\ E(\lambda)\ \bar{z}(\lambda)d\lambda \qquad (2.1.3)$$

Where K is a constant which depends on the units of E(λ) and the integration takes place over the visible range of wavelengths. It is convenient to store the illuminants in such a manner that the luminance of a perfectly *white* object in the scene (i.e. R(λ) = 1 for all λ) is 1 cd/m^2. All illuminant files are normalised so that

$$\int E(\lambda)\ \bar{y}(\lambda)d\lambda = 1 \qquad (2.1.4)$$

This approach has the advantage that when we require a luminance of L cd/m^2 for the *white* reflector, we may simply multiply the illuminant file by the factor L. In practice, the visible wavelengths are taken to be from 380nm to

760nm and both the illuminant and reflectance functions are measured at discrete intervals every 5nm (77 values from 380nm to 760nm). Thus equations 2.1, 2.2 and 2.3 become

$$X = \sum_{1}^{77} R(\lambda)\ E(\lambda)\ \bar{x}(\lambda)d\lambda \tag{2.5}$$

$$Y = \sum_{1}^{77} R(\lambda)\ E(\lambda)\ \bar{y}(\lambda)d\lambda \tag{2.6}$$

$$Z = \sum_{1}^{77} R(\lambda)\ E(\lambda)\ \bar{z}(\lambda)d\lambda \tag{2.7}$$

Given that we know the chromaticity coordinates of the monitor phosphors, we can compute the necessary luminance output from each phosphor to emulate the tristimulus values of the reflecting surface of interest under the given illuminant. Let x_r, y_r and z_r be the CIE 1931 chromaticity coordinates of the red phosphor and similarly x_g, y_g, z_g and x_b, y_b, z_b for the green and blue phosphors respectively. Let L_r, L_g, L_b be the required luminance outputs from the three phosphors. Then we have

$$X = \frac{L_r}{y_r}x_r + \frac{L_g}{y_g}x_g + \frac{L_b}{y_b}x_b \tag{2.8}$$

$$Y = L_r + L_g + L_b \tag{2.9}$$

$$Z = \frac{L_r}{y_r}z_r + \frac{L_g}{y_g}z_g + \frac{L_b}{y_b}z_b \tag{2.10}$$

The problem becomes that of solving these simultaneous equations.

$$\frac{L_r}{D_r} + \frac{L_g}{D_g} + \frac{L_b}{D_b} + \frac{1}{D} \tag{2.11}$$

Hence

$$L_r = \frac{D_r}{D} \quad ; \quad L_g = \frac{D_g}{D} \quad ; \quad L_b = \frac{D_b}{D} \tag{2.12}$$

Where D_r, D_g, D_b and D are determinants given by

$$D_r = \begin{vmatrix} X & x_g/y_g & x_b/y_b \\ Y & y_g/y_g & y_b/y_b \\ Z & z_g/y_g & z_b/y_b \end{vmatrix} \tag{2.13}$$

$$D_g = \begin{vmatrix} x_r/y_r & X & x_b/y_b \\ y_r/y_r & Y & y_b/y_b \\ z_r/y_r & Z & z_b/y_b \end{vmatrix} \tag{2.14}$$

$$D_b = \begin{vmatrix} x_r/y_r & x_g/y_g & X \\ y_r/y_r & y_g/y_g & Y \\ z_r/y_r & z_g/y_g & Z \end{vmatrix} \tag{2.15}$$

$$D = \begin{vmatrix} x_r/y_r & x_g/y_g & x_b/y_b \\ y_r/y_r & y_g/y_g & y_b/y_b \\ z_r/y_r & z_g/y_g & z_b/y_b \end{vmatrix} \tag{2.16}$$

So for each reflectance, illuminant combination the tristimulus values are computed and the corresponding determinants D, D_r, D_g and D_b. From these the required phosphor luminances are found. If any of the determinant values

are less than zero, then the emulation of these chromaticity coordinates is not possible.

Thus it is possible to compute the necessary phosphor luminances to emulate given tristimulus values, provided that the chromaticity coordinates of the phosphors are known. It then remains to measure and store a lookup table of the digital to analogue conversion for each of the phosphor electron guns so that the appropriate gun value may be selected for the required luminance. It should be noted that the spectral radiance distribution of the illuminant-reflector combination is not actually reproduced, rather a metamer of this combination is displayed on the monitor.

2.1.3 Equipment

The experiments presented in this thesis were carried out using Hewlett Packard D1187A 20" monitor. The calibration and chromaticity coordinates of this monitor are described below.

The computer programs (described in section 2.5) require the following hardware:-

An ISA/EISA compatible PC with minimum of 640 kbytes of RAM, a diskette drive and a hard disk drive,

System monitor and driver capable of supporting at least mono VGA,

MS or PC DOS version 4 of higher,

MS DOS mouse driver (mouse.sys) and HP-HIL mouse (for COLCON),

HP A1083A Intelligent Graphics Controller 20 (HPIGC20) with 2M VRAM installed and configured for 1280x1024 resolution with 256 colours.

The Texas Instruments Graphics Architecture (TIGA-340™) v1.1 or higher must be installed and its communications driver active to run the programs. The programs were compiled and linked with Microsoft C v6.0 using the large memory model and the TIGA graphics library (AI.LIB).

The light measurement instruments used were photometer and a telespectroradiometer. The latter allows the measurement of light output power in narrow band spectral regions and hence enables the complete characterisation of the signal emitted by each of the monitor phosphors. Light enters the telespectroradiometer through an EG&G Gamma Scientific High Efficiency photometric telescope (model 2020-31). All measurements were made with the telescope aperture set to 20' of visual arc and the monitor-telescope separation at 1m; this corresponds to an area 0.58cm in diameter on the screen. Light leaving the telescope passes into an Applied Photophysics monochromator F/3.4, which has a half power bandwidth of 4.0nm. The light is detected by a EG&G Gamma Scientific D-46B photomultiplier which is controlled by a model DR-2 digital radiometer. This produces a digital output which is interfaced with a PC for storage and manipulation. This same PC is used to set the monochromator wavelength via a scanning control unit and stepper motor.

The photometer permits the measurement of light output power over a broad spectral band and allows the measurement of luminances with considerably greater convenience than using a spectroradiometer. The photometer used was an LMT L1003 with an ultra stable Silicon semiconductor photodiode corrected to give a "fine" approximation to $V(\lambda)$, used with the aperture set to 20'.

2.2 Calibration

2.2.1 Calibration of Phosphor Chromaticity Coordinates

In order to compute the phosphor chromaticity coordinates it is necessary to measure each of the spectral radiance distributions. This was done using the telespectroradiometer described above. Each phosphor in turn was displayed alone over a patch in the centre of the screen. This stimulus arrangement was chosen to be similar to that used in the experiments. In order to minimise the effect of any residual contribution of other guns the monitor brightness control was turned to its minimum and the lookup table value of the displayed colour was 255. The spectral radiance distribution was scanned every 2nm from 380nm to 760nm. The results are shown in figure 2.2.1. The sharply peaked distribution of the red phosphor is typical of visual display unit output. The radiance values displayed were those obtained during measurement, but only the relative spectral distribution of each phosphor separately is necessary for the computation of the chromaticity coordinates and no importance should be attached to respective radiances of the red, green and blue phosphors.

The chromaticity coordinates obtained were: $x_{red} = 0.6226$, $y_{red} = 0.3505$; $x_{green} = 0.2885$, $y_{green} = 0.6075$; $x_{blue} = 0.1498$, $y_{blue} = 0.0675$. Figure 2.2.2 shows the chromaticity coordinates of the phosphors in the CIE 1931 chromaticity diagram as solid circles. The outer shape is the spectrum locus and the triangular area enclosed by the solid lines indicates the gamut of colours which can be reproduced on the monitor. It should be noted that the full gamut can only be reproduced at low luminances; at higher luminances the achievable gamut is further limited by the maximum luminance output of the phosphors (blue, red and green in increasing order).

The experimental work of this thesis was carried out in CIE Uniform Chromaticity Scale diagram (u', v' diagram) as this is more perceptually

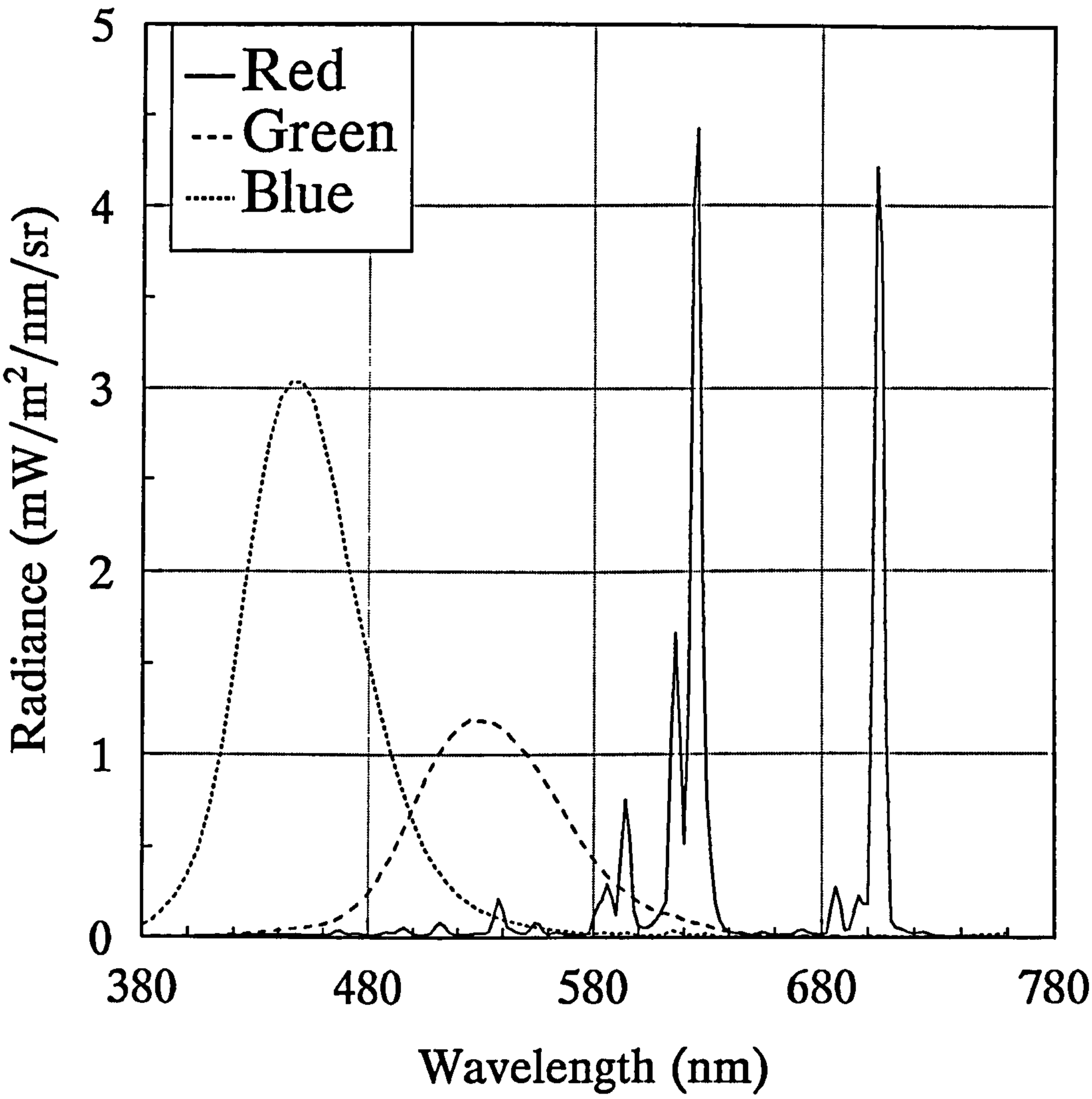

Figure 2.2.1 *The spectral radiance distributions of the outputs of the three phosphors of the Hewlett Packard D1187A 20" monitor used in the experiments of this thesis.*

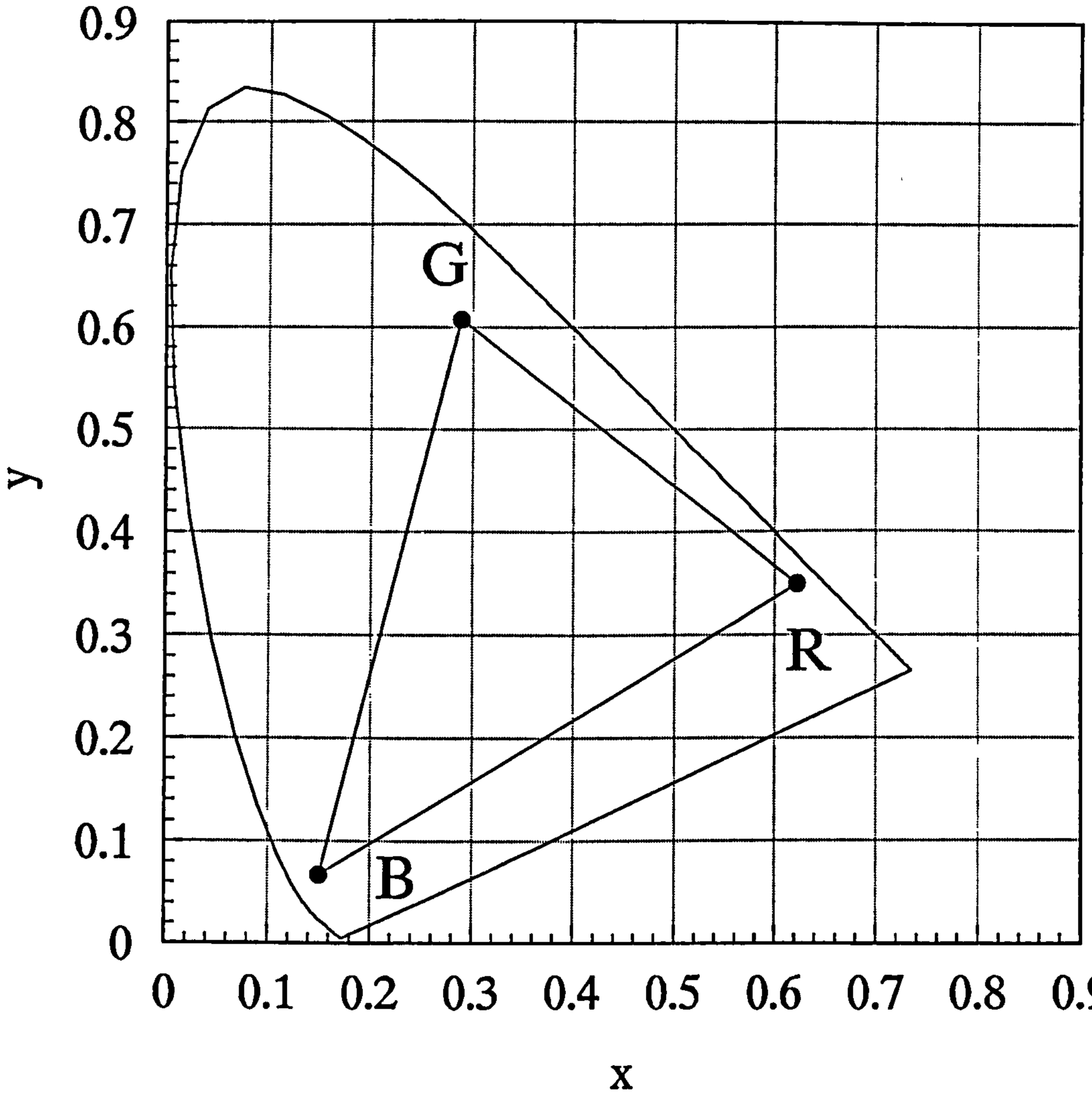

Figure 2.2.2 *The spectrum locus and the chromaticity co-ordinates of the phosphors of Figure 2.2.1 plotted in the CIE 1931 chromaticity diagram. The triangular area enclosed by the solid lines indicates the gamut of colours which can be reproduced on the monitor.*

uniform. Figure 2.2.3 shows the same data as figure 2.2.2 transformed into this diagram, the chromaticity coordinates being: $u'_{red} = 0.4180$, $v'_{red} = 0.5291$; $u'_{green} = 0.1188$, $v'_{green} = 0.5629$; $u'_{blue} = 0.1707$, $v'_{blue} = 0.1731$.

2.2.2 Calibration of Electron Gun Input to Phosphor Luminance Output

The monitor input output relationship was measured using the LMT photometer. A patch was displayed in the centre of the screen with at each lookup table value for each phosphor in turn and the luminance for each value recorded. Other authors (Brainard, 1989; Post and Calhoun, 1989; Lucassen and Walraven, 1990) have suggested that it is possible to extrapolate the input output relationship from a single function and a limited number of measurements (such as the maximum output of each phosphor) and that temporal instabilities could be accounted for by a single measurement in the appropriate stimulus configuration. However as the LMT photometer provides an analogue voltage output, which could be connect to an ADC card in the computer controlling the monitor it was not found inconvenient to measure all 768 values before each set of experiments.

Before carrying out each measurement, the monitor contrast control was set to maximum and the brightness raised from minimum until the luminance of a white patch (all input values at maximum) was greater than 100 cd/m^2. These settings were arbitrary, but were chosen so that a good range of luminance was available along with fine colour resolution. Once these settings had been achieved, the monitor controls were taped over so that they could not be altered during experimentation.

Typical results obtained for the input output relationship are shown in figure 2.2.4. As the spectral disribution of the green phosphor occupies the range over which the human eye is most sensitive, the luminance output of this phosphor is considerably higher than the red and blue. The ratio of

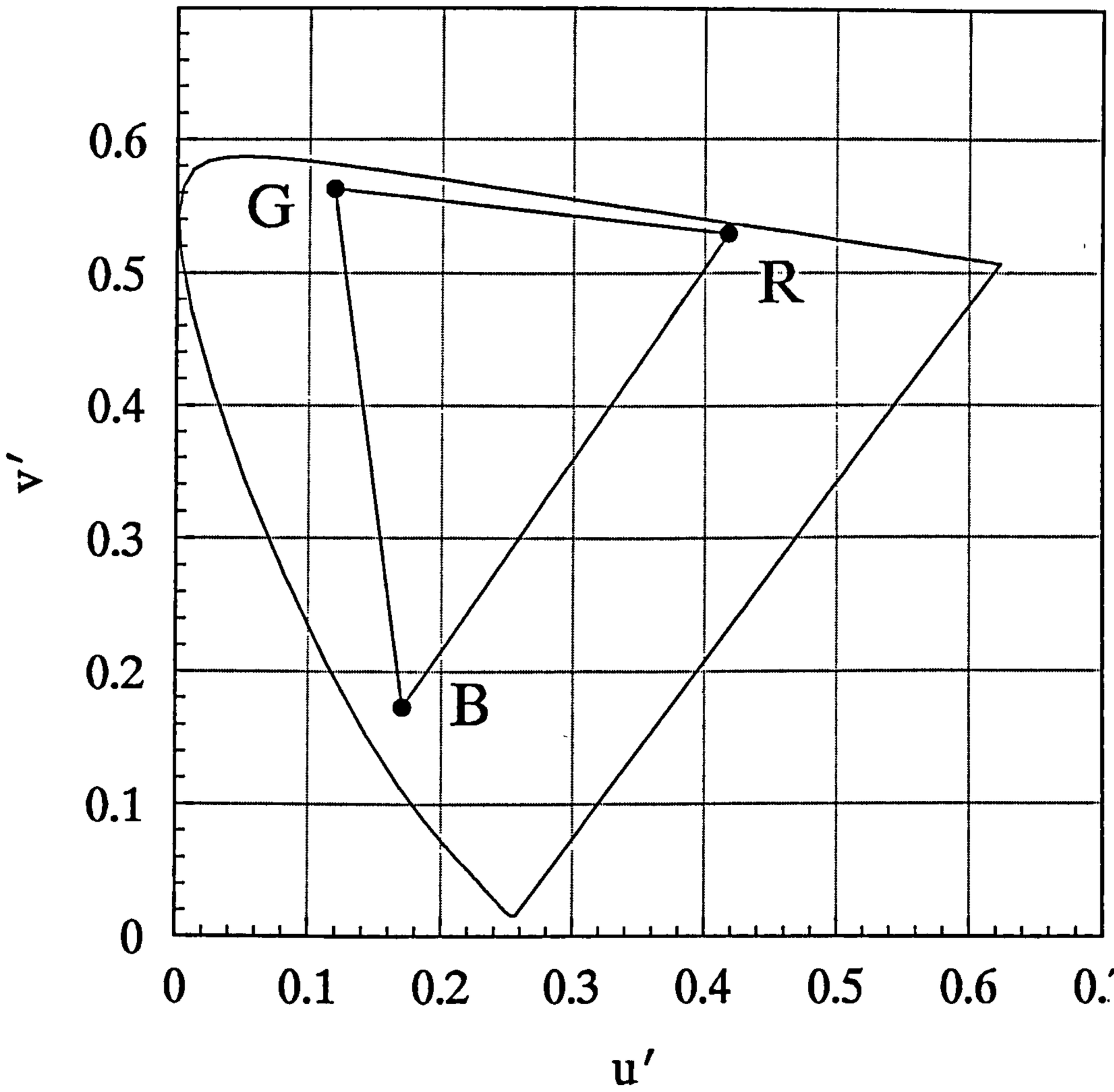

Figure 2.2.3 *The spectrum locus and chromaticity co-ordinates of the phosphors of Figure 2.2.1 plotted in CIE-UCS space. The triangular area enclosed by the solid lines indicates the gamut of colours which can be reproduced on this monitor.*

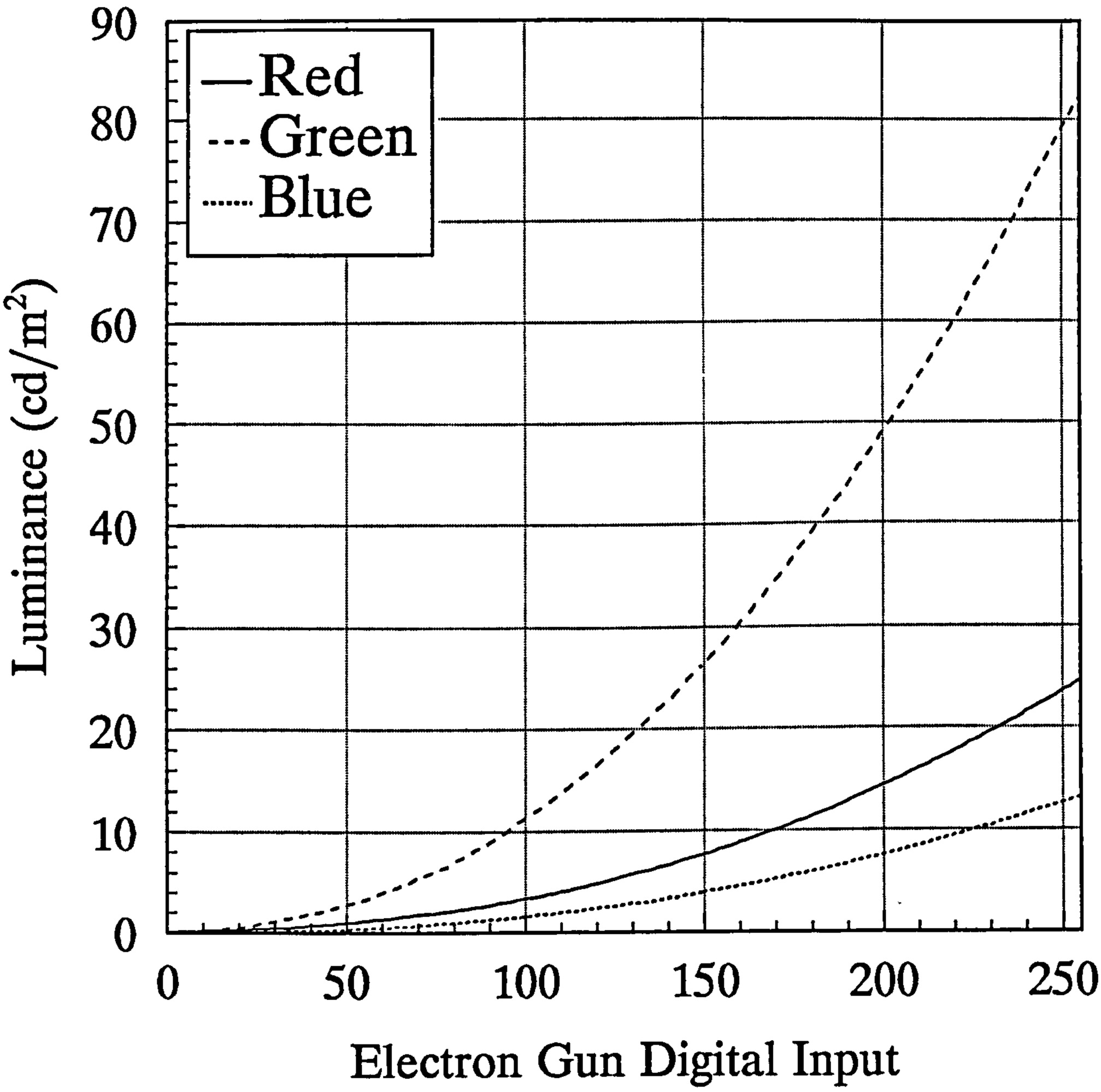

Figure 2.2.4 *The analog luminance output plotted against the electron gun digital input for the Hewlett Packard D1187A used for the experiment of this thesis adjusted so that the maximum total luminance output was a little over 100 cd/m².*

green : red : blue is approximately 6 : 3 : 1 , which is typical of a visual display unit. Figure 2.2.5 shows the data of figure 2.2.4 with the output of each phosphor plotted relative to its maximum. This shows, as per Brainard (1989), that the phosphor outputs do indeed follow very similar functions differing only by a multiplicative output.

The luminance output of a computer monitor will decrease, for a given input value, the further from the centre of the screen that it is specified (Lucassen & Walraven, 1990; Brainard, 1989). Figure 2.2.6 shows the luminance output of the three phosphors relative to the maximum of each, plotted against horizontal distance from the centre of the screen. There is considerably less variation than for the Barco 5351 monitor described by Brainard (1989), which shows a decrease of up to 20% at displacements of 8cm from screen centre. The similarity with which the relative luminances of the three phosphors decreases, is evidence for the single scale factor assumption of Brainard. This small variation (under 3% at 5cm) coupled with the human visual systems insensitivity to small luminance variations and the restricting of the target elements in the experiment, suggested that no correction need be made for elements displayed peripherally.

It is also important that the monitor output be stable with time. To this end, the luminance output of each of the phosphors was measured every few minutes after the monitor was switched on. The data are displayed in figure 2.2.7, which shows the luminance output of each phosphor relative to its maximum, plotted against time from monitor switch on. Each of the phosphors has reached 97% of its maximum value within 50 minutes of switch on and does not fluctuate by more than 1% after one hour (this fluctuation is likely to be due to measurement error). The practice was adopted, therefore, of switching on the monitor at least one hour before any experimentation or recalibration of the luminance input output relationship.

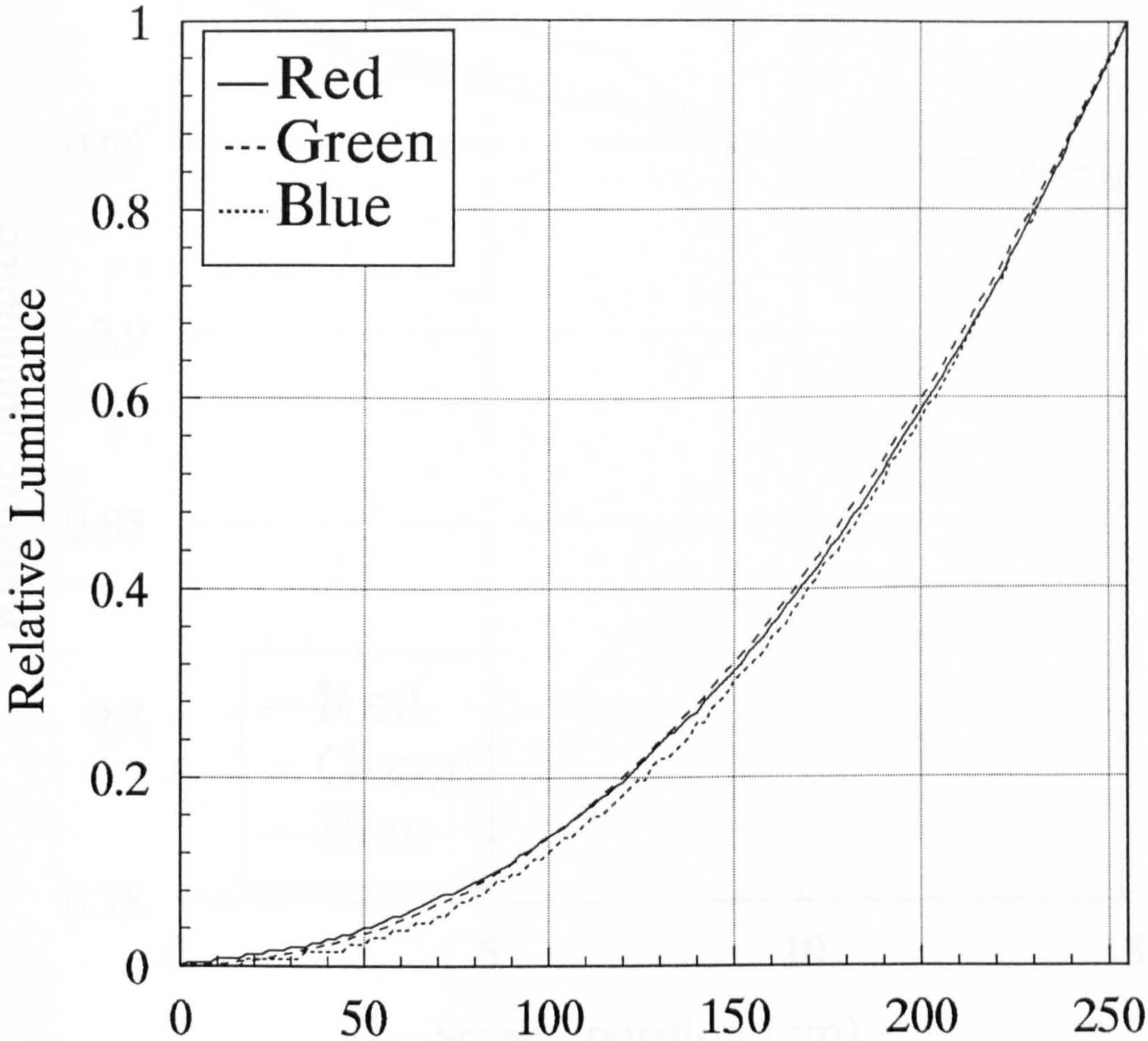

Figure 2.2.5 *The relative analog luminance output plotted against the electron gun digital input for each of the phosphors of the monitor of the Hewlett Packard D1187A.*

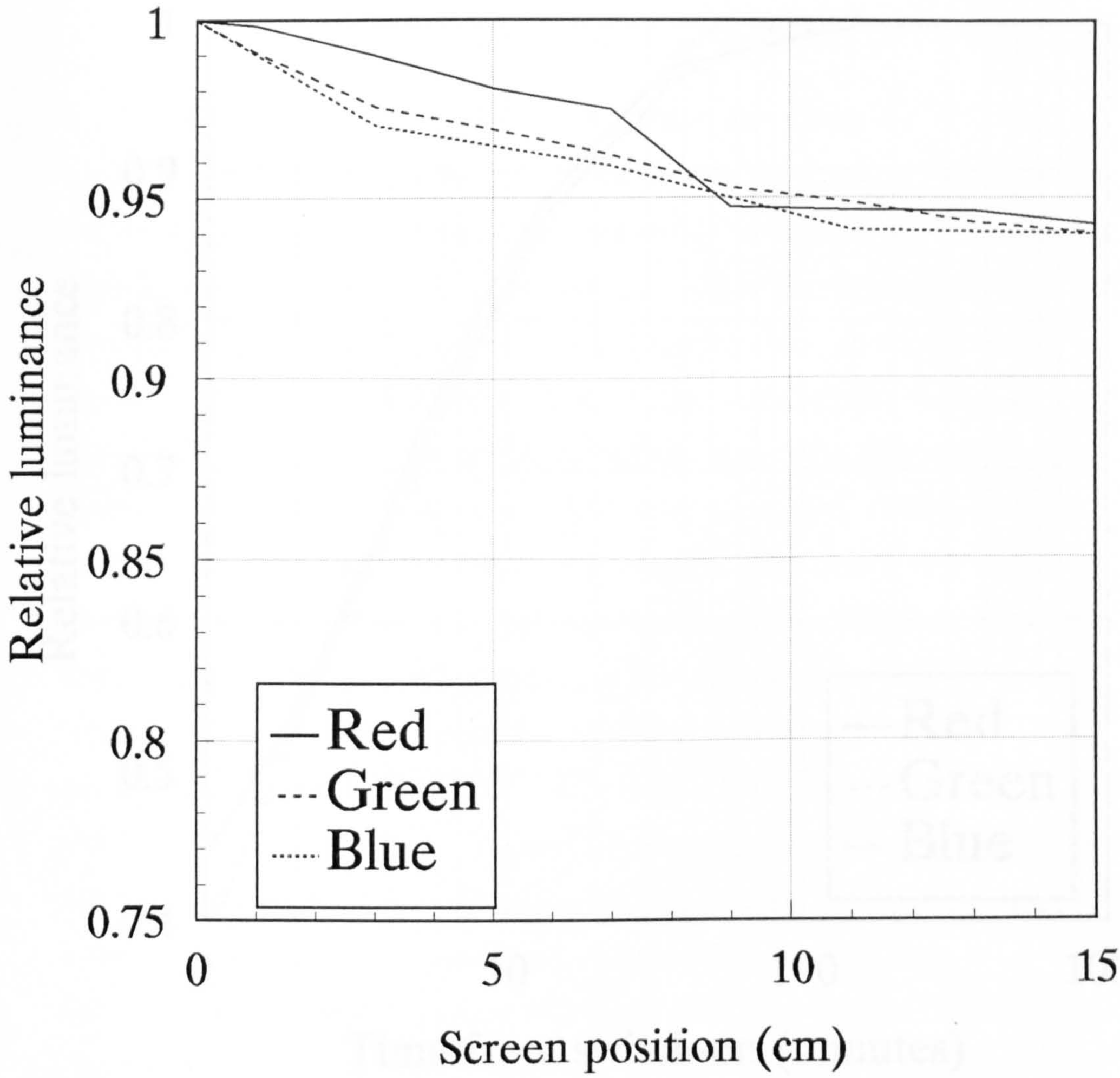

Figure 2.2.6 *The relative luminance output of each of the monitor phosphors, plotted against horizontal distance of the point of measurement from the centre of the screen.*

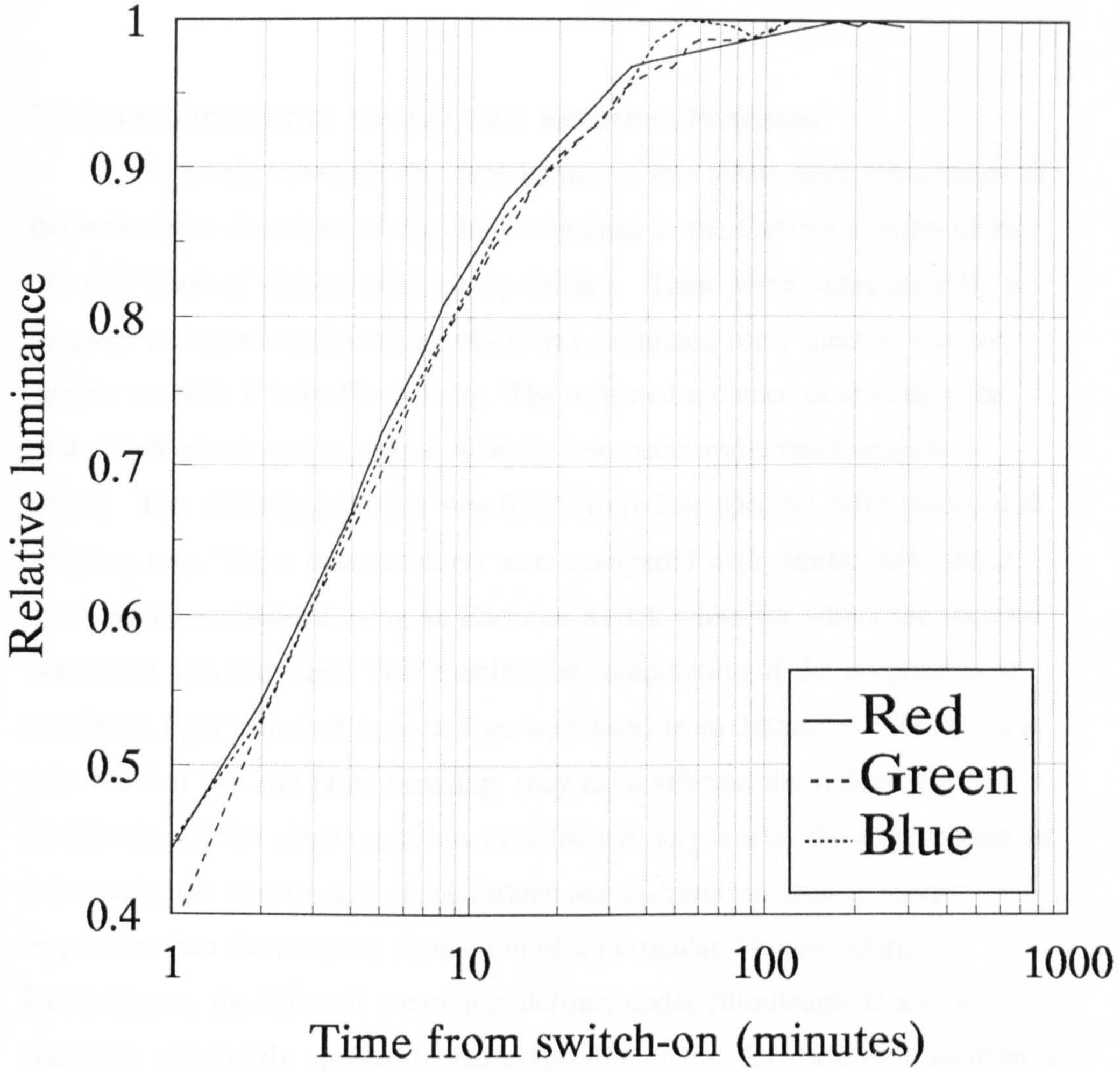

Figure 2.2.7 *The relative luminance of each of the monitor phosphors, displayed alone, plotted against time from switching on the monitor.*

2.2.3 Measurement of Munsell Chip Reflection Functions

The stimuli used for the experiments of this thesis were simulations of the reflectance functions of the chips contained in the Cabinet Edition of the Munsell Book of Colour 1963 glossy surface. These were illuminated by a tungsten halogen aviation lamp which was calibrated for a spectral intensity against an NPL Clarke-Berry lamp. The reflected radiance distribution for each patch of interest measured with the telespectroradiometer described above. The viewing geometry was 0°/45° to reduce spectral reflectance, with no gloss trap. These measurements were compared with similar reflectance measurements obtained using an Eastman Kodak white for which the spectral correction was provided. This enabled the computation of the proportion of incidental light reflected in each 5nm waveband from 380nm to 760nm. It is possible that age and prior handling may have affected the reflectance distribution of the chips used, however for the purposes of the experiments in this thesis, the consistency of the reflectance distribution used is more important than the accurate simulation of a particular Munsell chip. Furthermore, the Munsell notation is defined under Illuminants C and is therefore not strictly applicable under any illuminant. The Munsell notation is used in this thesis as a convenience of labelling. Figure 2.2.8 shows the reflectance distribution of four of the Munsell chips used in some of the experiments presented here. The distribution of other Munsell chips measured are given in Appendix A.

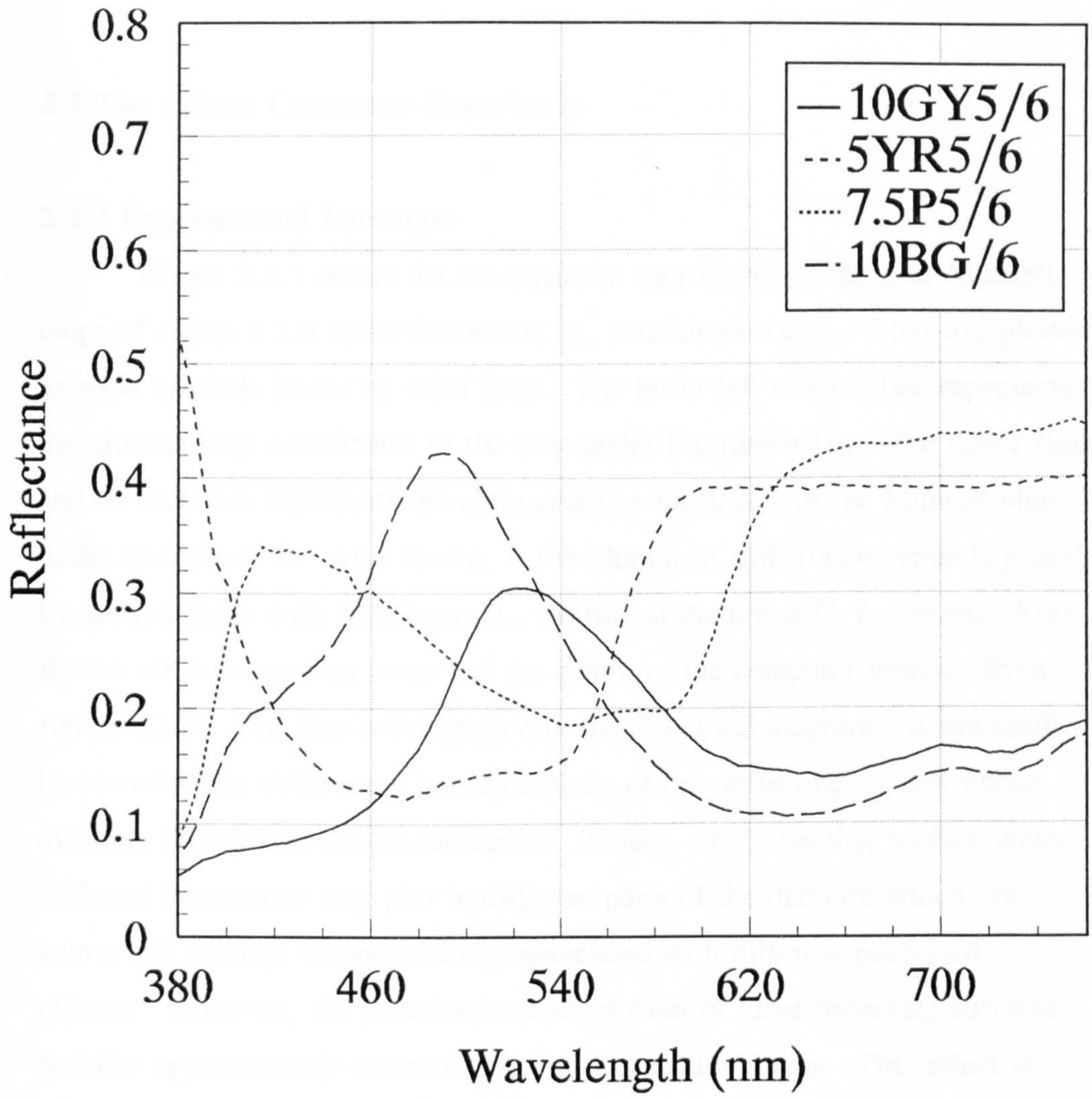

Figure 2.2.8 *The reflectance distribution of four Munsell chips.*

2.3 The Colour Constancy Experiment

2.3.1 Experimental Paradigm

Figure 2.3.1 shows the chromaticity coordinates of the four Munsell chips of figure 2.2.8 under Illuminant D_{65} and Illuminant A. They are plotted as solid symbols joined by solid lines. The lower left of each line represents the chromaticity coordinates of the chip under Illuminant D_{65}. The upper right end of each line represents the chromaticity coordinates of the Munsell chip under Illuminant A. Also shown, is the illuminant shift (open symbols joined by dashed lines) with Illuminant D_{65} plotting at the lower U-V- values. Also shown are the spectrum locus and the gamut of the computer monitor from figure 2.2.3. The data are displayed in the CIE-UCS diagram. It can readily be seen that the differences in chromaticity of one reflecting surface under different illuminants can be substantial. Indeed, one reflecting surface under different illuminants may plot in different parts of the diagram which are commonly (though inappropriately) associated with different perceived colours. However, the perceived colour of each of these reflecting surfaces remains approximately constant under different illuminants. This effect is only observed when objects are seen in the context of a full visual scene and does not occur of objects observed in isolation.

In order to quantify the ability of the visual system to account for changes in illumination and achieve a near constant colour percept of an object, it is necessary to present to an experimental subject the object and scene illuminated by each of two illuminants and perform a colour matching experiment between them. To this end, the experiments of this thesis employ a dynamic colour matching paradigm.

The experimental subject controls the colour of a test patch using the computer mouse. The initial chromaticity of the test patch is set by the computer for the experiment, and the motion of the mouse is interpreted as

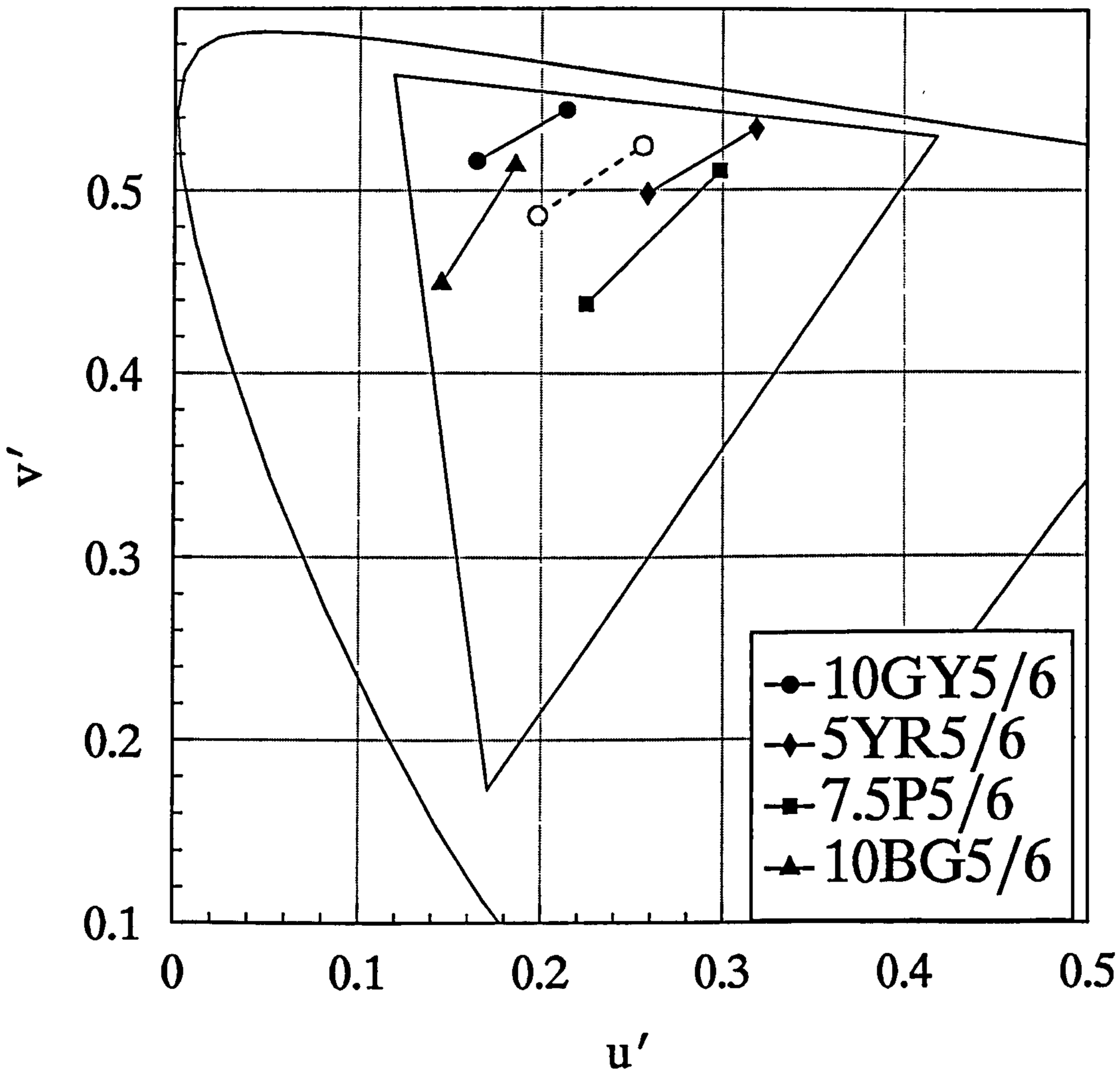

Figure 2.3.1 *A detail of Figure 2.2.3, showing part of the spectrum locus and the gamut of the computer monitor. The open symbols plot the chromaticity co-ordinates of Illuminant D65 and Illuminant A. The solid symbols plot the chromaticity co-ordinates of the four Munsell chips of Figure 2.2.6 illuminated by each of these illuminants respectively. The data are displayed in the CIE-UCS diagram.*

motion in the CIE-UCS chromaticity diagram. A practice programme is employed so that the subject may become familiar with the chromaticity diagram and with control of the chromaticity using the mouse. If the limit of the screen gamut is reached, an audible cue is given and further mouse motion in that direction has no effect. It is also possible to alter the illuminants of the test patch when the desired chromaticity has been achieved, the subject presses a mouse button to indicate this, and the next presentation is put on the screen. The colour matching paradigm is described as dynamic as the presentation to the subject alters in time between its appearance under the two illuminants, that is, the subject is presented initially with the test patch and surrounding scene under the first or reference illuminant. After a small amount of time (usually 800ms), the whole presentation flips so that the surrounding scene is under the second or test illuminant and the chromaticity of the test patch is under the control of the subject. The subject only has control of the chromaticity of the test patch when the surrounding scene is under the second or test illuminant. The experimental display flips back and forth between these two situations and there is no limit on the number of flips required by the subject to make the match. The subject is instructed to adjust the test patch when the surrounding scene is under the test illuminant to exactly match the same patch in saturation and hue when the surrounding scene is under the reference illuminant. That is, the test patch should appear not to change as the illuminant on the surrounding scene flips from test to reference. In order to achieve a constant state of photoreceptor adaptation between experiments before carrying out the initial colour match of an experimental run, the subject views the scene flipping between the two illuminants for some 10 minutes.

Using an experimental paradigm of this type, it is possible to investigate the effect of various spatial and chromatic properties of the surrounding scene on colour constancy. The shape and location of both the

test patch and elements in the surrounding scene may be varied, as may be their reflectance functions and the illuminants used.

2.3.2 The Definition of the C-Index

Figure 2.3.2 shows typical results of a dynamic colour matching experiment. Two points should be noted from these results. The first is that the colour matches by the subject cluster around the line joining the chromaticities of the test target under the reference illuminant and the test illuminant. The second point is that they cluster approximately half way along this line, that is, the colour matches do not equate to the chromaticity of the test patch under Illuminant D_{65}, which would be expected if the match were made purely on the basis of spectral radiance distribution. Nor do they equate to the chromaticity of the test patch under Illuminant A, which would be expected if the colour appearance of the test patch were entirely mediated by the surrounding scene. This gives us a quantitative index of the **C** index of colour constancy in any particular experiment. A **C** index of 0 for no colour constancy, is recorded when the subject matches the chromaticity of the test patch under the reference illuminant, in this case D_{65}. In this instance, the match is determined purely by the spectral radiance distribution of the patches involved. A **C** index of 1, or perfect colour constancy is recorded when the subject matches the chromaticity of the test patch to that which would be expected of it under the test illuminant, which indicates that the perceived colour has been entirely mediated by the surrounding scene. Between these two extremes of 0 for zero constancy and 1 for perfect colour constancy, the **C** index is defined as the ratio of the distance between the chromaticity of the colour matching made by the subject and the chromaticity of the test patch under the reference illuminant, and the distance between the chromaticities of the test patch under both the reference and test illuminants. These are measured as Euclidian distances in CIE-UCS space. This point is illustrated

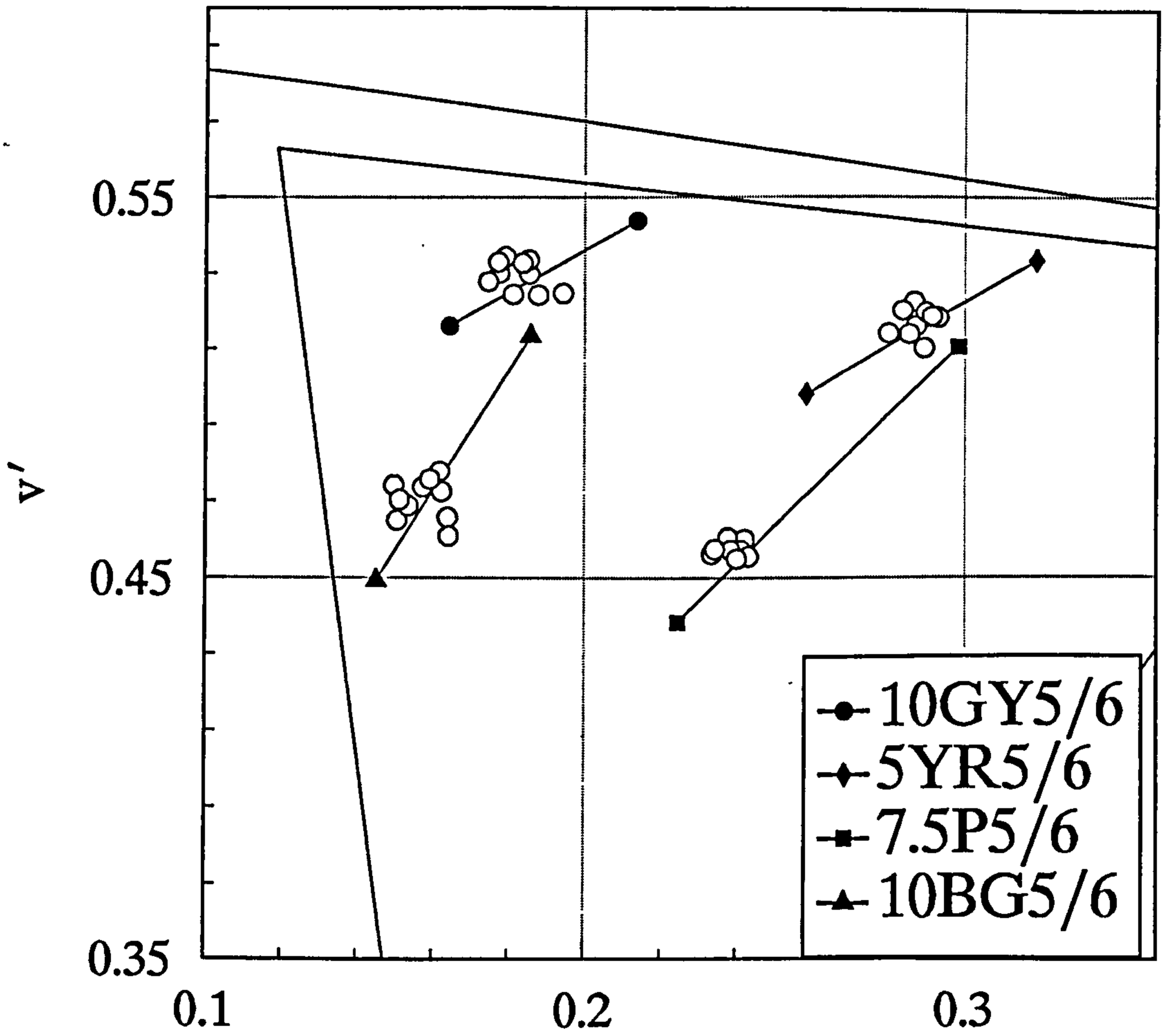

Figure 2.3.2 *Shows a detail of Figure 2.3.1 with a section of the spectrum locus as a section of the gamut of the computer monitor. The closed symbols plot the chromaticity co-ordinates of the four Munsell chips under the Illuminant D65 and Illuminant A. The open symbols plot the colour matches set by an experimental subject of a colour constancy experiment as described in the text.*

in great detail in figure 2.3.3, which shows and enlarged section of figure 2.3.2 for one particular colour match. T_D represents the chromaticity of the test patch under the reference illuminant. T_A is the chromaticity of the test patch under the test illuminant and T_M is the chromaticity of the colour match made by the subject. If, as in this case, the colour matching is not restricted to the line $T_D T_A$, a perpendicular is dropped from the chromaticity of the match made by the subject and this is represented by Point M. The **C** index is then defined simply as the ratio of the $(T_D\ M)/(T_D\ T_A)$.

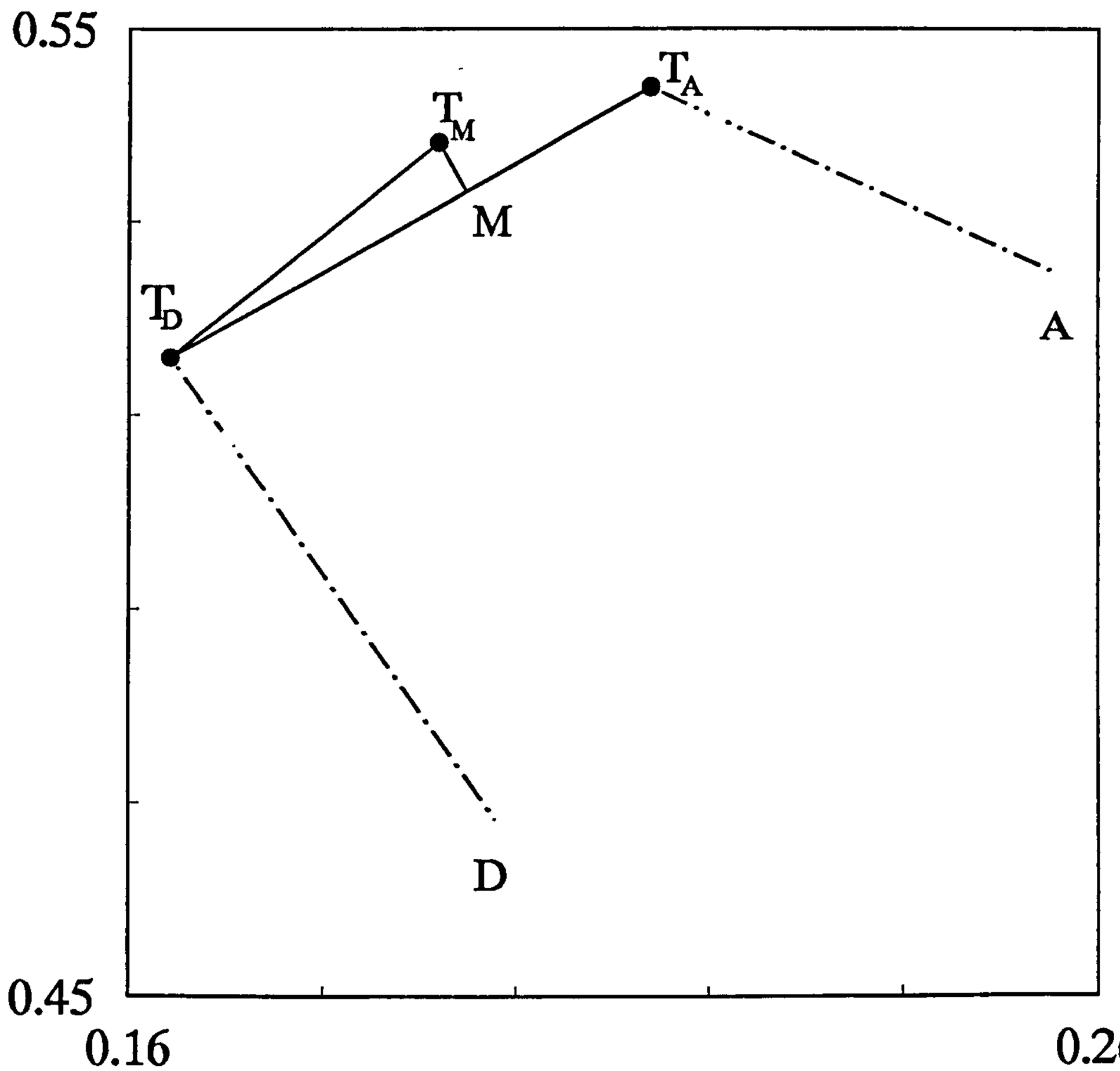

Figure 2.3.3 *Shows a detail of Figure 2.3.2. The chromaticities of the illuminants are plotted at points D and A, and the chromaticity of Munsell chip 10GY5/6 under Illuminant D are plotted at point T_D. The chromaticities of this Munsell chip under Illuminant A are plotted at point T_A. One of the matches made by the experimental subject is plotted at point T_M. A perpendicular is dropped from point T_M to the line T_DT_A to give point M. The 'C' Index is then defined as the ratio (T_DM / T_DT_A)*

2.4 The Effect of Scattered Light.

2.4.1 Experiment to Measure Light Scattered in the Human Eye.

Visual performance can be significantly affected by light scattered in the human eye from areas of the visual field other than those of interest (Stiles, 1929; Vos & Bouman, 1959; see section 1.1.2). This scattered light is characterised by Equation 1.1.1.

$$L_s(\theta) = Ek\theta^{-n} \qquad (1.1.1)$$

Figure 2.4.1 plots the results of a colour constancy experiment in which a circular target element is displayed inside a concentric uniform surround. The surround is held as a constant area and separated from the target element by a black annulus of varying size. This experiment is discussed in more detail in Chapter 3. The results show the **C** index the decreasing exponentially as the width of the black border increases. Jameson & Hurvich (1961) and Oyama & Hsia (1966), in experiments on the chromatic induction of a brightly coloured surround on a neutral centre, both obtained diminishing results as the coloured surrounds further separated from the centre. The former employed comparisons with Munsell colour samples and the latter a colour naming technique. Similarly, Tiplitz-Blackwell & Buchsbaum (1988) and Brenner & Cornelissen (1991) both found exponential decay in the chromatic induction of a neutral centre by a strongly coloured surround as centre surround separation increased, although the former only measured this for a very small range of centre surround separation. This diminishing effect is of similar form to that of the light scatter equation (Equation 1.1.1). Thus it may be possible that although these results are usually taken to reflect the spatial properties of a neural lateral mechanism they may be influenced by entopic stray light. Indeed, if the surround were to

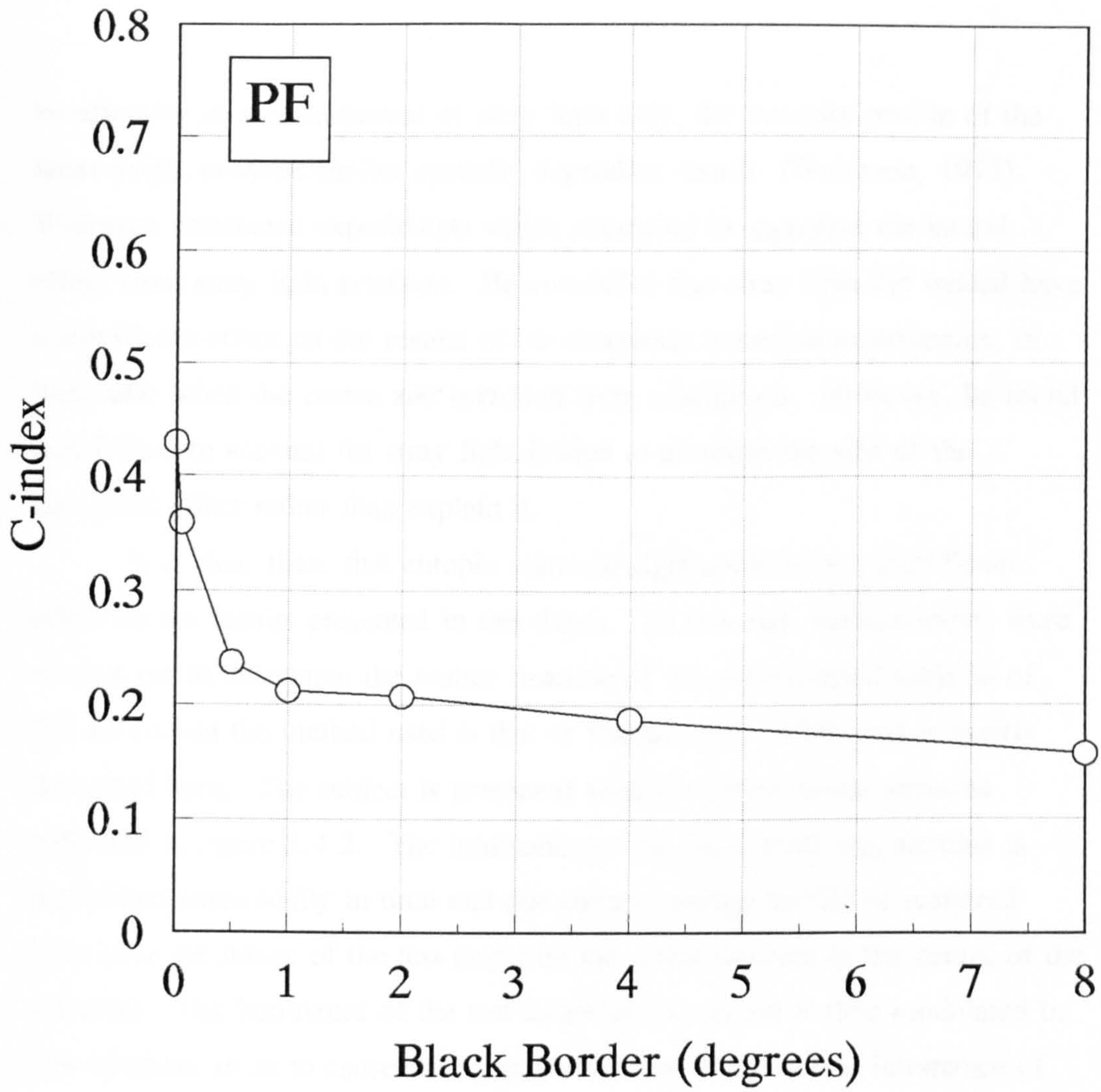

Figure 2.4.1 *Plots the results of a colour constancy experiment in which a central circular target element is displayed inside a concentric uniform surround. This surround is held at constant area and separated from the target element by a black annulus. The size of this annulus is varied. The* **C** *Index is plotted against the size of the annulus in degrees of visual angle.*

be effective as a consequence of stray light only, the intensity profile of the latter might produce similar spatially dependent results (Walraven, 1973). Walraven conducted experiments which attempted to segregate the lateral effect from stray light artefacts. He concluded that stray light did indeed have a significant effect on the results of his chromatic induction experiments, in particular when the centre and surround were contiguous. However, he found that failure to account for stray light tended to diminish the size of the measured effect rather than explain it.

It is clear then, that entopic scattered light could have a significant effect on the results presented in this thesis. To this end, measurements were carried out to determine the scatter function of the experimental subjects of this thesis and the method used is that of Barbur et al. (1992) and is briefly described here. The subject is presented with the experimental stimulus indicated in figure 2.4.2. The luminance of the large scattering annulus is modulated sinusoidally in time and this causes similar profile of scattered light over the image of the test target on the retina (located in the centre of the annulus). The luminance of the test target on the screen is then modulated in counterphase so as to cause the same modulation of the retinal luminance of the image of the target. This is illustrated in figure 2.4.3, which shows how the modulation for screen luminance cancels out the temporal modulation caused by scattered light. When the retinal illuminance of the test target caused by scattered light equals that caused by temporal modulation of screen luminance, little or no flicker is perceived. The screen luminance of the test target at minimum flicker is therefore a measure of the retinal illuminance caused by scattered light for that annulus eccentricity. The process is then repeated for a range of annulus sizes.

In order to increase the absolute level of scattered light in the eye so as to make it measurable at large annulus eccentricities, the illuminance generated in the plane by the scatter source must also be high and independent

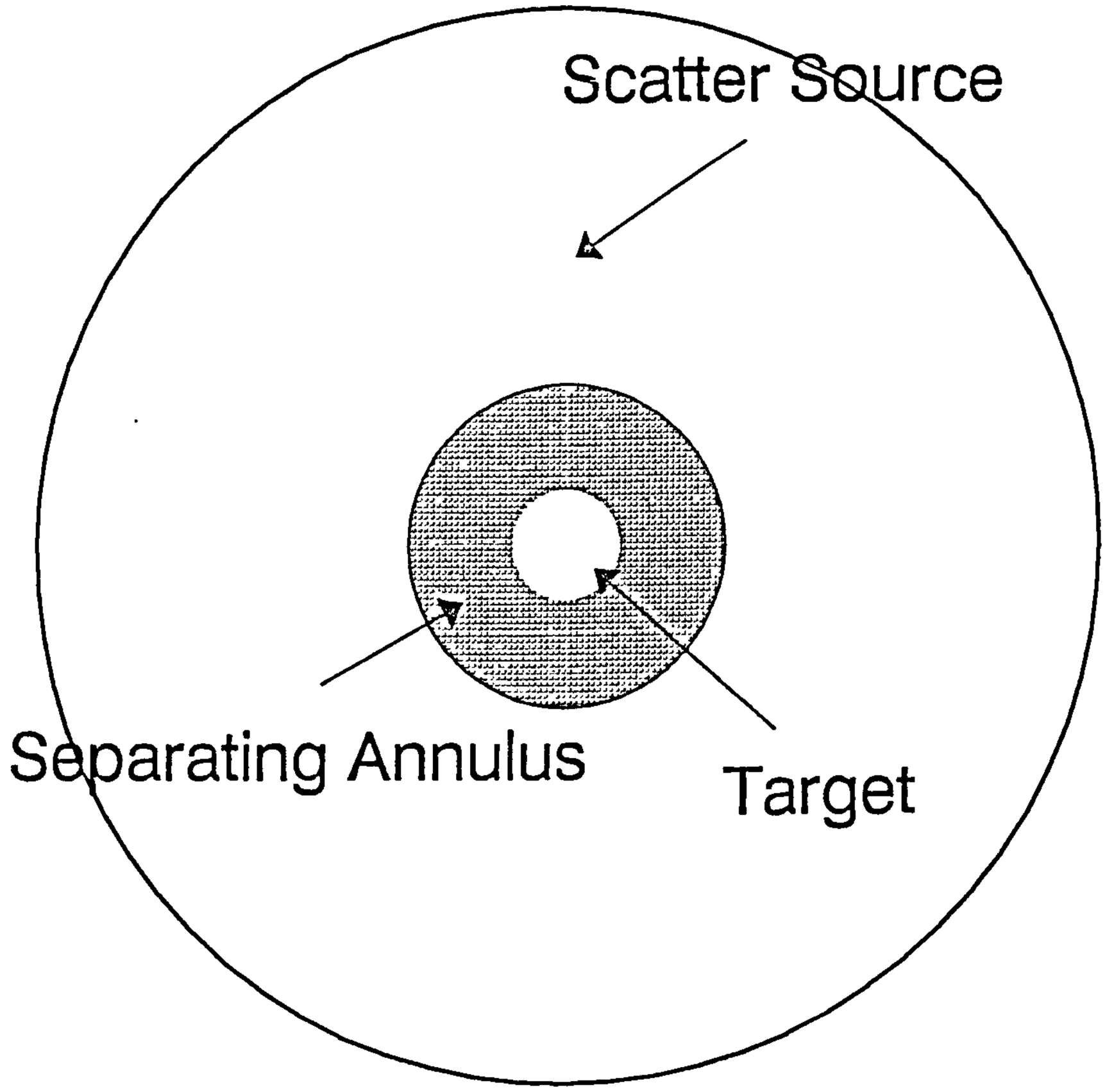

Figure 2.4.2 *Schematic diagram showing the stimulus arrangement for the light scatter measurement.*

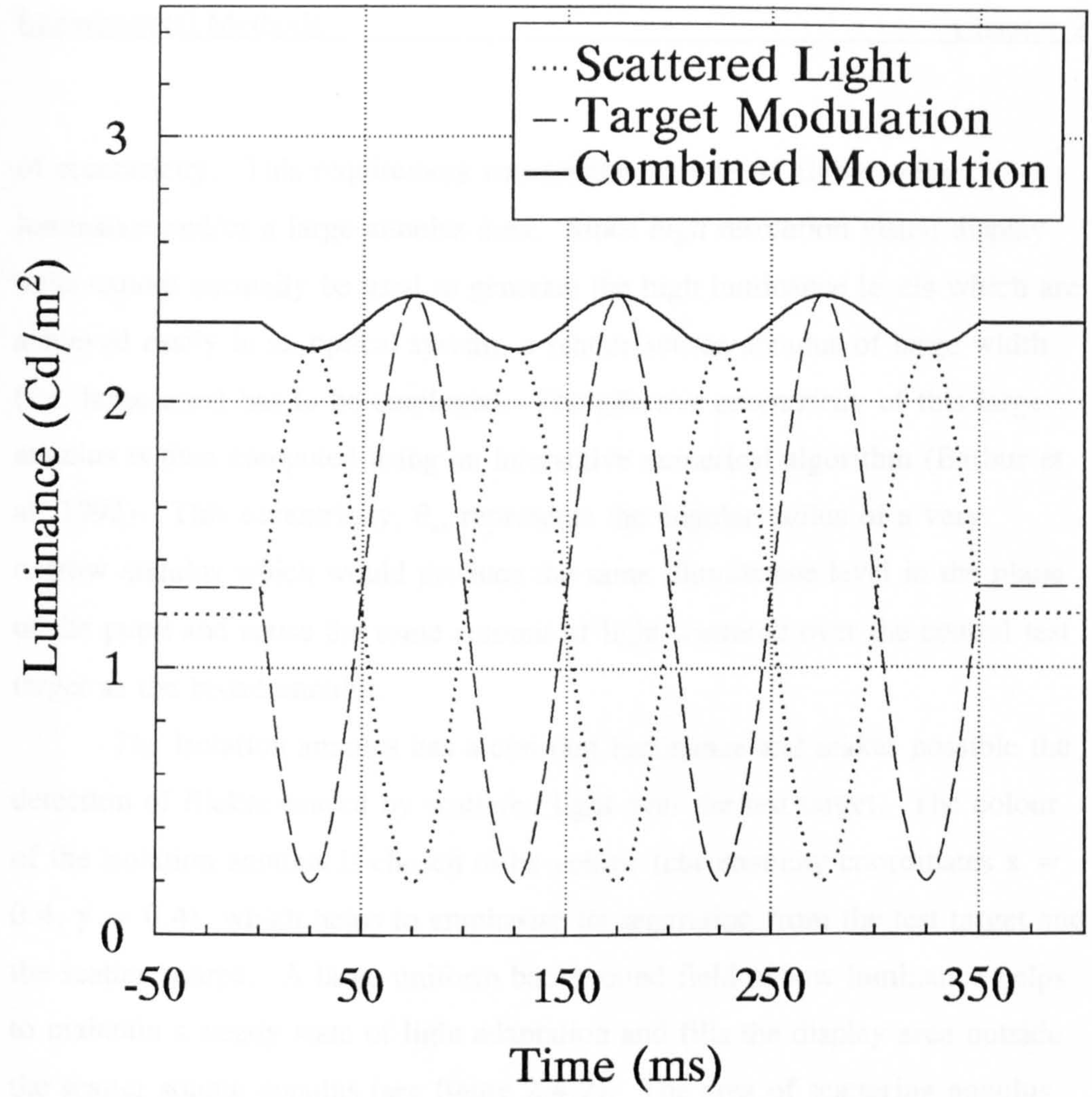

Figure 2.4.3 *Illustration of the sinusoidal modulation of retinal illuminance over the central test target area, caused by light scattered from the modulated annulus and its compensation achieved by counterphase modulation of screen luminance. When the two components are equal, the modulation cancels out completely and no flicker is perceived.*

of eccentricity. This requirement necessitates the use of high display luminance and/or a large annulus area. Since high resolution visual display units cannot normally be used to generate the high luminance levels which are achieved easily in an optical system, a scatter source annulus of large width (i.e. large area) has to be employed. The *effective eccentricity* of this large annulus is then computed using an interactive numerical algorithm (Barbur et al, 1992). This eccentricity, θ_e, represents the angular radius of a very narrow annulus which would produce the same illuminance level in the plane of the pupil and cause the same amount of light scattered over the central test target as the broad annulus.

The isolation annulus has a constant luminance and makes possible the detection of flicker caused by scattered light over the test target. The colour of the isolation annulus is chosen to be yellow (chromaticity coordinates x = 0.4, y = 0.4), which helps to emphasise its separation from the test target and the scatter source. A large uniform background field of low luminance helps to maintain a steady state of light adaptation and fills the display area outside the scatter source annulus (see figure 2.4.2). The area of scattering annulus changes appropriately with eccentricity so as to keep the illuminance in the plane of the pupil constant and independent of annulus eccentricity.

Figure 2.4.4 shows the results for three subjects used in many of the experiments used in this thesis. Subject CW is a 26 year old male; Subject JB a 40 year old male, both with uncorrected vision. Subject PF is a 63 year old male, who wore an optical correction for these measurements and for the colour constancy experiments. The dashed line indicates these data fitted with the scatter equation (Equation 1.1.1) for each subject. From these fitted equations, the stray light parameter **k** and the scatter index **n** may be obtained. These are: subject CW **n**=2.188, **k**=15.59; subject JB **n**=2.092, **k**=13.07; subject PF **n**=1.868, **k**=23.01. Knowledge of these parameters enables the

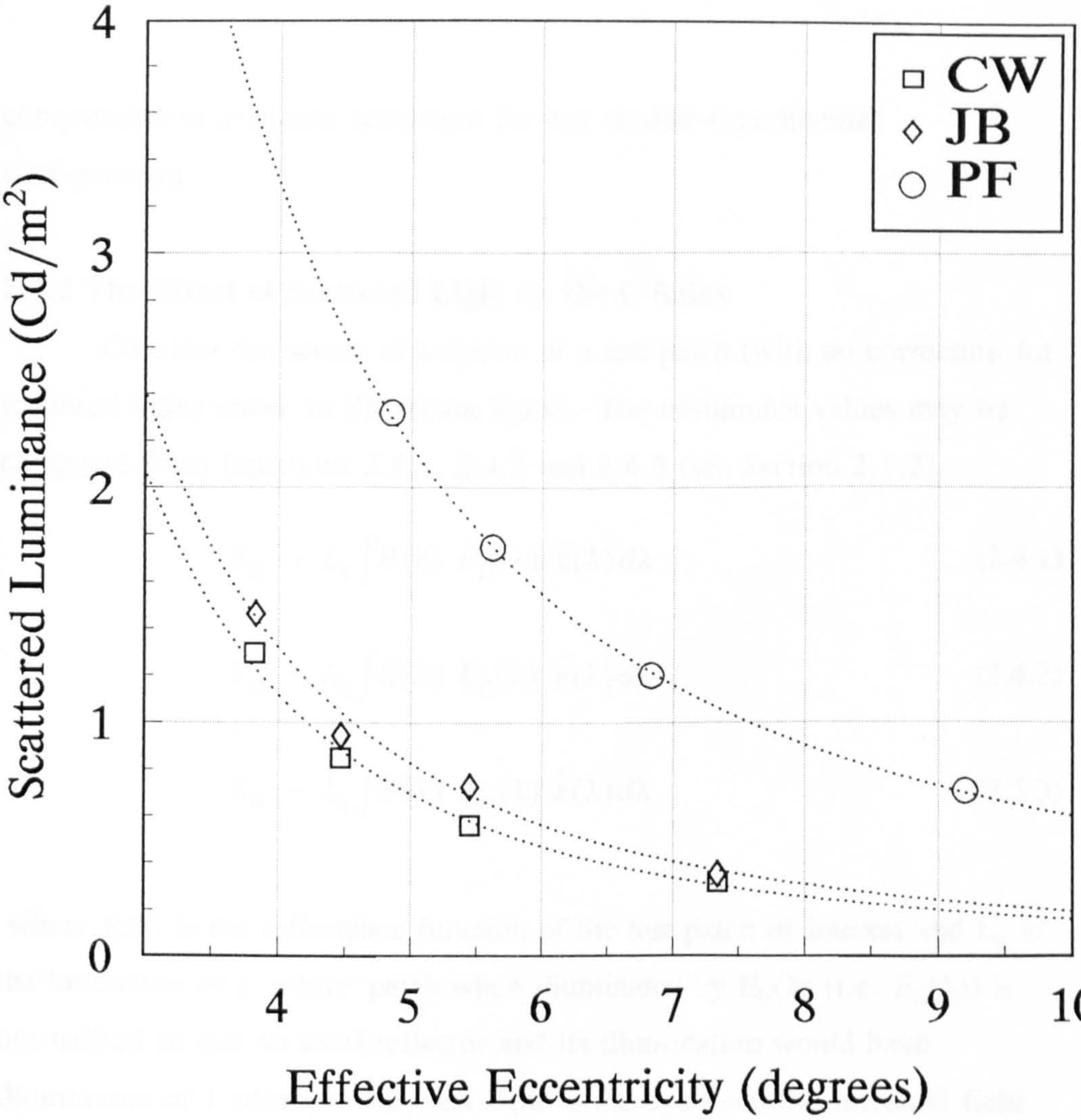

Figure 2.4.4 *Results of light scatter measures for three subjects. Subject CW is a 26 year old male, Subject JB, a 40 year old male (both with no optical correction), and Subject PF, a 63 year old male, who wore the same correction as used in the colour constancy experiments. The luminance scattered from the annular scattering source is plotted against the effective eccentricity (see text) of that source. The dotted lines show best fits of the form of the scatter equation:* $L_t = kE\theta^{-n}$. *For subject CW* $n=2.188$, $k=15.59$; *JB* $n=2.092$, $k=13.07$; *PF* $n=1.868$, $k=23.01$.

computation of scattered luminance for any similar experimental configuration.

2.4.2 The Effect of Scattered Light on the C index

Consider the screen description of a test patch (with no correction for scattered light) under an illuminant $E_D(\lambda)$. The tristimulus values may be computed from Equations 2.4.1, 2.4.2 and 2.4.3 (see Section 2.1.2),

$$X_D = L_\phi \int R(\lambda)\ E_D(\lambda)\ \bar{x}(\lambda) d\lambda \qquad (2.4.1)$$

$$Y_D = L_\phi \int R(\lambda)\ E_D(\lambda)\ \bar{y}(\lambda) d\lambda \qquad (2.4.2)$$

$$Z_D = L_\phi \int R(\lambda)\ E_D(\lambda)\ \bar{z}(\lambda) d\lambda \qquad (2.5.3)$$

where $R(\lambda)$ is the reflectance function of the test patch of interest and L_ϕ is the luminance of a 'white' patch when illuminated by $E_D(\lambda)$ (i.e. $E_D(\lambda)$) is normalised so that an ideal reflector and its illumination would have illuminance of 1 cd/m^2). Scattered light in the eye from the surround field increases the illuminance of a test patch by L_S cd/m^2. The spectral power distribution of the scattered light is the same as that of the background field ($E_D(\lambda)$).

The tristimulus values of the scattered light are given by Equations 2.4.4, 2.4.5, and 2.4.6. Note that it is only necessary to measure the luminance L_S of the scattered light in order to compute these tristimulus values.

$$X_{SD} = L_s \int E_D(\lambda)\ \bar{x}(\lambda) d\lambda \qquad (2.4.4)$$

$$Y_{SD} = L_s \int E_D(\lambda)\, \bar{y}(\lambda) d\lambda \qquad (2.4.5)$$

$$Z_{SD} = L_s \int E_D(\lambda)\, \bar{z}(\lambda) d\lambda \qquad (2.4.6)$$

Hence the tristimulus values of the retinal description of the test patch are given by Equations 2.4.7, 2.4.8 and 2.4.9.

$$X_{RD} = X_D + X_{SD} \qquad (2.4.7)$$

$$Y_{RD} = Y_D + Y_{SD} \qquad (2.4.8)$$

$$Z_{RD} = Z_D + Z_{SD} \qquad (2.4.9)$$

Now the wavelength radiance distribution of the surround field on the retina corresponds to Illuminant $E_D(\lambda)$. The modified tristimulus values caused by scattered light (Equations 2.4.7, 2.4.8 and 2.4.9) correspond to a modified reflectance function $R_S(\lambda)$. We need to know $R_S(\lambda)$ so as to be able to compute the expected change in test patch tristimulus values when the scene is illuminated with the second illuminant (the test illuminant). The spectral power distribution of the test patch on the retina given by combining the screen description and the scattered light may be equated to that spectral power distribution which would be obtained using this modified reflectance function $R_S(\lambda)$. This is shown in Equation 2.4.10.

$$L_\phi E_D(\lambda) R_s(\lambda) = L_\phi E_D(\lambda) R(\lambda) + L_s E_D(\lambda) \qquad (2.4.10)$$

This may be rearranged to give an expression for this modified reflectance function $R_S(\lambda)$ (Equation 2.4.11).

$$R_s(\lambda) = R(\lambda) + (L_s / L_\phi) \quad (2.4.11)$$

This modified reflectance function may be used to calculate the tristimulus values for the test patch when it is illuminated by the test illuminant $E_A(\lambda)$ (Equations 2.4.12, 2.4.13, 2.4.14).

$$X_A = L_\phi \int R_s(\lambda)\ E_A(\lambda)\ \bar{x}(\lambda) d\lambda \quad (2.4.12)$$

$$Y_A = L_\phi \int R_s(\lambda)\ E_A(\lambda)\ \bar{y}(\lambda) d\lambda \quad (2.4.13)$$

$$Z_A = L_\phi \int R_s(\lambda)\ E_A(\lambda)\ \bar{z}(\lambda) d\lambda \quad (2.4.14)$$

Now consider a colour match made by the subject in a colour constancy experiment. Let the tristimulus values of the colour match set by the experimental subject in screen co-ordinates be $X_M\ Y_M\ Z_M$. Given that the match is made under the test illuminant $E_A\lambda$, the tristimulus values of the scattered light are given by Equations 2.4.15, 2.4.16 and 2.4.17.

$$X_{SA} = L_s \int E_A(\lambda)\ \bar{x}(\lambda) d\lambda \quad (2.4.15)$$

$$Y_{SA} = L_s \int E_A(\lambda)\ \bar{y}(\lambda) d\lambda \quad (2.5.16)$$

$$Z_{SA} = L_s \int E_A(\lambda)\ \bar{z}(\lambda) d\lambda \quad (2.4.17)$$

The retinal description of the test patch when matched to the reference is therefore given by 2.4.18, 2.4.19 and 2.4.20.

$$X_{RM} = X_M + X_{SA} \quad (2.4.18)$$

$$Y_{RM} = Y_M + Y_{SA} \quad (2.4.19)$$

$$Z_{RM} = Z_M + Z_{SA} \quad (2.4.20)$$

The **C** Index which takes into account the light scattered in the eye, can be calculated in the manner described in Section 2.3.2, using the retinal tristimulus values, that is, Equations 2.4.7 to 2.4.9, 2.4.12 to 2.4.14, and 2.4.18 to 2.4.20.

The correction to the **C** Index is indicated graphically in figure 2.4.5. The open symbols plot the chromaticity co-ordinates of the reference illuminant D and the test illuminant A. The filled symbols joined by solid lines plot the screen chromaticity co-ordinates on the test target under the two illuminants and an example match set by the experimental subject, Point M. The retinal chromaticity co-ordinates of the test target under the two illuminants once scatter has been accounted for are shown by the solid symbols joined by the dashed line. The effect of scatter is to displace the chromaticity co-ordinates of the test target in the direction of the chromaticity co-ordinates of the illuminant surround. Similarly, the Match Point M is displaced towards Illuminant A (as this is the illuminant of the surround when the match is made) to arrive at Point M dashed. The **C** Index may now be calculated in the same way as before, but using the symbols joined by the dashed lines rather than solid lines. It should be noted that the computation accounting for the effect of scattered light always act to make the **C** index closer to one and that the size of the correction decreases the closer the **C** index is to one.

Figure 2.4.6 plots the same data as that of figure 2.4.1 with and without the correction for scatter. Similar data are plotted in figure 2.4.7 for

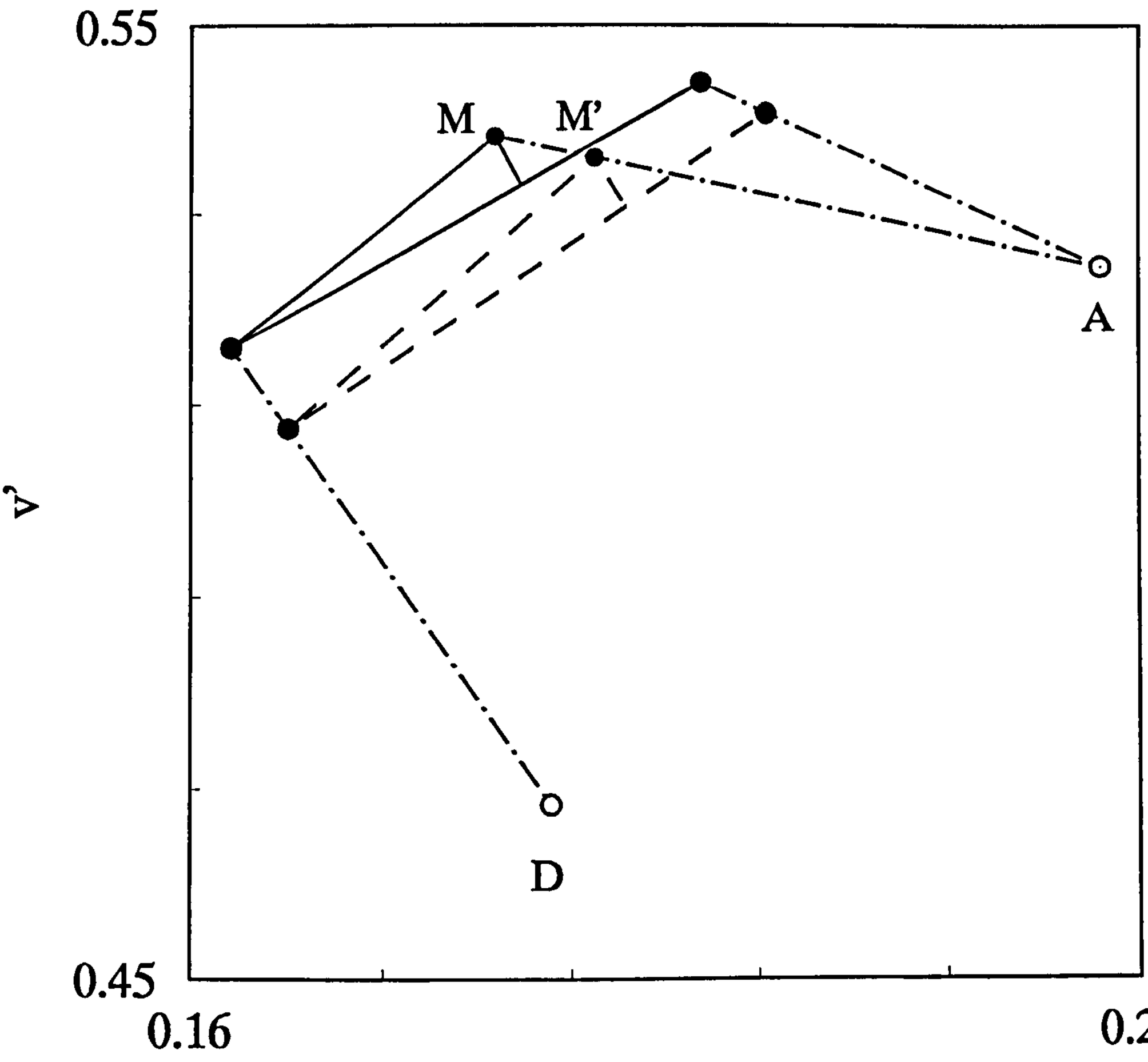

Figure 2.4.5 *Plots the same data as Figure 2.3.1, and indicates the correction for scattered light. Point M, the subject's match is recomputed to be at Point M- and the 'C' Index calculated as before using the points joined by the dashed lines.*

a different experimental subject. In both cases, it can readily be seen that the scatter correction has a significant effect on the size of the **C** Index. This effect decreases as the black border between the target and surround increases as the total amount of scattered light decreases with eccentricity of the scattering source. The correction for scatter has a larger effect for Subject PF, the oldest of the three subjects, as he has a larger stray light parameter, that is, a greater proportion of light from the surround is scattered onto the target area (see figure 2.4.4).

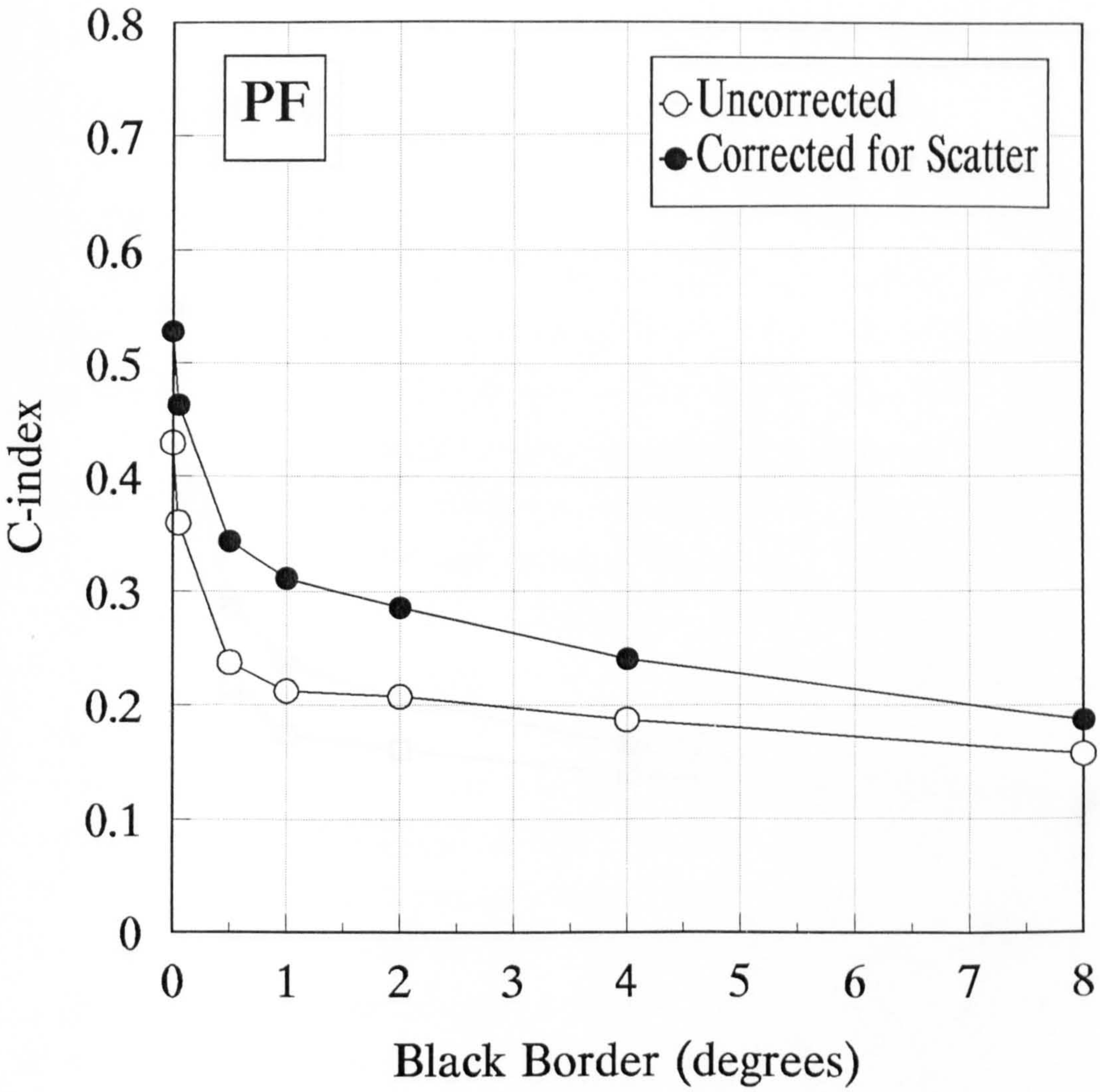

Figure 2.4.6 *Results of a colour constancy experiment for Subject PF. The 'C' Index is plotted against the side of a black border separating a uniform circular surround from the circular target. Open symbols plot the raw data in screen co-ordinates; the solid symbols plot the data corrected for the subject's scatter function.*

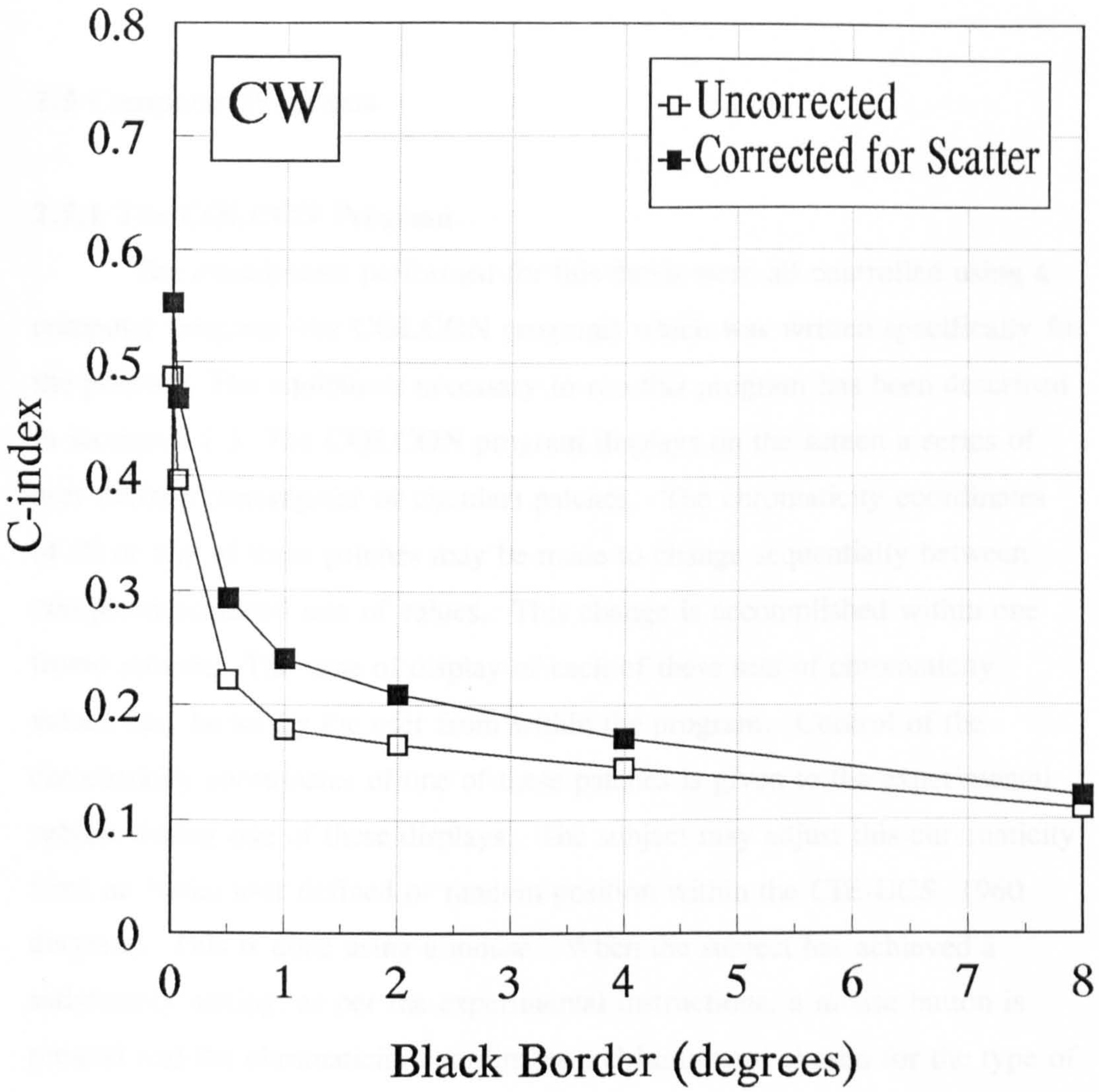

Figure 2.4.7 *Results of a colour constancy experiment for Subject CW. The 'C' Index is plotted against the side of a black border, separating a uniform circular surround from the circular target. Open symbols plot the raw data calculated in screen co-ordinates; solid symbols the data adjusted for the scatter function of this subject.*

2.5 Computer Programs

2.5.1 The COLCON Program

The experiments performed for this thesis were all controlled using a computer program (the **COLCON** program) which was written specifically for the purpose. The equipment necessary to run this program has been described in section 2.1.3. The **COLCON** program displays on the screen a series of user-defined (rectangular or circular) patches. The chromaticity coordinates of all or any of these patches may be made to change sequentially between two pre-determined sets of values. This change is accomplished within one frame refresh. The time of display of each of these sets of chromaticity values may be set by the user from within the program. Control of the chromaticity coordinates of one of these patches is given to the experimental subject during one of these displays. The subject may adjust this chromaticity from an initial user defined or random position within the CIE-UCS 1960 diagram. This is done using a mouse. When the subject has achieved a satisfactory setting, as per the experimental instructions, a mouse button is pressed and the chromaticity coordinates and luminance chosen for the type of patch are recorded. The program then displays the next experimental stimulus.

Different combinations of target chromaticity coordinates and stimulus spatial arrangements may be presented in a predetermined or random sequence and these combinations repeated for a number of iterations which is set within the program. At the end of an experimental run, the program can be instructed to file the results, including the chromaticity and luminance settings of each experimental presentation, the subject's matches, the **C** Index computed for each of these and some elementary statistics. It is also possible to set the program so that the user, rather than actively controlling the chromaticity of the test target, merely gives a two alternative forced choice

response. For example, as to whether or not a colour difference is seen. In this instance, the chromaticity of the test target is changed only in one direction of interest using a staircase procedure.

The **COLCON** program reads a series of user created files in order to define the parameters of any particular experiment. These are ASCII files, so that they may be edited using any standard editor outside the program.

The spatial arrangement of the patches in a given experiment are held in a pattern file, which contains one line of entry for each patch, this line specifying the position and size of the particular patch in screen pixels. These pattern files must be created by the user, using an ASCII editor.

To run an experiment, the program first reads a recipe file, which must also have been created by the user. This file contains the values of the global variables used by the program (although these may be changed while the program is running), and references to the other files necessary for the computation and display of the particular experiment. It is necessary to refer to the pattern file, the luminance files which will be used for each of the sequential displays and a reflectance file for each element in the pattern.

Upon reading this recipe file, the program first computes the tristimulus values of each element of the pattern under the two illuminants. These two sets of tristimulus values are then also filed and it is these tristimulus values which are produced on the screen. It is possible to set a switch within a program so that this calculation does not take place and pre-existing files of tristimulus values are read. This enables the input of tristimulus values calculated elsewhere to be used and enables the adjustment of tristimulus values calculated by the program if this is deemed necessary for any reason. At the end of each experimental run, the experimenter is prompted for a file name and the results are filed under this name.

2.5.2 The DISCON Program

The various colour constancy algorithms produce designators or lightness values for all the patches within the visual scene, but it is not immediately apparent how well they have performed. The **DISCON** program was developed to enable the direct visual comparison of the results of various algorithms, displayed simultaneously on the computer monitor. The screen is divided into four quadrants and in each quadrant either the appearance of a collection of reflecting surfaces under a chosen illuminant is displayed, or the results of one of the various colour constancy algorithms applied to that particular scene. The most common layout is to display a Mondrian under each of two illuminants in the top half of the screen, with the results of an algorithm for each illuminant displayed below. It is also possible to display a 'mondrian' occupying the full screen, but split vertically so that each side is illuminated by a different illuminant.

The program is controlled by a series of prompts on the system monitor to which the user must give appropriate numerical responses. It is used only to display the output of constancy algorithms. The files representing these must be created beforehand using the ALGOR program (see section 2.5.3) or an ASCII editor, in a similar fashion to that of the **COLCON** program. They differ from the files of the **COLCON** program in that the spatial pattern information, the reflectance functions, the illuminants and tristimulus values are all held in the one file. The assignation of a display file to each quadrant of the screen is specified in a description file and any combination of display files may be chosen.

2.5.3 The ALGOR Program

The ALGOR program is designed to read display files of section 2.5.2 and calculate the tristimulus values appropriate to the given reflectance, illuminant and algorithm combinations. The program is written as a template

so that user written algorithms may be easily embedded within the same format.

However, several algorithms have been explored. The output of any algorithm may not be in a form that is readily displayed. The convention has been adopted that the output is normalised so that a (hypothetical) white in the scene has tristimulus values each equal to the 'luminance of white' value in the display file. This is equivalent to normalising to an equi-energy illuminant. There follows a brief description of the algorithms which have been investigated:

Achromat (turns everything grey): This sets the tristimulus values of each patch to be equal to their Y value. This is useful as a demonstration that the aim of any colour constancy algorithm should not be to produce the same output for all illuminants, but that as much as possible of the original information should be preserved. It also serves to demonstrate the substantial variation in the luminance of patches illuminated by different illuminants.

AreaInt (integrated to grey): This measures the relative area of each patch to be displayed, taking account of any overlapping. It does this by examining each pixel of the TIGA screen to see which patch it finally appears in and incrementing a counter for that patch. Since this is a slow operation, the option is given of providing a sample of the pixels; one in 25 is probably adequate. The tristimulus values of each patch are then weighted by the relative displayed area of that patch and the weighted mean values of X, Y and Z are calculated. Since a patch with these tristimulus values is to be displayed as an equal energy grey, the X value for each patch is multiplied by the factor Y(mean)/X(mean) and similarly for Z. The Y value is left unchanged. The effect of this is to leave all patches at their input luminance

and adjust their chromaticities, so that the mean will have X = Y = Z. The function returns a low plausibility if there is only one patch in the pattern.

Highlight (the brightest patch is white): The Y tristimulus value of each patch is examined and the tristimulus values of the one with the highest Y value are used for normalising as above. The function returns a low plausibility if the brightest patch is less than twice the luminance of any other patch.

MaxLight (the maximum lightness in each channel represents white): All the tristimulus values are examined, and the highest individual values of X, Y and Z are selected as the normalising factors as above. The function returns a low plausibility of any of the highest X, Y or Z values is less than twice as large as the next highest corresponding value.

Retinex2 (a simplified version of Land's Retinex algorithm): This carries out Land's algorithm by directly comparing the log contrast of each tristimulus value of each patch with a large number (defined in the program as paths) of randomly selected pixels in the display. The assumption is made that there is not an illuminant gradient, so no thresholding step is necessary, and only the first and last points of Land's paths need to be considered. This is equivalent to computing a geometric mean, weighted by area, in each tristimulus channel and normalising that to 'white'.

At first it might be assumed that the most important measure is the similarity of output for a given algorithm applied to different conditions of illumination. However, it is also important to preserve as much as possible of the information present in the initial scene. An example of this is the *achromat* algorithm, which produces output very similar for a wide range of illuminants, but is clearly not appropriate as a colour constancy algorithm. It

should be borne in mind that in observing the results displayed on the screen, the observers apply the colour constancy of their own visual system. This tends to make the output appear more similar. Each of the algorithm described above could be made to perform well if the appropriate illuminant reflectance combinations were chosen. Equally, by judicious choice of conditions it was possible to demonstrate failures.

The main use of these programs has been for display and demonstration purposes and they have not been discussed further in this thesis.

Chapter 3. Illuminant Aspects of Instantaneous Colour Constancy

Chapter 3. Illuminant Aspects of Instantaneous Colour Constancy

3.1 Background

The purpose of this chapter is to present data from experiments which were carried out as a result of questions posed by the colour constancy models and algorithms discussed in Chapter One. Each of these algorithms makes certain implicit or explicit assumptions about the nature of the illumination and of the scene which is illuminated in order to arrive at colour constant designators, such as those described by Land and McCann (1971) and the various lightness algorithms summarised by Hurlbert (1986) or to deconfound the effects of illuminant and reflectant to arrive at illuminant invariant descriptions of the surface reflectants (Maloney & Wandell, 1986; D'Zmura & Lennie, 1986).

Land's original Retinex model incorporates an algorithm which calculates lightness values within each cone system. In fact, the principle underlying this model is akin to a Von Kries-type recalibration (Jameson & Hurvich, 1989; Valberg & Lange-Malecki, 1990). In the Von Kries colour transformation scheme, the output of each receptor is recalibrated so as to compensate for changes in the colour signal elicited by a (perfect) white reflector. That is, there is a linear scaling relative to a (reference) white. Land later suggested that this normalisation procedure could take place in each of his lightness channels separately (Land & McCann, 1971) and further that it may not be restricted to simply cone channels but may take place in any putative second stage channel which is a linear combination of the cone inputs (Land, 1983), such as the colour opponent channels. All other lightness algorithms are essentially derivatives of, or extensions to Land's original, this formal connection having been shown by Hurlbert (1986). Hurlbert states that

the process which she calls "spectral normalisation" must make some form of "grey world assumption". That is, the individual lightness channels are normalised with respect to some form of average value for that channel derived from the scene, although the averaging procedures, spatial sampling and boundary conditions vary considerably. It is therefore of particular interest to investigate the effect on colour constancy of varying the lightness values of our coloured target with respect to the scene average. This is achieved by using a simple centre surround paradigm consisting of a central target patch and a neutral surround and conducting experiments for which the luminance contrast between centre and surround is varied. These experiments are discussed in Section 3.3. It was also necessary to carry out control experiments, in which the global luminance of the whole scene was varied, as this enabled a wider range of contrast values to be achieved between target and surround. These global luminance experiments are described in Section 3.2. There is some evidence showing that (local) contrast, rather than lightness, is the stimulus variable, which underlies the computation of colour constancy (eg Fairchild & Lennie,1992; Shapley, 1986; Walraven et al., 1991; Lucassen & Walraven, 1993). If this is the case, it is interesting to investigate the form which this contrast variable takes. A subtractive measure of contrast between centre and surround would increase as global luminance increases, whereas a multiplicative one would not. These global luminance experiments have shed some light on this question.

The experiments of this thesis require that the subject is presented with the simulated appearance of a collection of Munsell chips under two illuminants usually chosen to be CIE illuminants D_{65} and A. It is important, then, to eliminate the choice of specific illuminants as of material importance in these results. To this end, experiments were carried out in which the size of the illuminant shift between pairs of illuminants selected from the Planckian locus was varied. These experiments are discussed in Section 3.4.

A series of colour constancy algorithms have been described in the literature which attempt to decouple and recover spectral descriptions of lights

and reflecting surfaces. See Lennie & D'Zmura (1988) for a summary and D'Zmura and Iveson (1993a; 1993b) for a formal exposition of models of this type. These all make assumptions with regard to the parameters which are necessary to represent the various light sources and reflecting surfaces. Essentially, they require that the illuminants may be represented by a linear sum of band limited basis functions (Maloney & Wandell, 1986) and that the visual system has a priori knowledge of the form of these basis functions. If this is the case, then colour constancy should be significantly impaired if unnatural illuminants which cannot be well represented by these basis functions are used in the colour constancy experiments. Data from experiments of this type are presented in Section 3.5.

The experimental technique employed in all the experiments of this chapter was that of the dynamic colour matching paradigm described in Chapter Two. This technique has the advantage of eliminating the long term temporal adaptation of the visual system to one or other of the illuminants employed; rather, the experimental subjects adapt for 10 minutes to the chromaticity and luminance of the two illuminants that are used in the experiment. The sequential flipping of the illuminants is the same as when the experiment is carried out. It has been shown that a long term adaptation of the photoreceptors could partially account for colour constancy (Worthey,1985; Worthey & Brill, 1986; Brill & West, 1986). These experiments do not address this question, but instead attempt to elucidate the properties of the second stage, which must involve near instantaneous mechanisms.

The use of the **C** index enables the degree of colour constancy achieved to be quantified and hence compared between experimental conditions. This in turn enables us to question the assumptions of colour constancy algorithms which have been presented in the literature. The experiments described in this chapter deal only with those properties of colour constancy which vary with the illuminant and with the reflectance properties of the experimental target element. To this end, the experiments all employed

a centre surround paradigm in which the subject was presented with a central circular target element subtending 1.5° of visual angle and a circular uniform neutral surround which subtended 15° of visual angle (Valberg and Lange-Malecki, 1989). Parameters effecting the illumination and reflectance properties of the target element were varied, but not those effecting the spatial configuration of the scene. All results shown have been corrected for scattered light as described in chapter 2. This does not effect the conclusions as there is little difference between values of **C** corrected for scattered light and those uncorrected for young normal subjects.

3.2 The Effect of Global Luminance

3.2.1 Method

Experiments were carried out to investigate the effect of global luminance on our measure of colour constancy. The centre surround arrangement described in the previous section and the dynamic colour matching paradigm described in chapter 2 were used. The surround was uniform, of reflectance 0.44, while the target area consisted of one of the four Munsell chips 10GY5/6, 5YR5/6, 7.5P5/6 and 10BG5/6. Although these Munsell chips all have the same Munsell value, their luminance under different illuminants does vary slightly. For this reason a small adjustment was made to their reflectance functions, which were scaled so that they all gave the same luminance value under the D_{65} illuminant whilst maintaining the expected chromaticity. This value was 0.24 of that which would be given by a perfect reflector. It is approximately the mean of the four values given by the original Munsell reflectance functions and provides a log luminance contrast with the surround of -0.6. This level of luminance contrast was used in all these experiments assessing the effect of global luminance. The luminance contrast is maintained when the surround is illuminated by both reference and test illuminants. This is because the luminance which the target has under the reference illuminant is used for the random start point of the user controllable target (the appearance of the target under the test illuminant is not usually displayed). The subjects had control of the target luminance along with its chromaticity, but did not need to adjust it to achieve a satisfactory match.

The experimental program contains a switch which allows the setting of the level of illumination. It is specified in terms of the luminance which a perfect reflector would have if there were one in the scene. Four values of this switch were chosen as the independent variable of these experiments; they were 20, 40, 80 and 120 cd/m^2. These values gave luminances of the surround element as 8.8, 17.6, 35.2 and 52.8 cd/m^2 respectively. Experiments

were carried out on two subjects: CW a 27 year old male with uncorrected vision and subject PF a 63 year old male who wore an optical correction for all the experiments of this thesis. Both subjects could read all the Ishihara isochromatic plates and complete the Farnsworth-Munsell 100 hue test without significant error. Testing with the Nägel anomaloscope revealed a normal matching range, but slight displacement towards the deuteranomalous direction for subject CW. As the data from the experiments were averaged over the colours employed, this was not taken to be significant. The dynamic colour matching paradigm described in chapter 2 was used, each of the four colours was presented in random order to the subject five times during each experimental session. Each subject carried out two experimental sessions, giving a total of ten colour matches, contributing to each point.

3.2.2 Results and Discussion

Figure 3.2.1 plots the mean **C** index of the four colours against the surround luminance for each of the two subjects. The error bars show 95% confidence limits obtained from the estimate of standard error in analysis of variance described below. It is possible that the **C** index measurements would vary with both the level of global luminance chosen and the particular target colour, and that there might be an interaction between these two factors. To test this, the data was modelled using a cross classification model, analysis of variance. As the target colours and the levels of the luminance switch are selected from larger sets the model is fully randomised. Individual data points x (measurements of C index) are categorised into i=(1..A) rows (levels of global luminance) and j=(1..B) columns (target colours), k=(1..n) observations are made for each row/column combination. The data are then modelled as:

$$x_{ijk} = \mu + a_i + b_j + + c_{ij} + e_{ijk} \qquad (3.2.1)$$

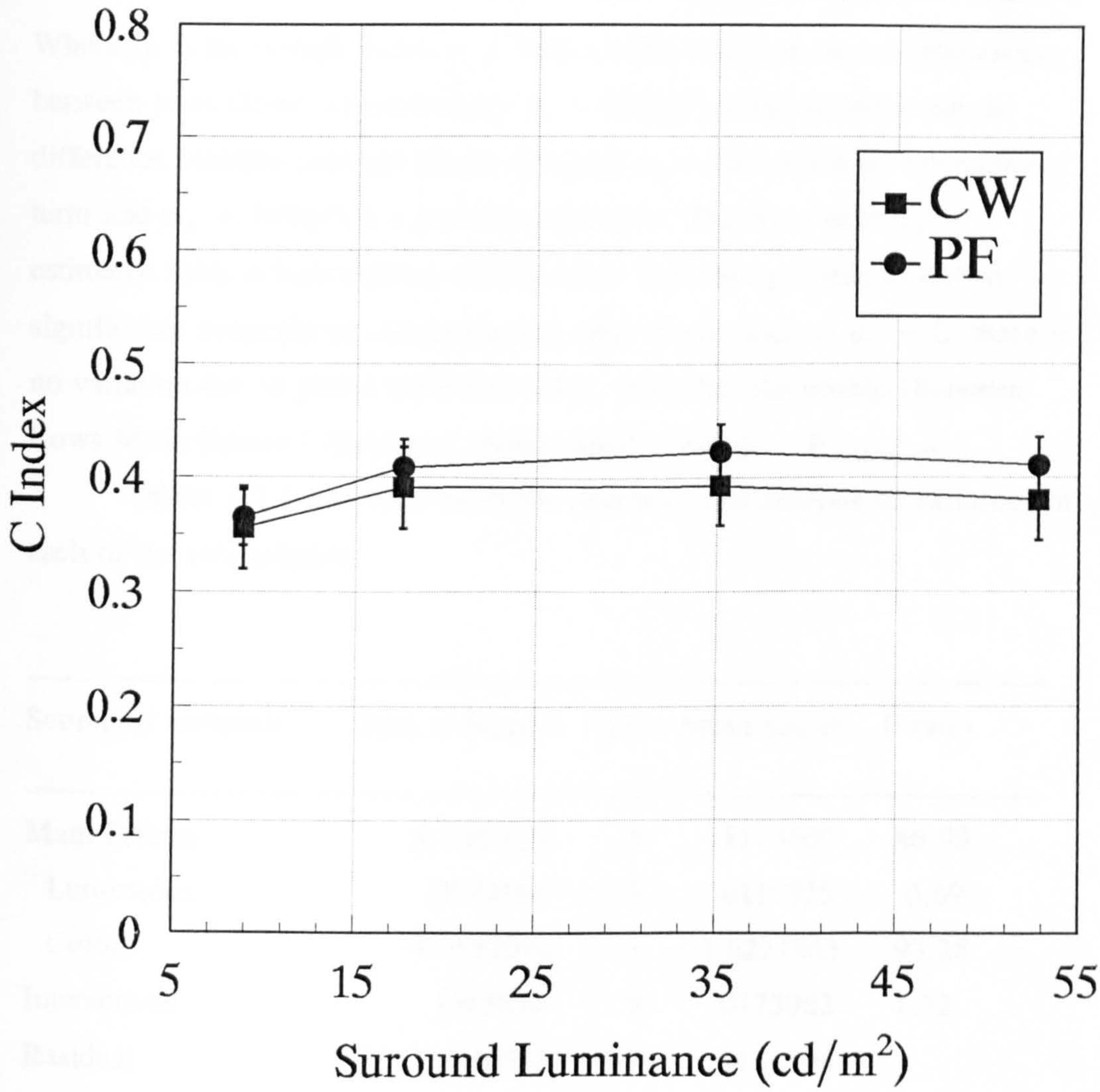

Figure 3.2.1 *C index measurements are plotted against the luminance of the uniform neutral surround field. Data are plotted for two subjects.*
The contrast between experimental target and surround was -0.6 and remained constant throughout this experiment. It can be seen from the data that changing the level of global luminance does not affect significantly our measurements of the **C** *index.*

Where, μ is the overall mean, $a_i \sim N(0,\sigma_a^2)$ the variation due to differences between rows (levels of luminance), $b_j \sim N(0,\sigma_b^2)$ is the variation due to difference between columns (target colours), $c_{ij} \sim N(0,\sigma_c^2)$ is an interaction term and $e_{ijk} \sim N(0,\sigma^2)$ is a residual error term. The error term e_{ijk} is estimated using a least squares minimisation. It is then possible to test for significance assumptions concerning the other terms; such as $\sigma_a^2 = 0$, there is no variation due to global luminance level, from the relationship (Between Rows Mean Square / Between Columns Mean Square) $\sim F_{(A-1),(A-1)(B-1)}$.

Tables 3.2.1 and 3.2.2 show the results of this analysis of variance for each of the two subjects.

Source of variation	Sum of Squares	d.f.	Mean square	F-ratio
Main Effects	4.9041654	6	.8173609	46.99
Luminance	.0359564	3	.0119855	0.69
Colour	4.8682090	3	1.6227363	93.28
Interactions	.1565654	9	.0173962	1.32
Residual	1.8936583	144	.0131504	
Total	6.9543891	159		

Table 3.2.1 *Analysis of variance for C index against global luminance, subject CW.*

The level of global luminance does not have a significant effect for subject CW ($p > 0.1$). For subject PF the effect is significant at the 95% level, but not the 99% level ($p > 0.025$) and the F ratio for the luminance effect is much smaller than that for the colour effect. Figure 3.2.1 shows this with the **C** index remaining constant against surround luminance with perhaps a small decrease as the surround luminance enters the near mesopic. From these results we may conclude that the level of global luminance does not affect our

measurements of **C** index and therefore this parameter need not be considered a critical factor in the luminance contrast experiments of the next section. Since these measurements were carried out similar results were also reported by Lucassen & Walraven (1993).

Source of variation	Sum of Squares	d.f.	Mean square	F-ratio
Main Effects	4.2375280	6	.7062547	109.08
Luminance	.0793771	3	.0264590	4.07
Colour	4.1581508	3	1.3860503	214.06
Interactions	.0582739	9	.0064749	1.06
Residual	.8765620	144	.0060872	
Total	5.1723639	159		

Table 3.2.2 *Analysis of variance for C index against global luminance, subject PF.*

3.3 The Effect of Luminance Contrast at the Border

3.3.1 Method

The contribution of the luminance contrast component between the test target and the surround was investigated using the same spatial configuration and Munsell chip reflectance functions as described in Section 3.2.1. The reflectance functions of the four Munsell chips were again scaled so that they gave equal luminance values under Illuminant D_{65} (the appearance under Illuminant A is not actually reproduced). Various such scale reflectances were presented against a neutral surround. Luminance contrast is defined as $\log_e(Y_T/Y_B)$, where Y_T is the luminance of the test target and Y_B of the surround and it is the independent variable in these experiments.

Table 3.3.1 details the luminances of target and surround elements used to achieve the indicated contrasts. Note that at high positive contrast the reproducibility of the target becomes a problem, so the illuminance of the target element is fixed and that of the neutral surround is lowered. The experiments of the previous sections suggest that this should not significantly affect the results.

Contrast	-1.2	-0.8	-0.6	0.0	0.2	0.6	0.8
Y_T	10.64	15.84	19.2	35.2	35.2	35.2	35.2
Y_B	35.2	35.2	35.2	35.2	28.8	23.6	15.84

Table 3.3.1 *Luminance values used to achieve indicated contrasts for experiments on the dependency of C index on contrast between test target and surround.*

Von Kries colour constancy requires a normalisation procedure which depends on the highest luminance or lightness value in a given channel observed in the scene (Worthey, 1985). This is also true of other algorithms (e.g. Brill, 1978). As the luminance of the target relative to the surround is

raised, it might be expected then that there is a discontinuity in the measured colour constancy around the isoluminant point. In order to investigate this further, experiments were carried out over a narrow range of contrasts about the isoluminant point. To account for possible differences in the photopic luminosity function of the two subjects, the luminance of the surround element under Illuminant A and of each of the target colours under Illuminant D_{65} were matched to that of the luminance of the surround element under D_{65} using heterochromatic flicker photometry, neither subject differed substantially from the CIE V(λ) function. The experiments were then repeated using a small range of luminance contrast around the isoluminant point. Table 3.2.2 details the range of luminance contrasts chosen and the luminance level necessary to achieve these for each subject.

Contrast	-0.05	-0.02	0.0	0.02	0.05
Y_T	35.2	35.2	35.2	35.2	35.2
Y_B	33.483	34.503	35.2	35.91	37.0

Table 3.3.2 *Luminance values used to achieve indicated contrasts for experiments on the dependency of C index on contrast between test target and surround, low contrast range.*

3.3.2 Results

Figure 3.3.1 plots the mean **C** index of the four colours against the luminance contrast between target and surround for each of the two subjects. The error bars show 95% confidence limits obtained from the estimate of standard error in analysis of variance. Tables 3.3.3 and 3.3.4 detail this analysis of variance.

Figure 3.3.1 shows a function which seems to decrease at both high and low levels of luminance contrast with a peak at $\log_e$(contrast) = -0.6. The analysis of variance, which compares the variation across luminance contrasts with the variation within each contrast-colour combination, is detailed below

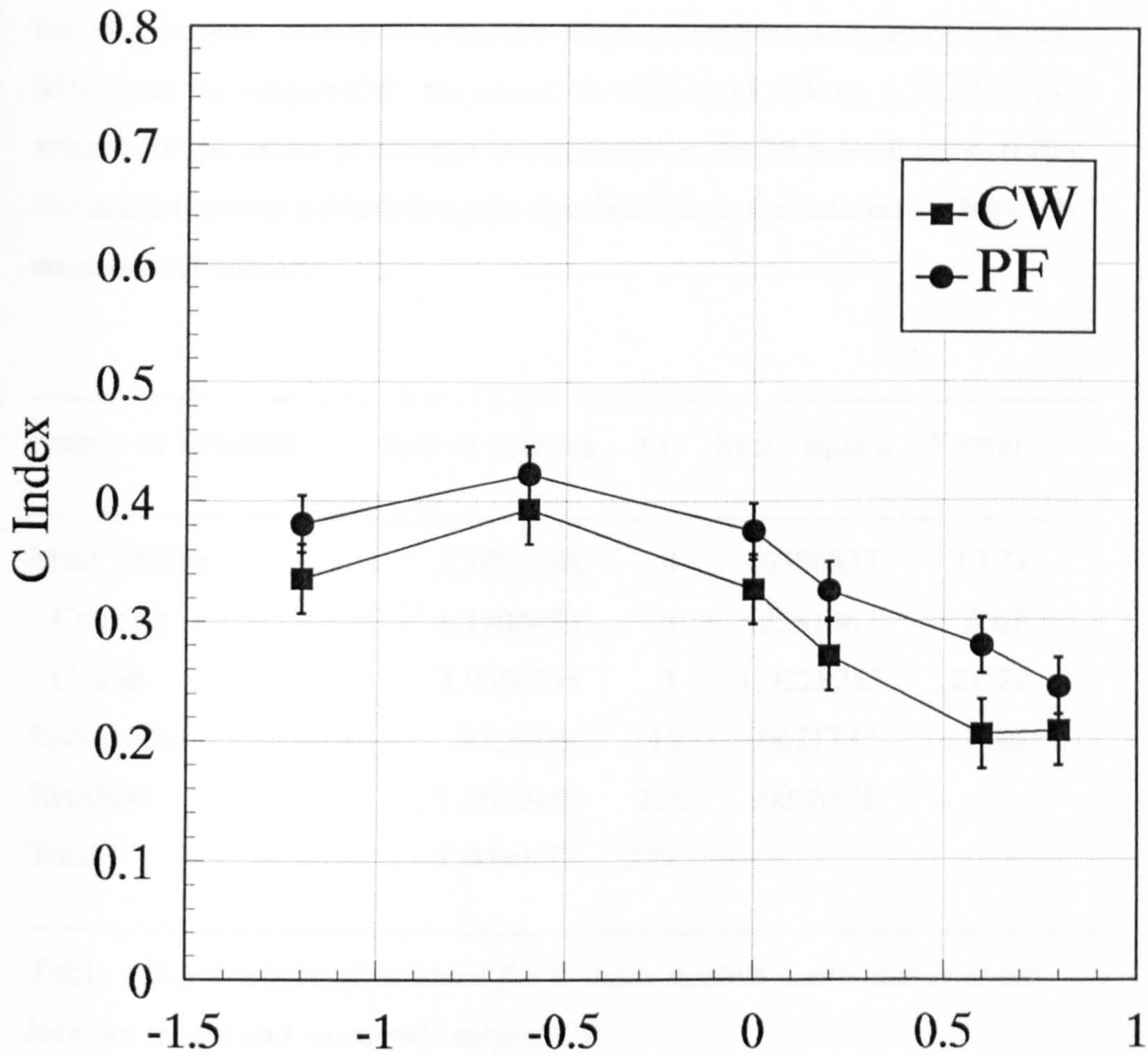

Figure 3.3.1 *C index measurements are plotted against luminance contrast between target and surround. Data are plotted for two subjects. Contrast is defined as* Log_e *(luminance of target/luminance of surround). The error bars are 95% confidence limits calculated from the estimate of standard error obtained from the analysis of variance.*

for each subject. This shows that the effect of contrast is significant at the 95% level for subject CW, but not at the 99% level CW ($p > 0.025$). For subject PF the effect of contrast is significant at the 99% level ($p < 0.01$). Variation between colours is again significant as is the interaction between contrast and colour.

Source of variation	Sum of Squares	d.f.	Mean square	F-ratio
Main Effects	5.1093098	8	.6386637	10.27
Contrast	1.1406833	5	.2281367	3.67
Colour	3.9686265	3	1.3228755	21.28
Interactions	.9326729	15	.0621782	7.20
Residual	1.8660445	216	.0086391	
Total	7.9080272	239		

Table 3.3.3 *Analysis of variance for C index against luminance contrast between target and surround, subject CW.*

Source of variation	Sum of Squares	d.f.	Mean square	F-ratio
Main Effects	4.2298543	8	.5287318	19.72
Contrast	.9118639	5	.1823728	6.80
Colour	3.3179904	3	1.1059968	41.24
Interactions	.4022745	15	.0268183	4.730
Residual	1.2245601	216	.0056693	
Total	5.8566889	239		

Table 3.3.4 *Analysis of variance for C index against luminance contrast between target and surround, subject PF.*

Figure 3.3.2 plots the mean **C** index of the four colours against the luminance contrast between target and surround for a low range of contrasts close to isoluminance, for each of the two subjects. The error bars show 95% confidence limits obtained from the estimate of standard error in analysis of variance. Tables 3.3.5 and 3.3.6 detail this analysis of variance.

Source of variation	Sum of Squares	d.f.	Mean square	F-ratio
Main Effects	3.0464264	7	.4352038	99.84
Contrast	.0812762	4	.0203190	4.66
Colour	2.9651502	3	.9883834	226.70
Interactions	.0523073	12	.0043589	.694
Residual	1.1308246	180	.0062824	
Total	4.2295584	199		

Table 3.3.5 *Analysis of variance for **C** index against luminance contrast (low contrast range) between target and surround, subject CW.*

Source of variation	Sum of Squares	d.f.	Mean square	F-ratio
Main Effects	2.3566003	7	.3366572	78.12
Contrast	.0249191	4	.0062298	1.45
Colour	2.3316812	3	.7772271	180.36
Interactions	.0517102	12	.0043092	.735
Residual	.7031481	120	.0058596	
Total	3.1114585	139		

Table 3.3.6 *Analysis of variance for **C** index against luminance contrast (low contrast range) between target and surround, subject PF.*

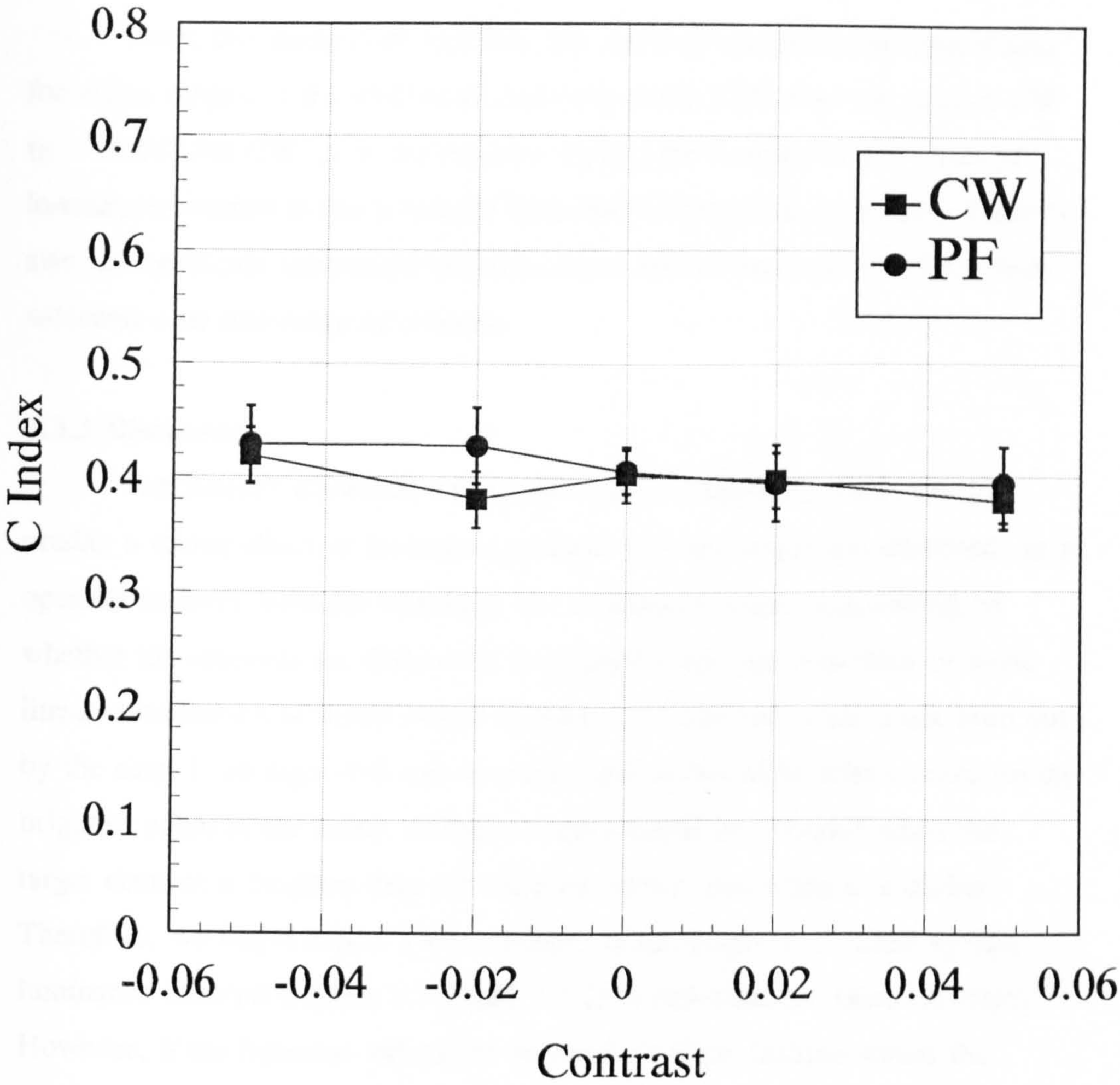

Figure 3.3.2 *C index data are plotted against luminance contrast between target and surround. Contrast is as defined for* ***Figure 3.3.1****. Data are plotted for two subjects. The error bars are 95% confidence limits calculated from the estimate of standard error obtained in the analysis of variance. The data of this figure plot the results of similar experiments to those of* ***Figure 3.3.1****, but a much smaller range of luminance contrasts are used close to the isoluminant point.*

From this analysis of variance, the effect of contrast is not significant for either subject at the 99% level, but is so at the 95% level for subject CW ($p > 0.025$ for CW, $p > 0.1$ for PF). Again, the F ratio for the effect of luminance contrast is much smaller than that for the effect of colour. There is also no significant interaction between colour and contrast ($p > 0.1$ for both subjects) over this range of contrast.

3.3.3 Discussion

The Retinex algorithm and its derivatives (Hurlbert, 1986) would predict a strong effect of luminance contrast between target and surround, as it operates in three lightness channels, one or more of which (depending on whether the channels are defined by individual cone type responses or some linear combination of them) would increase with contrast. This is not born out by the data. If an algorithm uses a normalisation procedure which relies on the brightest patch in the scene, different results would be obtained when the target element is brighter than the surround rather than when it is darker. Therefore, we might expect a discontinuity in the graph of **C** index against luminance contrast (figures 3.3.1 and 3.3.2) at isoluminance (zero contrast). However, if the lightness values are averaged in some fashion across the whole scene, including the target element, then increasing the luminance of target would increase its contribution to these averages and the **C** index should monotonically decrease as luminance increases. Neither of these is the case.

Figure 3.3.1 shows a decrease in **C** index at high positive contrasts (target brighter than surround). It is possible that the mechanisms which mediate instantaneous colour constancy operate differently when the target is significantly brighter than the surround and that the lightnesses are averaged across the whole scene. This would lead to the observed decrease in the effect of the surround on the target as the target made a larger contribution to the lightness average in each channel. However it should be borne in mind that the level of the subjects' adaptation was to the light level of the surround. If the opponent colour channels are driven to their limits (as may happen for

very bright targets), they will saturate and it will no longer be possible to alter their relative values (that is observe the effects of constancy).

These data and those of the previous section suggest that instantaneous colour constancy is mediated through channels which exclude the effect of luminance, over a wide range of luminance contrasts. Some form of simultaneous contrast mechanism in the colour opponent channels seems the best mechanism. This is consistent with suggestions put forward by Valberg and Lange-Malecki (1989) and with Tiplitz Blackwell and Buchsbaum (1988a).

3.4 Size of Illuminant Shift

3.4.1 Method

Experiments were carried out to investigate the effect of changing the size of the illuminant shift on the measurements of **C** index. Eight illuminants were chosen to give four shift sizes, within the range of normally occurring illuminant shifts. These illuminants were selected from the Planckian locus, which lies very close to the daylight locus (Wyszecki & Styles, 1982). Planckian illuminants at 6,500K and 2,855K are very similar to the CIE illuminants D_{65} and A respectively and are visually indistinguishable from them. These two illuminants were chosen and three further pairs were selected; two with a smaller difference in colour temperature (and hence chromaticity) and one pair with a larger. The illuminants were chosen so that for each pair, each illuminant was equidistant in mireds (a more perceptually uniform scale) from the midpoint of the 6,500K to 2,855K shift. The colour temperatures and the equivalent mired values for the illuminant shifts chosen are given in Table 3.4.1.

Colour Temperature (k)		Shift	Equivalent Mireds		Shift
7353	2717	4636	136.00	368.05	232.05
6500	2855	3645	153.85	350.26	196.41
5495	3110	2385	181.98	321.54	139.56
4854	3355	1499	206.02	298.06	092.04

Table 3.4.1 *Colour temperatures and equivalent mireds for the different illuminant shift sizes. 1 mired = $(10^6/T_c)$*

Experiments were carried out on three subjects. Subjects CW and PF are described above, subject DW, a 27-year old male who had uncorrected vision and normal colour vision as assessed by the Farnsworth-Munsell 100 Hue Test and the Rayleigh Anomaloscope. Each experimental session

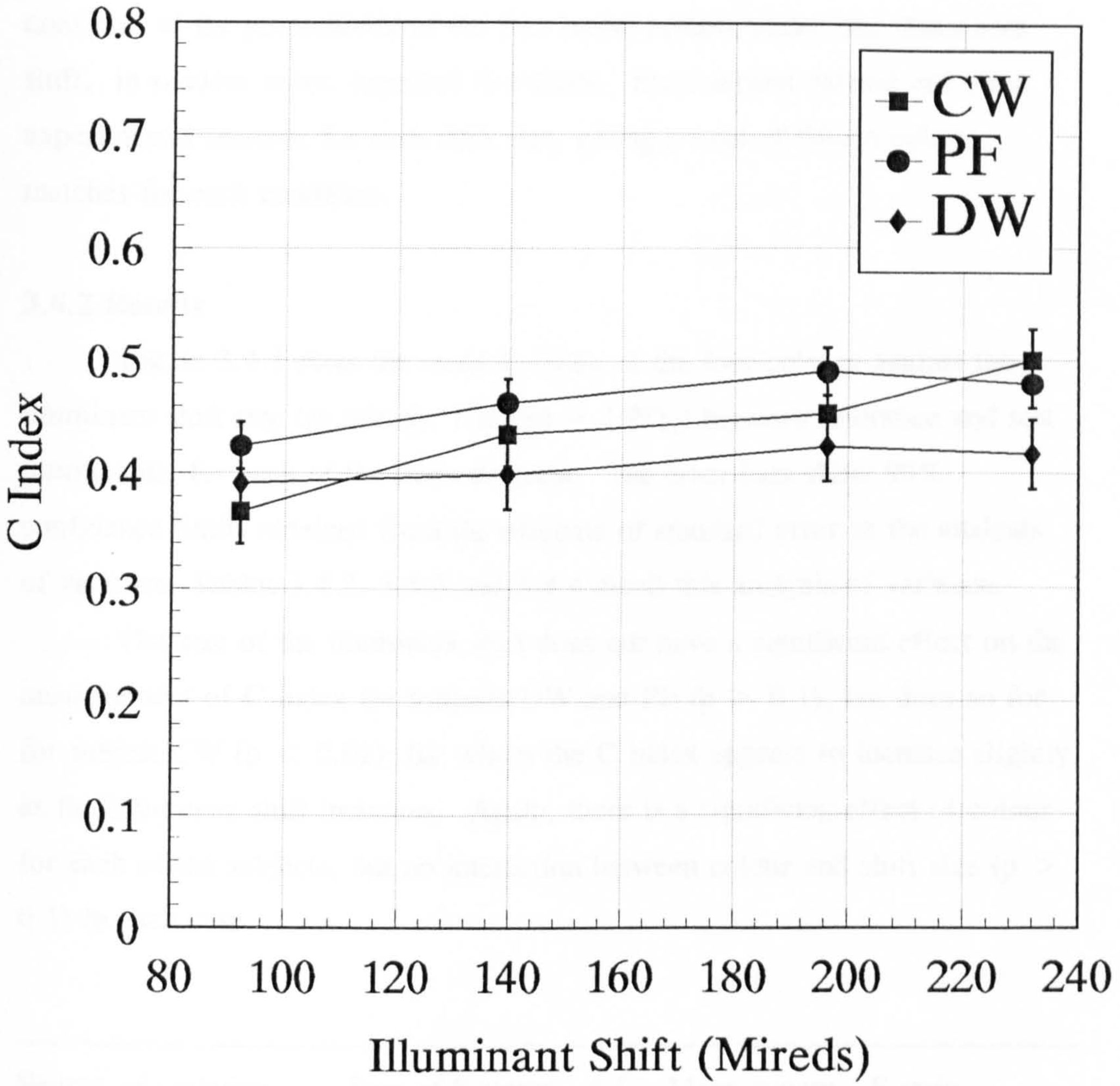

Figure 3.4.1 *Data for C index measurements are plotted against the difference between the reference and test illuminants used in the experiment. The illuminant shift data are plotted as a difference in the mired values of the two illuminants (one mired equals $10^6/T_c$ where T_c is the colour temperature of the illuminant on the Planckian locus). Data are plotted for three subjects. The error bars are 95% confidence limits calculated from the estimate of standard error obtained from the analysis of the variance.*

consisted of the presentation of the four target colours under one illuminant shift, in random order, repeated five times. Each subject carried out three experimental sessions for each shift size, giving a total of fifteen colour matches for each condition.

3.4.2 Results

Figure 3.4.1 plots the mean **C** index of the four colours against the illuminant shift size (in mireds, 1 mired = $10^6/T_c$) between reference and test illuminants, for each of the three subjects. The error bars show 95% confidence limits obtained from the estimate of standard error in the analysis of variance. Tables 3.4.2, 3.4.3 and 3.4.4 detail this analysis of variance.

The size of the illuminant shift does not have a significant effect on the measurement of **C** index for subjects DW and PF ($p > 0.1$), but does so for for subject CW ($p < 0.01$), for whom the **C** index appears to increase slightly as the illuminant shift increases. Again, there is a significant effect of colour for each of the subjects, but no interaction between colour and shift size ($p > 0.1$) in each case.

Source of variation	Sum of Squares	d.f.	Mean square	F-ratio
Main Effects	5.5731792	6	.9288632	78.73
Illuminant shift	.5448581	3	.1816194	15.39
Colour	5.0283211	3	1.6761070	142.07
Interaction	.1061787	9	.0117976	.98
Residual	2.7056554	224	.0120788	
Total	8.3850133	239		

Table 3.4.2 *Analysis of variance for C index against Luminance shift size along the Planckian locus, subject CW.*

Source of variation	Sum of Squares	d.f.	Mean square	F-ratio
Main Effects	1.0255629	6	.1709272	13.72
Illuminant shift	.0270956	3	.0090319	0.72
Colour	.9984674	3	.3328225	26.72
Interaction	.1120876	9	.0124542	1.31
Residual	1.3719867	144	.0095277	
Total	2.5096372	159		

Table 3.4.3 *Analysis of variance for C index against Luminance shift size along the Planckian locus, subject DW.*

Source of variation	Sum of Squares	d.f.	Mean square	F-ratio
Main Effects	4.7706905	6	.7951151	36.24
Illuminant shift	.1494255	3	.0498085	2.27
Colour	4.6212650	3	1.5404217	70.21
Interaction	.1974643	9	.0219405	3.25
Residual	1.5118516	224	.0067493	
Total	6.4800063	239		

Table 3.4.4 *Analysis of variance for C index against Luminance shift size along the Planckian locus, subject PF.*

3.4.3 Discussion

Tiplitz Blackwell and Buchsbaum (1988a) suggest that " colour constancy is strong enough to eliminate perceptual differences caused by slightly different illuminants, but it can only partly remove perceptual

differences caused by extremely different illuminants." However they make this judgement on the basis of the size of colour shift induced in their experiment. When this colour shift is compared with the appropriate expected shift, as is the case in the calculation of the **C** index, instantaneous colour constancy remains approximately the same across illuminant shifts.

This observed independence of the size of illuminant shift would be expected of an algorithm which made use of a priori knowledge of the properties of the Planckian locus (Lennie and D'Zmura, 1988), or the daylight locus (Wyszecki and Stiles, 1982) to which it is very similar. However, it would also be expected of a mechanism which directly compared contrasts across channels.

3.5 Natural versus Unnatural Illuminants

3.5.1 Method

Experiments were conducted to investigate the dependency of the **C** index on the use of unnatural, rather than natural illuminant shifts. Two experiments are described in this section. In the first experiment, **C** index measurements for the 6,500k to 2,855k illuminant shift along the Planckian locus are compared with measurements for an "equivalent" shift between two artificial illuminants. In the second experiment, different shift sizes of artificial illuminants "equivalent" to those of the previous section are investigated. For a given pair of illuminants on the Planckian locus, a pair of artificial illuminants with an "equivalent" difference between them are generated in the following manner. The line joining the chromaticity coordinates of the two illuminants of the Planckian locus in CIE-UCS space is found. A perpendicular of the same length is constructed through its midpoint to define two new chromaticities; one which may be referred to as "magenta" and the other as "green", in terms of their location on the UCS diagram. Linear combinations of the radiance outputs of the three monitor phosphors are then found which have these chromaticities. The wavelength radiance distributions of our artificial illuminants were then defined by these combinations. This method produces artificial illuminants which, to a good approximation, have the same colour temperature and so are not well distinguished by any illuminant model which relies on basis functions derived from naturally occurring illuminants. Figure 3.5.1 shows the relative spectral radiance distribution of two of the illuminants from the Planckian locus and the magenta "equivalent" illuminant. Figure 3.5.2 shows the chromaticity coordinates of the illuminants at 6,500k and 2,855k from the Planckian locus and of their artificial "equivalents"; it also shows the chromaticity coordinates of each of the four Munsell chips used as targets in this experiment under each illuminant.

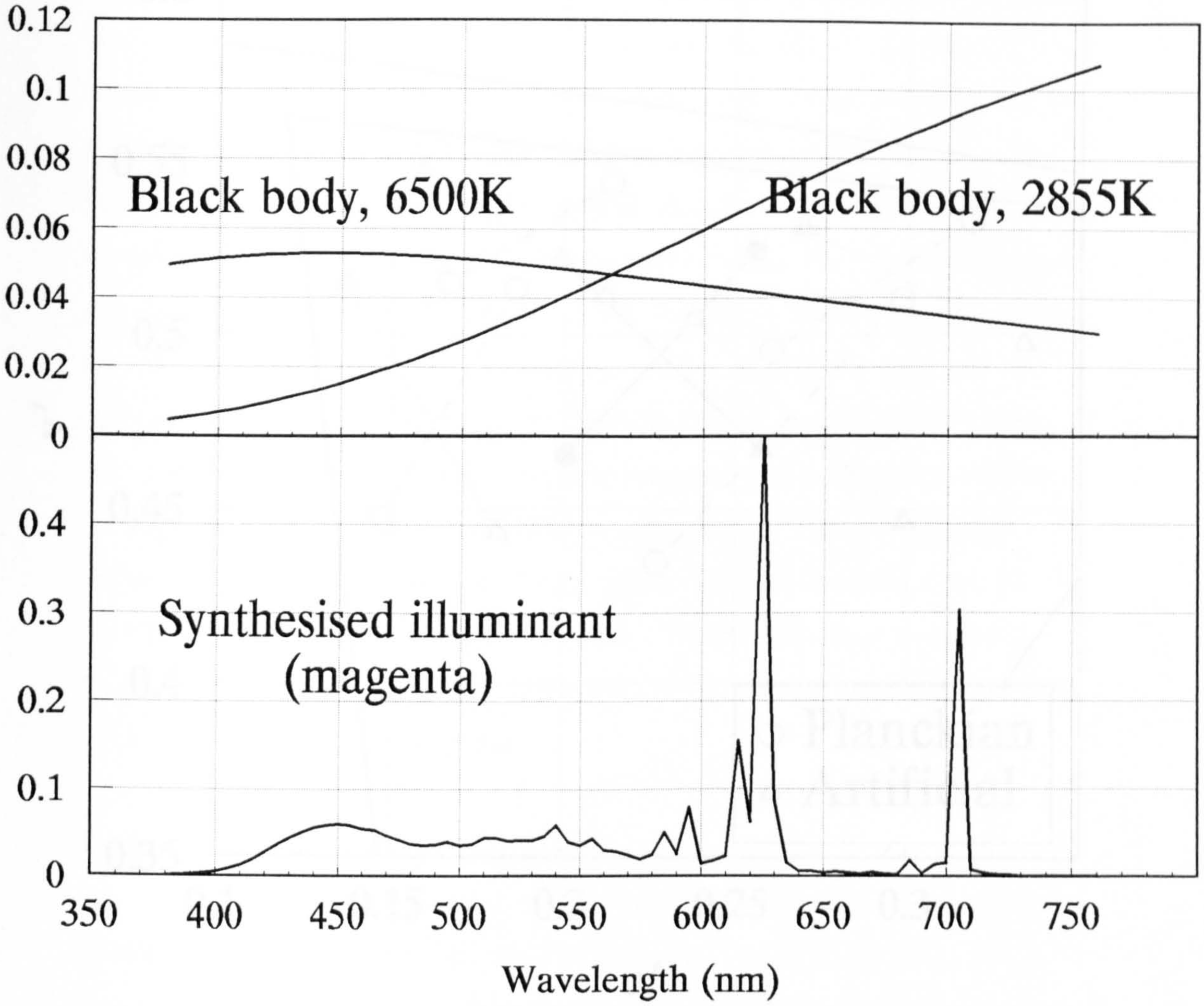

Figure 3.5.1 Relative spectral radiance distributions for illuminants used in the artificial versus natural illuminant experiments. The illuminants are normalised so that a perfect reflector so illuminated would have a luminance of 1cd/m^2. The upper portion shows the distribution for two illuminants from the Planckian locus (Wysecki & Styles, 1984) with the indicated colour temperatures. The lower portion shows one of the artificial illuminants (magenta) constructed from linear combinations of the monitor phosphor outputs. The sharp peaks of the red phosphor can readily be seen.

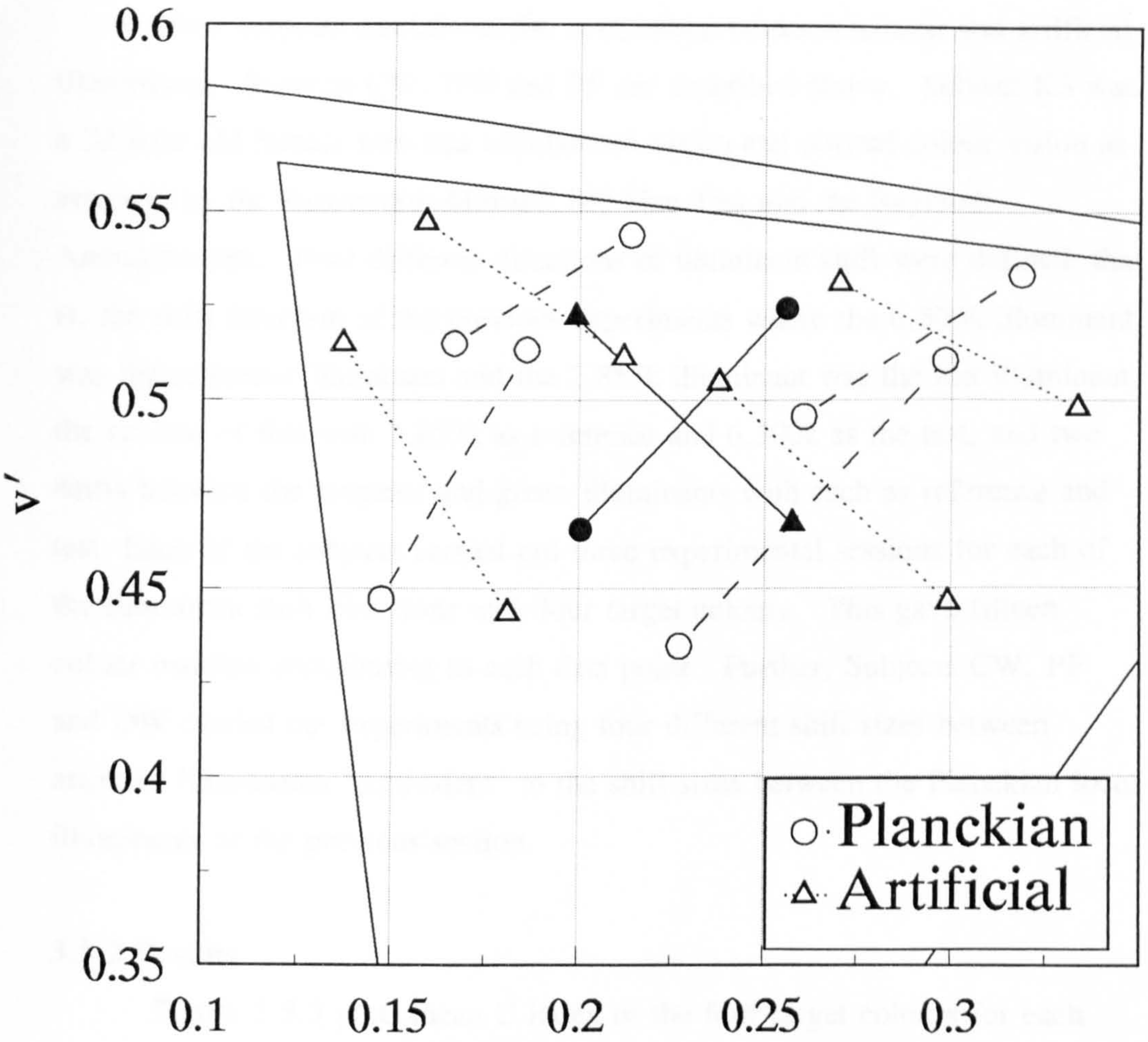

Figure 3.5.2 *Chromaticities of the four illuminants used in the natural versus artificial illuminant experiment and of the four target Munsell chips under each of these illuminants. Filled symbols joined by solid lines plot the chromaticities of the illuminants; open circles joined by dashed lines plot the chromaticities of the target colours under the Planckian illuminant; open triangles joined by dotted lines plot the chromaticities of the target under the artificial illuminants.*

Four subjects carried out the comparison between natural and artificial illuminants. Subjects CW, DW and PF are described above. Subject KS was a 32-year old female who had uncorrected vision and normal colour vision as assessed by the Farnsworth-Munsell 100 Hue Test and the Rayleigh Anomaloscope. Four different directions of illuminant shift were defined; that is, the shift direction of the previous experiments where the 6,500k illuminant was the reference illuminant and the 2,855k illuminant was the test illuminant, the reverse of this with 2,855k as reference and 6,500k as the test, and two shifts between the magenta and green illuminants with each as reference and test. Each of the subjects carried out three experimental sessions for each of the illuminant shift directions with four target colours. This gave fifteen colour matches contributing to each data point. Further, Subjects CW, PF and DW carried out experiments using four different shift sizes between artificial illuminants "equivalent" to the shift sizes between the Planckian locus illuminants of the previous section.

3.5.2 Results

Figure 3.5.3 plots mean C index of the four target colours for each direction of illuminant shift, for the four subjects. The order of shifts is: Planckian 6,500K to 2,855K; Planckian 2,855K to 6,500K; artificial magenta to green; artificial green to magenta; with the test illuminant specified first in each case. The error bars are 95% confidence limits calculated from the estimate of standard error in the analysis of variance. Tables 3.5.1, 3.5.2, 3.5.3 and 3.5.4 detail this analysis of variance.

The analysis of variance shows that there are significant effects of both shift direction and target colour alone ($p < 0.01$ for all subjects for each condition), and that there is a significant interaction between them for all the subjects. However, figure 3.5.3 shows no clear trend with shift direction and considerable variation between subjects.

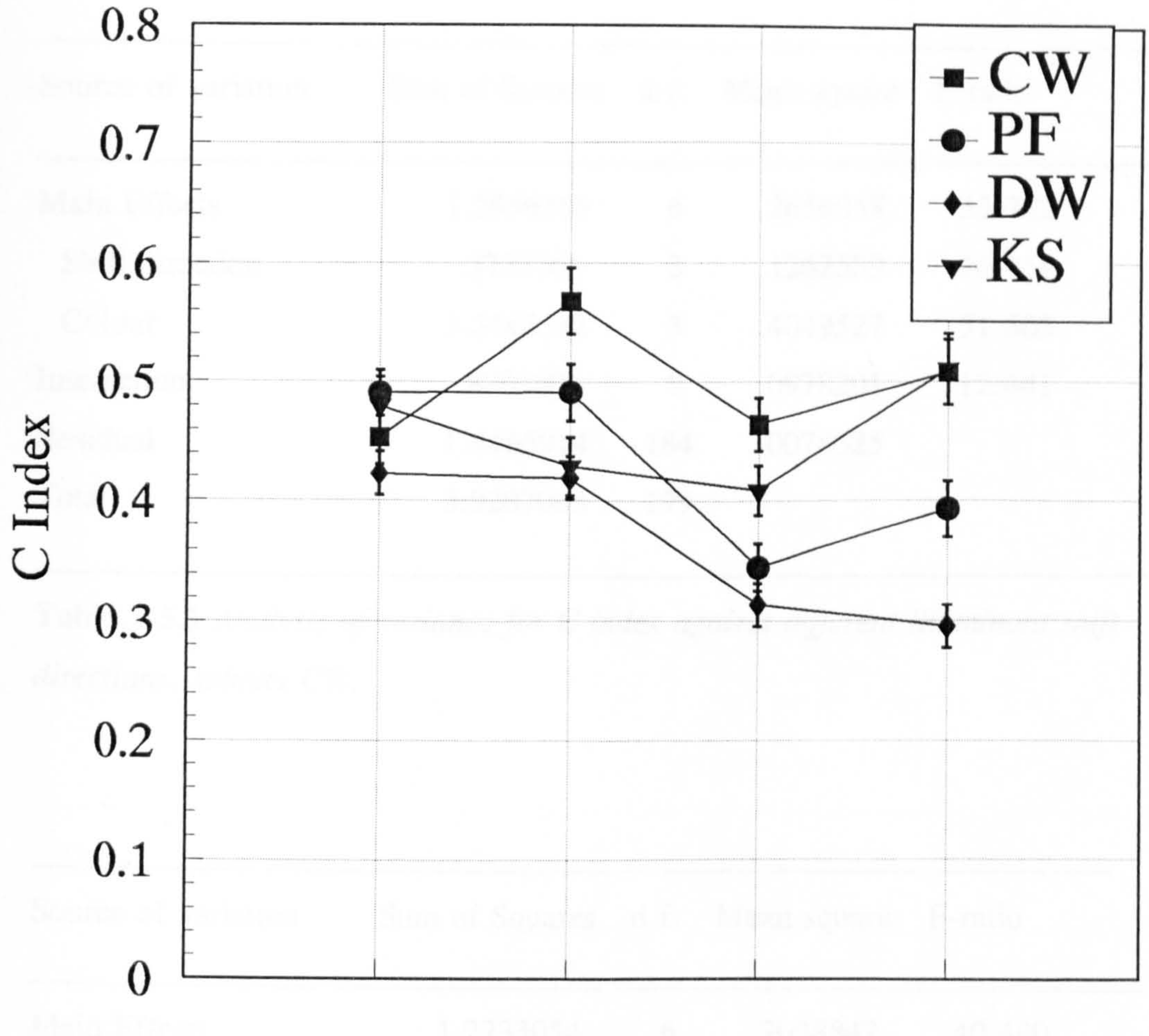

Figure 3.5.3 *C index measurements plotted for each of the four illuminant shifts of the natural versus artificial illuminant experiments. Data are plotted for four subjects. The order in which the shifts are displayed is: Planckian 6,500K - 2,855K, Planckian 2,855K - 6,500K, Artificial Magenta - Green, Artificial Green - Magenta, the first illuminant being reference and the second illuminant the test in each case. This order is arbitrary.*

Source of variation	Sum of Squares	d.f.	Mean square	F-ratio
Main Effects	1.5936348	6	.2656058	33.782
Shift direction	.3787766	3	.1262589	16.058
Colour	1.2148582	3	.4049527	51.505
Interaction	.8803806	9	.0978201	12.441
Residual	1.4466914	184	.0078625	
Total	3.9207068	199		

Table 3.5.1 *Analysis of variance for C index against different illuminant shift directions, subject CW.*

Source of variation	Sum of Squares	d.f.	Mean square	F-ratio
Main Effects	1.2233054	6	.2038842	40.480
Shift direction	.8284738	3	.2761579	54.830
Colour	.3948316	3	.1316105	26.131
Interaction	.6732251	9	.0748028	14.852
Residual	1.1282101	224	.0050367	
Total	3.0247406	239		

Table 3.5.2 *Analysis of variance for C index against different illuminant shift directions, subject DW.*

Source of variation	Sum of Squares	d.f.	Mean square	F-ratio
Main Effects	1.8057740	6	.3009623	32.532
Shift direction	.3650635	3	.1216878	13.154
Colour	1.4407104	3	.4802368	51.911
Interaction	.6362674	9	.0706964	7.642
Residual	2.0722638	224	.0092512	
Total	4.5143052	239		

Table 3.5.3 *Analysis of variance for* **C** *index against different illuminant shift directions, subject KS.*

Source of variation	Sum of Squares	d.f.	Mean square	F-ratio
Main Effects	2.2937380	6	.3822897	65.574
Shift direction	.8655800	3	.2885267	49.491
Colour	1.4281581	3	.4760527	81.657
Interaction	1.6239126	9	.1804347	30.950
Residual	1.0727029	184	.0058299	
Total	4.9903536	199		

Table 3.5.4 *Analysis of variance for* **C** *index against different illuminant shift directions, subject PF.*

Figure 3.5.4 plots the **C** index against shift direction and colour, for one subject in each quadrant. Each group of joined points are data for one shift direction, each point plots data for one target colour for that shift direction. The shift directions are in the order: Planckian 6,500K to 2,855K; Planckian 2,855K to 6,500K; artificial magenta to green; artificial green to

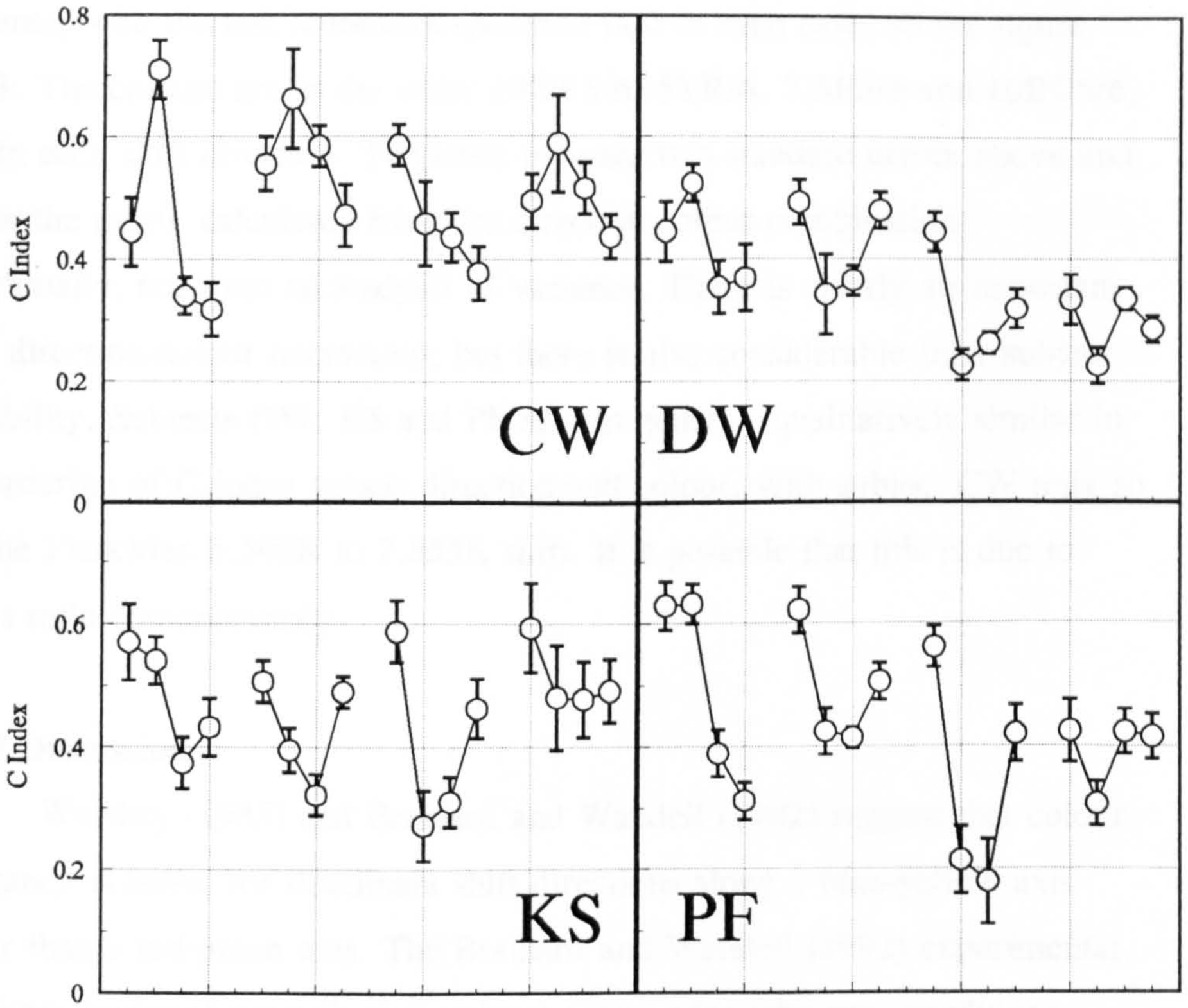

Figure 3.5.4 *Each quadrant plots* **C** *index measurements against illuminant shift direction and target colour, for one subject. Each group of joined points plots data for one shift size, with each point within the group representing one of the four target colours. The order of target colours within each group is 10GY5/6, 5YR/6, 7.5P5/6 and 10BG5/6 and the order of the illuminants is as for* ***Figure 3.5.3****. The error bars plot two standard errors above and below the mean calculated from the* **C** *index measurements for that particular colour-shift combination, not from an analysis of variance.*

magenta; with the test illuminant specified first in each case, as for figure 3.5.3. The colours are in the order 10GY5/6, 5YR/6, 7.5P5/6 and 10BG5/6, within each shift direction. The error bars are two standard errors above and below the mean, calculated from the direction-colour combination individually, not from an analysis of variance. There is clearly an important shift direction-colour interaction, but there is also considerable inter subject variability. Subjects DW, KS and PF are, in general, qualitatively similar in the ordering of C index versus direction and colour, with subject CW only so for the Planckian 6,500K to 2,855K shift. It is possible that this is due to CW's mild deuteranomaly.

3.5.3 Discussion

Worthey (1985) and Brainard and Wandell (1992) suggest that colour constancy is better for illuminant shift directions along a blue-yellow axis rather than a red-green axis. The Brainard and Wandell (1992) experimental paradigm involved remembering colours seen under reference conditions, whilst the Worthey (1985) paradigm involved viewing test and reference stimuli with different eyes. In both cases the subjects were differentially adapted to the test and reference conditions. Indeed the authors of both papers couch their explanation in terms Von Kries type adaptation, for which reg-green contrasts are better preserved under blue-yellow illuminant shifts due to the similarity between the spectral sensitivity of human long and middle wavelength sensitive cones.

The data presented here do not have an effect of differential adaptation between test and reference conditions and they do not show any difference for the direction of illuminant shift, consistent across subjects. This is not consistent with a colour constancy algorithm which models common illuminants with a sum of basis functions of which the visual system has a priori knowledge (Lennie and D'Zmura, 1988; D'Zmura and Iveson, 1993 a & b) and suggests that such a mechanism is not employed here.

Several authors have presented results of colour constancy experiments for which the degree of constancy varied significantly with the choice of target colour (e.g.McCann et al., 1976; Worthey, 1985; Arend and Reeves, 1986; Troost et al., 1992). Troost et al. (1992) found greater constancy for stimuli which differed only slightly from the average surround chromaticity. That does not seem to be born out by the data presented here (figure 3.5.5). Indeed there seems to be no such simple explanation based on the colour differences of the targets from the two illuminants (figure 3.5.2).

3.6 Summary

The data presented here show that although instantaneous colour constancy is not perfect, the **C** index is never one, it can nevertheless account for a large percentage of the colour constancy observed in human vision. This is in agreement with the findings of numerous other studies (e.g. McCann et al., 1976; Worthey, 1985; Arend and Reeves, 1986; Tiplitz Blackwell and Buchsbaum, 1988 a&b; Valberg and Lange-Malecki, 1990; Troost et al., 1992; Brainard and Wandell, 1992). However, the data of this thesis describe instantaneous constancy when there is no difference between adaptation states for the test and reference conditions. Most of the other authors allow differential adaptation by using a haploscopic viewing technique (McCann et al.,1976) or a memory paradigm (Brainard and Wandell, 1992). This does produce some differences in results. More recently, Hurlbert (personal communication) has suggested that by carefully adapting each eye separately and appropriate arrangement of the viewing conditions it is possible to obtain **C** indices of nearly one.

Neither the level of global luminance nor the luminance contrast between the test target and surround affected the **C** index significantly. This is inconsistent with the predictions of the Retinex theory (Land, 1983) or any algorithm which normalises its response according to the maximum value in any channel or a simple average.

The **C** index does not depend on the size of the illuminant shift along the Planckian locus, nor on the direction of the illuminant shift, be it along the Planckian locus or between artificial illuminants. The equivalence of natural and artificial illuminants for producing the effect of instantaneous colour constancy suggests that algorithms such as those reviewed by Lennie and D'Zmura (1988), which rely on approximating the illuminant by a linear sum of three basis functions, do not describe the operation of the human visual system in this case.

The importance of the choice of target colour and the interaction of target colour with illuminant shift direction suggest a mechanism which is

driven by spectrally specific contrast. This is more in line with the findings of Tiplitz Blackwell and Buchsbaum (1988a) and Lucassen and Walraven (1993). As neither the global luminance nor the luminance contrast between target and surround do not effect the **C** index, this contrast mechanism is likely to operates at the level of cone opponency or higher in the visual system

Chapter 4. Spatial Aspects of Instantaneous Colour Constancy

Chapter 4. Spatial Aspects of Instantaneous Colour Constancy

4.1 Background

Recent computational approaches to colour constancy (see D'Zmura & Lennie, 1986 for review) assume that spectral information is sampled over a large area of the visual field in order to estimate the spectral distribution of the illuminant. In so doing they take no specific account of spatial structure within the area of sampling. The processing of spatially distributed (chromatic) information by the visual system is perhaps one of the least well understood issues of colour constancy. The experiments described in this chapter were carried out in order to investigate some of the properties of instantaneous colour constancy with respect to this spatial distribution of chromatic information and to address some of the questions posed by the models and algorithms described in chapter one.

Land's Retinex theory (Land, 1959 a&b; Land & McCann, 1971) proposed the first algorithm for the spatial sampling of the retinal light distribution. To determine colour designators for each patch within a Mondrian, The Land algorithm (described in chapter one) samples from a large number of points along randomly defined paths within the visual field and compares contrast for each cone system between each point and its predecessor (under conditions of uniform illumination the thresholding step may be ignored), the designator is then updated appropriately. In order to achieve a constant description within Land's designator three space, it is required that the visual field contains a wide variety of different coloured patches (Land, 1983; 1986a). Valberg and Lange-Malecki (1989) computed the designator values (normalised cone absorbtion values or scaled integrated reflectances; McCann et al., 1976) from experiments comparing the effect of Mondrian and uniform grey surrounds and found that they were indeed different. However, this difference was not born out by their experimental

results (Valberg & Lange-Malecki, 1987; 1989). The authors used a haploscopic viewing technique and showed that appropriate choice of "equivalent" neutral surround (Valberg & Lange-Malecki, 1987) would elicit the same degree of colour constancy. Similar experiments are presented here, using our dynamic matching paradigm to compare the effect of Mondrian and uniform neutral surrounds on instantaneous colour constancy. These experiments are described in section 4.2.

One of the most important aspects of Land's algorithm was that it highlighted the effect of borders between coloured patches in the visual scene on the computation of colour constancy (Marr, 1982). The thresholding step (Land, 1983) carries out a filling in process which effectively ascribes uniform colour to each patch within a Mondrian so that only contrast between patches contributes to the designator computation. The connection between image segmentation by object colour and colour constancy (Brill, 1990) is beyond the scope of this thesis, but it is of interest to investigate the effect of target perimeter length on colour constancy. To this end, experiments were carried out in which the size and shape of the experimental target were varied. These experiments are described in section 4.3.

Land (1986b) in his most recent version of the Retinex algorithm, acknowledges that the contribution of different areas of the visual scene to the computation of the lightness designators for the patch of interest may be spatially weighted. The triplet of cone specific lightness designators are computed by sampling the visual scene with a "two aperture" light integrator. The designators are computed as the logarithm of the ratio of the fluxes from a 4' field and a 24° field respectively. The field sizes are empirical and were suggested (Land, 1986b) in conjunction with a $1/r^2$ cone sensitivity profile, where r denotes distance from the point of interest. Hurlbert (1986) described a solution to the Laplacian of Horn's algorithm, the multiple scales algorithm. The multiple scales algorithm filters the intensity signal through a $-\nabla^2 G$ operator (where G is a Gaussian), thresholds the result and sums over a continuum of scales. This is equivalent to the sum over difference of

Gaussians (DOG) in which all but the smallest and largest scale Gaussians are cancelled. The resulting operator has a narrow centre with a large shallow surround with a Gaussian profile. Hurlbert and Poggio (1988) synthesised a lightness algorithm from a set of examples which had a "nonclassical" profile of this type.

Studies of chromatic induction (Jameson and Hurvich, 1961; Valberg, 1974) have shown a decreasing effect as the inducing surround is separated from the experimental target. Walraven (1973) suggested that this decrease was exponential. Tiplitz Blackwell and Buchsbaum (1988 a&b) related chromatic induction to colour constancy and also found an exponential decrease as the inducing surround was separated from the target. Brenner and Cornelissen (1991) suggested that this exponential decay was dependent more specifically on the distance between the outer boundary of the target element and the inner boundary of the surround element. A lightness operator with a fairly narrow centre and a wide, Gaussian surround would be expected to give such an exponential decrease (Hurlbert, 1986; Hurlbert and Poggio, 1988). It was therefore of interest to see if our dynamic matching paradigm would give similar results. Experiments describing the effect of introducing a black border of various size between the target and surround are described in section 4.4.

The earlier incarnations of the Retinex algorithm (Land and McCann, 1971; Land, 1983) implied that colour constancy was improved for complex (Mondrian) scenes and that the particular location of a patch within the Mondrian was immaterial (Valberg and Lange-Malecki, 1989). Land's last Retinex (1986b) had an operator which took ratios from a "two aperture" light integrator. This was much more like the multiple scales difference of Gaussians from Hurlbert (1986) and the simulated operator from Hurlbert and Poggio (1988), all be it an inverse square rather than Gaussian surround profile. It should be noted that these operators sum the surround effects over a large area (24° in the case of Land, 1986b) and hence do not imply significant differences between complex and simple surrounds.

4.2 Complex versus Uniform Surrounds

4.2.1 Method

Experiments were carried out to compare the effects of a complex Mondrian surround with a uniform neutral surround on instantaneous colour constancy. The Mondrian used by McCann (McCann, McKee and Taylor, 1976) was used as the complex surround. The arrangement of Munsell chips used in this Mondrian is indicated in figure 4.2.1. The neutral surround was obtained by replacing each of the Munsell chip reflectance functions of the McCann Mondrian with a uniform reflectance of 0.44. This value was chosen as it gave the same luminance as the mean of the McCann Mondrian under illuminant D_{65}. Patch M of the Mondrian was replaced with the target element. Four target colours were used against each of the two surrounds. These were: 10GY5/6, 5YR5/6, 7.5P5/6, 10BG5/6.

Experiments were carried out on three subjects. Subjects CW and PF have been described earlier, subject JB was a 40 year old male, experienced observer with uncorrected vision and normal colour vision. The dynamic colour matching paradigm described in chapter two was used. Each target colour was presented in random order five times during each run. Each subject carried out two experimental runs for each of the two surround conditions, giving a total of ten colour matches contributing to each point.

4.2.2 Results

Figure 4.2.2 plots the **C** index against target colour for the two surround conditions, for subject CW. The filled symbols indicate the Mondrian surround, open symbols indicate the uniform neutral surround. The error bars show two standard errors above and below the means, calculated for each target colour-surround combination. Figures 4.2.3 and 4.2.4 plot similar data for subjects JB and PF respectively. An analysis of variance, using a cross classified model with random effects, as in the previous chapter,

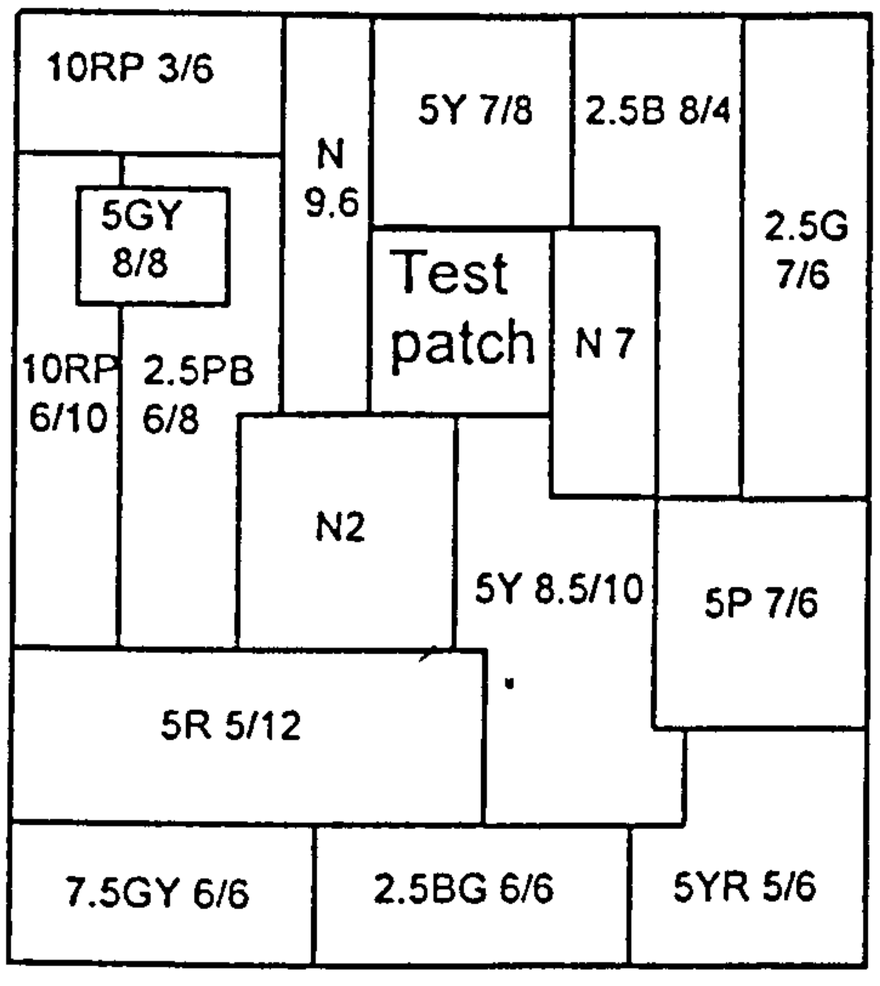

Figure 4.2.1 Diagram *of the 17 area Mondrian used by McCann et al. (1976). The Munsell designation of each coloured area is printed on the photograph. From McCann, McKee and Taylor (1976).*

was carried out for each subject. Tables 4.2.1, 4.2.2 and 4.2.3 detail this analysis of variance for subjects CW, JB and PF, respectively.

Source of variation	Sum of Squares	d.f.	Mean square	F-ratio
Main Effects	3.7600363	4	.9400091	40.29
Surround	.4328712	1	.4328712	18.55
Colour	3.3271651	3	1.1090550	47.52
Interactions	.0700154	3	.0233385	.075
Residual	.5465104	72	.0075904	
Total	4.3765621	79		

Table 4.2.1 *Analysis of variance for C index against complex or uniform surround, subject CW.*

Source of variation	Sum of Squares	d.f.	Mean square	F-ratio
Main Effects	.6071162	4	.1517791	3.91
Surround	.0018470	1	.0018470	.048
Colour	.6052692	3	.2017564	5.205
Interactions	.1162858	3	.0387619	5.719
Residual	.4879842	72	.0067776	
Total	1.2113862	79		

Table 4.2.2 *Analysis of variance for C index against complex or uniform surround, subject JB.*

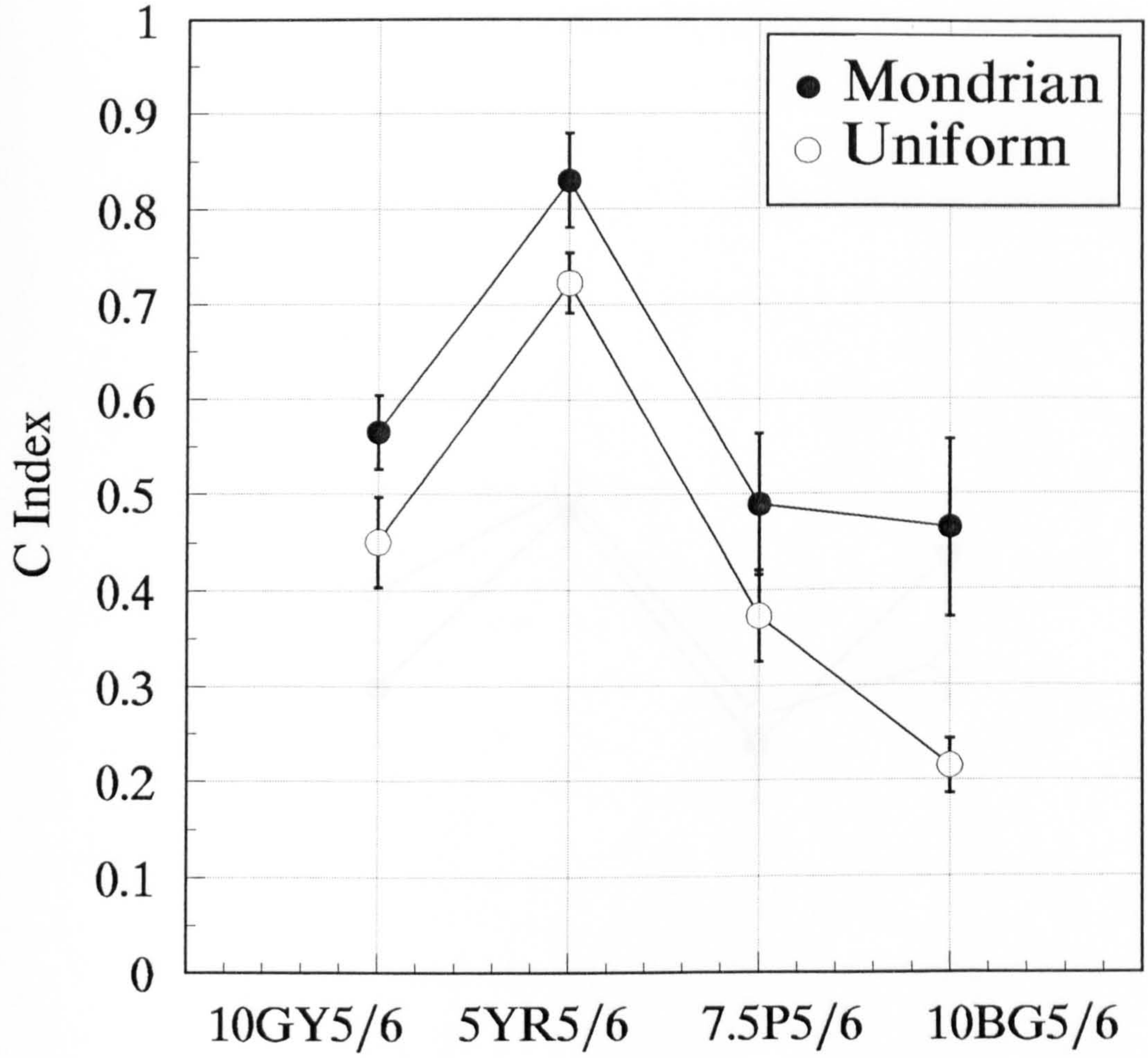

Figure 4.2.2 *C index measurements plotted against target colour for subject CW. Filled circles plot data obtained with the Mondrian surround, open circles plot data obtained with the uniform, neutral surround. Error bars show plus and minus two standard errors, calculated from the measurements made for each target colour and surround condition.*

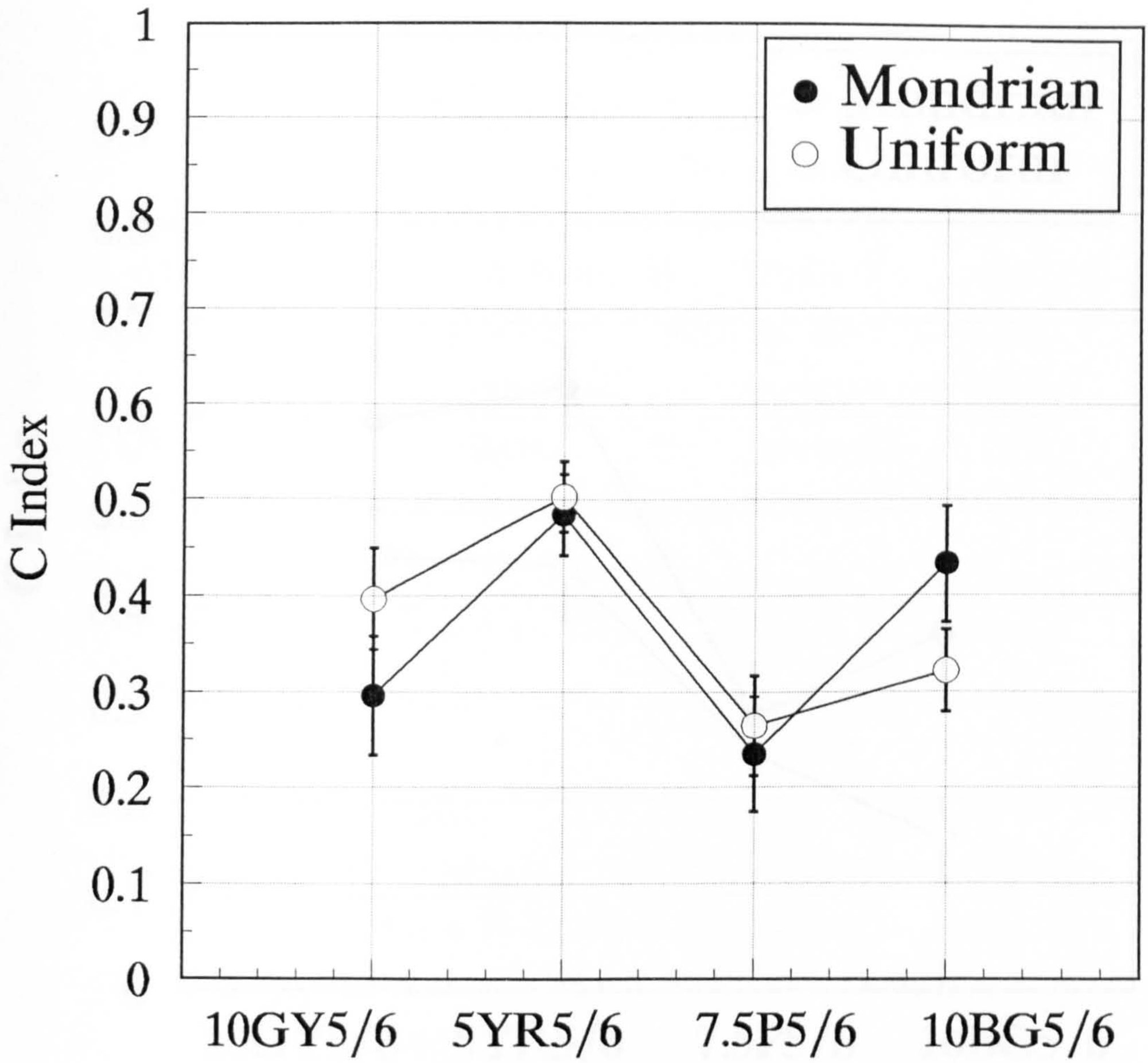

Figure 4.2.3 *C index measurements plotted against target colour for subject JB. Filled circles plot data obtained with the Mondrian surround, open circles plot data obtained with the uniform, neutral surround. Error bars show plus and minus two standard errors, calculated from the measurements made for each target colour and surround condition.*

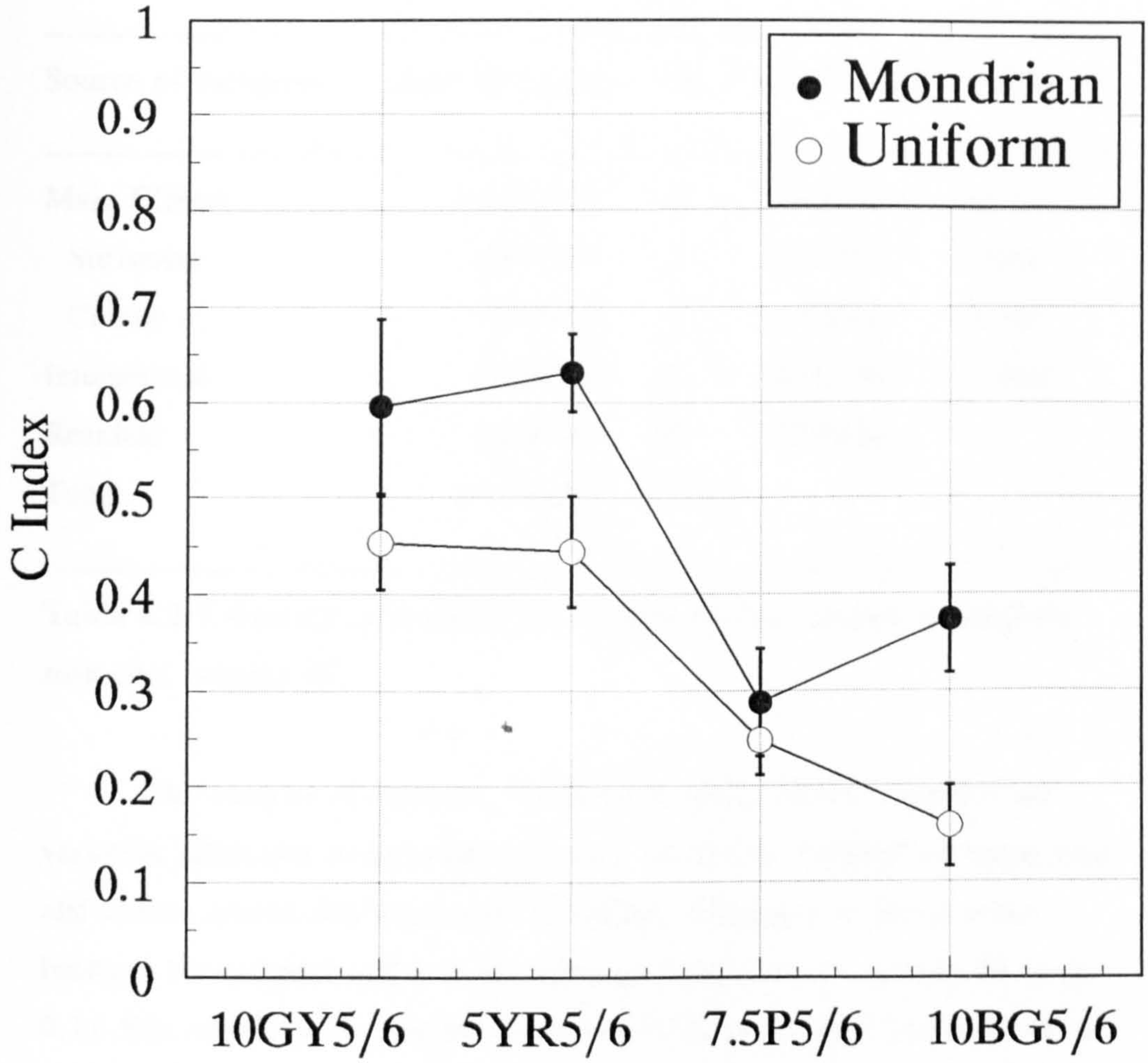

Figure 4.2.4 *C index measurements plotted against target colour for subject PF. Filled circles plot data obtained with the Mondrian surround, open circles plot data obtained with the uniform, neutral surround. Error bars show plus and minus two standard errors, calculated from the measurements made for each target colour and surround condition.*

Source of variation	Sum of Squares	d.f.	Mean square	F-ratio
Main Effects	1.8243944	4	.4560986	15.27
Surround	.4267143	1	.4267143	14.29
Colour	1.3976801	3	.4658934	15.60
Interactions	.0895794	3	.0298598	3.826
Residual	.5618789	72	.0078039	
Total	2.4758526	79		

Table 4.2.3 *Analysis of variance for C index against complex or uniform surround, subject PF.*

The analysis of variance, which for random effects compares the variation effect due to surround type with interaction between surround type and colour, shows that there is no significant difference in the **C** index between the complex and uniform surround conditions for subject JB ($p > 0.1$). For subjects CW and PF the choice of surround type is significant at the 5% level, but not the 99% level ($p > 0.025$ for PF, $p > 0.01$ for CW). As can be seen from figures 4.2.2, 4.2.3 and 4.2.3, the variation between the two surround conditions is smaller than the variation between colours. A comparison of the effect of surround was performed on each colour separately, for each subject, using Student's t test. The pattern of results varied between subjects. There were significant ($p < 0.05$) differences for all colours for subject CW; significant differences for colours 10GY5/6 and 10BG5/6 (but with the uniform surround producing the larger **C** index for 10GY5/6 and the smaller for 10BG5/6) for subject JB; and significant differences for all colours except 7.5P5/6 for subject PF. These differences can more readily be seen from figures 4.2.2, 4.2.3 and 4.2.4.

It should be noted that, due to the complexity of the surrounds, no correction has been made for the effect of light scattered in the eye (see

chapter two). The size of the correction to the **C** index due to light scatter (see figures 2.4.6 and 2.4.7) is of the same order as the differences in **C** index shown in figures 4.2.2, 4.2.3 and 4.2.4. This may be a confounding factor which cannot be easily taken into account in this study.

4.2.3 Discussion

The lack of significant difference between the **C** indices measured using complex and uniform surrounds is similar to the results of the chromatic induction experiments of Valberg and Lange-Malecki (1987, 1989) and Tiplitz Blackwell and Buchsbaum (1988a). This finding is contrary to the predictions of Land's earlier Retinex algorithms (Land, 1983; 1986a; Valberg and Lange-Malecki, 1989). It is more in keeping with lightness operators which respond to a large area of the surround field (Hurlbert, 1986; Hurlbert and Poggio, 1988).

The results show variation in the effect of different surround type between colours. There is also variation between subjects. It is possible that much of this may be accounted for by light scatter within the eye, for which the **C** index measurements have not been corrected. Valberg and Lange-Malecki (1989) suggested that the immediate chromatic contrast between target and surround might account for surround effects. An effect might be observed if the colours of those elements of the surround which abutted the target were biased in some way. However the data presented here show considerable variation between subjects. An explanation of the type put forward by Valberg and Lange-Malecki (1989) cannot explain this variability with consistency.

4.3 The Effect of Target Area and Perimeter Length

4.3.1 Method

Experiments were carried out to investigate the effect of target area and perimeter length on the measurement of instantaneous colour constancy. A series of differently shaped target elements was used against a uniform neutral surround, which has been shown in the previous section to have an equivalent effect to a more complex Mondrian surround. The target shapes used were a series of squares and crosses. They were chosen (in increasing dimension) so that each cross had the same area as the preceding square (but a larger perimeter) and each square had the same perimeter as the preceding cross (but a larger area). Figure 4.3.1 shows the six target shapes relative to each other. Their dimensions are given in table 4.3.1.

Shape	Square	Cross	Square	Cross	Square	Cross
Dimension	70	112x24	112	150x50	150	175x85
Perimeter	280	448	448	600	600	700
Area	4900	4800	12544	12500	22500	22525

Table 4.3.1 *Dimensions of targets used to investigate the effect of target area and perimeter. The side of each square and the length and breadth of one arm of each cross is given in screen pixels. Each pixel is 0.266mm on screen, which is equivalent to 0.0217° visual angle at 700mm viewing distance.*

Experiments were carried out on two subjects, CW and PF who have been described before. During each experimental run, the four target colours, 10GY5/6, 5YR/6, 7.5P5/6 and 10BG5/6, were each presented five times in random order for one target shape. Each subject carried out three experimental runs for each target shape, giving a total of 15 colour matches contributing to each point. The subjects were instructed to fixate at the centre

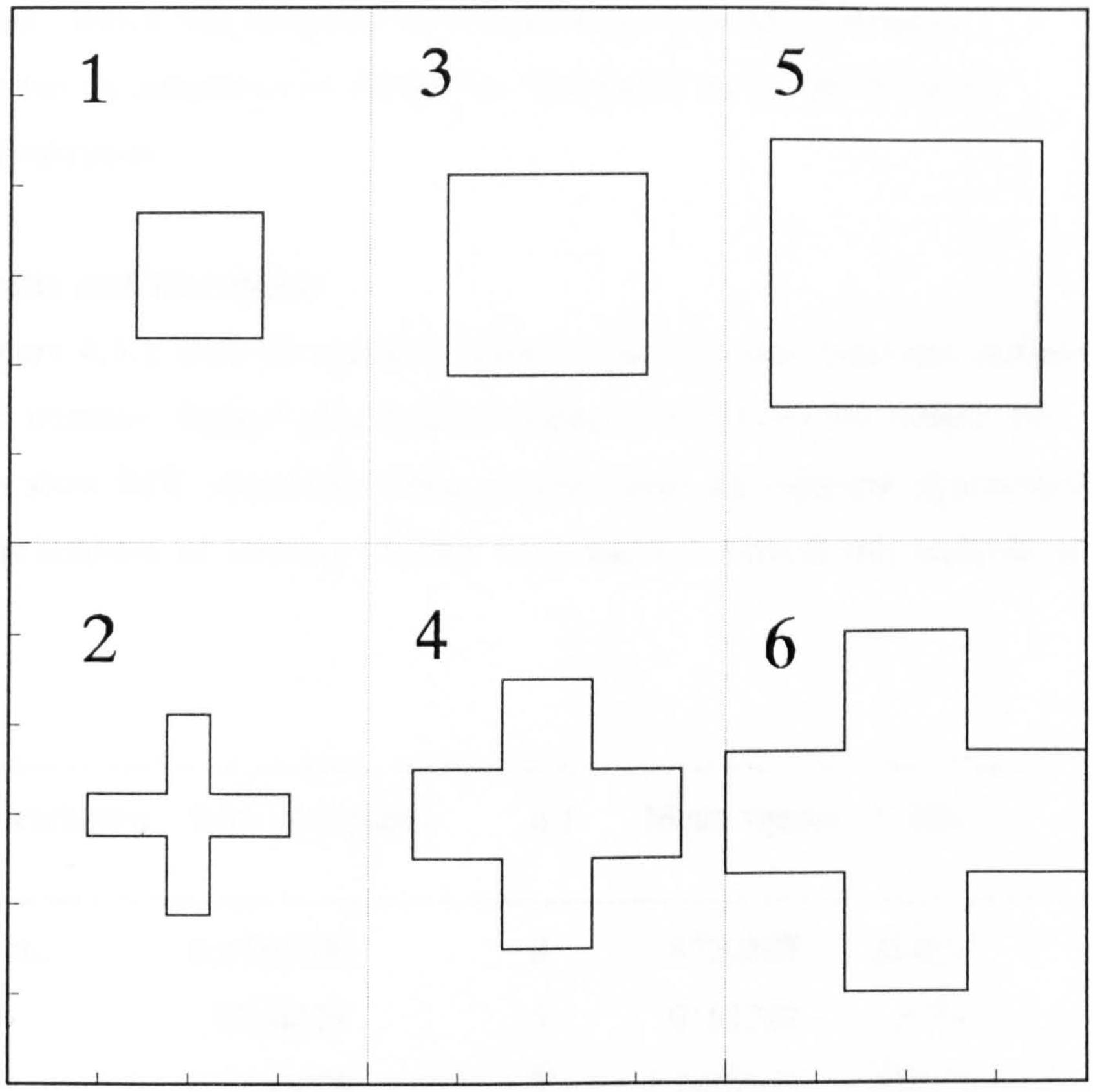

Figure 4.3.1 *Relative sizes of the targets used in the experiments investigating the effect of target area and perimeter length.*

of the target, which was indicated by a small black spot. Both subjects reported a strong temptation to change the fixation to the border between target and surround.

4.3.2 Results and Discussion

Figure 4.3.2 plots the mean **C** index for the four target colours against the pattern number. Squares plot data for subject CW, circles for subject PF. Error bars show 95% confidence limits obtained from the estimate of standard error in the analysis of variance. Tables 4.3.2 and 4.3.3 detail this analysis of variance.

Source of variation	Sum of Squares	d.f.	Mean square	F-ratio
Main Effects	6.9761656	8	.8720207	214.94
Pattern	.0766228	5	.0153242	3.78
Colour	6.7463028	3	2.2487676	554.31
Interactions	.0608538	15	.0040569	1.05
Residual	1.2917500	336	.0038445	
Total	8.3287694	359		

Table 4.3.2 *Analysis of variance for C index against target shape, subject CW*

The data show that at the 99% level ($p > 0.01$) there is no significant effect of target shape on instantaneous colour constancy, either as the target perimeter gets larger or as the target area increases, for either subject. For subject CW the differences are significant at the 95% level ($p < 0.05$), but the variation due to pattern is considerably smaller than that due to colour. The earlier versions of the Retinex theory (Land and McCann, 1971; Land, 1983) would predict an effect of border perimeter (Marr, 1982; Valberg and Lange-Malecki, 1989) which is not observed here. That there is no effect of

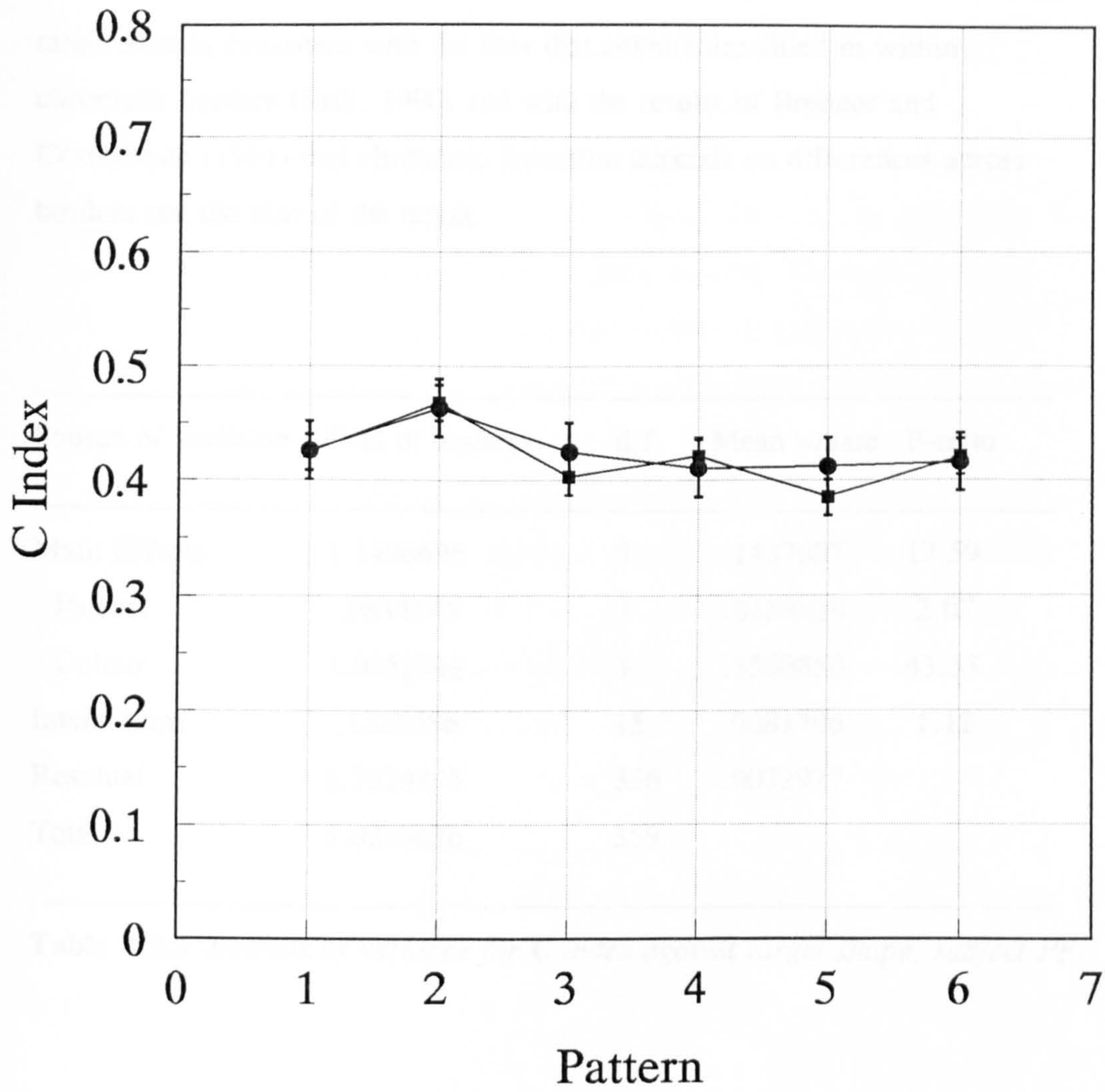

Figure 4.3.2 *Mean C index for the four target colours plotted against pattern number for the experiments investigating the effect of target area and perimeter length. The error bars plot 95% confidence limits obtained from the estimate of standard error in the analysis of variance detailed in the text.*

target area is consistent with the idea that colours are filled in within chromatic borders (Brill, 1990) and with the results of Brenner and Cornelissen (1991) that chromatic induction depends on differences across borders not the size of the target.

Source of variation	Sum of Squares	d.f.	Mean square	F-ratio
Main Effects	1.1496695	8	.1437087	17.59
Pattern	.0844145	5	.0168829	2.07
Colour	1.0652549	3	.3550850	43.55
Interactions	.1225586	15	.0081706	1.12
Residual	1.7514395	336	.0072977	
Total	3.0236676	359		

Table 4.3.3 *Analysis of variance for C index against target shape, subject PF*

4.4 The Effect of a Black Annulus Separating Target and Surround

4.4.1 Method

Experiments were carried out to investigate the effect of separating the target element from the surround with a black annulus. The circular target subtended 1.5° of visual angle and was surrounded by a uniform, neutral circular surround. Seven sizes of separating annulus were chosen. These were: 0° (abutting), 0.05°, 0.5°, 1°, 2°, 4° and 8°. The outer diameter of the surround element was adjusted for each separating annulus size so that its total area remained constant. This arrangement was in part chosen to facilitate the corrections for light scattered in the eye, which were made to all the data reported in this section. Table 4.4.1 details the parameters of the surrounds used in the experiments of this section.

Annulus	0°	0.05°	0.5°	1°	2°	4°	8°
Inner Radius	30	32	50	70	110	190	340
Outer Radius	300	300	303	307	319	355	455

Table 4.4.1 *Sizes of surround elements used with the different sizes of black separating annulus between target and surround. Element sizes are given in screen pixels. Each pixel is 0.266mm on the screen, equivalent to 0.0217° visual angle at 700mm viewing distance.*

Experiments were carried out on two subjects, CW and PF who have been described before. During each experimental run, each of the annulus sizes was presented for one of the four target colours, 10GY5/6, 5YR/6, 7.5P5/6 and 10BG5/6. Each subject carried out three experimental runs for each target colour, giving a total of 15 colour matches contributing to each point. The subjects were instructed to fixate at the centre of the target, which was indicated by a small black spot.

4.4.2 Results

Figure 4.4.1 plots the mean **C** index for the four target colours against the size of the black, separating annulus in degrees of visual angle. The error bars indicate 95% confidence limits obtained from the estimate of standard error in an analysis of variance, computed for each annulus size. The dotted line shows the results of a least squares regression, taking the form of a power law described below. Figures 4.4.2 and 4.4.3 plot equivalent data for subjects JB and PF respectively.

The data for each subject were fitted using a least squares regression procedure to a multiplicative equation of the form $y = ax^b$ and to an exponential equation of the form $y = e^{(a + bx)}$, where a and b are arbitrary constants in each case. Table 4.4.2 details results of the fitting procedure for the multiplicative equation. Table 4.4.3 details results of the fitting procedure for the exponential equation. The procedures were carried out by taking logarithms of the data and fitting a linear regression model. Hence the parameters a and b are referred to as intercept and slope.

Subject	CW	JB	PF
Intercept (log a)	-1.456	-1.354	-1.213
Slope (b)	-0.255	-0.196	-0.168
Correlation coeff.	-0.985	-0.925	-0.971
R squared	97.02%	85.59%	94.42%

Table 4.4.2 Results of fitting the **C** index versus black border size data with an equation of the form $\mathbf{C} = a.(\text{border})^b$, for three subjects.

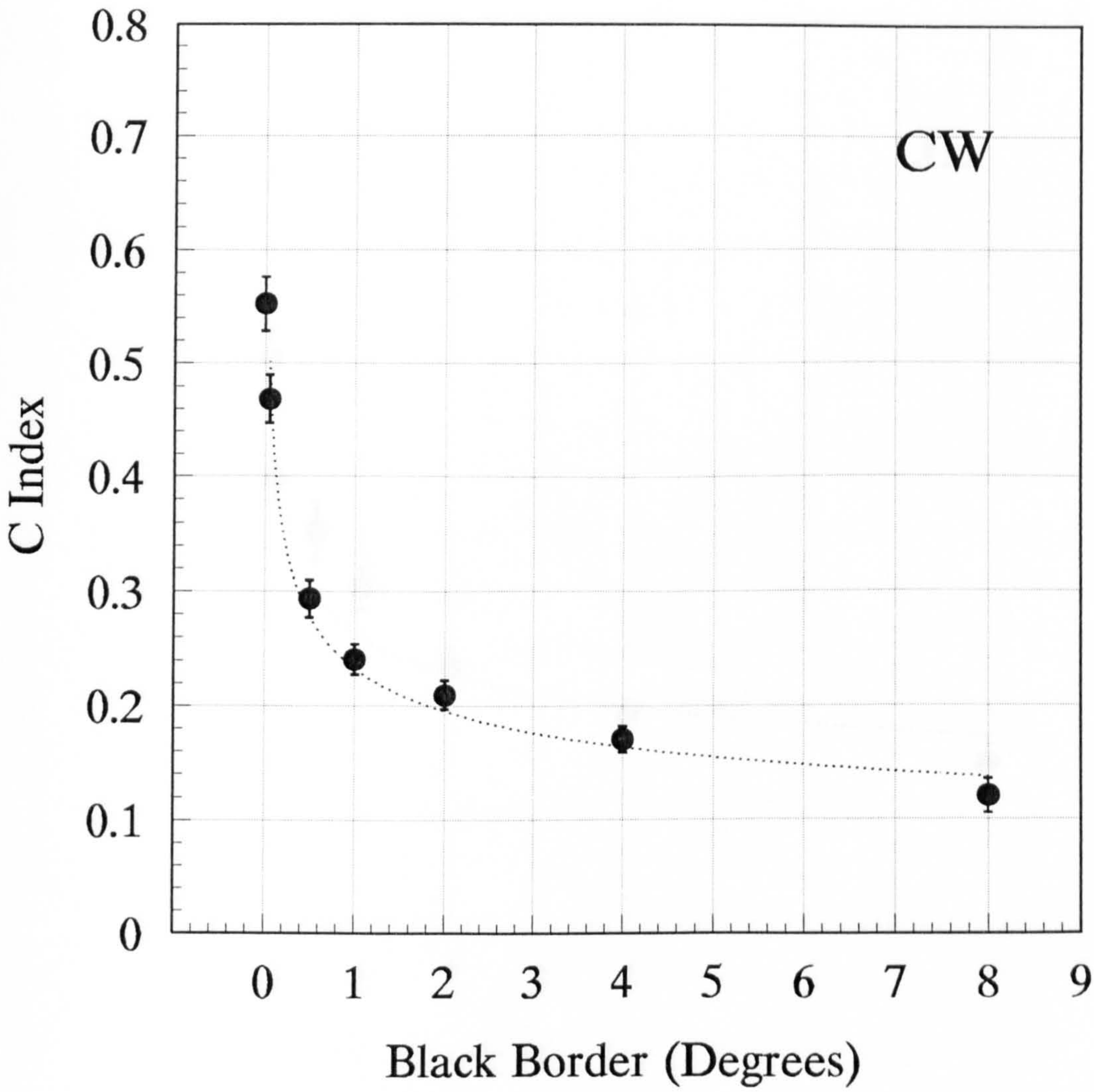

Figure 4.4.1 *Mean C index for the four target colours plotted against the size of black, separating annulus between target and surround (degrees) for subject CW. The error bars plot 95% confidence limits obtained from the estimate of standard error in an analysis of variance carried out for each point separately. The dotted line plots the results of a least squares regression to these data of the form* $y = a.x^b$.

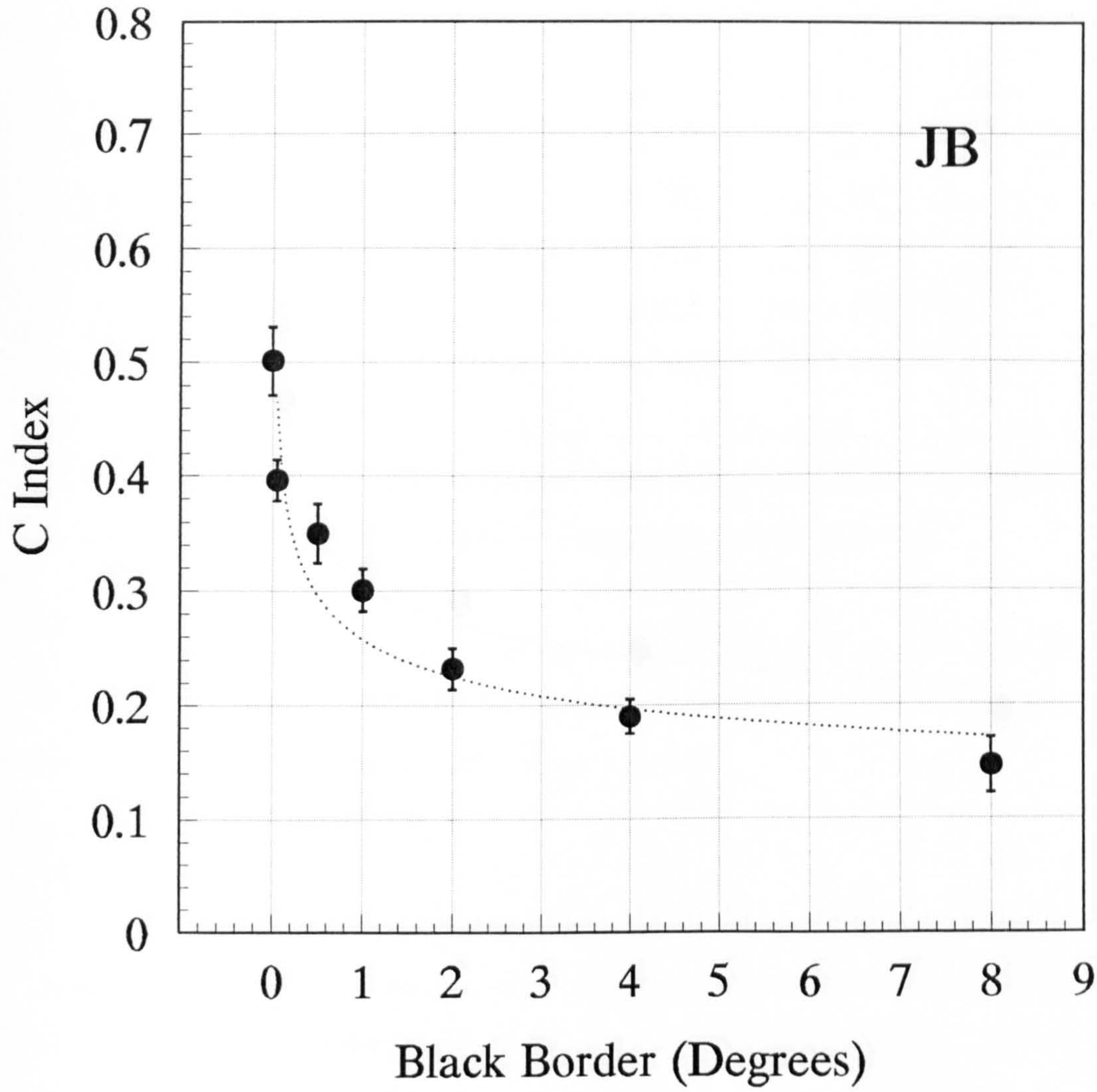

Figure 4.4.2 *Mean C index for the four target colours plotted against the size of black, separating annulus between target and surround (degrees) for subject JB. The error bars plot 95% confidence limits obtained from the estimate of standard error in an analysis of variance carried out for each point separately. The dotted line plots the results of a least squares regression to these data of the form* $y = a.x^b$.

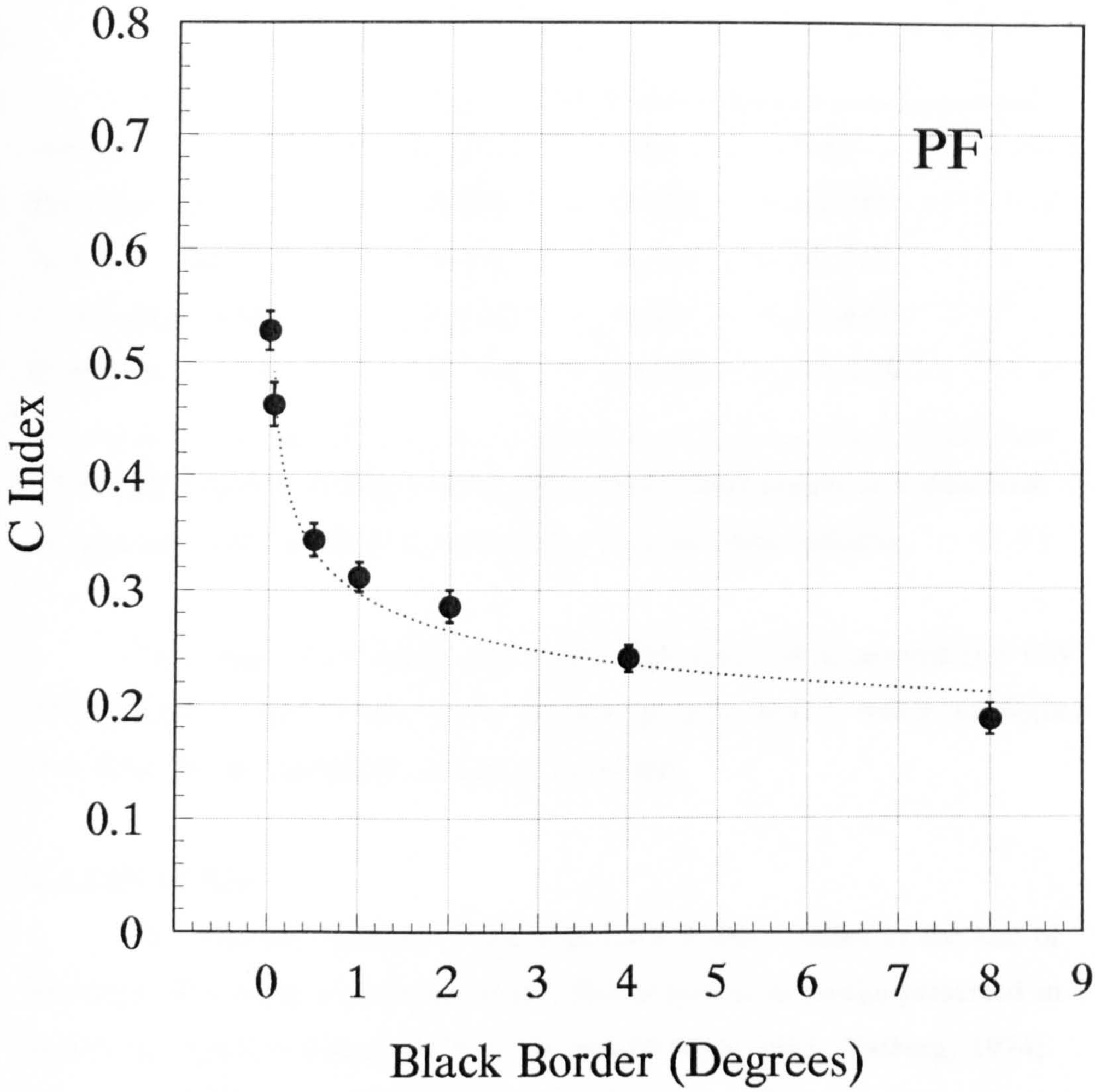

Figure 4.4.3 *Mean C index for the four target colours plotted against the size of black, separating annulus between target and surround (degrees) for subject PF. The error bars plot 95% confidence limits obtained from the estimate of standard error in an analysis of variance carried out for each point separately. The dotted line plots the results of a least squares regression to these data of the form* $y = a.x^b$.

Subject		CW	JB	PF
Intercept	(a)	-0.990	-0.970	-0.897
Slope	(b)	-0.162	-0.136	-0.111
Correlation coeff.		-0.872	-0.917	-0.892
R squared		76.11%	84.14%	79.67%

Table 4.4.3 *Results of fitting the C index versus black border size data with an equation of the form* $C = exp(a+b.border)$*, for three subjects.*

The results of the model fitting give high values of R squared (for CW 97%, JB 85.6% and PF 94.4%) for the multiplicative model, which are higher than those of the exponential model in each case.

4.4.3 Discussion

The data presented here show a decrease in the C index as the size of the black, separating annulus increases. This is similar to results presented in studies of chromatic induction (Jameson and Hurvich, 1961; Valberg, 1974; Walraven, 1973; Tiplitz Blackwell and Buchsbaum, 1988a; Brenner and Cornelissen, 1991). This sort of decrease of effect is consistent with an operator which has a narrow centre and a wide, shallow, spatially opponent surround (Hurlbert, 1986; Hurlbert and Poggio, 1988).

The operators proposed in the literature (Hurlbert, 1986; Hurlbert and Poggio, 1988) have Gaussian surrounds, which would give an exponential decrease. Previous experimental results have also suggested an exponential form of the decrease (Walraven, 1973; Tiplitz Blackwell and Buchsbaum, 1988a; Brenner and Cornelissen, 1991). However, the data of these experiments are better modelled using a multiplicative equation. Land (1986b) proposed a spatial weighting factor for the surround of $1/r^2$, and Valberg et al. (1985) reported colour opponent cells in the primate whose remote surrounds

had an effect up to 20 to 25 degrees in the periphery and had a spatial weighting factor of $1/r^n$, where n was between 2 and 3.

The weighting factors reported here are considerably smaller (b ranges from -0.17 to -0.25). It should be stressed that the data discussed above come from studies on chromatic induction.

The differences noted are important since they suggest that instantaneous colour constancy, measured using the dynamic colour matching technique employed in this study, may reflect different processes from those associated with chromatic induction mechanism. The spatial characteristics of instantaneous colour constancy may well be different from those of chromatic induction.

4.6 Summary

The data presented in this chapter show the dependency of colour constancy on spatial structure within the visual scene. As for the data of chapter three, instantaneous constancy is never perfect. **C** index values of approximately 0.5 are typically obtained.

Land's Retinex algorithm (Land and McCann, 1971; Land, 1983) would predict that colour constancy is better for complex scenes than for simple ones (Valberg and Lange-Malecki, 1989). However, studies on chromatic induction (Valberg and Lange-Malecki, 1987; 1989; Tiplitz Blackwell and Buchsbaum, 1988a) have found that appropriately chosen neutral surrounds produce the same effects as complex Mondrian ones. The data presented here show similar findings for instantaneous colour constancy.

The Retinex algorithm also predicts an effect of target perimeter (Marr, 1982; Valberg and Lange-Malecki, 1989). Such an effect is not observed here. There is also no effect due to target area which is consistent with the idea that colours are filled in within chromatic borders (Brill, 1990). The results are again similar to chromatic induction experiments (Brenner and Cornelissen, 1991), which suggests that both chromatic induction and instantaneous colour constancy depend on differences across borders rather than the size of the target.

The lack of significant difference between the results obtained with complex and uniform surrounds is in keeping with lightness operators which respond to a large area of the surrounding field. The data from the experiments which separated the surround from the target with a black annulus seem to agree with this. However, the lightness operators in the literature (Hurlbert, 1986; Hurlbert and Poggio, 1988) are modelled with a Gaussian surround, which would produce an exponential decrease in effect, while the data presented here are better modelled by a multiplicative equation. This difference is important as previous results from experiments on chromatic induction (Walraven, 1973; Tiplitz Blackwell and Buchsbaum, 1988a; Brenner and Cornelissen, 1991) have also suggested an exponential decrease in effect.

This suggests that the instantaneous colour constancy elucidated with the dynamic colour matching technique may reflect different processes from those associated with chromatic induction mechanisms.

Chapter 5. An Investigation of Instantaneous Colour Constancy in Subjects with Damage to the Cerebral Cortex.

Chapter 5. An Investigation of Instantaneous Colour Constancy in Subjects with Damage to the Cerebral Cortex.

5.1 The Relevance of using Subjects with Damage to Cerebral Cortex in Investigations of Colour Constancy

Colour constancy, the ability of the visual system to maintain near constant coloured percepts of objects under different illuminants, certainly aids in object recognition. However, it is known that object colour may also subserve the segmentation of an image by the visual system (e.g. Brill, 1990), and that chromatic signals contribute to motion perception (Cavanagh and Anstis, 1991). Studies on subjects with cerebral achromatopsia suggest that they may sometimes detect stimulus borders or chromatic gratings without seeing colour (Mollon et al., 1980; Heywood et al., 1987; 1991; Victor et al., 1989). These observations suggest that chromatic signals are either independent or can be separated completely from confounding achromatic contrast changes. Further, these signals carry information which allows the visual system to construct spatially structured patterns independently of the generation of a colour percept. It is however very difficult to isolate the use of pure chromatic signals in the visual system.

Background perturbation techniques have been developed to investigate the spatial (Barbur and Ruddock, 1980) and the temporal (Barbur et al., 1981) properties of achromatic vision. These techniques were extended to enable the study of chromatic signals in human vision without having to be concerned with the detection of luminance contrast signals. This was done using a spatiotemporal luminance masking technique (Barbur et al., 1992; 1993a), which makes use of isoluminant stimuli embedded in a pattern of random luminance modulation. Using this technique, Barbur et al. (1993b, 1994) investigated the colour vision of the three subjects with cerebral

achromatopsia, described in this chapter. The results are summarised in figure 5.1.1. In subjects with normal trichromatic colour vision and in dichromats, whose deficiency in colour discrimination is caused by a difference at the retinal level (Wright, 1946) there was no difference between structure thresholds and colour thresholds. This was not the case for the subjects with (incomplete) cerebral achromatopsia whose structure and colour thresholds differed substantially. For two of the three subjects, their ability to detect structure using achromatic signals was markedly better than their ability to detect a colour change. However, for the third subject, the reverse was the case. These results suggest that the processing of chromatic signals to generate the spatial representation of an object in terms of its structure is separate from the processing required to generate perceived object colour (Barbur et al., 1994) and that the neural substrates which are involved in these functions can be affected differently by the exact location and extent of the cortical lesion.

Approximately 80% of ganglion cells, in primates, have spatial, temporal and chromatic properties which enable them to respond to both intensity and/or wavelength changes in the retinal image (De Monasterio and Gouras, 1975; Perry et al., 1984; Shapley and Perry, 1986). These cells connect, via the four uppermost layers of the dorsal lateral geniculate nucleus, to the primary visual cortex (Area V1) and may account for both colour vision and discrimination of fine spatial detail (Merigan, 1989; Schiller et al., 1990). In general, most parvocellular retinal ganglion cells have a centre surround receptive field organisation that is chromatically and spatially opponent. Such neurons respond to both achromatic and chromatic contrast components in the image (Wiesel and Hubel 1966; De Valois and Pease, 1971; De Valois and De Valois, 1975). Cells have also been described which exhibit only spectral opponency with no trace of centre surround organisation (Wiesel and Hubel, 1966; Dreher et al., 1976). How the various components of these chromatic signals may be separated in their contribution to different visual attributes is not yet clear. The presence of direct projections from the lateral geniculate

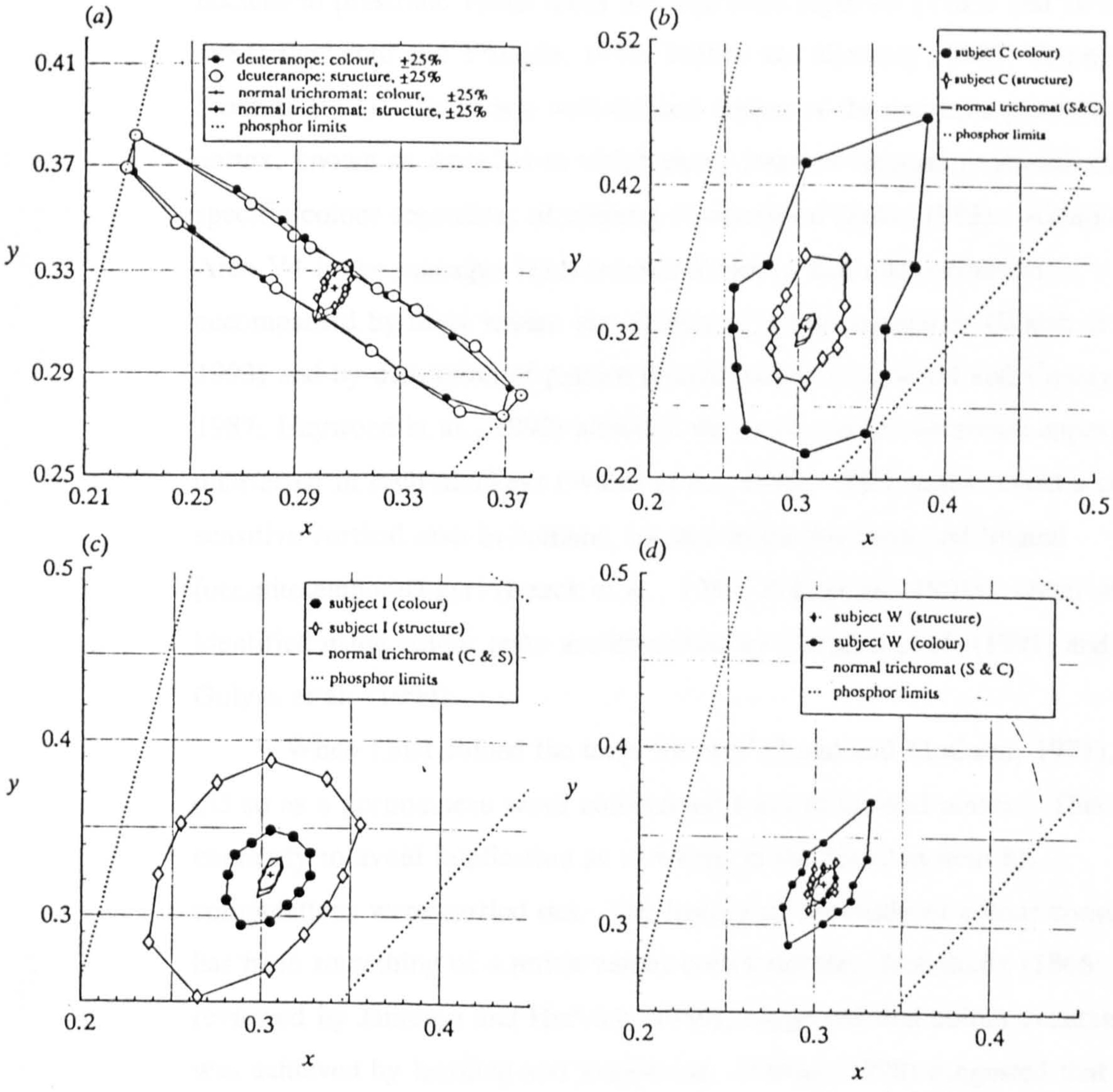

Figure 5.1.1 *Direct comparison of chromatic displacement thresholds for detection of vertical bars (structure thresholds) or colour changes only (colour thresholds). (a) Data for a normal trichromat (diamonds) and for a deuteranope (circles). (b), (c) and (d) Data for the three subjects with cerebral achromatopsia. Unlike thresholds measured in normal trichromats and in dichromats (a), the two tests yield markedly different threshold values. Remarkable is the reversal of thresholds observed in subjects IK and CG when comparing structure and colour responses. While subject CG needs a larger chromatic displacement to see that a square object defined by achromatic luminance contrast has changed colour without changing shape (b), subject IK shows larger thresholds when the task is to detect vertical bars from chromatic signals only.*

nucleus to prestriate visual areas has also been reported (Yukie and Iwai, 1981; Benvento and Yoshida, 1981; Bullier and Kennedy, 1983; Cowey and Stoerig, 1991). There is a well defined region of the macaque prestriate cortex, known as Area V4 in which many neurons respond to stimuli of a specific colour regardless of spectral composition (Zeki, 1983). Ablation of Area V4 in the macaque leads to mild losses of hue discrimination, accompanied by more severe impairment of colour constancy (Walsh et al., 1993) and by disruption of pattern discrimination (Heywood and Cowey, 1987; Heywood et al., 1992) although the basic colour categories appear to be unaffected in such monkeys (Walsh et al., 1992). PET scans reveal a colour sensitive cortical area in humans, located in the fusiform and lingual (occipitotemporal) gyri (Leuck et al., 1989; Zeki et al., 1991). Other areas identified using colour tasks are described by Corbetta et al. (1991) and Gulyas et al. (1994).

When Land coined the term 'retinex' (Land and McCann, 1971), he did so as a portmanteau word constructed from retina and cortex. This was expressly to avoid implication as to where in the visual system his computations were carried out. The history of the study of colour constancy has been something of a retina versus cortex debate; Helmholtz (1866; reviewed by Jameson and Hurvich, 1989), suggested that colour constancy was achieved by learning and judgement; Hering (1878) suggested that colour constancy could be achieved by adaptation of his opponent mechanisms. Since then, most approaches have attempted to identify one particular mechanism for achieving colour constancy, or emphasise the importance of the contribution of one mechanism over any others. Several authors have attempted to explicitly separate the reflectance from the illuminant by computational theory (eg. Buchsbaum, 1980; Maloney and Wandell, 1986; D'Zmura and Lennie, 1986; Brainard and Wandell, 1991; D'Zmura and Iverson, 1993 a,b). These mechanisms all require a priori knowledge of the visual environment and this, together with their complexity suggest that they are high level functions of the visual system. Retinal theories of colour

constancy include those based on the adaptation of photoreceptors (e.g. Helson, 1938; Judd, 1940; Brill and West, 1986; Brainard and Wandell, 1992) and on cone-specific contrast (Lucassen and Walraven, 1993). The need for two types of processing, one slow and multiplicative, one fast and subtractive (Hayhoe et al., 1987) to explain colour constancy and colour induction data has been advanced. Courtney et al. (1995) used a neural network simulation to explore possible interaction between these retinal and cortical mechanisms. They hypothesise a multi-stage system which is advantageous for producing colour constancy over each of the stages individually and is able to act over a wider range of stimulus conditions.

Interest in the specific cortical colour mechanisms, particularly V4 has developed relatively recently. Zeki (1980; 1983) recorded from individual cells in V4 whose responses unlike those in V1, appeared to follow colour perception, rather than wavelength. Ablation of Area V4 in the macaque leads to mild losses of hue discrimination accompanied by more severe impairment of colour constancy (Walsh et al., 1993) and by disruption of pattern discrimination (Heywood and Cowey, 1987; Heywood et al., 1992) although the basic colour categories appear to be unaffected (Walsh et al., 1992). Schein and Desimone (1990) reported receptive field regions, for the macaque, which they called silent surrounds. They found these regions to be quite distant (up to 16 degrees) from the classically defined receptive fields of V4 cells and that they could influence a cell's response if the centre of its classical receptive field is also stimulated. These silent surrounds in V4 are sensitive to nearly the same wavelengths as the centre of the receptive field, creating a spectrally specific response which is functionally similar to 'cone specific contrast' (see Lucassen and Walraven, 1993). Some authors have suggested that cone specific contrast appears, from psychophysical experiments, to be a necessary component of human colour constancy (Tiplitz Blackwell and Buchsbaum, 1988b; Lucassen and Walraven, 1993; McCann, McKee and Taylor, 1976). However, because of modifications to the cone inputs preceding cortical stages, it is difficult to quantify the response of the

V4 cells directly in terms of cone specific contrast (Courtney et al., 1995). Long range lateral connections have been found in macaque V4 (Yoshioka, Levitt and Lund, 1992), which suggest that these large silent surround mechanisms may be mediated by a mechanism within V4. Connections across the Corpus Callosum are also implicated by the dramatic reduction in ipsilateral surround suppression after its section (Desimone, Moran, Schein and Mishkin, 1993).

Evidence for a significant influence from cortical processing in constancy and induction phenomena also exists for human subjects. Land et al. (1983) carried out colour constancy experiments using a patient with a split corpus callosum, who gave different verbal reports for the inducing surround in each hemifield. Using binocularly fused stimuli Shevell, Holliday and Whittle (1992), reported two brightness inducing mechanisms. Both these experiments provide evidence of information transference across the Corpus Callosum in constancy/induction phenomena. In addition, regions significantly separated from the test area have been demonstrated by psychophysical experiments to be very influential in determining perceived colour (Tiplitz, Blackwell and Buchsbaum, 1988a; Valberg and Lange-Malecki, 1990; Wesner and Shevell, 1992; see also chapter four). The spatial dimensions of these phenomena are too large to be easily explained by known retinal structures. Further, the speed with which a significant portion of this effect occurs, rules out the combination of receptor adaptation and eye movements as the sole mechanism for colour constancy.

Cerebral achromatopsia is an acquired deficiency of colour vision found in association with neurological events which effect the cortical visual areas. In typical cases, the subjects have bilateral lesions in the ventral, occipitotemporal cortex (Meadows, 1974; Zeki, 1990a, b; Plant, 1991). This region of the brain, in particular the fusiform gyrus, is also activated strongly in normal subjects when presented with coloured stimuli (Zeki et al., 1991). The loss of colour perception is rarely total. Subjects report colours as appearing 'washed out' and exhibit naming errors. These naming errors vary

considerably between subjects, although blues and greens are most frequently involved. Indeed, some authors have suggested that the blue sensitive cone mechanism is selectively impaired in achromatopsia (Pearlman et al., 1979; Young and Fishman, 1980). Most subjects perform abnormally on pseudo-isochromatic plates (e.g. Heywood et al., 1987; Rizzo et al., 1992,1993) although others respond normally (e.g. Meadows, 1974). Subjects also have abnormally high error scores on the Farnsworth-Munsell (FM) 100-hue test, although confusions are sometimes restricted to blue hues (e.g. Rondot et al., 1967). Reasons for these differences have been discussed above. Other neurological conditions, especially prosopagnosia and topographical agnosia, are frequently found in association with achromatopsia, but dissociations among all three conditions are also reported. Preservation of spatial vision is indicated by the fact that some subjects have normal or near normal visual acuity, and retention of various degrees of lightness discrimination has been reported by Heywood et al. (1987) and Rizzo et al. (1992, 1993). Localisation of the underlying lesions in cerebral achromatopsia has been achieved by autopsy and by MRI brain scanning, and in patients with unilateral cortical damage, colour vision is disturbed in the contralateral hemifield (e.g. Verrey, 1888; Kolmel, 1988). As discussed earlier, neurons in area V4 of the monkey prestriate cortex respond selectively to colour appearance, that is, they demonstrate colour constancy under change of illumination (Zeki, 1980). It might be expected that lesions of a cortical area corresponding to V4 in humans would result in failure of this aspect of visual performance. Rizzo et al. (1993) comment, however, that the consequences of cerebral achromatopsia are greater than would be expected simply from failure of colour constancy.

It has been shown that chromatic signals may contribute differentially to the generation of various visual attributes. The site of the various mechanisms by which the visual system may achieve colour constancy is still a source of debate. It is therefore of great interest to investigate colour constancy in subjects with damage to the occipitotemporal region of the

cortex. The experiments described in this chapter investigated the instantaneous colour constancy of three such subjects. To explore the possibility that the mechanisms involved are purely retinal, a further experiment was conducted on a subject with a lesion of the primary visual area (V1), which has resulted in an homonymous visual field defect, or hemianopia.

5.2 Experiments on Subjects with Cerebral Achromatopsia

5.2.1 The subjects

The Subjects discussed in this section were those investigated by Barbur et al. (1993b, 1994) and the descriptions are taken from there.

Subject IK (male) is a 53 year-old translator who suddenly developed blurred vision and topographical disorientation. Colours and chromatic contours appeared washed out and difficult to identify. His achromatic visual acuity was 6/6 bilaterally, and measurements of visual field sensitivity revealed an upper homonymous visual field defect which was particularly dense in the upper left quadrant. This subject has great difficulty in reading any of the Ishihara pseudoisochromatic plates, and his error score on the Farnsworth-Munsell 100 hue test was 588. He has persistent prosopagnosia in addition to achromatopsia. MRI revealed bilateral ventral occipitotemporal infarction, with right sided infarct being larger than the left.

Subject CG (male) is a 74 year-old retired engineer who developed a occipital infarct at the age of 65. A right homonymous quadrantonopia was noted, together with dysphasia and dysgraphia. Three months later, C recovered from all symptoms except the field defect. Three years later he suddenly developed blurred vision and he was unable to recognise faces, including that of his own daughter. Chromatic borders appeared washed out and saturated colours were often described as pastel shades. Subsequent imaging studies revealed a second right occipital infarct. At the time C was examined for the present study he had bilateral, upper, homonymous quadrantic field defects and his visual acuity was 6/9 with correct near vision of N8. C was unable to read any of the Ishihara pseudoisochromatic plates with either eye, and his error score on the Farnsworth-Munsell 100 hue test was greater than 800. Magnetic resonance imaging confirmed results from previous CT scans and revealed a bilateral ventral, occipitotemporal infarction

involving cortex and underlying white matter. C's achromatopsia is accompanied by severe prosopagnosia.

Subject WW (male) is a 54 year-old retired professional man who suddenly developed a right homonymous hemianopia at the age of 44. A left occipital infarct was demonstrated on CT scanning. Four years later, W suddenly became confused and topographically disoriented, his vision became unclear, and he was unable to recognise faces or to identify colours. When first examined for the present study, W's visual acuity was 6/5 bilaterally, and measurements of visual field sensitivity revealed right homonymous hemianopia with some loss also affecting his left upper quadrant. W can read all of the Ishihara plates, despite having great difficulties in identifying the colours, but makes some errors on the Farnsworth-Munsell 100 hue test. His severe prosopagnosia has persisted. MRI scans show a large left occipital infarct and a smaller ventral infarct on the right.

The discrimination ellipses for both colour and structure thresholds for all three subjects are shown in figure 5.1.1. The ability of each of the subjects to detect achromatic contrast against the background of random luminance noise was similar to that of normal subject (Barbur et al., 1995). The distribution of light scattered within the eye was measured as described in Chapter 2 from each of the subjects. These data and the corresponding scatter functions are plotted in figure 5.2.1. It should be noted that each of the three subjects with cerebral achromatopsia have a significantly higher stray light parameter **k** than the normal subject CW, whose data are also plotted. Hence, light scattered in the eyes of these subjects will have a larger effect on the colour discrimination tasks described below. As an example of the impairment of the subjects in a visual task, contrast sensitivity functions for each of them are plotted in figure 5.2.2. Note the deterioration in contrast sensitivity at high spatial frequencies. The effect of light scattered in the eye is to blur out fine spatial detail.

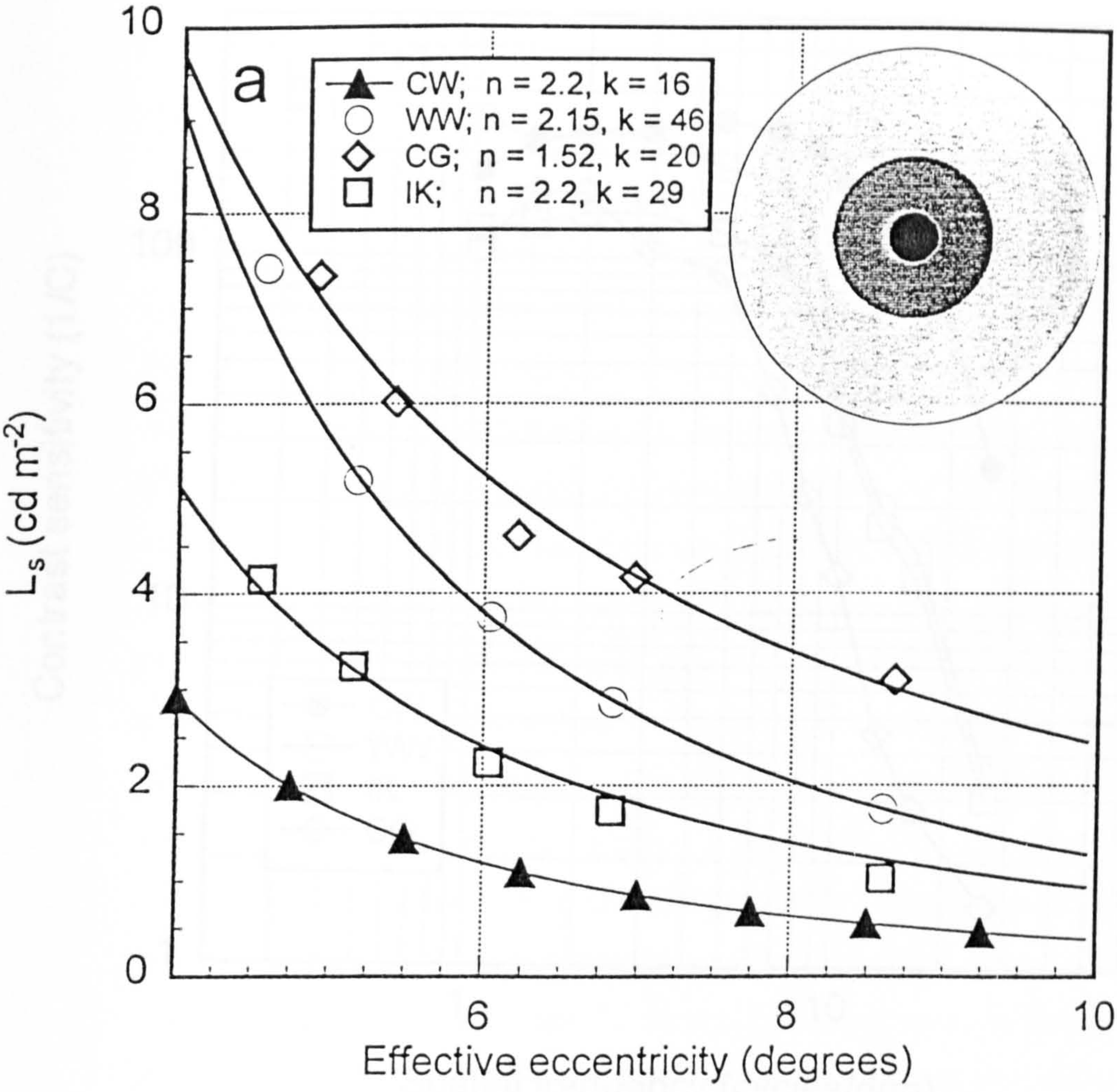

Figure 5.2.1 *The distribution of light scattered within the eye and the corresponding scatter functions measured for the three subjects with cerebral achromatopsia and a normal.*

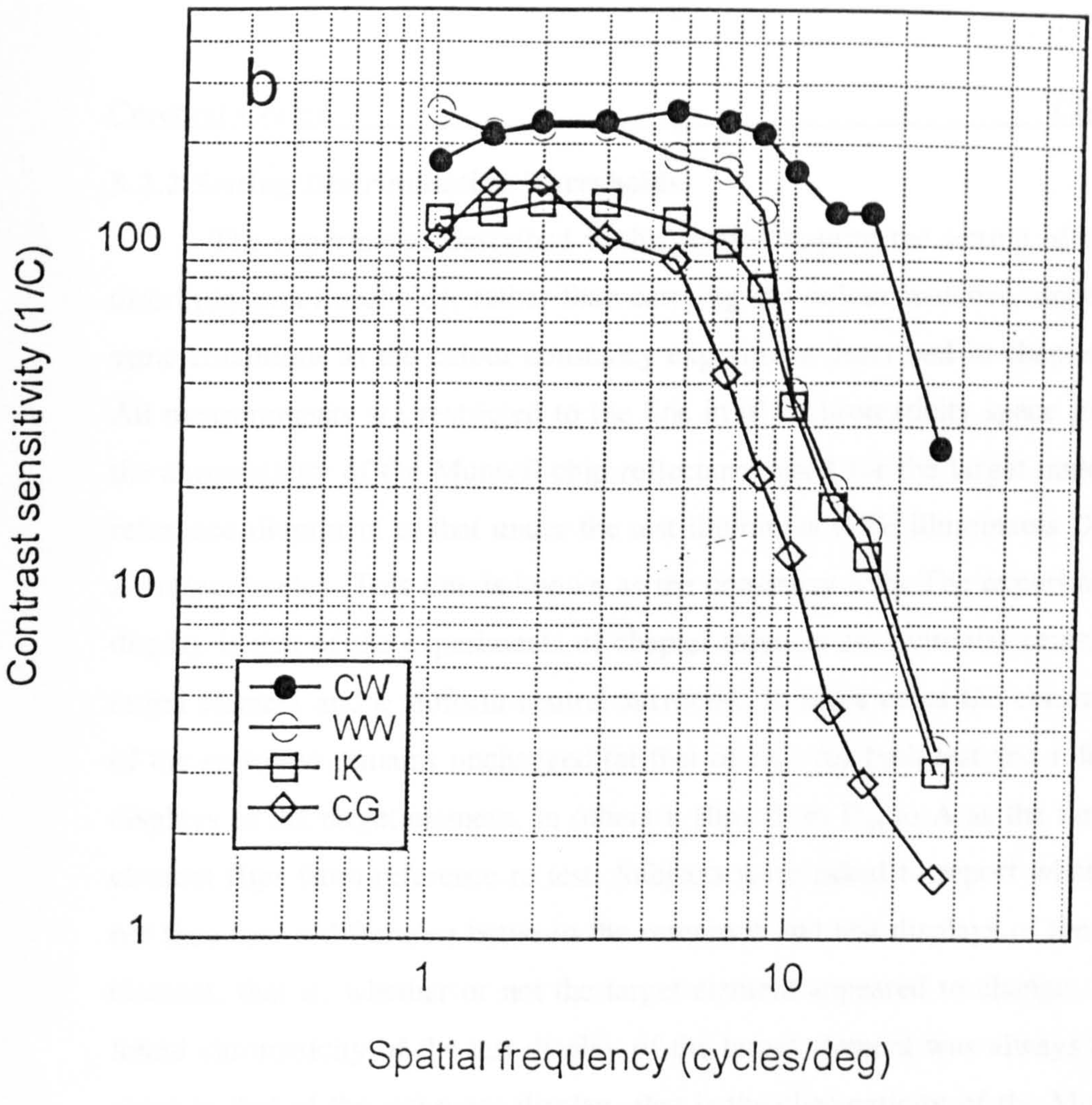

Figure 5.2.2 *Measurements of achromatic contrast sensitivity for the three subjects with cerebral achromatopsia, showing a significant loss in the high frequency range.*

5.2.2 Setting Discrimination Thresholds

The experiments described in this section require the setting of colour discrimination thresholds, rather than carrying out colour matches, under the same conditions as the colour constancy experiment described in chapter two. All measurements are restricted to the line in u'v' chromaticity space joining the chromaticity of the Munsell chip reflectance used for the target under the reference illuminant to that under the test illuminant (CIE illuminants D_{65} and A, respectively). This line is known as the constancy line. The experimental display is that of the experiments of chapter three, with a circular central target element and a uniform neutral surround. In some cases the chromaticity of the surround remains unchanged (at that of D_{65}) for both test and reference displays of the target element, in others it flips from D_{65} to A as the target element flips from reference to test. Subjects were asked to report whether or not they saw a difference between the reference and test displays of the target element, that is, whether or not the target element appeared to change. The initial chromaticity of the test display of the target element was always the same as that of the reference display, that is the chromaticity of the Munsell chip under D_{65}. A single staircase procedure was used, with a negative response from the subject causing the difference in chromaticity to increase and a positive one causing it to decrease. The initial step size was 0.1 times the distance (in u'v' space) between the chromaticities of the target Munsell chip under D_{65} and A; this decreased exponentially to a step of 0.02, after six reversals of direction. The mean of the last three reversal points was taken as the discrimination threshold. It should be noted that the subjects are asked only to report when they see a difference in the target element, they are not asked to identify its colour. As the target element changes in chromaticity every 0.8 seconds and the spatial arrangement of the display does not alter, it is not apparent which, if either, of the two colour discrimination mechanisms differentiated in figure 5.1.1 is the limiting factor in this case. However, the discrimination thresholds measured using this method for a normal subject are not different for those using structure or colour thresholds as described earlier.

Figure 5.2.3 plots the chromaticities of the CIE illuminants D_{65} and A. It also plots the chromaticities of two Munsell chips (5GY5/6 and 7.5P5/6) under each of these illuminants, joined by the constancy (dashed) line. The open circles plot colour discrimination thresholds for a normal subject obtained using the staircase procedure described above. The data for the open squares was obtained using the dynamic colour matching technique described in Chapter 2 with the surround chromaticity flipping between D_{65} and A (i.e. a typical constancy experiment) and the subject's range of movement in the u'v' diagram was restricted to the constancy line. It can readily be seen that the shift in chromaticity caused by instantaneous constancy is many times larger than the discrimination threshold. The size of these shifts are indicated by the grey arrows displaced arbitrarily from the constancy line. Figure 5.2.4 plots similar data for a subject with cerebral achromatopsia (subject CG), with the open circles plotting his discrimination thresholds.

The discrimination thresholds obtained in this manner for the subject with cerebral achromatopsia are significantly larger than those for the normal subject. Therefore, if the colour constancy experiment were to be attempted, it is quite likely the shift due to instantaneous constancy would lie within the range of these enlarged thresholds. The grey arrows in figure 5.2.4 are the same as those in figure 5.2.3, indicating the shift due to constancy for a normal subject. The solid squares plot the discrimination thresholds of the subject with cerebral achromatopsia shifted by this amount. These two ranges of discrimination overlap substantially. It is for this reason that many tests of colour constancy in subjects with cerebral achromatopsia may fail. The subjects do not have sufficiently fine chromatic discrimination to perceive a change in hue under the conditions of the experiment. In view of such findings a new method of testing colour constancy had to be devised instead of performing colour matching experiments. We proposed to determine if there were any shift in chromatic discrimination thresholds when measured using the same sequential presentation technique as used in the dynamic colour matching experiments. That is for one half of the sequential presentation the test target

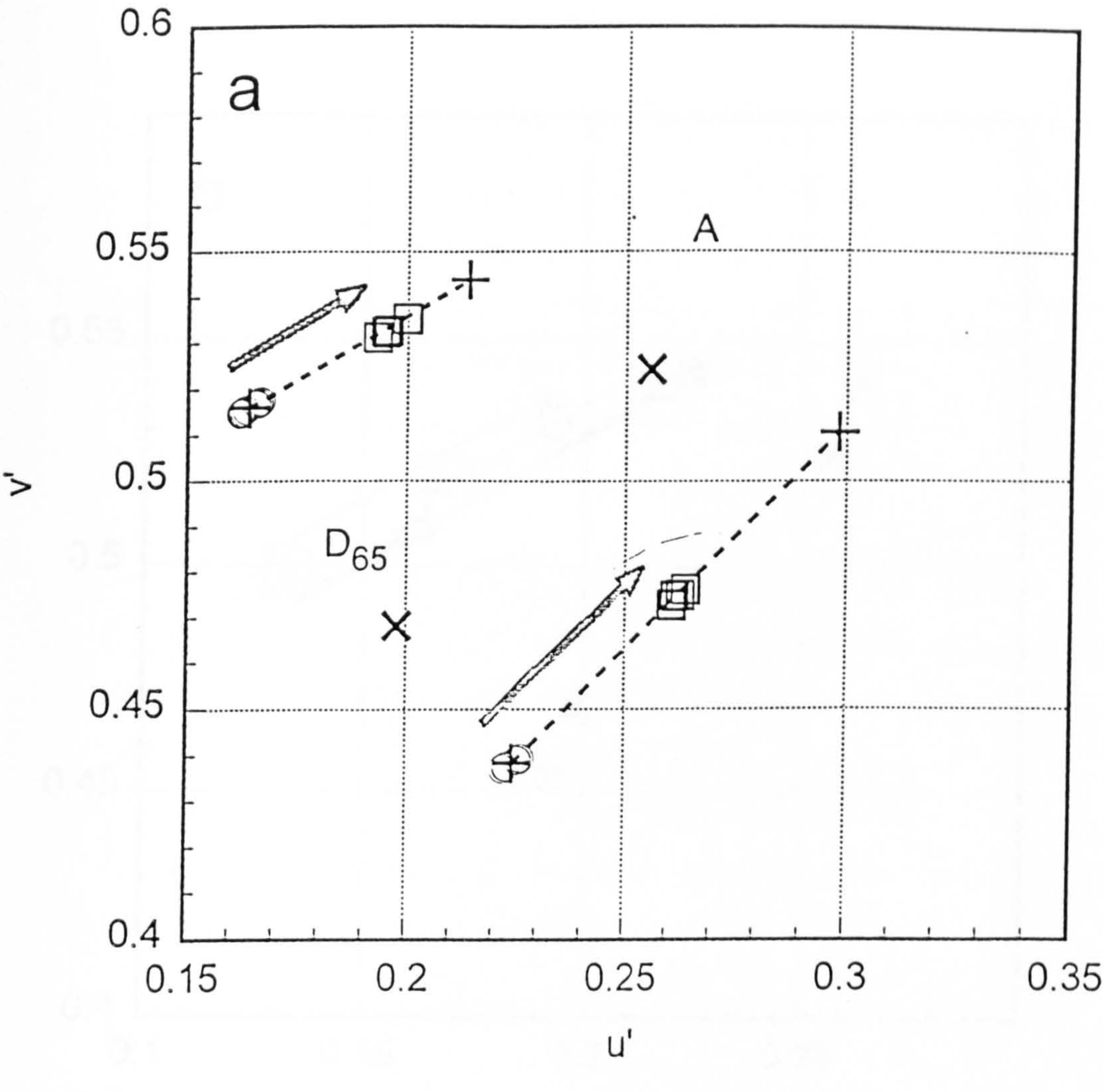

Figure 5.2.3 *The chromaticities of illuminants D_{65} and A are plotted as crosses. The chromaticities of Munsell chips 5GY5/6 and 7.5P5/6 under each of these illuminants are plotted as crosses joined by the constancy (dashed) line. The open circles plot colour discrimination thresholds for a normal subject. The open squares plot the results of a typical constancy experiment. The size of the shifts in chromaticity required to cancel the effect of instantaneous constancy are indicated by the grey arrows displaced arbitrarily from the constancy line.*

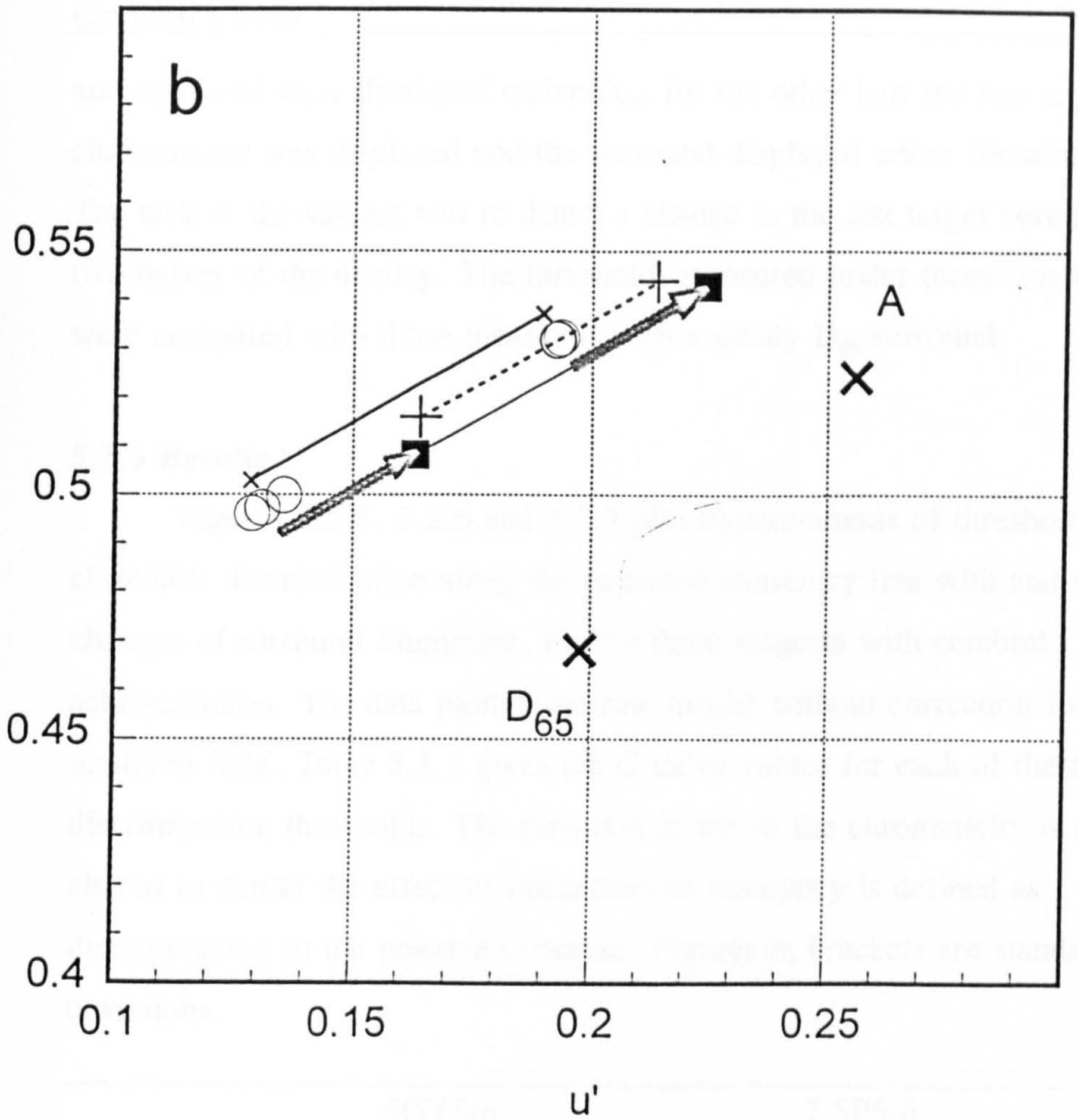

Figure 5.2.4 *The chromaticities of illuminants D_{65} and A are plotted as crosses. The chromaticities of Munsell chip 5GY5/6 under each of these illuminants are plotted as crosses joined by the constancy (dashed) line. The open circles plot colour discrimination thresholds for a subject with cerebral achromatopsia (CG). The grey arrows indicate the shifts in chromaticity due to instantaneous constancy for a normal subject (from figure 5.2.3). The filled squares plot the chromatic discrimination thresholds shifted by this amount (displaced arbitrarily from the constancy line). It is not possible to use test for instantaneous colour constancy in the usual way as the discrimination thresholds are larger than the shifts required to cancel the effect of instantaneous constancy.*

and surround were displayed under D_{65}, for the other half the test target chromaticity was displaced and the surround displayed under illuminant A. The task of the subject was to detect a change in the test target between the two halves of the display. The thresholds measured under these conditions were compared with those measured with a steady D_{65} surround.

5.2.3 Results

Figures 5.2.5, 5.2.6 and 5.2.7 plot measurements of thresholds for chromatic discrimination along the expected constancy line with and without changes of surround illuminant, for the three subjects with cerebral achromatopsia. The data plotted are raw results without correction for scattered light. Table 5.1.1 gives the **C** index values for each of these discrimination thresholds. The direction in which the chromaticity is usually altered to cancel the effect of instantaneous constancy is defined as discrimination in the positive direction. Figures in brackets are standard deviations.

		5GY5/6		7.5P5/6	
		Constant	Changing	Constant	Changing
IK	pos.	0.205	0.758	0.149	0.602
		(0.045)	(0.184)	(0.056)	(0.074)
	neg.	-0.335	0.033	-0.126	0.027
		(0.051)	(0.043)	(0.054)	(0.028)
CG	pos.	0.579	1.247	0.296	1.197
		(0.071)	(0.143)	(0.055)	(0.096)
	neg.	-0.654	-0.437	-0.273	-0.193
		(0.056)	(0.111)	(0.063)	(0.10)
WW	pos.	0.456	0.192	0.335	0.238
		(0.225)	(0.076)	(0.098)	(0.174)
	neg.	-0.448	-0.338	-0.271	-0.174
		(0.013)	(0.097)	(0.042)	(0.077)

Table 5.1.1 *C index values for chromatic discrimination thresholds measured for three subjects with cerebral achromatopsia (not corrected for scatter).*

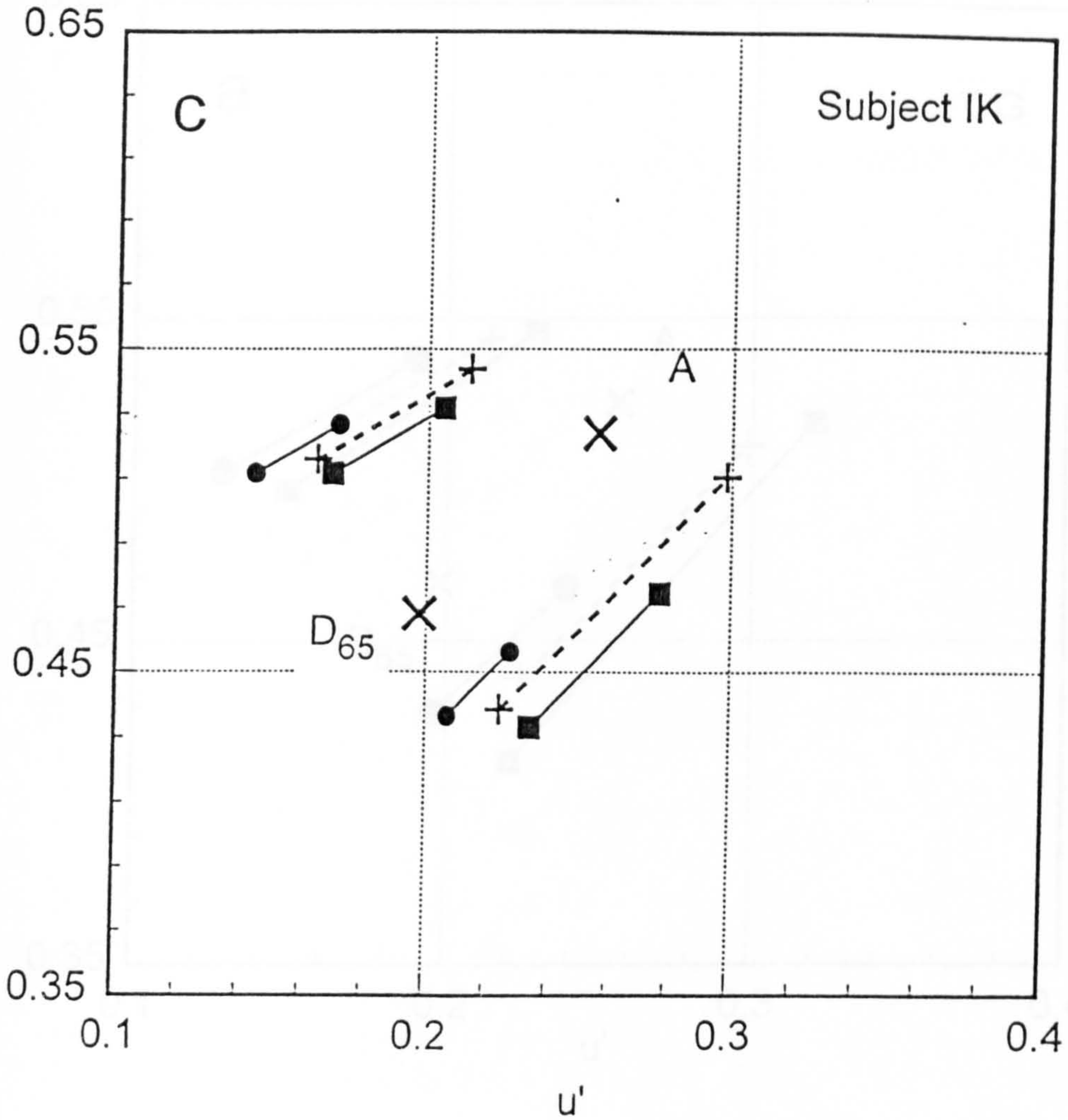

Figure 5.2.5 *Measurement of thresholds for chromatic discrimination along the expected constancy line with and without changes of surround illuminant for subject IK. Data are shown for two Munsell chips (5GY5/6 and 7.5P5/6). Circles plot thresholds measured without illuminant changes and squares plot the same thresholds measured with sequential changes of background illuminant. The data plotted are raw results without correction for scattered light.*

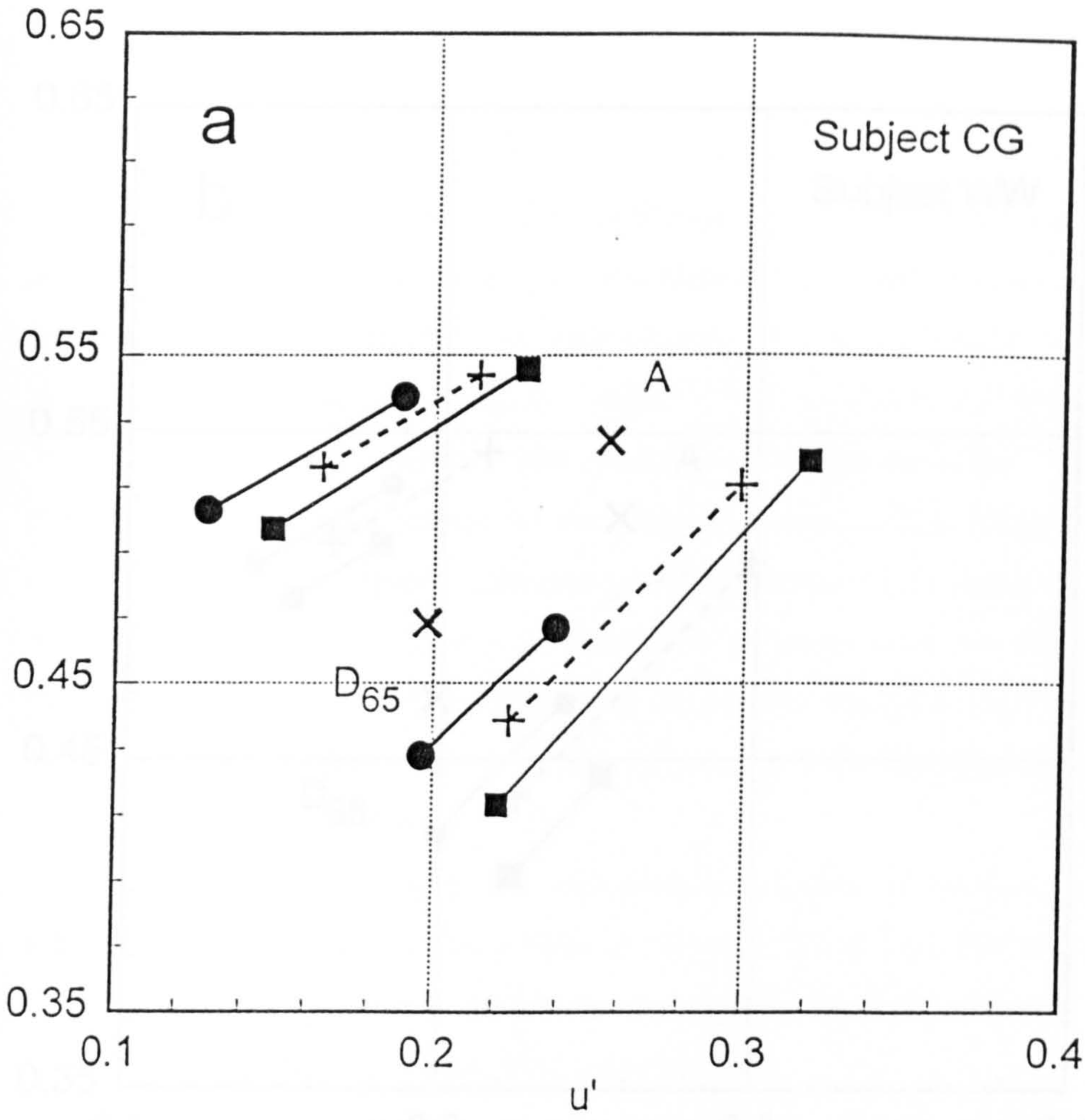

Figure 5.2.6 *Measurement of thresholds for chromatic discrimination along the expected constancy line with and without changes of surround illuminant for subject CG. Data are shown for two Munsell chips (5GY5/6 and 7.5P5/6). Circles plot thresholds measured without illuminant changes and squares plot the same thresholds measured with sequential changes of background illuminant. The data plotted raw results without correction for scattered light.*

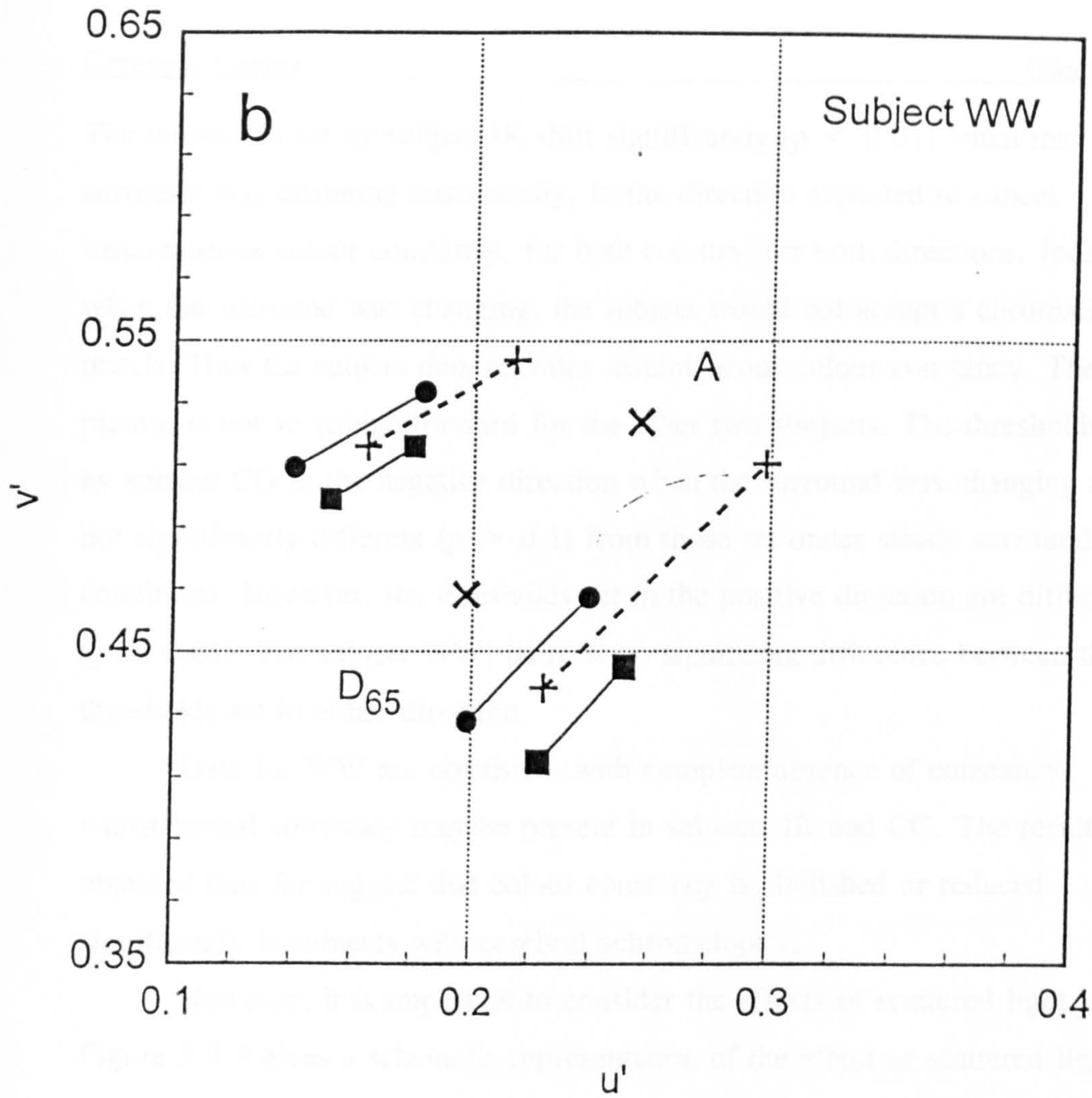

Figure 5.2.7 *Measurement of thresholds for chromatic discrimination along the expected constancy line with and without changes of surround illuminant for subject WW. Data are shown for two Munsell chips (5GY5/6 and 7.5P5/6). Circles plot thresholds measured without illuminant changes and squares plot the same thresholds measured with sequential changes of background illuminant. The data plotted are raw results without correction for scattered light.*

The thresholds set by subject IK shift significantly ($p < 0.01$) when the surround was changing sequentially, in the direction expected to cancel instantaneous colour constancy, for both colours, for both directions. Indeed, when the surround was changing, the subject would not accept a chromaticity match. Thus the subject demonstrates instantaneous colour constancy. The picture is not so straightforward for the other two subjects. The thresholds set by subject CG in the negative direction when the surround was changing are not significantly different ($p > 0.1$) from those set under steady surround conditions. However, the thresholds set in the positive direction are different ($p < 0.01$). For subject WW, there is no significant difference between the thresholds set in either direction.

Data for WW are consistent with complete absence of constancy, whilst partial constancy may be present in subjects IK and CG. The results obtained thus far suggest that colour constancy is abolished or reduced significantly in subjects with cerebral achromatopsia.

However, it is important to consider the effects of scattered light. Figure 5.2.8 gives a schematic representation of the effect of scattered light on the measurements for a steady surround (light scattered only from the D_{65} illuminant). Figure 5.2.9 plots the similar correction made when the surround illuminant changes sequentially from D_{65} to A. Details of the correction to chromaticity coordinates are given in chapter two. It should be noted that in the case of the changing surround conditions, the chromaticity of the reference target is displaced towards that of the D_{65} surround, whilst the chromaticities of the discrimination thresholds are displaced towards that of the A surround. If the amount of scattered light is large, it could mask the shift in chromaticity required to cancel the effect of instantaneous colour constancy.

Figures 5.2.10, 5.2.11 and 5.2.12 plot measurements of thresholds for chromatic discrimination along the expected constancy line with and without changes of surround illuminant, for the three subjects with cerebral achromatopsia. The data plotted are corrected for scattered light. Table 5.1.2

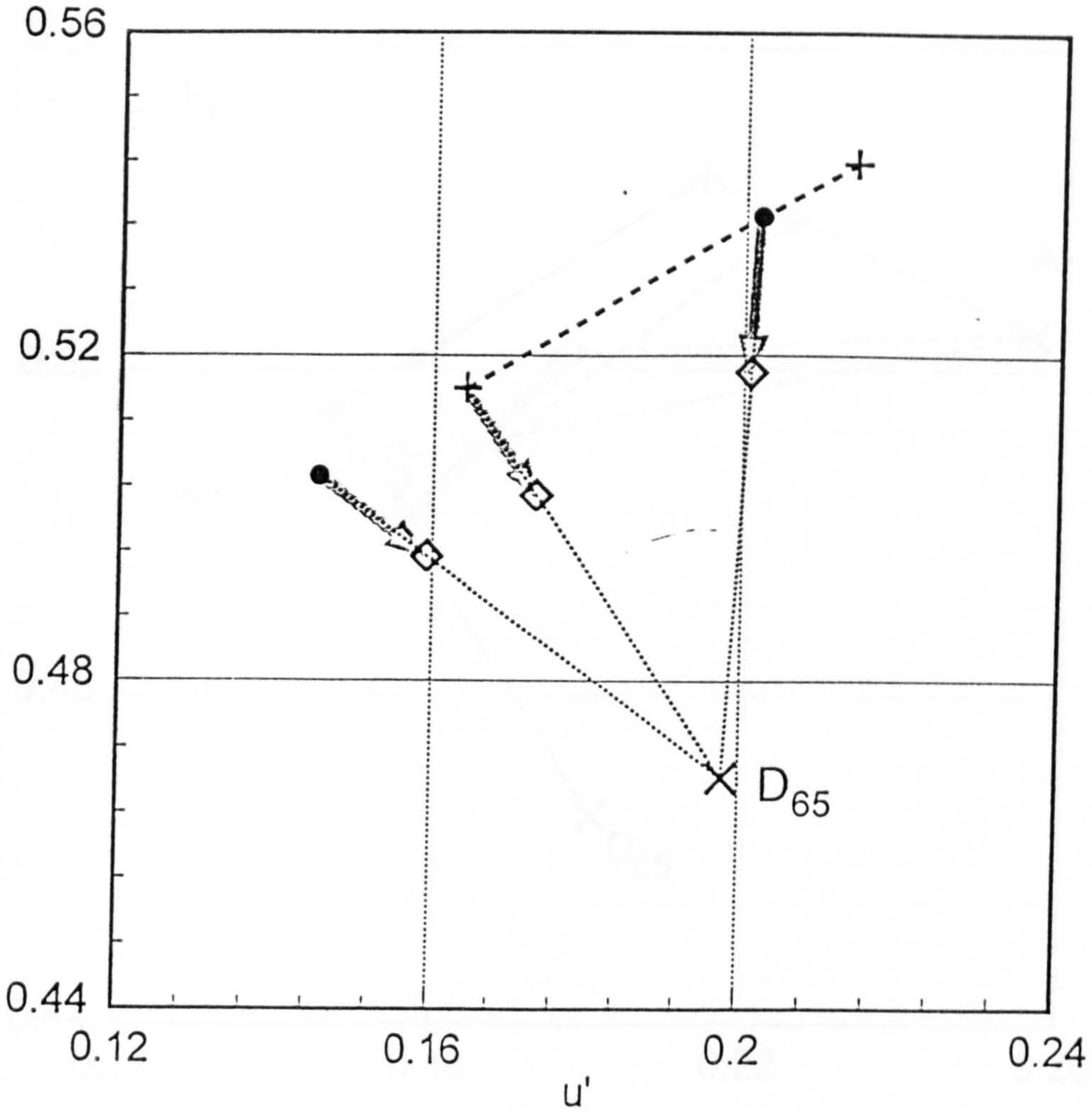

Figure 5.2.8 *Schematic representation of the effect of scattered light on the measurement of chromatic discrimination thresholds, measured with a steady surround. Light is scattered from the D_{65} illuminant only, so all chromaticities are displaced towards the chromaticity of D_{65}. The solid circles plot the threshold settings as measured in screen coordinates. The open circles show the actual chromaticity changes involved after correction for light scatter from the surrounding background.*

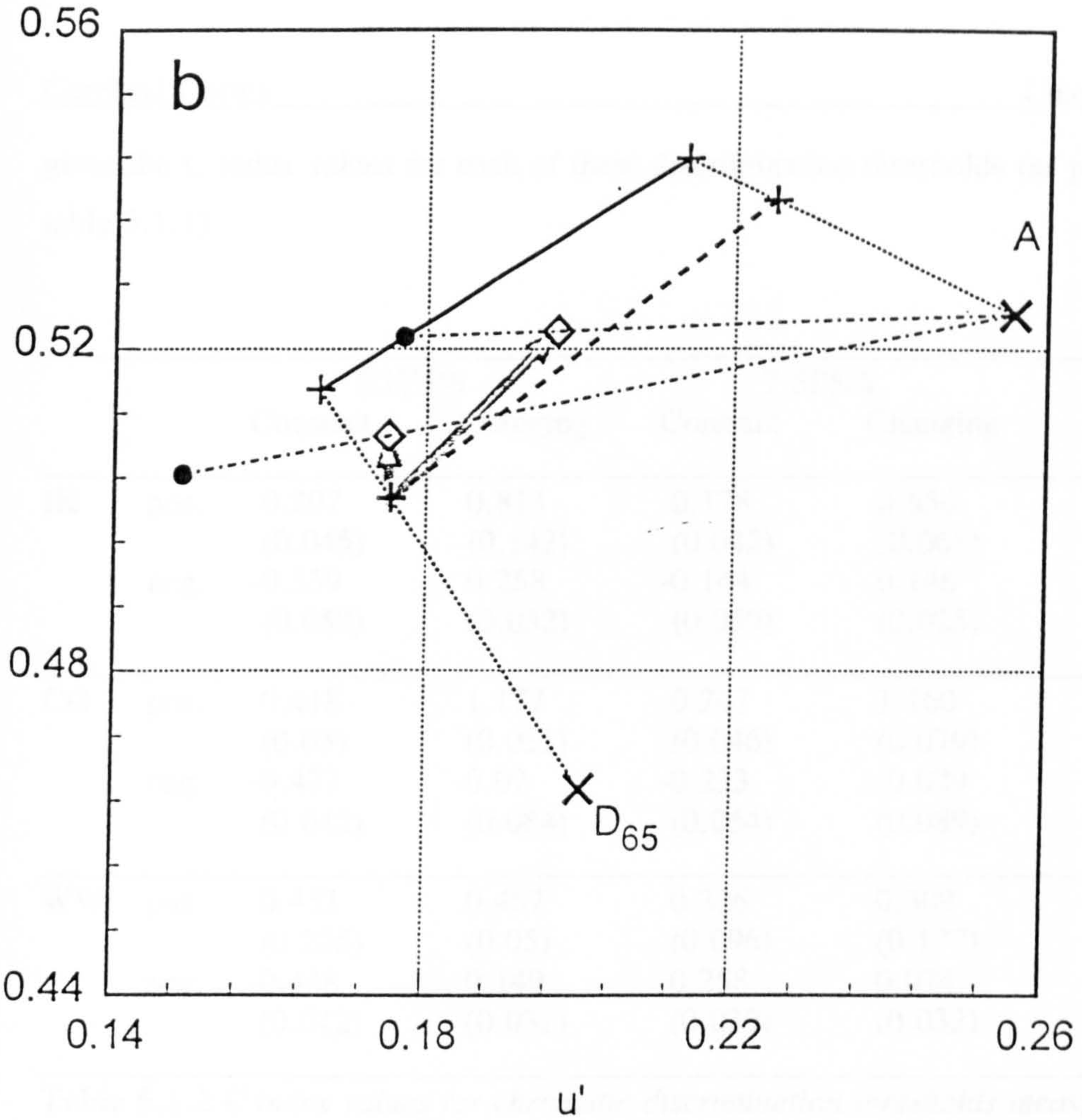

Figure 5.2.9 *Schematic representation of the effect of scattered light on the measurement of chromatic discrimination thresholds, measured when the surround illuminant changes sequentially from daylight to tungsten (D_{65} and A). The solid circles plot the threshold settings as measured in screen coordinates. The open circles show the actual chromaticity changes involved after correction for light scatter from the surrounding background.*

gives the **C** index values for each of these discrimination thresholds (as per table 5.1.1).

		5GY5/6		7.5P5/6	
		Constant	Changing	Constant	Changing
IK	pos.	0.207	0.813	0.178	0.656
		(0.045)	(0.142)	(0.042)	(0.065)
	neg.	-0.339	0.258	-0.144	0.146
		(0.052)	(0.032)	(0.059)	(0.025)
CG	pos.	0.418	1.177	0.247	1.160
		(0.05)	(0.031)	(0.046)	(0.079)
	neg.	-0.477	-0.07	-0.233	-0.029
		(0.042)	(0.084)	(0.054)	(0.089)
WW	pos.	0.453	0.457	0.326	0.309
		(0.225)	(0.05)	(0.096)	(0.177)
	neg.	-0.438	0.149	-0.258	0.074
		(0.012)	(0.032)	(0.039)	(0.032)

Table 5.1.2 *C index values for chromatic discrimination thresholds measured for three subjects with cerebral achromatopsia (corrected for scattered light in the eye).*

Once the effects of scattered light have been accounted for, the chromaticity discrimination thresholds shift significantly for all three subjects. The pattern of results obtained suggests that instantaneous constancy mechanisms are present in each subject.

5.2.4 Discussion

The results show that these three subjects with cerebral achromatopsia examined in our study do indeed show shifts in their colour discrimination thresholds due to instantaneous colour constancy. The need to consider the effects of scattered light within the eyes of these subjects has also become apparent. The effect of scattered light is to decrease the measured shift due to

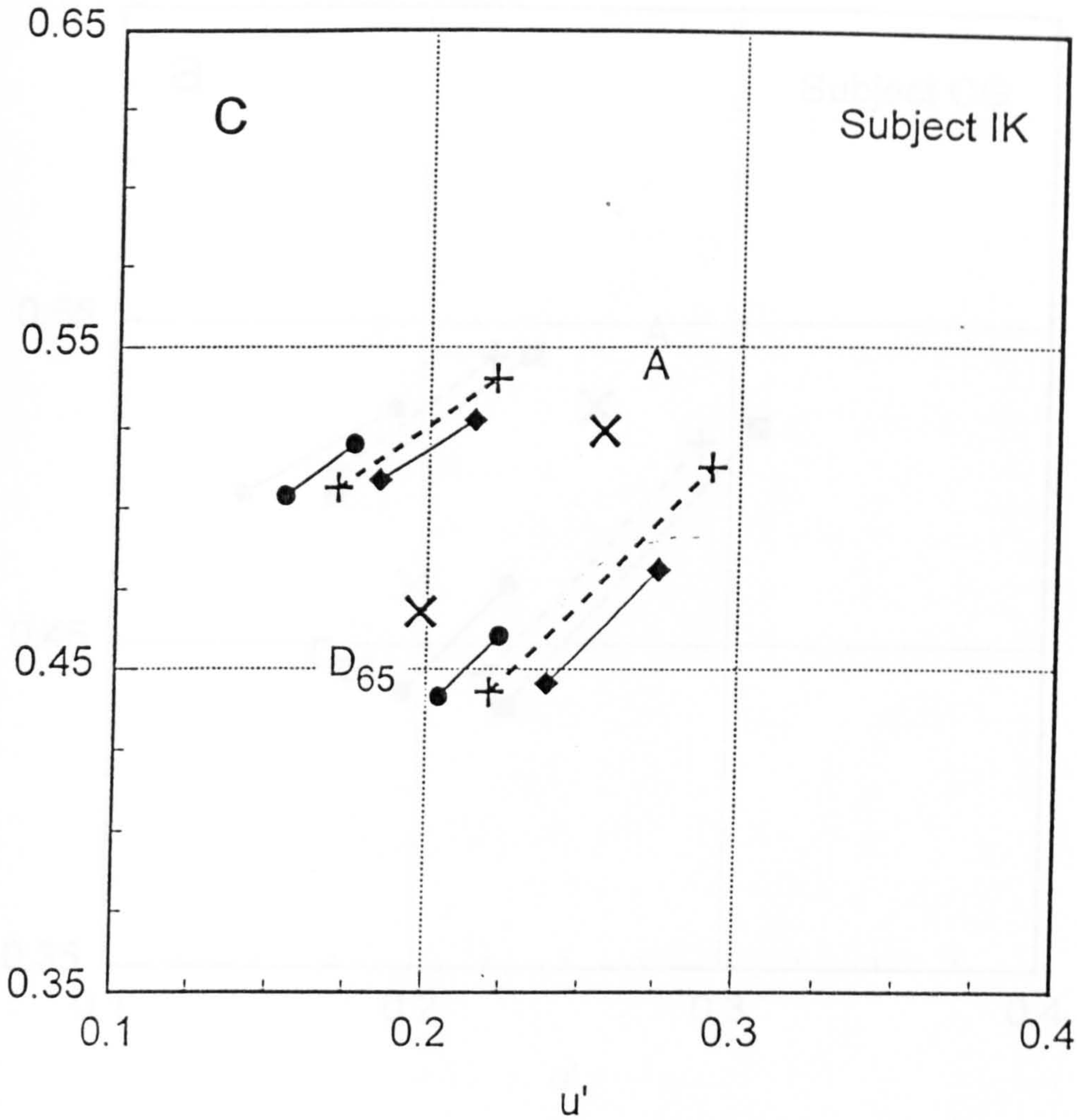

Figure 5.2.10 *Measurement of thresholds for chromatic discrimination, after correction for scattered light, with and without surround illuminant changes for subject IK. Data are shown for two Munsell chips (5GY5/6 and 7.5P5/6). Circles plot thresholds measured without illuminant changes and squares plot the same thresholds measured with sequential changes of background illuminant.*

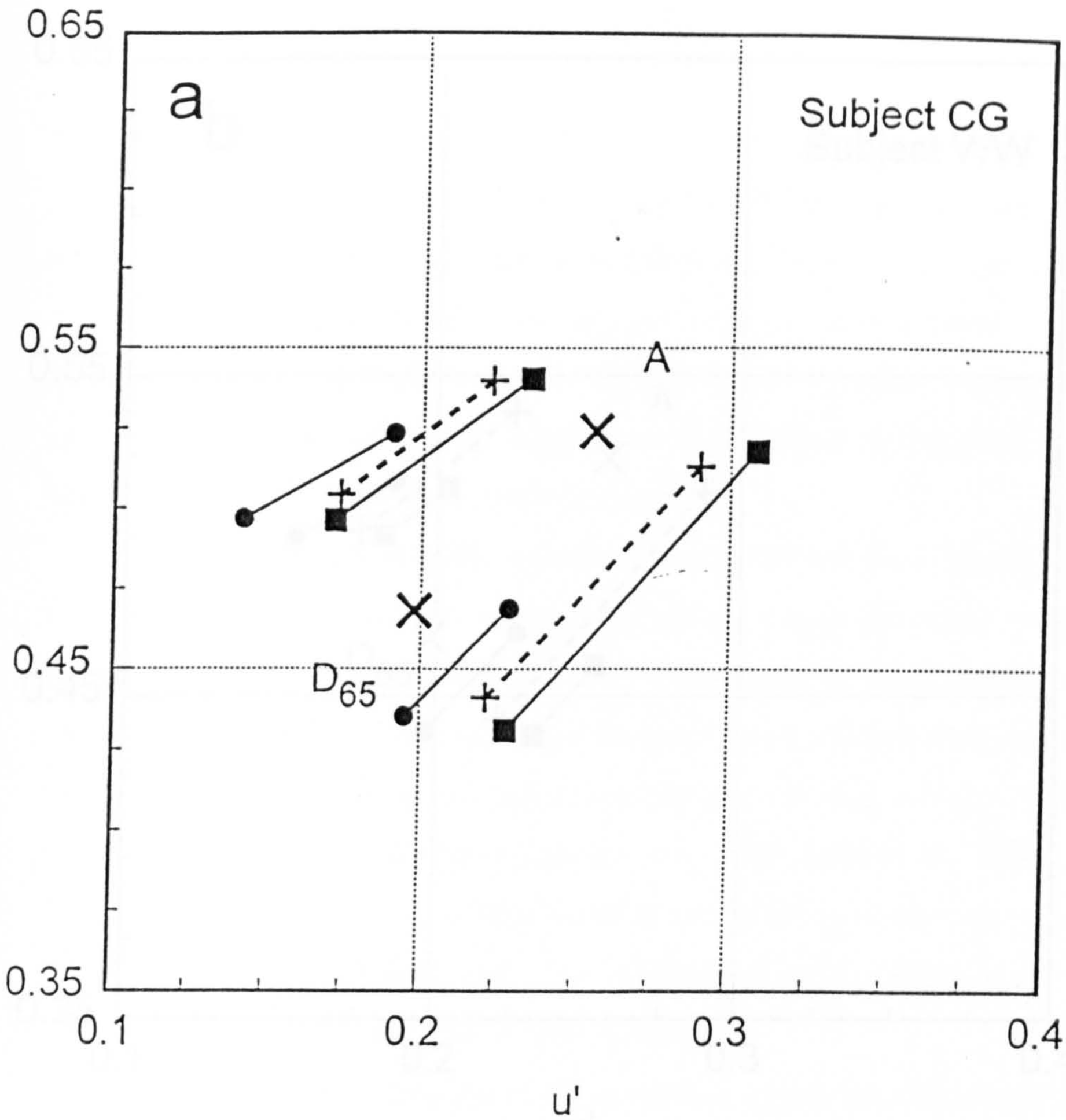

Figure 5.2.11 *Measurement of thresholds for chromatic discrimination, after correction for scattered light, with and without surround illuminant changes for subject CG. Data are shown for two Munsell chips (5GY5/6 and 7.5P5/6). Circles plot thresholds measured without illuminant changes and squares plot the same thresholds measured with sequential changes of background illuminant.*

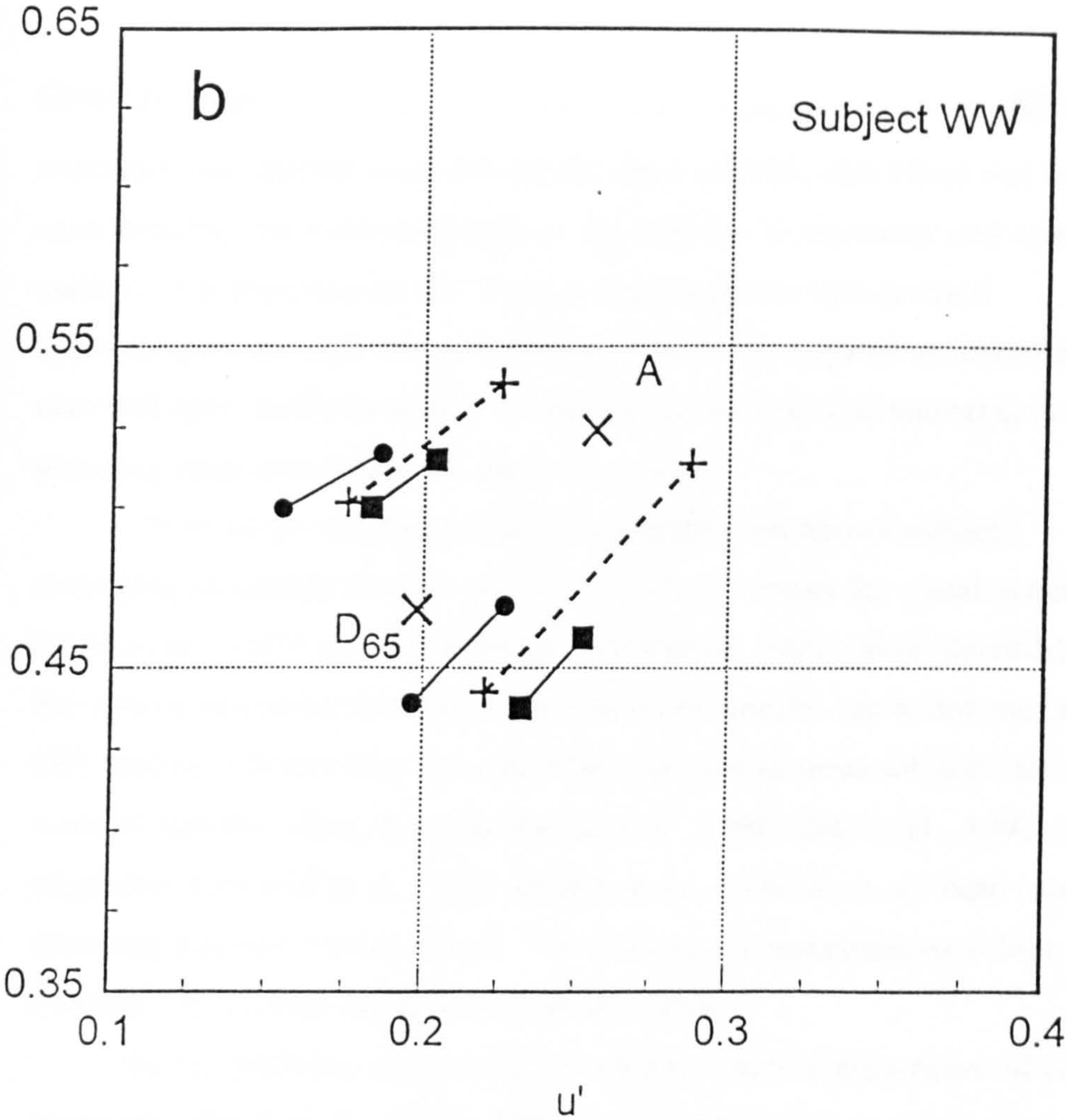

Figure 5.2.12 *Measurement of thresholds for chromatic discrimination, after correction for scattered light, with and without surround illuminant changes for subject WW. Data are shown for two Munsell chips (5GY5/6 and 7.5P5/6). Circles plot thresholds measured without illuminant changes and squares plot the same thresholds measured with sequential changes of background illuminant.*

constancy (see chapter two). For two of these subjects, this effect was of approximately the same magnitude as the shift due to constancy and served to mask it. It is important to note that, as many subjects with cerebral achromatopsia are well above the average age of the population, the effect of scattered light should be always considered in any fine discrimination or matching tasks which they are asked to perform.

Previous psychophysical experimentation with human subjects, attempting to identify the site of colour constancy within the visual system (Land et al., 1983; Shevell, Holliday and Whittle, 1992), have identified the importance of cortical function, rather than any specific site within the cortex. PET studies, whether they have identified the area of these subjects' lesion as a site of specific colour function (Lueck et al., 1989; Zeki et al., 1991) or other sites (Corbetta et al., 1991; Gulyas et al., 1994) have not been carried out using a colour constancy task. The existence of instantaneous colour constancy is not then inconsistent with this work.

In the macaque, ablation of V4 leads to a severe impairment of colour constancy (Walsh et al., 1993). Although our instantaneous colour constancy may only be one contributory mechanism to the phenomenon of colour constancy as we experience it, its preservation in subjects with damage to the lingual and fusiform gyri suggests that these areas in humans may not be the homologue of cortical area V4 in the monkey. This is in agreement with Heywood et al., who found differences between the abilities of monkeys with bilateral removal of area V4 (Heywood et al., 1992) and a cortically colour blind human observer (Heywood, et al., 1991) to discriminate between two rows of coloured or grey stimuli. Further, these results suggest that the computations for this instantaneous colour constancy in humans occur earlier in the visual system.

5.3 Experiments on a Subject with Hemianopia

5.3.1 The Subject

The subject tested in this experiment, GY, has been investigated in several previous studies and his visual deficits have been documented (Barbur et al., 1980, 1988; Blythe et al., 1987; Weiskrantz et al., 1991; 1995). He has a complete right homonymous hemianopia with approximately 3° of macular sparing as a result of a road accident at the age of eight years. A comparison of field plots of the hemianopic field, taken immediately after the accident, some fourteen years later by Barbur et al. (1980) and in recent perimetric testing (Barbur et al., 1994) show no significant change. A CT scan on this subject (Barbur et al., 1988) shows unilateral destruction of the left striate cortex. GY is emmetropic and has no other loss of function following the accident.

5.3.2 Retinal Function

After lesions of the occipital cortex or optic radiations, transneural retrograde degeneration in primates may take place. However this is not always complete. Studies have shown that eight years after a striate lesion some 20% of retinal beta ganglion cells and a small number of LGN neurones may survive (Cowey and Stoerig, 1991). Retinal beta ganglion cells have been found to project to the surviving LGN neurones either directly or via interneurons (Cowey and Stoerig, 1991; Stoerig and Cowey 1992; Cowey,1993). The surviving LGN cells project to the extrastriate areas including area V4 (Cowey and Stoerig, 1991). In addition, beta ganglion cells may project to the pulvinar where some colour opponent activity has been reported (Felsten et al.,1983).

Stoerig and Cowey (1992) discuss the contributions of these pathways and of pathways originating in retinal alpha and gamma cells to colour discrimination ability in blindsight. For the purposes of the experiments of this section, it is

necessary only to demonstrate retinal function specific to different coloured stimuli, in human subjects.

Several authors have reported chromatic discrimination ability or cone functions in the blind hemifields of subjects with hemianopia. Dark adaptation traces for monochromatic adaptive fields presented in a subject's blind hemifield (Bender and Krieger, 1951) implied the involvement of more than one type of retinal receptor. They also reported that for sufficiently long and intense stimuli, subjects had an "appreciation of colour". Correct colour identification of foveally presented large coloured stimuli was reported by Perenin et al. (1980) for a subject with complete bilateral cortical blindness. In experiments where a visual stimulus contained both colour and luminance components, the existence of a pupillary constriction despite large decrements in stimulus luminance, has been demonstrated (Barbur et al., 1987). The response amplitudes were found to be much reduced in the absence of any chromatic change, indicating the contribution of chromatic processes to the pupil responses. Stoerig (1987) reported that six out of ten subjects with central lesions tested had significant performance levels when asked to discriminate between red and green targets in a forced choice paradigm. Later, increment threshold spectral sensitivity was measured in three hemianopic subjects by Stoerig and Cowey (1989; 1991; 1992). These findings provide evidence of both rod and cone activity in cortically damaged subjects and show that opponent colour mechanisms of at least blue/yellow opponency contribute to the responses in the blind field. Ruddock (1993) has also measured wavelength discrimination in the hemianopic subject who performed the experiments of this chapter (GY) using large monochromatic stimuli generated in a Maxwellian viewing system, and found evidence for cone activity and colour discrimination in the blind hemifield. Discrimination between red, green and blue achromatic flashes under conditions when GY cannot make use of luminance contrast cues has also been demonstrated (Barbur et al., 1994).

For the purposes of this investigation, an experiment first carried out by Pöppel (1986) was repeated on subject GY. The subject fixates a point within a rectangular area of the screen, chosen so that half the remaining screen area is within his blind field and that the rectangular area occupies the region of macular sparing. This rectangular area remains white throughout the whole experiment. The surrounding area of the screen is set to high saturation colour; either with the whole surround the same colour, or with the sighted and blind hemifields set to different colours. The subject maintains fixation on this presentation for 30s, whereupon the whole display becomes white and the subject is asked to describe what he sees. Fatigue within a receptor population causes complementary after images (Pöppel, 1986). That is for a normal subject, if the whole of the surround is green, after adaptation for 30s, the after image of the surround area is magenta, while the central rectangle becomes a pale green. However, if half the surround is green and the other half red, the after image of the green area is magenta as before, the red area becomes cyan or pale blue while the central white area remains neutral (grey) in colour. It is interesting to note that the central area is homogeneously coloured and does not show a tendency towards either of the surround colours close to its edges.

These stimuli were presented to subject GY several times, with several minutes in daylight between each presentation, and his responses recorded. He was unable to distinguish the two adapting conditions (full green surround and split green/red surround) consciously. However, he reported the after images of the full green surround condition as the outside being "a purplish colour" and the centre a "pale green"; while for the split surround condition he reported the outside as "the usual pink" and the centre "like a shadow, no colour". These results are similar to those of Pöppel's (1986) subject. That colour induction is effected by stimuli in the blind hemifield is evidence for cone function in the part of the retina which represents that hemifield.

5.3.3 Colour Constancy Experiment

The experiments of this section were carried out to investigate whether a changing surround in Subject GY's blind hemifield would contribute to instantaneous constancy. The figure used for these experiments was similar to that of the experiments with the achromatopsics in that it consisted of a central circular target and a circular surround. However, the target element subtended 6^0 visual angle in diameter. It should be noted that this is larger than the previous target size and may have an effect on the results. There was a fixation spot displaced 2^0 to the left of the centre of the target (i.e. 1^0 from the left hand side) and strict fixation was an instruction to the subject. The surround, on which the changing illuminant acts, was divided into two halves, which could change independently. Three experiments were carried out. The illuminant was changed from D_{65} to A over the whole surround (experiment 1), changed on the left hand side (sighted hemifield) only, while the right hand side remains illuminated by D_{65} all the time (experiment two) or changed on the right hand side (blind hemifield) only with the left hand side remaining under D_{65} (experiment three). It should be noted that Subject GY was not aware of the difference between experiments 1 and 2. Dynamic colour matching was carried out in the usual manner. Two normal subjects (CW and JB) and subject GY performed a total of fifteen colour matches for each of the experiments, for each of the target colours (Munsell chips 5GY5/6 and 7.5P5/6).

Figure 5.3.1 shows the configuration of the experimental display and plots the data obtained in each of the three experiments for Subject CW. Figure 5.3.2 and 5.3.3 plot similar data for subjects JB and GY, respectively. The data are plotted as pairs of points indicating a range from two standard errors below the mean to two above. The data for experiments 2 and 3 are displaced arbitrarily from the colour constancy line. This is merely for ease of presentation, as all colour matching was restricted to this line. The solid circles plot data for Experiment 1 with the full surround change. The open diamonds plot data for Experiment 2 with just the sighted hemifield change.

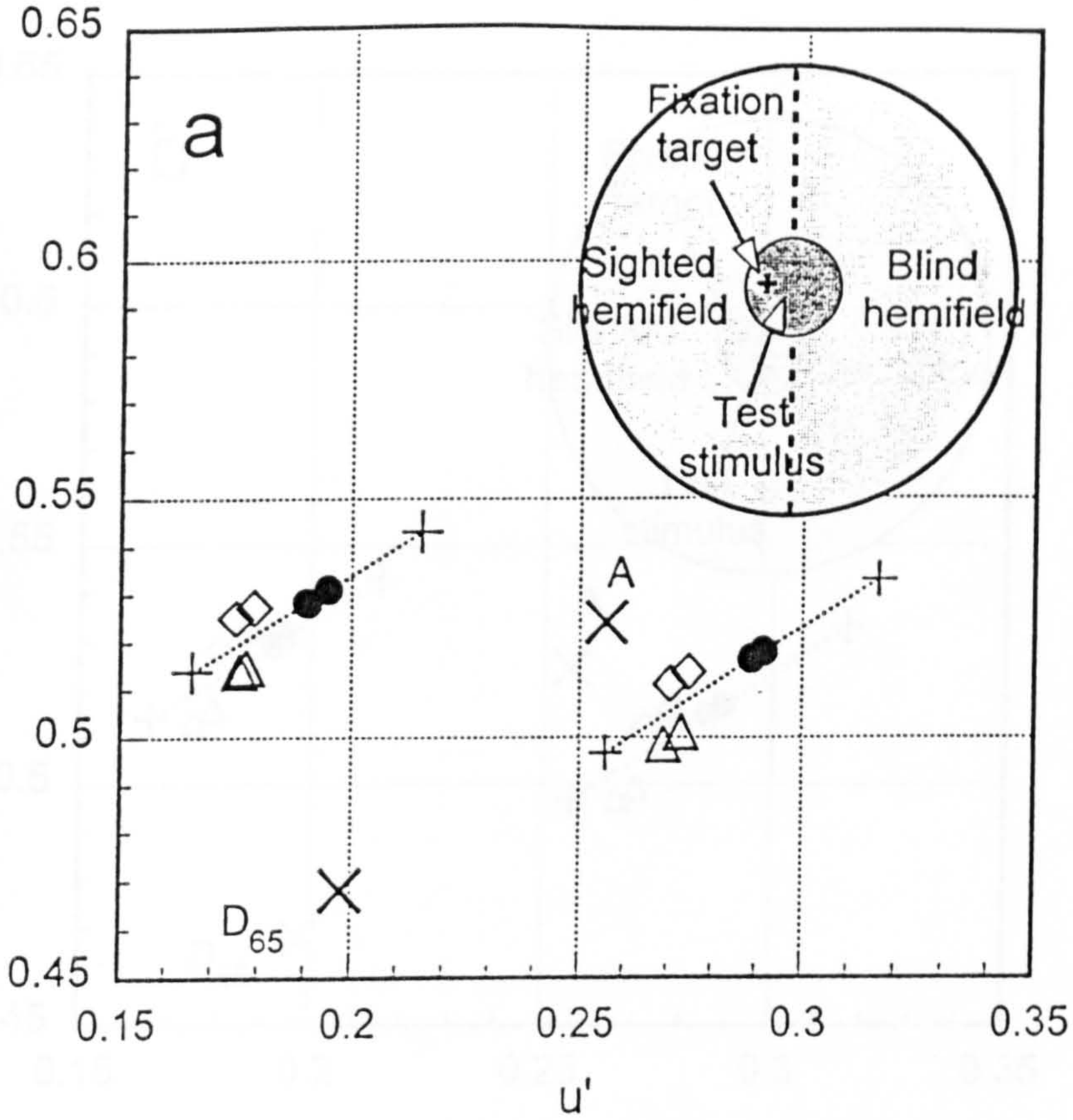

Figure 5.3.1 *Colour constancy measurements for subject CW for the special pattern developed for GY. (see inset showing pattern covering the sighted and the blind hemifields of GY). Data shown when the changing illuminant covered the blind, sighted or the whole of the visual field (full field: solid circles; sighted hemifield stimulus: diamonds and blind hemifield stimulus: triangles). The half field symbols are displaced with respect to the constancy line for clarity of presentation. Data show that a reduced but significant shift in chromaticity is required to null out the effect of constancy mechanisms for the half field condition. The difference between the two hemifields has been attributed to the difference in the geometry of the pattern as illustrated in the inset. All data are corrected for the effects of scattered light.*

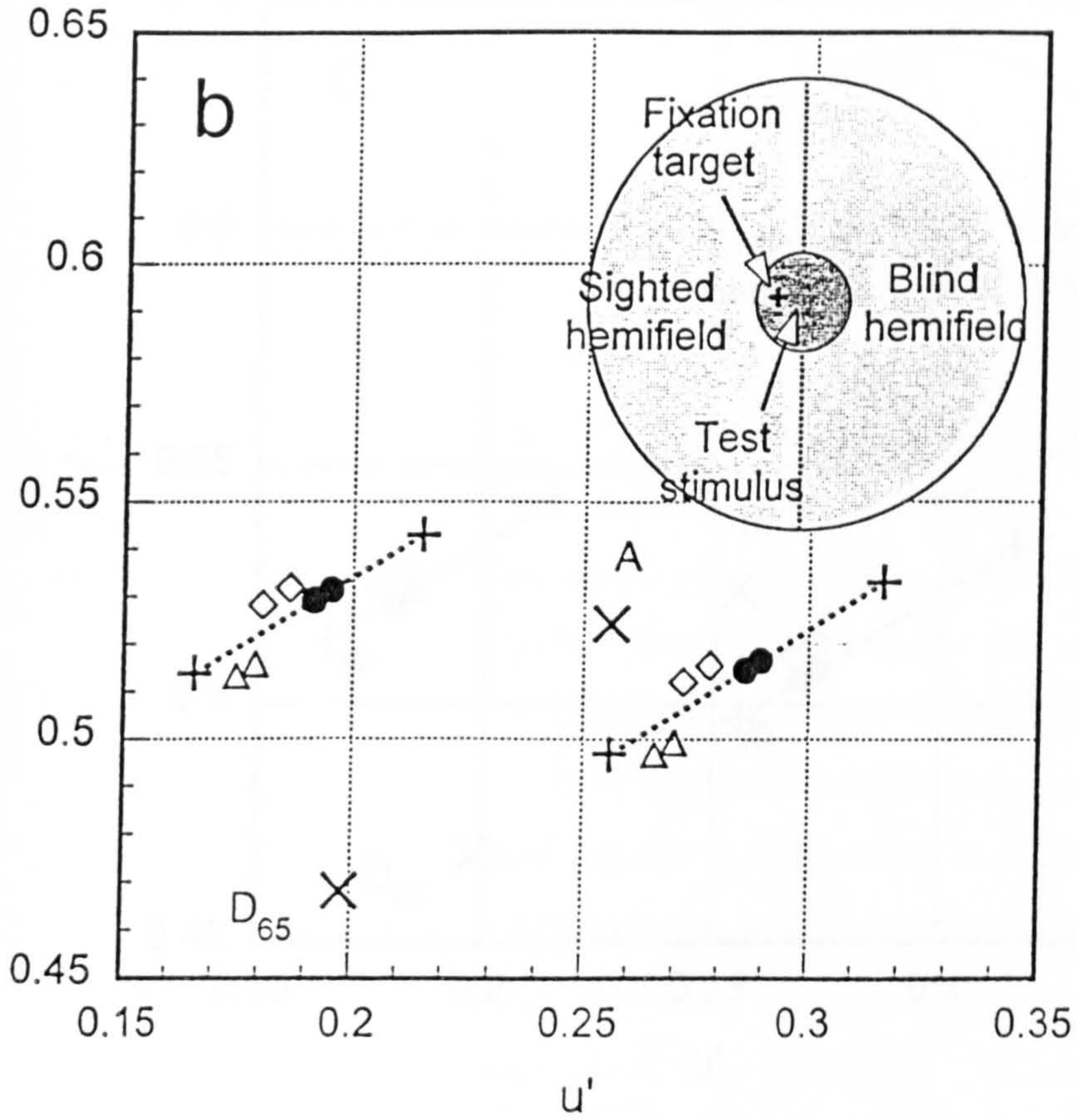

Figure 5.3.2 *Colour constancy measurements for subject JB for the special pattern developed for GY. (see inset showing pattern covering the sighted and the blind hemifields of GY). Data shown when the changing illuminant covered the blind, sighted or the whole of the visual field (full field: solid circles; sighted hemifield stimulus: diamonds and blind hemifield stimulus: triangles). The half field symbols are displaced with respect to the constancy line for clarity of presentation. Data show that a reduced but significant shift in chromaticity is required to null out the effect of constancy mechanisms for the half field condition. The difference between the two hemifields has been attributed to the difference in the geometry of the pattern as illustrated in the inset. All data are corrected for the effects of scattered light*

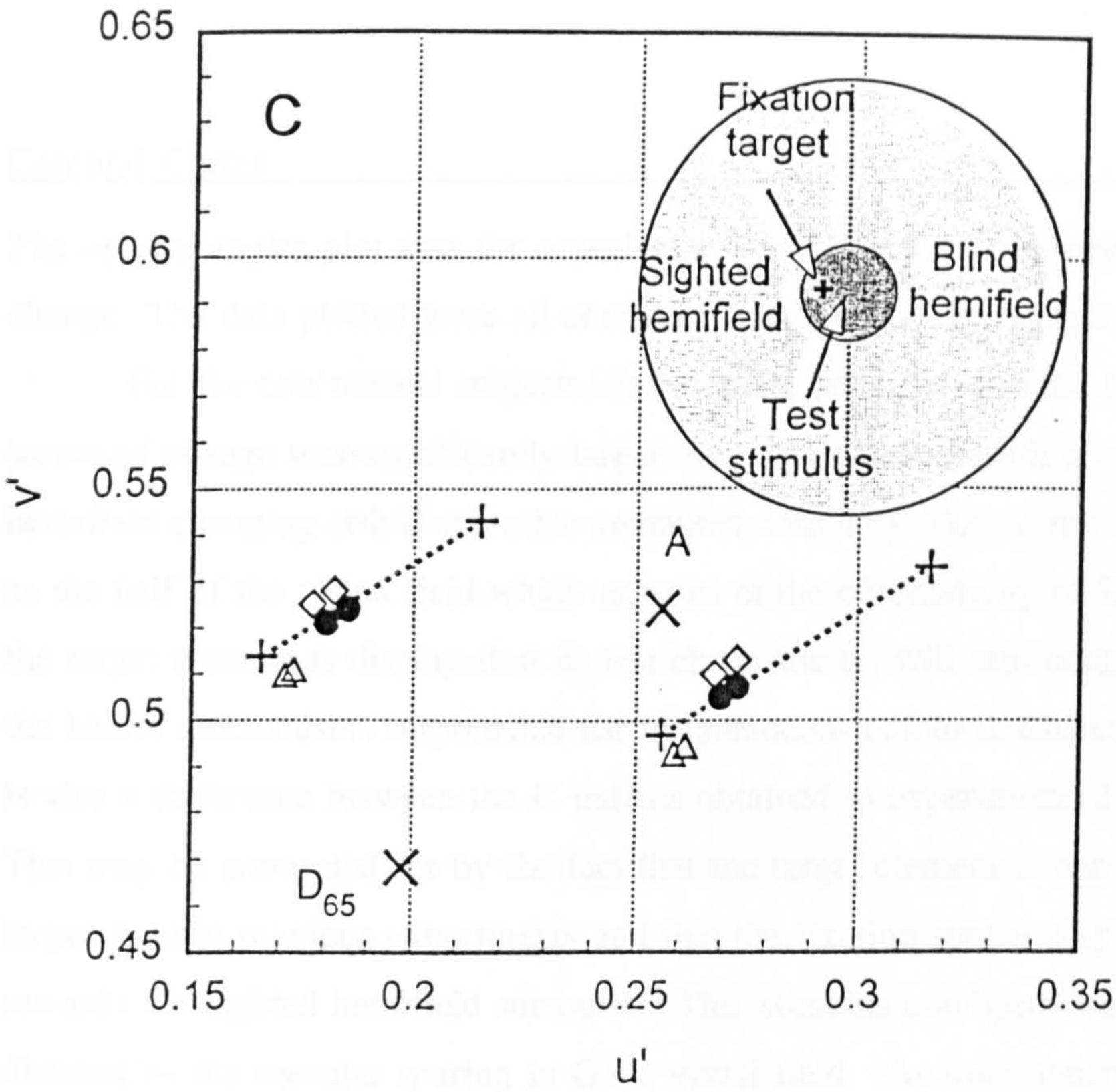

Figure 5.3.3 *Colour constancy measurements for hemianopic subject GY for the special pattern developed for GY. (see inset showing pattern covering the sighted and the blind hemifields of GY). Data shown when the changing illuminant covered the blind, sighted or the whole of the visual field (full field: solid circles; sighted hemifield stimulus: diamonds and blind hemifield stimulus: triangles). The half field symbols are displaced with respect to the constancy line for clarity of presentation. The data show clearly that there is no significant difference between the full field and the sighted hemifield conditions and that the data for the sighted field condition is very close to zero. This suggests that the blind hemifield does not contribute significantly to instantaneous constancy.*

The open triangles plot data for experiment 3 with just the blind hemifield change. The data plotted were all corrected appropriately for scattered light.

For the two normal subjects, the **C** index obtained with the full surround change was significantly larger than that obtained with just one hemifield changing (while the other remained constant). This is not surprising, as the half of the visual field which remains at the chromaticity of D_{65} when the target element is displayed at its test chromaticity, will also contribute to the lateral mechanisms responsible for instantaneous colour constancy. There is also a difference between the **C** indices obtained in experiments 2 and 3. This may be accounted for by the fact that the target element is considerably larger than in previous experiments and that the fixation spot is displaced towards the sighted hemifield surround. This stimulus configuration was dictated by the macular sparing in GY's visual field. As instantaneous constancy can be shown to depend markedly on the distance between the target element and the inducing surround (see Chapter 4), it is to be expected that when the changing surround is closer to the fixation spot (i.e. experiment 2) a larger **C** index will be induced.

For Subject GY, a different pattern of results is observed. There is no significant difference between the results obtained in experiments 1 and 2. That is, flipping only the sighted hemifield during the dynamic colour matching procedure induces the same degree of instantaneous constancy as flipping the whole of the surround. The **C** index in each case is approximately that obtained for a normal when only the sighted hemifield is flipped. When only the blind hemifield is flipped the **C** index is very close to zero, although statistically significantly just larger. However, scattered light from the blind hemifield onto the sighted hemifield cannot be eliminated as the blind hemifield changes. This effectively causes a small change of illuminant in the sighted hemifield, which could well account for the very small **C** index observed.

5.3.4 Discussion

Pöppel (1986) suggested that the colour induction phenomenon he observed was as mediated by the retina. Subject GY demonstrated the same induction phenomenon and this was taken as evidence of retinal cone function. However the constancy experiment suggests that stimuli in the blind hemifield do not contribute to instantaneous colour constancy. It is interesting to note that these two properties of the visual system are mediated differently within it and by implication have different neural substrates. It may be concluded that instantaneous colour constancy is not achieved by the retina, rather it is a function of a higher stage in the parvocellular - striate cortex - prestriate cortex pathway.

5.4 Summary

In this chapter results of experiments on four subjects with damage to the cerebral cortex have been discussed. The aim was to shed some light on the question of the location within the visual system of the neural substrate underlying instantaneous colour constancy.

Three of the subjects suffered from cerebral achromatopsia due to lesions of the ventral, occipitotemporal cortex (the lingual and fusiform gyri). This area has been put forward a putative homologue of monkey area V4 (Zeki, 1991). If this were the case an impairment of colour constancy would be expected for these subjects (Walsh et al., 1993). This was not found to be the case which suggests that the area of the lingual and fusiform gyri is not the homologue of V4 (Heywood et al., 1991; 1992) and that instantaneous colour constancy is mediated elsewhere in the visual system.

The fourth subject was a hemianope who was investigated in order to explore the possibility that instantaneous colour constancy was achieved by the retina. Retinal cone function was demonstrated using a colour induction experiment (Pöppel, 1986). The constancy experiment showed no contribution from the blind hemifield. This suggests that instantaneous colour constancy is not mediated by the retina.

The two experiments together suggest that the parvocellular pathway must be intact at least as far as the primary visual cortex for instantaneous colour constancy. The results are not inconsistent with the hypothesis that the primary visual cortex is itself the neural substrate of instantaneous colour constancy.

Chapter 6. Concluding Remarks

Colour constancy has been defined as the ability of the visual system to maintain a constant colour percept of a surface despite varying conditions of illumination. Much of the previous work has attempted to explain this phenomenon as a single stage process. This has varied from comparatively simple models of photoreceptor adaptation (von Kries, 1905), through highly detailed mathematical models of the requirements of achieving this invariance (Hurlbert, 1986; Iverson and D'Zmura, 1994), to more general assertions that it is due to high level cognitive processes (Arend and Reeves, 1986). However, more recently some authors have proposed multistage processes (Dannemiller, 1989; Courtney et al., 1995).

In this thesis the concept of instantaneous colour constancy has been used, to distinguish effects which happen very rapidly with the change of illuminant on a scene from those effects which result from photoreceptor adaptation. To this end a dynamic colour matching technique has been devised to conduct the constancy experiments. This meets the objection of Brill and West (1986) to previous work that the context of viewing should be preserved between test and reference samples, but maintains a steady state of adaptation which is the same for both eyes. The technique also enables a quantitative measure of the degree of colour constancy to be derived, which has led to the definition of the **C** index.

Various aspects of visual performance can be affected significantly by light scattered within the human eye from areas of the visual field other than those of interest (Stiles, 1929; Vos and Bouman, 1959). It has also been suggested that this Forward light scatter in the eye may partially explain some colour constancy phenomena that have been reported in the literature (Walraven, 1973). The technique of Barbur et al. (1992) is used to measure the scatter functions for the experimental subjects of this thesis and a method

described for the correction of the **C** index. It turns out that the effects of scattered light do not substantially alter the experimental results for most normal subjects. However, the age of the experimental subjects is of particular importance and in older subjects the effects of scattered light can be large and should be considered carefully (Barbur et al., 1995).

The data presented in this thesis show that although instantaneous colour constancy is never perfect, the **C** index is never one, it can account for a large percentage of the colour constancy performance observed in human vision. It is possible that photoreceptor adaptation and other, cognitive factors would be able to account for the level of functional constancy observed.

The level of luminance contrast between the experimental target and its surround does not have a significant effect on the degree of colour constancy. Further, there is no discontinuity in the **C** index as the test target is made brighter than the surround. This is inconsistent with models of constancy which normalise responses to the brightest patch within a scene or to any simple average, such as the Retinex theory (Land, 1983). The **C** index also does not depend on whether the illuminant shift is along the Plankian locus, or between artificial illuminants defined so that the shift between them is at right angles to the Plankian locus. Some of the more recent computational models in the literature require *a priori* knowledge of basis functions to describe common reflectances and illuminants (Lennie and D'Zmura, 1988; Iverson and D'Zmura, 1994). The use of artificial illuminants which cannot be well modelled by the same basis functions would cause colour constancy to fail in humans if the human visual system operated such a mechanism. The result presented in this thesis suggest quite the reverse, that colour constancy is maintained despite using artificial illuminants. It seems likely that the human visual system employs a method which relies on some computation on or comparison of receptor signals without knowledge of prevailing conditions in the outside world.

Of the computational models in the literature, only the Retinex algorithm (Land, 1983) and other lightness models (Hurlbert, 1986) explicitly

consider the contribution of spatial aspects of the visual scene to colour constancy. The retinex algorithm predicts that constancy should be better for more complex scenes and that for a target of constant area there should be an effect of target perimeter (Marr, 1982; Valberg and Lange-Malecki, 1990). Neither of these is found to be the case here. The equivalence of complex and simple surrounds is similar to the results of experiments on chromatic induction reported in the literature (Valberg and Lange-Malecki, 1987; Tiplitz Blackwell and Buchsbaum, 1988a). Although it is difficult to set the parameters of the Retinex algorithm to achieve this equivalence (Brainard and Wandell, 1986), other lightness operators (Hurlbert, 1986; Hurlbert and Poggio, 1988) can do so. It is an assumption of all these lightness algorithms that the colour of each patch within a Mondrian is uniform (Hurlbert, 1986). This requires some form of filling in (Brill, 1990), which, with appropriate averaging, would account for there being no effect of test target perimeter.

Studies on chromatic induction have found a decrease in the size of the effect as the inducing field is separated from the target by a black annulus (Walraven, 1973; Tiplitz Blackwell and Buchsbaum, 1988a; Brenner and Cornelissen, 1991). This decrease is reported to be exponential and ascribed to a difference of Gaussians function such as that of the lightness operator of Hurlbert and Poggio (1988). The results presented here for instantaneous colour constancy show a decrease in effect that cannot be well modelled by an exponential decay. This suggests that the mechanism of instantaneous colour constancy may not be identical to those of chromatic induction and that the contribution of the field of view surrounding the test target may not be well modelled by a Gaussian spatial profile.

There has been much debate in the literature as to the location within the human visual system of the computations achieving colour constancy. To this end experiments were performed on subjects with damage to the cerebral cortex. Zeki (1980; 1983) has identified area V4 in the macaque as responsible for colour constancy. Damage to the region of the lingual and fusiform gyrus in humans has been shown to result in cerebral achromatopsia

(Meadows, 1974; Plant 1991). This area has been put forward as the human homologue of V4 (Zeki, 1991). If this is the case an impairment of colour constancy would be expected for subjects with damage to this region (Walsh et al., 1993). Colour matching experiments on subjects with cerebral achromatopsia are difficult to perform due to the subjects' poor colour discrimination. Effects due to colour constancy may not be apparent if the shifts in chromaticity caused are not significantly larger than the much increased chromatic discrimination thresholds of these subjects. In order to investigate the presence of "hidden" constancy, a novel colour discrimination test was developed. The colour discrimination thresholds of three subjects with cerebral achromatopsia were investigated. The subjects' task was to set thresholds of chromatic discrimination along the "expected" constancy line, both with steady surround conditions and the surround conditions of the instantaneous colour constancy experiment. It was found that the discrimination thresholds did indeed shift in the direction expect due to constancy. However, this shift was masked by the effect of scattered light. The effects of scattered light and constancy were approximately equal in size for two of the subjects (and acted in opposite directions). These findings stress the importance of accounting for light scatter within the eyes of older subjects. The conclusion of these experiments was that instantaneous colour constancy remains in the three subjects with cerebral achromatopsic studied. The results therefore suggest that the area of the fusiform gyrus does not act as a human homologue of V4 (Heywood et al., 1991; 1992). The colour constancy of a fourth subject who suffered from hemianopia due to a traumatic injury to the primary visual cortex was also investigated. No contribution to instantaneous constancy could be found from this subject's blind hemifield. Together, these results suggest that the parvocellular pathway must be intact at least as far as the primary visual cortex for instantaneous colour constancy to occur. The results are therefore not inconsistent with the hypothesis that V1 is itself the principal neural substrate which mediates instantaneous colour constancy.

Appendix. Spectral Reflectance Functions of various Munsell chips.

Munsell reflectances for chips specified in McCann, McKee and Taylor (1976).

λ	N6	5YR5/6	2.5BG6/6	7.5GY6/6	5R5/12	10RP6/10	2.5PB6/8	5GY8/8
380	0.6304	0.5238	0.5676	0.6073	0.5829	0.748	0.6552	0.655
385	0.5753	0.4812	0.5119	0.5532	0.5319	0.6999	0.5826	0.5834
390	0.5235	0.3995	0.4513	0.4693	0.4622	0.629	0.5264	0.4899
395	0.4813	0.3292	0.4127	0.4028	0.3957	0.588	0.521	0.4387
400	0.4992	0.3091	0.4027	0.3617	0.3441	0.5424	0.5704	0.4048
405	0.4838	0.2654	0.3816	0.3133	0.3158	0.4983	0.6017	0.3644
410	0.4656	0.2354	0.3659	0.2664	0.2733	0.4784	0.611	0.3358
415	0.4539	0.2193	0.3562	0.2527	0.2603	0.4535	0.6214	0.3179
420	0.4438	0.1982	0.3536	0.2279	0.2344	0.441	0.6358	0.2903
425	0.4462	0.1786	0.3426	0.2137	0.2199	0.4213	0.6398	0.2744
430	0.441	0.1668	0.3477	0.2046	0.2052	0.4244	0.6809	0.2686
435	0.4273	0.1558	0.3458	0.193	0.1883	0.4087	0.6908	0.2635
440	0.4227	0.1458	0.3523	0.1843	0.1755	0.3955	0.6938	0.2516
445	0.4086	0.1363	0.3501	0.1779	0.1669	0.3845	0.6963	0.2487
450	0.4015	0.132	0.3612	0.1784	0.157	0.3745	0.7063	0.2502
455	0.3952	0.1293	0.3661	0.1799	0.1497	0.3609	0.7127	0.2521
460	0.3942	0.1293	0.3825	0.1831	0.1454	0.3566	0.7324	0.2597
465	0.3829	0.1254	0.3967	0.1876	0.137	0.3393	0.7455	0.2669
470	0.383	0.1248	0.4249	0.1967	0.1326	0.324	0.7667	0.2844
475	0.3693	0.122	0.4500	0.2117	0.1229	0.3123	0.7496	0.2941
480	0.3737	0.1272	0.4663	0.2287	0.1193	0.3018	0.7498	0.3251
485	0.377	0.1283	0.4891	0.2506	0.1143	0.2946	0.7348	0.3631
490	0.38	0.1363	0.5099	0.283	0.1113	0.2891	0.724	0.4152
495	0.3754	0.1361	0.5181	0.3091	0.1064	0.2782	0.6928	0.4627
500	0.3789	0.1392	0.5233	0.3411	0.1031	0.2719	0.6624	0.5239
505	0.378	0.1421	0.5267	0.375	0.09964	0.2635	0.6259	0.5968
510	0.3781	0.143	0.5247	0.4131	0.09653	0.2564	0.5881	0.691
515	0.3812	0.1448	0.5264	0.4386	0.09303	0.251	0.5545	0.7835
520	0.378	0.1454	0.5152	0.4471	0.09146	0.2462	0.5177	0.838
525	0.371	0.1437	0.5004	0.4477	0.08942	0.2424	0.4828	0.8586
530	0.3746	0.1445	0.4899	0.4429	0.09148	0.2434	0.4549	0.8722
535	0.3713	0.1488	0.4728	0.4379	0.09235	0.2404	0.4297	0.8686
540	0.3695	0.1536	0.4566	0.4324	0.09422	0.2415	0.407	0.8626
545	0.3726	0.1595	0.4422	0.4262	0.09603	0.2411	0.3883	0.8594
550	0.3767	0.1791	0.4237	0.4209	0.1011	0.2446	0.3675	0.859
555	0.3771	0.2005	0.4004	0.4095	0.1055	0.2452	0.3496	0.8376
560	0.3776	0.2316	0.3747	0.3986	0.1114	0.2498	0.3322	0.8216

λ	N6	5YR5/6	2.5BG6/6	7.5GY6/6	5R5/12	10RP6/10	2.5PB6/8	5GY8/8
565	0.3812	0.2691	0.3532	0.3886	0.121	0.2636	0.3204	0.8076
570	0.3827	0.3036	0.3319	0.378	0.1405	0.2948	0.3081	0.7895
575	0.3838	0.3277	0.3125	0.3643	0.1707	0.3435	0.2983	0.7709
580	0.3829	0.3502	0.2934	0.3535	0.2272	0.4229	0.2912	0.7535
585	0.3819	0.3682	0.272	0.3395	0.3056	0.5173	0.2836	0.7343
590	0.3825	0.3802	0.2506	0.3238	0.4081	0.6296	0.2767	0.7083
595	0.3797	0.3866	0.2334	0.3076	0.5035	0.733	0.2721	0.6901
600	0.3808	0.3914	0.2166	0.2945	0.5847	0.8011	0.2688	0.6652
605	0.3752	0.3917	0.2032	0.2833	0.6585	0.8458	0.2645	0.6494
610	0.3753	0.3907	0.1951	0.2763	0.7158	0.8721	0.2641	0.6389
615	0.3749	0.3919	0.1894	0.2708	0.7404	0.8864	0.2639	0.6301
620	0.3736	0.3906	0.1867	0.2676	0.7608	0.8985	0.2663	0.6336
625	0.3726	0.3893	0.1829	0.2656	0.7698	0.9036	0.2695	0.6247
630	0.3734	0.3916	0.1818	0.2626	0.7882	0.9146	0.2748	0.6253
635	0.3731	0.3924	0.1803	0.2604	0.7956	0.9157	0.2799	0.6195
640	0.3713	0.3924	0.1771	0.2565	0.8023	0.9218	0.2892	0.6173
645	0.3713	0.3884	0.1759	0.2541	0.8022	0.9203	0.2964	0.6108
650	0.3731	0.3926	0.1742	0.2538	0.8162	0.9322	0.3061	0.617
655	0.3714	0.3931	0.1745	0.2552	0.814	0.9319	0.3142	0.6148
660	0.3705	0.3921	0.1767	0.2549	0.8167	0.9325	0.324	0.6153
665	0.3712	0.3923	0.1795	0.2574	0.8214	0.9378	0.3374	0.6209
670	0.3701	0.391	0.1847	0.2585	0.8223	0.9341	0.3515	0.6257
675	0.3728	0.3912	0.191	0.2655	0.8243	0.9398	0.3699	0.6345
680	0.3721	0.3922	0.1956	0.2704	0.8313	0.9455	0.3907	0.6424
685	0.3723	0.3914	0.2023	0.2741	0.8345	0.9469	0.4122	0.6517
690	0.3689	0.3908	0.207	0.2773	0.8352	0.9503	0.4334	0.6632
695	0.3686	0.3897	0.2102	0.2804	0.8393	0.9454	0.4462	0.6639
700	0.3723	0.3921	0.215	0.2839	0.8448	0.9547	0.4645	0.6756
705	0.3710	0.391	0.2164	0.2846	0.8434	0.9581	0.4816	0.6736
710	0.3700	0.3909	0.2156	0.2868	0.8466	0.958	0.492	0.6773
715	0.3688	0.3906	0.2121	0.2823	0.8488	0.9622	0.4996	0.6718
720	0.3668	0.3919	0.2096	0.2814	0.8543	0.9617	0.5069	0.6691
725	0.37	0.3946	0.2064	0.2817	0.8558	0.9675	0.5138	0.6623
730	0.3715	0.393	0.2098	0.2841	0.8628	0.9726	0.5222	0.6639
735	0.3735	0.3962	0.214	0.2886	0.8645	0.9784	0.533	0.6729
740	0.3747	0.3963	0.222	0.2935	0.8646	0.9865	0.5441	0.6782
745	0.3771	0.3995	0.2289	0.3008	0.8698	0.9905	0.5614	0.6905
750	0.3766	0.3989	0.2408	0.3082	0.8692	0.9915	0.5788	0.7012
755	0.3772	0.3999	0.2523	0.3187	0.8647	1.00	0.5921	0.7148
760	0.3813	0.4013	0.2629	0.3273	0.8734	1.000	0.6054	0.7281

λ	10RP3/6	N2	5Y7/8	2.5B8/4	N7	5P7/6	2.5G7/6
380	0.5049	0.5093	0.6246	0.6101	0.6413	0.8249	0.6355
385	0.4262	0.4600	0.5597	0.5604	0.5952	0.8185	0.5711
390	0.3863	0.3793	0.4669	0.5091	0.5211	0.7751	0.4985
395	0.317	0.3170	0.4008	0.5125	0.4965	0.7665	0.4533
400	0.2831	0.2698	0.3357	0.5866	0.5441	0.7725	0.4493
405	0.2496	0.2326	0.296	0.6625	0.558	0.7644	0.4232
410	0.2265	0.1997	0.2546	0.6822	0.5677	0.7603	0.3975
415	0.2067	0.1821	0.2332	0.7214	0.571	0.7597	0.3867
420	0.1885	0.1604	0.215	0.7261	0.5701	0.7627	0.3676
425	0.1708	0.1421	0.1951	0.7453	0.5619	0.7577	0.3542
430	0.1505	0.1288	0.1872	0.7762	0.5803	0.7859	0.3635
435	0.1445	0.1140	0.1729	0.7903	0.5644	0.766	0.3565
440	0.1364	0.1035	0.1599	0.7874	0.5624	0.7503	0.3584
445	0.1284	0.09714	0.1500	0.7849	0.55	0.7363	0.3559
450	0.1239	0.08743	0.1499	0.8027	0.5401	0.7179	0.3594
455	0.1195	0.08211	0.1455	0.8122	0.5334	0.6995	0.3598
460	0.1121	0.07806	0.1512	0.8322	0.5361	0.6954	0.3745
465	0.1079	0.07306	0.1519	0.8325	0.5301	0.6642	0.3901
470	0.1014	0.06997	0.1604	0.851	0.5276	0.6512	0.4128
475	0.09238	0.06542	0.1693	0.8563	0.5152	0.623	0.4245
480	0.08775	0.06266	0.1849	0.8716	0.5188	0.6164	0.4544
485	0.08401	0.0601	0.2103	0.8772	0.5278	0.6066	0.5007
490	0.07927	0.0596	0.2416	0.8943	0.5328	0.5942	0.5483
495	0.07729	0.05777	0.2745	0.8904	0.5286	0.5764	0.581
500	0.07412	0.05626	0.3146	0.8864	0.5268	0.5662	0.6162
505	0.07066	0.05543	0.3615	0.8846	0.5247	0.5493	0.6463
510	0.06756	0.05541	0.4119	0.8788	0.5283	0.5429	0.682
515	0.06505	0.05457	0.4575	0.8838	0.5339	0.54	0.6952
520	0.06245	0.05311	0.473	0.8625	0.5346	0.5242	0.693
525	0.06125	0.05228	0.4826	0.8363	0.5273	0.5112	0.6838
530	0.06082	0.05177	0.4851	0.8225	0.531	0.4974	0.679
535	0.06012	0.05097	0.4876	0.8029	0.5285	0.4857	0.6586
540	0.05916	0.05062	0.4951	0.781	0.5229	0.4756	0.6405
545	0.0583	0.05053	0.5073	0.7607	0.5271	0.4755	0.6186
550	0.05782	0.05121	0.5241	0.7383	0.5286	0.4878	0.6034
555	0.05772	0.05008	0.5355	0.7104	0.5281	0.4939	0.5771
560	0.05866	0.05004	0.5584	0.6842	0.5291	0.4962	0.5515
565	0.06013	0.05044	0.5896	0.6588	0.5326	0.5002	0.5278
570	0.06499	0.05004	0.6166	0.6417	0.5347	0.4994	0.5032
575	0.07587	0.04996	0.628	0.6217	0.5354	0.4886	0.4814
580	0.09308	0.05011	0.6343	0.6048	0.54	0.4793	0.4594
585	0.1182	0.05008	0.644	0.5895	0.5373	0.4708	0.4348
590	0.1544	0.0488	0.647	0.5717	0.5404	0.4773	0.4086
595	0.183	0.04915	0.6529	0.5529	0.5376	0.4948	0.3875

λ	10RP3/6	N2	5Y7/8	2.5B8/4	N7	5P7/6	2.5G7/6
600	0.2018	0.04897	0.6543	0.5324	0.539	0.5304	0.3665
605	0.2133	0.04835	0.6511	0.5115	0.5311	0.5678	0.3474
610	0.2186	0.04804	0.649	0.5001	0.536	0.6141	0.3396
615	0.2218	0.04753	0.6543	0.4962	0.5342	0.6495	0.3327
620	0.2217	0.04743	0.6546	0.4947	0.5359	0.6768	0.3277
625	0.2229	0.04808	0.6531	0.4896	0.5316	0.7052	0.3222
630	0.2228	0.04748	0.6574	0.4898	0.5384	0.7339	0.3212
635	0.2232	0.04749	0.6573	0.4923	0.5399	0.7503	0.3177
640	0.2224	0.04764	0.6586	0.4908	0.5362	0.7664	0.3137
645	0.2238	0.04728	0.6584	0.4943	0.5381	0.7785	0.3092
650	0.2241	0.04768	0.6632	0.4998	0.541	0.7947	0.3097
655	0.2243	0.04711	0.6636	0.5034	0.5498	0.8049	0.3102
660	0.2225	0.04745	0.6616	0.5103	0.5448	0.8137	0.3094
665	0.2222	0.04737	0.665	0.5181	0.5446	0.8255	0.3131
670	0.2238	0.0477	0.6647	0.5248	0.5409	0.8353	0.3167
675	0.2223	0.0475	0.6687	0.5361	0.5442	0.8464	0.3246
680	0.2215	0.04799	0.6677	0.5404	0.5475	0.8596	0.3321
685	0.2219	0.04788	0.6701	0.5444	0.5455	0.8692	0.341
690	0.222	0.04805	0.6725	0.5471	0.544	0.8829	0.3456
695	0.2218	0.04878	0.6712	0.5462	0.5441	0.8866	0.3478
700	0.2228	0.0494	0.6767	0.555	0.5496	0.8987	0.3547
705	0.2217	0.04891	0.6714	0.5568	0.5491	0.9074	0.3573
710	0.2229	0.04936	0.6739	0.558	0.5489	0.9125	0.355
715	0.2235	0.05043	0.6741	0.5596	0.5502	0.9197	0.3505
720	0.2245	0.05027	0.6753	0.5593	0.5469	0.9272	0.3443
725	0.2235	0.0518	0.6779	0.5623	0.5507	0.9364	0.3429
730	0.2272	0.05228	0.6804	0.5706	0.5514	0.9383	0.3451
735	0.228	0.05272	0.6873	0.585	0.5509	0.9496	0.3504
740	0.2272	0.05329	0.6872	0.5985	0.5513	0.9549	0.3568
745	0.2279	0.05386	0.6873	0.619	0.5568	0.9651	0.37
750	0.2253	0.05597	0.6876	0.6445	0.5548	0.9677	0.3803
755	0.2273	0.05643	0.6916	0.6684	0.5581	0.9817	0.3909
760	0.2301	0.05973	0.7018	0.6904	0.559	0.99	0.4002

Further Munsell chips.

λ	N5	5G5/6	10GY5/6	7.5Y5/6	5YR5/6	2.5R5/6	7.5P5/6
380	0.09986	0.05639	0.05437	0.0316	0.5238	0.07871	0.08661
385	0.1196	0.06455	0.06072	0.02922	0.4812	0.09368	0.1093
390	0.1487	0.07763	0.06775	0.02844	0.3995	0.1185	0.1488
395	0.1766	0.08822	0.07081	0.02945	0.3292	0.1399	0.2052
400	0.2047	0.09843	0.0761	0.02956	0.3091	0.1596	0.2611
405	0.2114	0.1032	0.07654	0.02832	0.2654	0.169	0.2998
410	0.2168	0.1089	0.07838	0.0281	0.2354	0.1765	0.3237
415	0.2210	0.1110	0.07982	0.02758	0.2193	0.1768	0.3409
420	0.2189	0.1121	0.08297	0.02899	0.1982	0.1763	0.3357
425	0.2188	0.115	0.0835	0.03053	0.1786	0.1744	0.3383
430	0.2217	0.119	0.08681	0.03146	0.1668	0.1752	0.3346
435	0.2224	0.1223	0.0893	0.03238	0.1558	0.1737	0.3369
440	0.2218	0.1292	0.09284	0.03433	0.1458	0.1774	0.3295
445	0.2177	0.1346	0.09667	0.03561	0.1363	0.1752	0.3219
450	0.2198	0.1422	0.1023	0.03842	0.132	0.1764	0.3192
455	0.2195	0.1532	0.1088	0.04211	0.1293	0.1743	0.3002
460	0.2194	0.1652	0.1165	0.04697	0.1293	0.1728	0.3032
465	0.2199	0.1777	0.1265	0.05176	0.1254	0.1723	0.2929
470	0.2206	0.1926	0.1394	0.05876	0.1248	0.1684	0.285
475	0.2213	0.2077	0.1533	0.06698	0.122	0.1676	0.2754
480	0.2218	0.2239	0.1658	0.07551	0.1272	0.1635	0.267
485	0.2198	0.2411	0.1845	0.08806	0.1283	0.1613	0.2571
490	0.2219	0.2583	0.2052	0.103	0.1363	0.1581	0.2486
495	0.2206	0.2768	0.2314	0.1209	0.1361	0.1566	0.2399
500	0.2225	0.2938	0.2552	0.1445	0.1392	0.1539	0.2299
505	0.2228	0.3066	0.2765	0.166	0.1421	0.1501	0.2218
510	0.2212	0.3128	0.2934	0.1818	0.143	0.1461	0.2171
515	0.2203	0.3151	0.3023	0.1934	0.1448	0.1443	0.2107
520	0.2208	0.312	0.3047	0.2004	0.1454	0.1422	0.206
525	0.2213	0.3074	0.3048	0.2044	0.1437	0.1422	0.2006
530	0.2198	0.3004	0.3023	0.2065	0.1445	0.1431	0.1959
535	0.2212	0.2917	0.2976	0.209	0.1488	0.1454	0.1908
540	0.2195	0.2804	0.2888	0.213	0.1536	0.1447	0.186
545	0.2193	0.2676	0.2809	0.2158	0.1595	0.1462	0.1857
550	0.2201	0.2514	0.2719	0.2214	0.1791	0.1499	0.1869
555	0.2232	0.2387	0.263	0.2306	0.2005	0.1562	0.1919
560	0.2222	0.2256	0.2524	0.2363	0.2316	0.1628	0.1955
565	0.2251	0.2111	0.2419	0.2455	0.2691	0.1724	0.197
570	0.2243	0.1974	0.2321	0.2505	0.3036	0.1911	0.1976
575	0.2253	0.1846	0.2195	0.2565	0.3277	0.22	0.1986
580	0.2254	0.1691	0.207	0.2585	0.3502	0.2685	0.197
585	0.225	0.1552	0.1959	0.2587	0.3682	0.3161	0.1981

λ	N5	5G5/6	10GY5/6	7.5Y5/6	5YR5/6	2.5R5/6	7.5P5/6
590	0.2238	0.1435	0.1842	0.2579	0.3802	0.3517	0.2028
595	0.2239	0.1333	0.1743	0.2575	0.3866	0.3741	0.2176
600	0.2218	0.1248	0.1649	0.2553	0.3914	0.3871	0.2389
605	0.2207	0.1177	0.1591	0.2551	0.3917	0.3947	0.2664
610	0.2197	0.1133	0.1556	0.2562	0.3907	0.4007	0.301
615	0.2198	0.1102	0.1495	0.2531	0.3919	0.4009	0.3274
620	0.2174	0.1076	0.1494	0.2517	0.3906	0.4012	0.3552
625	0.2191	0.1057	0.1469	0.2511	0.3893	0.4034	0.3758
630	0.2194	0.1052	0.1459	0.2501	0.3916	0.4049	0.3905
635	0.2175	0.1038	0.1454	0.2487	0.3924	0.4015	0.4033
640	0.2154	0.1026	0.1427	0.249	0.3924	0.4039	0.4098
645	0.2155	0.09984	0.1429	0.2482	0.3884	0.4042	0.4146
650	0.2153	0.1001	0.1398	0.2478	0.3926	0.4043	0.42
655	0.216	0.1009	0.1399	0.2491	0.3931	0.4044	0.4233
660	0.2159	0.1019	0.1409	0.248	0.3921	0.4042	0.4265
665	0.2146	0.104	0.1435	0.247	0.3923	0.4052	0.43
670	0.2144	0.1058	0.1478	0.2449	0.391	0.4023	0.4298
675	0.214	0.1089	0.1496	0.2456	0.3912	0.4025	0.4291
680	0.2107	0.1114	0.1534	0.2443	0.3922	0.4036	0.4291
685	0.2108	0.1152	0.155	0.2431	0.3914	0.4055	0.43
690	0.2108	0.1166	0.1587	0.244	0.3908	0.4036	0.4323
695	0.2093	0.1201	0.163	0.2425	0.3897	0.4026	0.4339
700	0.2113	0.1225	0.1662	0.2422	0.3921	0.404	0.4384
705	0.2102	0.1237	0.1654	0.2433	0.391	0.4059	0.4378
710	0.2096	0.1219	0.1639	0.2407	0.3909	0.402	0.4387
715	0.2081	0.1197	0.1634	0.24	0.3906	0.4037	0.437
720	0.2064	0.1167	0.1596	0.2399	0.3919	0.4012	0.4392
725	0.2071	0.1149	0.1604	0.2387	0.3946	0.403	0.4346
730	0.2075	0.1151	0.1594	0.2387	0.393	0.4047	0.4392
735	0.2091	0.12	0.1645	0.2405	0.3962	0.4065	0.4425
740	0.2057	0.1227	0.1666	0.2393	0.3963	0.4034	0.4396
745	0.2084	0.1273	0.1756	0.2398	0.3995	0.4033	0.4448
750	0.2098	0.1338	0.1813	0.2436	0.3989	0.4084	0.4475
755	0.2075	0.1387	0.1838	0.2435	0.3999	0.4065	0.4507
760	0.2066	0.1425	0.1879	0.239	0.4013	0.406	0.4466

λ	7.5PB5/6	10BG5/6	5G5/2	5YR5/2	7.5P5/2	5RP5/10	7.5GY5/6
380	0.09045	0.07125	0.06968	0.06976	0.08862	0.0837	0.03992
385	0.1135	0.0858	0.08528	0.08456	0.1059	0.1029	0.04378
390	0.1533	0.1094	0.1029	0.1062	0.1396	0.137	0.04947
395	0.2137	0.137	0.1258	0.1284	0.1722	0.1765	0.05242
400	0.2824	0.1652	0.1456	0.1444	0.2114	0.212	0.05588
405	0.3300	0.1807	0.1572	0.1542	0.2251	0.2291	0.0541
410	0.3701	0.1956	0.1627	0.161	0.2355	0.2362	0.05716
415	0.3787	0.2000	0.1644	0.1633	0.24	0.2369	0.05695
420	0.3888	0.2055	0.1659	0.1626	0.2441	0.2387	0.05629
425	0.39	0.2169	0.1683	0.1614	0.2427	0.2409	0.05911
430	0.3911	0.2259	0.1751	0.1648	0.2473	0.2429	0.06041
435	0.3915	0.2339	0.1759	0.1655	0.245	0.2433	0.06374
440	0.3907	0.2444	0.1824	0.1666	0.2458	0.2472	0.06669
445	0.3879	0.2581	0.1843	0.1671	0.2467	0.2466	0.07023
450	0.387	0.276	0.1872	0.168	0.2467	0.2448	0.07318
455	0.381	0.2908	0.1916	0.1684	0.2455	0.2411	0.07791
460	0.3726	0.3185	0.1962	0.169	0.2434	0.2343	0.08616
465	0.3654	0.3452	0.2052	0.174	0.2435	0.2265	0.09341
470	0.3577	0.3714	0.2105	0.1747	0.2439	0.2177	0.1038
475	0.3499	0.3909	0.2154	0.1759	0.2387	0.2068	0.1143
480	0.3436	0.4079	0.2209	0.1792	0.2363	0.1981	0.1269
485	0.3335	0.4208	0.2245	0.1812	0.2342	0.1877	0.1413
490	0.323	0.4226	0.2333	0.1808	0.2318	0.1784	0.1621
495	0.3115	0.4212	0.2358	0.1819	0.2287	0.1695	0.1867
500	0.301	0.4117	0.2395	0.1844	0.2253	0.162	0.2136
505	0.2901	0.3951	0.2429	0.1862	0.2209	0.153	0.2373
510	0.2784	0.3784	0.2417	0.1879	0.2189	0.1446	0.2552
515	0.2681	0.3573	0.2406	0.1867	0.2174	0.1374	0.2658
520	0.2586	0.3383	0.2435	0.1863	0.2131	0.1332	0.271
525	0.2498	0.324	0.243	0.1886	0.2125	0.1312	0.2757
530	0.2397	0.3041	0.2404	0.1889	0.2107	0.1288	0.2747
535	0.2299	0.2847	0.2404	0.1917	0.2094	0.1274	0.2717
540	0.2201	0.265	0.2365	0.1937	0.2093	0.1243	0.2655
545	0.2139	0.2461	0.2339	0.1979	0.2068	0.1208	0.2603
550	0.2087	0.2277	0.2318	0.2049	0.2032	0.1162	0.2514
555	0.2075	0.2167	0.2299	0.2142	0.2032	0.1132	0.2471
560	0.2041	0.1996	0.2241	0.2249	0.2031	0.1112	0.2385
565	0.1999	0.1863	0.2213	0.2342	0.2038	0.1111	0.2315
570	0.1946	0.1747	0.2149	0.2474	0.2062	0.1199	0.2215
575	0.1905	0.1643	0.2109	0.2535	0.2149	0.141	0.2142
580	0.1853	0.1511	0.2057	0.2572	0.2244	0.1853	0.2037
585	0.1811	0.1417	0.1984	0.2609	0.2288	0.2479	0.1939
590	0.1811	0.1319	0.1925	0.2626	0.2355	0.304	0.1851

λ	7.5PB5/6	10BG5/6	5G5/2	5YR5/2	7.5P5/2	5RP5/10	7.5GY5/6
595	0.1853	0.1261	0.1871	0.2639	0.2405	0.3591	0.1751
600	0.1897	0.1192	0.1805	0.2637	0.2442	0.4061	0.1677
605	0.1962	0.1145	0.1764	0.2634	0.2475	0.4493	0.1615
610	0.2046	0.1107	0.1755	0.2647	0.2515	0.4876	0.1589
615	0.2106	0.1093	0.1721	0.2621	0.2552	0.5193	0.1531
620	0.2170	0.1075	0.1698	0.2637	0.256	0.543	0.1508
625	0.2236	0.1075	0.1696	0.2628	0.256	0.5634	0.1483
630	0.2314	0.1081	0.1685	0.2637	0.2572	0.5768	0.147
635	0.2392	0.1056	0.1677	0.2633	0.2576	0.5866	0.1461
640	0.2459	0.1067	0.1668	0.2602	0.2597	0.5916	0.1448
645	0.2532	0.1067	0.1653	0.2607	0.2591	0.5954	0.1443
650	0.2635	0.1072	0.1649	0.2603	0.2603	0.6013	0.1433
655	0.2731	0.109	0.1644	0.2618	0.2613	0.6017	0.1425
660	0.2824	0.1125	0.1669	0.262	0.2601	0.6046	0.1442
665	0.2969	0.1152	0.1675	0.262	0.26	0.6068	0.1457
670	0.3076	0.1183	0.169	0.2597	0.2592	0.6059	0.1486
675	0.3202	0.1227	0.1693	0.2607	0.2594	0.609	0.1505
680	0.333	0.1282	0.1722	0.2603	0.2576	0.6076	0.1538
685	0.3455	0.1323	0.1736	0.2589	0.2595	0.6094	0.1556
690	0.3575	0.1382	0.1753	0.2614	0.2586	0.6111	0.1574
695	0.3719	0.1417	0.1768	0.2599	0.258	0.612	0.1597
700	0.3883	0.1438	0.1781	0.2598	0.2597	0.616	0.1631
705	0.3984	0.1459	0.1791	0.2596	0.2596	0.6154	0.1624
710	0.4065	0.146	0.1785	0.2588	0.2588	0.6162	0.1608
715	0.4184	0.143	0.1774	0.259	0.2577	0.6169	0.1595
720	0.4256	0.1422	0.1749	0.261	0.2579	0.6182	0.1587
725	0.4304	0.1415	0.1745	0.2535	0.255	0.6168	0.1563
730	0.4407	0.1415	0.1738	0.2577	0.255	0.6174	0.1573
735	0.4448	0.1464	0.1757	0.2573	0.2573	0.6254	0.1586
740	0.445	0.1501	0.1759	0.2557	0.2523	0.6175	0.1614
745	0.4542	0.1572	0.1829	0.2573	0.256	0.6242	0.1679
750	0.4597	0.1656	0.1863	0.2573	0.2568	0.6327	0.1721
755	0.4613	0.1723	0.1876	0.2574	0.2576	0.6309	0.1762
760	0.4599	0.1758	0.1882	0.2586	0.2572	0.6281	0.177

References

Allman, J.M. and Kass, J.H. (1971). A representation of the visual field in the caudal third of the middle temporal gyrus of the owl monkey (*Aotus trivirgatus*). *Brain Research*, **31**, 85-105.

Alpern, M. (1979). Lack of uniformity in colour matching. *Journal of Physiology, London*, **288**, 85-105.

Alpern, M. and Pugh, E.N., Jr. (1977). Variation in the action spectrum of erythrolabe among deuteranopes. *Journal of Physiology, London*, **266**, 613-646.

Arend, L.E. and Goldstein, R. (1987). Lightness models, gradient illusions and curl. *Perception and Psychophysics*, **42**, 65-80.

Arend L. and Reeves A. (1986) Simultaneous colour constancy. *Journal of the Optical Society of America A*, **3**, 1743-1751

Arend L.E., Reeves A., Schirillo J. and Goldstein R. (1991). Simultaneous color constancy: papers with diverse Munsell values. *Journal of the Optical Society of America*, **8**, 661-672.

Baker, H.D. and Rushton, W.A.H. (1965). The red sensitive pigment in normal cones. *Journal of Physiology, London*, **176**, 56-72.

Barbur, J.L., Birch, J. and Harlow, J.A. (1992). Threshod and suprathreshold responses to chromatic stimuli using psychophysical and pupillometric methods. In: *Noninvasive assessment of the visual system technical digest*, **vol.I**, 51-54. Washington DC: Optical Society of America.

Barbur J.L., Birch J. and Harlow J.A. (1993a) Colour vision testing using spatiotemporal luminance masking. In: *Colour vision deficiencies*, **vol. XI** (ed.B.Drum), 417-426. Dordrecht: Kluwer Academic Publishers.

Barbur J.L., De Cunha D., Harlow A.J. and Woodward E.G. (1992). Methods for the measurement and analysis of light scattered in the human eye. In: *Noninvasive assessment of the visual system Technical Digest*, Washington D.C.: Optical Society of America.

Barbur, J.L., Forsyth, P.M. and Findlay, J.M. (1988). Human Saccadic Eye Movements in the Absence of the Geniculocalcarine Projection. *Brain*, **111**, 63-82.

Barbur J.L., Harlow A.J. and Plant G.T. (1994). Insights into the different exploits of colour in the visual cortex. *Proceedings of the Royal Society of London B,* **258,** 327-334.

Barbur J.L., Harlow J.A., Plant G. and Williams C.B. (1993b). Colour discrimination measurements in patients with cerebral achromatopsia. In: *Noninvasive assesment of the visual system technical digest (1993),* **vol.III,** 356-359. Washington DC: Optical Society of America.

Barbur J.L., Harlow J.A. and Weiskrantz L. (1994). *Philosophical Transactions of the Royal Society of London, B,* **343,** 157-166.

Barbur, J.L., Holliday, I.E., Ruddock, K.H. and Waterfield, V.A. (1980). Spatial Characteristics of Movement Detection Mechanisms in Human Vision. *Biological Cybernetics*, **37**, 99-105.

Barbur J.L., Ruddock K.H., Waterfield V.A. (1980) Human visual responses in the absence of the geniculo-calcarine projection. *Brain,* **103,** 905-928.

Barbur J.L., Williams C.B. and Plant G.T. (1995). Studies of instantaneous colour constancy in subjects with cerebral achromatopsia. In: *Colour Vision Deficiencies,* **vol. XIII**. Dordrecht: Kluwer Academic Publishers (submitted).

Bender M.B., Krieger H.P. (1951) Visual function in perimetrically blind field. *Archives of Neurology and Psychiatry,* Chicago **65,** 72-79.

Benvento L.A. and Yoshida K. (1981). The afferent and efferent organisation of the lateral geniculate-prestriate pathways in the macaque monkey. *Journal of Comparative Neurology,* **203,** 455-474.

Blake A. (1985). Boundary conditions for lightness computation in Mondrian world. *Computer Vision, Graphics and Image Processing* **32,** 314-327.

Blythe I.M., Kennard C., Ruddock K.H. (1987) Residual vision in patients with retrogeniculate lesions of the visual pathways. *Brain*, **110,** 887-905.

Bowmaker, J.K. and Dartnall, H.J.A. (1980). Visual pigments of rod and cones in a human retina. *Journal of Physiology, London*, **298**, 501-511.

Boycott B.B. and Dowling J.E. (1969). Organisation of the primate retina: light microscopy. *Philosophical Transactions of the Royal Society B,* **255,** 109-184.

Boynton, R.M. (1988) Approaches to visual cortical function (Review). *Annual Review of Psychology*, **39**, 69-100.

Brainard, D.H. (1989). Calibration of a computer controlled color monitor. *Color Research and Application*, **14**, 23-34.

Brainard K. H. and Wandell B. A. (1986) Analysis of the retinex theory of color vision. *Journal of the Optical Society of America A*, **3**, 1651-1661

Brainard D.H. and Wandell B. (1991) A bilinear model of the illuminant's effect on color appearance. In: *Computational models of visual processing* (Movshon J.A. and Landy M.S. eds.), Cambridge Mass: MIT Press.

Brainard D.H. and Wandell B.A. (1992). Asymmetric colour matching: how colour appearance depends on the illuminant. *Journal of the Optical Society of America A*, **9**, 1433-1448.

Brenner, E. and Cornelissen, F.W. (1991). Spatial interactions in color vision depend on distances between boundaries. *Naturwissenschaften*, **78**, 70-73.

Brenner E. and Cornelissen F. (1993). Eye movements are influenced by matching instructions in experiments on colour constancy. *Perception*, **22s.**

Brenner E., Cornelissen F. and Nuboer J.F.W. (1989). In: *Seeing contour and colour* (Kulikowski J.J., Dickinson C.M. and Murray I.J., eds.) Oxford: Pergammon.

Brent P.J., Kennard C. and Ruddock K.H. (1994). *Proceedings of the Royal Society of London, B*, **256**, 219-225.

Brent, P.J. and Ruddock, K.H. (1990). Colour-opponent responses in human vision: psychophysical measurement of spectral responses. *Journal of Physiology, London*, **430**, 108.

Brill, M.H. (1978). A device performing illuminant invariant assessment of chromatic relations. *Journal of Theoretical Biology*, **71**, 473-478.

Brill M.H. (1979) Further features of the illuminant invariant trichromatic photosensor. *Journal of Theoretical Biology*, **78**, 305-308.

Brill, M.H. (1990) Image segmentation by object colour: a unifying framework and connection to colour constancy. *Journal of the Optical Society of America A*, **7**, 2041-2047.

Brill D. H. and West G. (1986) Chromatic adaptation and color constancy: A possible dichotomy. *Color Research and Application*, **11**, 196-204

Brindley, G.S. (1960). Physiology of the retina and visual pathway. London: Edward Arnold Ltd.

Brindley, G.S. and Willmer, E.N. (1952). The reflexion of light from the macular and peripheral fundus oculi in man. *Journal of Physiology, London*, **116**, 350-356.

Brodmann K. (1909) Vergleichende Lokalisationslehre der Grosshirnrinde. In: *Prinzipien dargestellt auf Grund des Zellenbaues.* Leipzig: J. A. Barth

Brown, P.K. and Wald, G. (1964). Visual pigments in single rods and cones of the human retina. *Science*, **144**, 45-52.

Buchsbaum, G. (1980). A spatial processor model for object colour perception. *Journal of the Franklin Institute*, **310**, 1-26.

Buchsbaum, G. and Gottschalk, A. (1983). Trichromacy, opponent colours coding and optimum colour infomation transmission in the retina. *Proceedings of the Royal Society of London B*, **220**, 89-113.

Buchsbaum, G. and Gottschalk, A. (1984). Chromaticity coordinates of frequency-limited functions. *Journal of the Optical Society of America A*, **1**, 885.

Bullier J. and Kennedy H. (1983). Projections of the lateral geniculate nucleus onto cortical area V2 in the macaque monkey. *Experimental Brain Research*, **53**, 168-172.

Bunt, A.H. and Minckler, D.S. (1977). Foveal Sparing. *Arch. Ophthalmology*, **95**, 1445-1447.

Campbell, F.W. and Gubisch, R.W. (1966). Optical Quality of the Human Eye. *Journal of Physiology, London*, **186**, 437-445.

Campbell, F.W. and Rushton, W.A.H. (1955). Measurement of the scotopic pigment in the living human eye. *Journal of Physiology, London*, **130**, 131-147.

Cavanagh P. and Anstis A.M. (1991). The contribution of color to motion in normal and color-deficient observers. *Vision Research*, **31**, 2109-248.

Chan R.Y. and Naka K. (1976). The amacrine cell. *Vision Research*, **16**, 1119-1129.

Clark, V.P., Courchesne, E. and Grafe, M. (1992). In vivo myeloarchitectonic analysis of human striate and extrastriate cortex using magnetic resonance imaging. *Cerebral Cortex*, **2**, 417-424.

Cohen, J. (1964). Dependency of the spectral reflectance curves of the Munsell color chips. *Psychonomic Science*, **1**, 369-370.

Corbetta M., Miezin F.M., Dolmeyer S., Shulman G.L. & Peterson S.E. (1991). Selective and divided attention during visual discriminations of shape, colour and speed: funtional anatomy by positron emission tomography. *Journal of Neurosciience* **11** 2383-2402.

Courtney S.M., Finkel L.H. and Buchsbaum G. (1995). Network simulations of retinal and cortical contributions to color constancy. *Vision Research,* **35,** 413-434.

Cowan, B. and Rowell, N. (1986). On the gun independence and phosphor constancy of color video monitors. *Color Research and Application*, **11**, 543-538.

Cowey A. (1979). Cortical maps and visual perception. *Quarterly Journal of Experimantal Psychology,* **31,** 1-17.

Cowey A. (1985) Aspects of cortical organisation related to selective attention and selective impairment of visual perception. In: *Attention and performance,* **XI,** 41-62. (Posner M.I. and Marin O.M., eds.).

Cowey A. (1993). Is blindsight colour blind? Lecture given at Colour Vision Deficiencies, City University. January 1993.

Cowey A., Stoerig P. (1991a) Reflections on blindsight. In: *The neuropsychology of consciousness,* pp 11-37. (Milner D. and Rugg M., eds.), Academic Press.

Cowey A., Stoerig P. (1991b) The neurobiology of blindsight. *Trends in Neuroscience*, **14,** 140-145.

Cowey A., Stoerig P., Perry V.H. (1989) Transneuronal retrograde degeneration of retinal ganglion cells after damage to striate cortex in macaque monkey: selective loss of Pβ cells. *Neuroscience*, **29,** 65-80.

Cowey A., Weiskrantz L. (1963) A perimetric study of visual field defects in monkeys. *Quarterly Journal of Experimental Psychology,* **15,** 91-115.

Craven B.J. and Foster D.H. (1992). An operational approach to colour constancy. *Vision Research,* **32,** 1359-1366.

Crescitelli, F. and Dartnall, H.J.A. (1953). Human visual purple. *Nature*, **172**, 195-200

Curcio C.A. and Allen K.A. (1990). Topography of ganglion cells in human retina. *Journal of Comparative Neurology,* **300,** 5-25.

D'Zmura, M. and Lennie, P. (1986). Mechanisms of color constancy. *Journal of the Optical Society of America A,* **3,** 1662-1672.

D'Zmura, M. and Iverson, B. (1993a). Color constancy I. Basic theory of two-stage linear recovery of spectral descriptions for lights and surfaces. *Journal of the Optical Society of America A,* **10,** 2148-2165

D'Zmura, M. and Iverson, B. (1993b). Color constancy II. Results for two stage linear recovery of spectral descriptions for lights and surfaces. *Journal of the Optical Society of America A,* **10,** 2148-2165

Damasio A.R. and Damasio H. (1986). Hemianopia, hemiachromatopsia and the mechanisms of alexia. *Cortex,* **22,** 161-169.

Damasio A.R., Yamada T., Damasio H., Corbett J. and McKee J. (1980). Central achromatopsia: Behavioural, anatomic and physiologic aspects. *Neurology,* **30,** 1064-1071.

Dannemiller, J.L. (1989). Computational approaches to color constancy: adaptive and ontogenetic considerations. *Psychological Review,* **96,** 255-266.

Dannemiller, J.L. (1992). Spectral reflectance of natural objects: how many basis functions are necessary? *Journal of the Optical Society of America A,* **9,** 507-515.

Dartnall, H.J.A. (1953). The interpretation of spectral sensitivity curves. *British Medical Bulletin.,* **9,** 24.

Dartnell H.J.A. (1957). The Visual Pigments. London: Methuen.

Dartnell H.J.A., Bowmaker J.K. and Mollon J.D. (1983). Microspectrophotometry of human photoreceptors. In: *Colour Vision, Physiology and Psychophysics* (Mollon J.D. and Sharpe L.T., eds.), London: Academic press.

Davidoff J. (1991). Cognition through Color. London: MIT Press

Daw N.W. (1968). Color-coded ganglion cells in the goldfish retina: Extension of their receptive fields by a means of new stimuli. *Journal of Physiology,* **197,** 567-592.

Daw N. W. (1984) The psychology and physiology of colour vision. *Trends in NeuroScience,* **September,** 330-335

de Monasterio, F.M. (1978a). Properties of concentrically organised X and Y ganglion cells of macaque retina. *Journal of Neurophysiology*, **41**, 1394-1417.

de Monasterio, F.M. (1978b). Properties of ganglion cells with atypical receptive-field organization in retina of macaques. *Journal of Neurophysiology*, **41**, 1435-1448.

de Monasterio, F.M. and Gouras, P. (1975). Functional properties of ganglion cells of the rhesus monkey retina. *Journal of Physiology, London*, **251**, 167-195.

De Valois R.L. and De Valois K.K. (1975). Neural coding of colour. In: *Handbook of Perception,* **V**, (Carterette E.C. and Friedman M.P., eds.), pp 117-166. New York: Academic Press.

De Valois, R.L. and De Valois, K.K. (1993). A multi-stage colour model. *Vision Research*, **33**, 1053-1065.

De Valois R.L. and Pease P.L. (1971). Contours and contrast: Responses of monkey lateral geniculate nucleus cells to luminance and colour figures. *Science, Washington,* **171**, 694-696.

Derrington A.M., Krauskopf J., Lennie P. (1984) Chromatic mechanisms in lateral geniculate nucleus of macaque. *Journal of Physiology, London,* **357**, 241-265.

Desimone R., Moran J., Schein S.J. and Mishkin M. (1993). A role for the corpus callosum in visual area V4 of the Macaque. *Visual Neuroscience,* **10**, 159-171.

Dixon, E.R. (1978). Spectral distribution of Australian daylight. *Journal of the Optical Society of America*, **68**, 437-450.

Dowling J.E., Boycott B.B. (1966) Organisation of primate retina: electron microscopy. *Proceedings of the Royal Society of London, B,* **166,** 80-111.

Dowling J.E. and Werblin F.S. (1971). Synaptic organisation of the vertebrate retina. *Vision Research,* **s3**, 1-15.

Dreher B., Fukada Y. and Rodieck R.W. (1976). Identification, classification and anatomical segregation of cells with X-like and Y-like properties in the lateral geniculate nucleus of old world primates. *Journal of Physiology, London,* **258**, 433-452.

Enroth-Cugell C., Robson J.G. (1966) The contrast sensitivity of retinal ganglion cells of the cat. *Journal of Physiology, London,* **187**, 517-552.

Estevez, O. and Cavonius, C.R. (1977). Human color perception and Stiles' pi mechanisms. *Vision Research*, **17**, 417-422.

Fairchild M.D. & Lennie P. (1992). Chromatic adaption to natural and incandescent illuminants. *Vision Research*, **32**, 2077-2085.

Felsten G., Benvento L.A. and Burmann D. (1983). Opponent-colour responses in macaque extrageniculate visual pathways: the lateral pulvinar. *Brain Research*, **288**, 363-367.

Foster, D.H., Craven, B.J. and Sale, R.H. (1992). Immediate colour constancy. *Ophthalmic and Physiological Optics*, **12**, 157-160.

Gouras P. (1968). Identification of cone mechanisms in monkey ganglion cells. *Journal of Physiology, London*, **204**, 407-419.

Gulyas B., Heywood C.A., Popplewell D.A., Roland P.E. & Cowey A. (1994). Visual form discrimination from colour or motion cues. Functional anatomy by positron emission tomography. *Proceedings of the National Academy of Science, USA*, **91**, 9965-9969.

Hayhoe M.M., Benimoff N.I. and Hood D.C. (1987). The time course of multiplicative and subtractive adaptation processes. *Vision Research*, **27**, 1981.

Helson H., Judd D.B. and Warren M.H. (1952). Object-color changes from daylight to incandescent filament illumination. *Transactions of the Illumination Engineering Society*, **47**, 221-233.

Helson, H. (1938). Fundamental problems in color vision. I. The principle governing changes in non-selective samples in chromatic illumination. *Journal of Experimental Pyschology*, **23**, 439-476.

Hering, E. (1920/1964). *Outlines of the theory of light sense*, Translated from German by Hurvich, L.M. and Jameson, D. (1964) Cambridge, MA: Harvard University Press.

Heywood C.A. & Cowey A. (1987). On the role of cortical area V4 in the discrimination of hue and pattern in macaque monkeys. *Journal of Neuroscience*, **7**, 2601-2617.

Heywood C.A., Cowey A. and Newcombe F. (1991). Chromatic discrimination in a cortically blind observer. *European Journal of Neuroscience*, **3**, 802-812.

Heywood C.A., Gadotti A. & Cowey A. (1992). Cortical area V4 and its role in the perception of colour. *Journal of Neuroscience*, **12**, 4056-4065.

Heywood C. A., Wilson B. and Cowey A. (1987) A case study of cortical colour "blindness" with relatively intact achromatic discrimination. *Journal of Neurology, Neurosurgery and Psychiatry*, **50**, 22-29.

Holladay L.L. (1926). The fundamentals of glare and visibility. *Journal of the Optical Society of America,* **12,** 271-319.

Holmes G. (1918) Disturbances of vision by cerebral lesions. *British Journal of Ophthalmology,* **2,** 353-384.

Horn B.P.K. (1974). On lightness. MIT Artificial Intelligence Lab. memo 295 (Massachusetts Institute of Technology, Cambridge, MA). cited by Hurlbert, 1986.

Horton H.C. and Hubel T.N. (1981). A regular patchy distribution of cytochrome oxidase staining in primary visual cortex of the macaque monkey. *Nature,* **292,** 762-764.
Hubel D.H. (1988) Eye, brain and vision. *Scientific American Library series,* **22,** ISBN 0-7467-5020-1.

Hubel K. H. and Livingstone M. S. (1987) Segregation of form, color and stereopsis in primate area 18. *Journal of Neuroscience*, **7**, 3378-3415

Hubel K. H. and Wiesel T. N. (1965) Receptive fields and functional architecture in two nonstriate visual areas (18 and 19) of the cat. *Journal of Neurophysiology*, **28**, 229-289

Hurlbert, A.C. (1986). Formal connections between lightness algorithms. *Journal of the Optical Society of America A*, **3**, 684-1693.

Hurlbert, A. (1990). Color algorithms for machine vision. *A V A meeting on Modelling in Vision,* **12**, 297-314.

Hurlbert A. (1993). Real world colour constancy. *Perception,* **22s**, 2.

Hurlbert A. C. and Poggio T. A. (1988) Synthesizing a color algorithm from examples. *Science, New York*, **239**, 482-285

Hurvich L.M. (1981). Color Vision. Sunderland, MA: Sinauer.

Ingle, D.J. (1985). The goldfish as a retinex animal. *Science*, **227**, 65-654.

Ingling C.R. and Drum B.A. (1972). Retinal receptive fields: Correlations between psychophysics and electrophysiology. *Vision Research,* **13**, 151-1163.

Iverson G. and D'Mura M. (1994). Criteria for color constancy in trichromatic bilinear models. *Journal of the Optical Society of America A,* **7,** 1970-1975.

Ives H.E. (1912). The Relation between the color of the illuminant and the color of the illuminated object. *Transactions of the Illumination Engineering Society,* **7,** 62-72.

Jaeger, W. and Kroker, K. (1952). Uber das Verhalten der Protanopen und Deuteranopen bie grossen Reizflachen. *Klin.Monatsbl.Augenheilkd.*, **121,** 445-449.

Jameson D. and Hurvich L.M. (1972). Color adaptation: sensitivity, contrast, after images. In: *Handbook of Sensory Physiology, Visual Psychophysics,* (Jameson D. and Hurvich L.M., eds.) Berlin: Springer-Verlag.

Jameson, D. and Hurvich, L.M. (1986). Complexities of perceived brightness. *Science*, **133**, 174-179.

Jameson, D. and Hurvich, L.M. (1989). Essay concerning color constancy. *Annual Review of Psychology,* **40,** 1-22

Jordan G. and Mollon J.D. (1993). A study of women heterozygous for colour deficiencies. *Vision Research,* **33,** 1495-1508.

Judd, D.B. (1940). Hue, saturation and lightness of surface colors with chromatic illumination. *Journal of the Optical Society of America*, **50**, 2-32.

Judd, D.B. (1960). Appraisal of Land's work on two-primary color projections. *Journal of the Optical Society of America*, **50**, 254-268.

Judd, D.B., MacAdam, D.L. and Wyszecki, G. (1964). Spectral distributions of typical daylight as a function of correlated color temperature. *Journal of the Optical Society of America*, **54**, 1031-1040.

Kaplan, E. and Shapley, R.M. (1986). The primate retina contains two types of ganglion cells, with high and low contrast sensitivity. *Proceedings of the National Academy of Science, USA*, **83**, 2755-2757.

Kilbride, P.E., Alexander, K.R., Fishman, M. and Fishman, G.A. (1989). Human macular pigment assessed by imaging fundus reflectometry. *Vision Research*, **29**, 663-674.

Kinney J. A. S. (1962) Factors affecting induced colour. *Vision Research*, **2**, 503-525

Kölmel H.W. (1988). Pure homonymous hemiachromatopsia: findings with neuro-ophthalmologic examination and imaging procedures. *European Archives of Psychiatry and Neurological Science,* **237,** 237-243.

Krinov E. (1947). Spectral Reflectance Properties of Natural Formations. *Technical translation TT-439.* National Research Council of Canada, Ottawa.

Kuffler S.W. (1953). Discharge patterns and functional organisation of mammalian retina. *Journal of Neurophysiology,* **16,** 37-68.

Land E. H. (1959a) Color vision and the natural image, Part I. *Proceedings of the National Academy of Sciences, U.S.A.,* **45,** 115-129.

Land E.H. (1959b). Colour vision and the natural image, Part II. *Proceedings of the National Academy of Science, USA,* **45** 636-644.

Land E. H. (1959c) Experiments in color vision. *Scientific American,* **May,** 1-14.

Land, E.H. (1964). The retinex. *American Scientist,* **52,** 247-264.

Land E. H. (1974) The retinex theory of color vision. *Proceedings of the Royal Institution of Great Britain,* **47,** 23-58.

Land E. H. (1983) Recent advances in retinex theory and some implications for cortical computations: Color vision and the natural image. *Proceedings of the National Academy of Sciences. U.S.A.,* **80,** 5163-5169

Land E.H. (1986a). Recent advances in retinex theory. *Vision Research,* **26,** 7-21.

Land E.H. (1986b). An alternative technique for the computation of the designator in the retinex theory of colour vision. *Proceedings of the National Academy of Science, USA,* **83,** 3078-3080.

Land E. H., Hubel D. H., Livingstone M. S., Perry S. H. and Burns M. M. (1983) Colour-generating interactions across the corpus callosum. *Nature, London,* **303,** 616-618

Land E. H. and McCann J. J. (1971) Lightness and retinex theory. *Journal of the Optical Society of America,* **61,** 1-11

Lee, H.C. (1986). Method for computing the scene-illuminant chromaticity from specular highlights. *Journal of the Optical Society of America A,* **3,** 1694-1699.

Lennie, P. (1984). Recent developments in the physiology of colour vision. *Trends in NeuroScience*, **7**, 243-248.

Lennie, P. and D'Zmura, M. (1988). Mechanisms of colour vision. *Critical Reviews in Neurobiology*, **3**, 333-400.

Lennie P., Haake P.W. and Williams D.R. (1991). The design of chromatically opponent receptive fields. In: *Computational models of visual processing*, (Landy M.S. and Movshon J.A., eds.), Cambridge MA.: MIT Press.

Livingstone M.S., Hubel D.H. (1984a) Anatomy and physiology of colour system in the primate visual cortex. *Journal of Neuroscience*, **4**, 309-356.

Livingstone M.S., Hubel D.H. (1984b) Specificity of intrinsic connections in primate primary visual cortex. *Journal of Neuroscience*, **4**, 2830-2835.

Livingstone M.S., Hubel D.H. (1987a). Psychophysical evidence for separate channels for the perception of form, colour, movement and depth. *Journal of Neuroscience*, **7**, 3416-3468.

Livingstone M.S., Hubel D.H. (1987b). Connections between layer 4B of area 117 and the thick cytochrome oxidase stripes of area 18 in the squirrel monkey. *Journal of Neuroscience*, **7**, 3416-3468.

Lucassen, M.P. and Walraven, J. (1990). Evaluation of a simple method for color monitor recalibration. *Color Research and Application*, **15**, 32-326.

Lucassen, M. and Walraven, J. (1993). Quantifying color constancy: Evidence for nonlinear processing of cone-specific contrast. *Vision Research*, **33**, 739-757.

Lueck C.J., Zeki S., Friston K.J., Dieber M.P., Cope P., Cunningham V.J., Lammerstsina A.A., Kennard C. & Frakowiak R.S.J. (1989). The colour centre in the cerebral cortex of man. *Nature, London*, **340**, 386-389.

MacNichol, E.F.(Jr.), Levine, J.S., Mansfield, R.J.W., Lipetz, L.E. and Collins, B.A. (1983). Microspectrophotometry of visual pigments in primate photoreceptors. In: *Colour Vision, Physiology and Psychophysics* (Mollon, J.D. and Sharpe, L.T., eds.). Academic Press, London.

Maloney L. (1986). Evaluation of linear models of surface spectral reflectance with a small number of parameters. *Journal of the Optical Society of America A*, **3**, 1673-1683.

Maloney, L.T. and Wandell, B.A. (1986). Color constancy: a method for recovering surface spectral reflectance. *Journal of the Optical Society of America A*, **3**, 29-33.

Malpeli L.G., Schiller P.H. and Colby C.L. (1981). Response properties of single cells in monkey striate cortex during reversible inactivation of individual lateral geniculate laminae. *Journal of Neurophysiology*, **46**, 1102-1119.

Mariani A.P. (1984a). Bipolar cells in monkey retina selective for the cones likely to be blue sensitive. *Nature*, **308**, 184-186.

Mariani A.P. (1984b). The neuronal organisation of the outer plexiform layer in the primate retina. *International Review of Cytology*, **86**, 285-320.

Marks, W.B., Dobelle, W.H. and MacNichol, E.F., Jr. (1964). Visual pigments of single primate cones. *Science*, **143**, 1181-1183.

Marr, D. (1982). *Vision*. Freeman, San Francisco.

Maunsell, J.H. and Newsome, W.T. (1987). Visual processing in monkey extra striate cortex (Review). *Annual Review of Neuroscience*, **10**, 363

McCann J. J., McKee S. P. and Taylor T. H. (1976) Quantitative studies in retinex theory. *Vision Research*, **16**, 445-458

McCann, J.J. and Houston, K.L. (1983). Calculating color sensation from arrays of physical stimuli. *IEEE Transactions on Systems, Man and Cybernectics*, **13**, 1000-1007.

Meadows J. C. (1974a) Disturbed perception of colours associated with localized cerebral lesions. *Brain*, **97**, 615-632

Meadows J. C. (1974b) The anatomical basis of prosopagnosia. *Journal of Neurology, Neurosurgery and Psychiatry*, **37**, 489-501

Merigan W.H. (1989). Chromatic and achromatic vision of macaques: role of P pathway. *Journal of Neurosci,* **9,** 776-783.

Michael C.R. (1988). Retinal afferent arborization patterns, dendritic field orientations, and the segregation of function in the lateral geniculate nucleus of the monkey. *Proceedings of the National Academy of Science, USA,* **85,** 4194-4198.

Millodot M. (1982). Image formation in the eye. In: *The Senses,* (Barlow H.B. and Mollon J.D. eds.) pp46-61. Cambridge University Press.

Mollon J.D., Newcombe F., Polden P.C. and Ratcliff C. (1980). On the presence of three cone mechanisms in a case of total achromatopsia. In: *Colour vision deficiencies* (Verriest C., ed.), pp 130-135. Bristol:A.Hilger.

Moreland, J.D. and Bhatt, P. (1984). Retinal Distribution of the Macular Pigment. In: *Colour Vision Deficiencies*, vol VII. (Verriest, C., ed.). The Hague: Dr.W.Junk.

Morland, A.B. and Ruddock, K.H. (1993). Variations in colour matching data associated with light losses in the macular pigment. In: *Colour Vision Deficiencies*, **XI.** Kluwer Academic Publishers, Netherlands.

Motter B.C. (1994a). Neural correlates of feature selective memory and pop-out in extrastriate area V4. *Journal of Neuroscience,* **14,** 2190-2199.

Motter B.C. (1994b). Neural correlates of attentive selection for color or luminance in extrastriate area V4. *Journal of Neuroscience,* **14,** 2178-2189.

Mullen K.T. and Plant G.T. (1986). Colour and luminance vision in human optic neuritis. *Brain,* **109,** 1-13.

Nagy, A.L. (1980). Large-field substitution in Rayleigh matches of dichromats. *Journal of the Optical Society of America*, **70**, 778-784.

Nathans, J., Piantanida, T.P., Eddy, R.L., Shows, T.B. and Hogness, D.S. (1986). Molecular genetics of inherited variation in human color vision. *Science*, **232**, 203-210.

Neitz, J. and Jacobs, G.H. (1986). Polymorphism of the long-wavelength cone in normal human colour vision. *Nature*, **323**, 623-635.

Neitz J. and Jacobs G.H. (1990). Polymorphism in normal human color vision and its mechanism. *Vision Research,* **30,** 620-636.

Neitz J., Neitz M. and Jacobs G.H. (1991). Spectral tuning of pigments underlying red-green color vision. *Science,* **252,** 971-974.

Neitz J., Neitz M. and Jacobs G.H. (1992). The molecular genetic basis of polymorphism in normal color vision. *Optical society of America Technical Digest.* **4,** 14-16.

Neitz J., Neitz M. and Jacobs G.H. (1993). More than three cone pigments among people with normal color vision. *Vision Research,* **33,** 117-122.

Norren, D.V. and Vos, J.J. (1974). Spectral transmission of the human ocular media. *Vision Research,* **14,** 1237-1243.

Oppel O. (1967) Untersuchungen über die Verteilung und Zahl der retinalen Ganglienzellen beim Menschen. *Grafes Arch Klin. Exp. Ophthalmol.*, **172,** 1-22.

Osterberg, G. (1935). Topography of the layer of rods and cones in the human retina. *Acta Opthalmologica,* **s6.**

Oyama, T. and Hsia, Y. (1966). Compensatory hue shift in simultaneous color contrast as a function of separation between inducing and test fields. *Journal of Experimental Psychology,* **71,** 405-413.

Parkkinen, J.P.S., Hallikainen, J. and Jaaskelainen, T. (1989). Characteristic spectra of Munsell colors. *Journal of the Optical Society of America A,* **6,** 38-322.

Pearlman A.L. (1987) The central visual pathways. In: *Adler's physiology of the eye (clinical application)* (Moses R.A and Hart Jr W.M., eds.) 8th ed. The C.V. Mosby Company.

Pearlman A.L., Birch J. & Meadows J.C. (1979). Cerebral colour blindness; an acquired defect in hue discrimination. *Annals of Neurology,* **5,** 253-261.

Pease, P.L., Adams, A.J. and Nuccio, E. (1987). Optical density of human macular pigment. *Vision Research,* **27,** 705-710.

Peichl, L. and Wässle, H. (1979). Scatter, size and coverage of ganglion cell receptive field in the cat retina. *Journal of Physiology, London,* **291,** 117-141.

Perenin M.-T, Ruel J., Hécaen H. (1980) Residual visual capacities in a case of cortical blindness. *Cortex,* **16,** 605-612.

Perry, V.H. and Cowey, A. (1984). Retinal ganglion cells that project to the superior colliculus and pretectum in the macaque monkey. *Neuroscience*, **12**, 1125-1137.

Perry, V.H., Oehler, R. and Cowey, A. (1984). Retinal ganglion cells that project to the lateral geniculate nucleus in the macaque monkey. *Neuroscience*, **12**, 1101-1123.

Plant G.T. (1991). Disorders of colour vision in diseases of the nervous system. *Vision and Visual Disorders,* **17,** 173-198.

Pöppel E. (1986) Long-range colour-generating interactions across the retina. *Nature* **320,** 523-525.

Post, D.L. and Calhoun, C.S. (1989). An evaluation of methods for producing desired colors on CRT monitors. *Color Research and Application*, **14**, 172-186.

Pugh, E.N. and Mollon, J.D. (1979). A theory of the π_1 and π_3 color mechanisms of Stiles. *Vision Research*, **18**, 317-330.

Rayleigh (1912). *The Scientific papers of Lord Rayleigh, vol 1 and 4,* New York: Cambridge University Press.

Reading, V.M. and Weale, R.A. (1974). Macular pigment and chromatic aberration. *Journal of the Optical Society of America*, **64**, 231-234.

Rizzo M., Nawrot M., Blake R. & Damasio A. (1992). A human visual disorder resembling area V4 dysfunction in the monkey. *Neurology,* **42,** 1175-1180.

Rizzo M., Smith V., Pokorny J. & Damasio A.R. (1993). Colour perception profiles in central achromatopsia. *Neurology,* **43,** 995-1001.

Rodieck, R.W. (1973). *The Vertebrate Retina.* Freeman, San Francisco.

Rondot P., Tzavaras A. and Garcin R. (1967). Sur un cas de prosopagnosie persistant depuis quinze ans. *Rev. Neurolology,* **117,** 424-428.

Ruddock, K.H. (1963). Evidence for macular pigmentation from colour matching data. *Vision Research*, **3**, 417-429.

Ruddock, K.H. (1971). Parafoveal colour vision responses of four dichromats. *Vision Research*, **11**, 143-156.

Ruddock K.H. and Svaetichin G. (1973). Fast and slow components of intracellularly recorded responses from retinal units of a teleost fish. *Vision Research,* **13,** 1785-1788.

Rushton, W.A.H. (1963). A cone pigment in the protanope. *Journal of Physiology, London*, **168**, 345-359.

Rushton, W.A.H. (1965). A foveal pigment in the deuteranope. *Journal of Physiology, London*, **176**, 24-37.

Rushton, W.A.H. (1972). Visual pigments in man. In: *Handbook of Sensory Physiology,* Vol II Photochemistry of Vision. (H.J.A.Dartnall, Ed.) New York: Springer-Verlag.

Ruskell G. (1993) Personal communications and unpublished notes on "Anatomy and physiology of visual pathways". Dept. Optometry and Visual Science, City University.

Said, F.S. and Weale, R.A. (1959). The variation with age of the spectral transmissivity of the living crystalline lens. *Gerontology*, **3**, 213-231.

Sallstrom, P. (1973). Colour and physics: some remarks concerning the physical aspects of human colour vision. Report 73-09. Stockholm, University of Stockholm, Institute of Physics.

Schein S. J., Marrocco R. T. and Monasterio F. M. de (1982) Is there a high concentration of color-selective cells in area V4 of monkey visual cortex? *Journal of Neurophysiology*, **47**, 193-213

Schein S.J. and Desimone R. (1990). Spectral properties of V4 neurons in the macaque. *Journal of Neuroscience,* **10,** 3370-3389.

Schiller P.H., Logothetis N. and Charles E. (1990). Functions of the colour-opponent and broad band channels of the visual system. *Nature, London.* **343,** 368-370.

Schiller P.H., Malpeli J.G. (1978) Functional specificity of lateral geniculate nucleus laminae in the rhesus monkey. *Journal of Neurophysiology*, **41,** 788-793.

Schneider G.E. (1969) Two visual systems. *Science*, **163,** 895-902.

Schultze, M. (1866). Anatomie und Physiologie der Netzhaut. *Arch. Mikr. Anat.*, **2**, 175-286.

Shapley, R. (1986). The importance of contrast for the activity of single neurons, the VEP and perception. *Vision Research,* **26,** 45-61.

Shapley R. and Perry V.H. (1986). Cat and monkey retinal ganglion cells and their functional roles. *Trends in Neuroscience,* **9,** 229-235.

Shevell S.K. (1978). The dual role of chromatic backgrounds in color perception. *Vision Research,* **18,** 1649-1661.

Shevell S.K., Holliday I. and Whittle P. (1992). Two separate neural mechanisms of brightness induction. *Vision Research,* **32,** 2331-2340.

Smith, V.C. and Pokorny, J. (1977). Large field trichromacy in protanopes and deuteranopes. *Journal of the Optical Society* of America, **67,** 213-220.

Smith, V.C., Pokorny, J. and Starr, S.J. (1976). Variability of color mixture data- I. Interobserver variability in the unit coordinates. *Vision Research,* **16,** 1087-1094.

Stabell, U. and Stabell, B. (1980). Variation in density of macular pigmentation and in the short-wave cone sensitivity with eccentricity. *Journal of the Optical Society* of America, **70,** 706-711.

Stiles W.S. (1929). The effect of glare on the brightness difference threshold. *Proceedings of the Royal Society, B,* **104** 322-355.

Stiles W.S. (1939) The directional sensitivity of the retina and the spectral sensitivities of the rods and cones. *Proc. R. Soc.,* **B127,** 64-105.

Stiles W.S. (1949) Increment thresholds and the mechanisms of colour vision. *Doc. Ophthalmol.,* **3,** 138-165.

Stiles, W.S. (1953). Further Studies of Visual Mechanisms by the Two-Colour Threshold Method. *Coloq.Probl.Opt.Vis.,* **1,** 65-103.

Stiles W.S. (1978) Mechanisms of colour vision. Academic Press.

Stiles W.S. and Crawford B.H. (1957). The effect of a glaring source on extrafoveal vision. *Proceedings of the Royal Society, B,* **122,** 255-280.

Stiles W.S., Wyszecki G. and Ohta N. (1977). Counting metameric object-color stimuli using frequency-limited spectral reflectance functions. *Journal of the Optical Society of America,* **67,** 779.

Stoerig P. (1987) Chromaticity and achromaticity: evidence of a functional differentiation in visual field defects. *Brain*, **110,** 869-886.

Stoerig P. and Cowey A. (1989) Wavelength sensitivity in "blindsight". *Nature, London*, **342**, 916-918

Stoerig P. and Cowey A. (1991). Increment-threshold spectral sensitivity in blindsight. Evidence for colour-opponency. *Brain,* **114,** 1487-1512.

Stoerig P. and Cowey A. (1992). Wavelength sensitivity in blindsight. *Brain,* **115,** 425-444.

Stryer L. (1986). Cyclic GMP cascade of vision. *Annual Review of Neuroscience,* **9,** 87-119.

Teuber H. L., Battersby W. S. and Bender M. B. (1960) Visual field defects after penetrating missile wounds of the brain. Cambridge, MA: Harvard University Press.

Tiplitz Blackwell, K. and Buchsbum, G. (1988a). Quantitative studies of color constancy. *Journal of the Optical Society of America A*, **5**, 1772-1780.

Tiplitz Blackwell, K. and Buchsbaum, G. (1988b). The effect of spatial and chromatic parameters on chromatic induction. *Color Research and Application*, **13**, 166-173.

Tootell R. B. H., Silverman M. S., De Valois R. L. and Jacobs G. H. (1983) Functional organization of the second cortical visual area in primates. *Science*, **220**, 737-739

Troost, J.M. and de Weert, C.M.M. (1991a). Surface reflectance and human color constancy: comment on Dannemiller (1989). *Psychological Review*, **98**, 143-145.

Troost, J.M. and de Weert, C.M.M. (1991b). Naming vs matching in color constancy. *Perception and Psychophysics*, **50**, 591-602.

Troost J.M., Wei L. and de Weert C.M.M. (1992). Binocular measurements of chromatic adaption. *Vision Research,* **10,** 1987-1997.

Uchikawa H., Uchikawa K and Boynton R.M. (1989). Influence of chromatic surrounds on categorical perception of surface colours. *Vision Research,* **29,** 881-890.

Valberg A. (1974) Colour induction: Dependence on luminance, purity and dominant or complementary wave-length of inducing stimuli. *Journal of the Optical Society of America*, **65**, 1531-1540

Valberg A. and Lange-Maclecki B. (1987). Mondrian complexity does not improve "colour constancy". *Investigative Ophtalmology and Visual Science (Suppl.)* **28**.

Valberg A. and Lange-Maclecki B. (1989). The lack of colour constancy in a complex Mondrian and its equivalent surround. In: *Seeing contour and colour* (Kulikowski J., ed.) London: Academic Press.

Valberg, A. and Lange-Malecki, B. (1990), Colour constancy in Mondrian patterns: a partial cancellation of physical chromaticity shifts by simultaneous contrast. *Vision Research*, **30**, 371-380.

Valberg A., Lee B.B., Tigwell D.A. and Creutsfeldt O. D. (1985). A simultaneous contrast effect of steady remote surrounds on response of cells in macaque lateral geniculate nucleus. *Experimental Brain Research,* **58**, 604-608.

Veiweg und Sohn I. S. (1933) Partial cortical blindness with preservation of color vision: report of a case following asphyxia due to carbon monoxide poisoning: a consideration of the question of colour vision and its cortical localization. *Archives of Ophthalmology*, **9**, 957-965

Verrey D. (1888). Hémiachromatopsie droite absolue. *Archives d'Ophthalmologie, Paris,* **8**, 289-301

Victor J.D., Maiese K., Shapley R., Sidtis J. and Gazzaniga M.S. (1989). Acquired central dyschromatopsia: analysis of a case with preservation of colour discrimination. *Clinical Vision Science,* **4**, 183-196.

Viénot, F. (1983). Can variation in macular pigment account for the variation of colour matches with retinal position? In: *Colour Vision: Physiology and Psychophysics* (Mollon, J.D., Sharpe, L.T., Eds.). London: Academic Press.

von Helmholtz, H. (1866). Handbuch der Physiologischen Optik. Translation (entitled *Helmholtz's Treatise on Physiological Optics*) by Southall, J.P.C. Rochester, NY: Optical Society of America. Republished by Dover Publications, New York, 1962.

von Kries J. (1905) Die Gesichtesempfindungen. In: *Handbuch der Physiologie des Menschen,* (Nagel W., ed.). Brunswick, NJ: Vieweg.

Vos J.J. and Bouman M.A. (1959). Disability Glare: theory and practice. *Proceedings of the CIE, Brussels,* 298-306.

Walraven, J. (1973). Spatial characteristics of chromatic induction: the segregation of lateral effects from straylight artifacts. *Vision Research*, **11**, 1739-1753.

Walraven J., Benzschawel T.L. and Rogowitz B.E. (1987). Color-constancy interpretation of chromatic induction. *Die Farbe,* **34**, 269-273.

Walraven, J., Benzschawel, T., Rogowitz, B.E. and Lucassen, M.P. (1991). Testing the contrast explanation of colour constancy. In: *From Pigments to Perception.* (Valberg, A. and Lee, B.B Eds.) p369-378. New York: Plenum Press.

Walraven, J. and Werner, J.S. (1991). The invariance of unique white:Possible implications for normalizing cone action spectra. *Vision Research,* **31**, 2185-2193.

Walsh, V., Carden, D., Butler, S.R. and Kulikowski, J,J. (1993). The effects of V4 lesions on the visual abilities of macaques: hue discrimination and colour constancy. *Behavioural Brain Research*, **53**, 51-62.

Walsh, V., Kulikowski, J.J., Butler, S.R. and Carden, D. (1992). The effects of lesions of area V4 on the visual abilities of macaques: colour categorisation. *Behavioural Brain Research*, **52**, 81-89.

Wassle H., Grunert U., Rohrenbeck J. and Boycott B.B. (1989). Cortical magnification factor and the ganglion cell density of the primate retina. *Nature,* **341**, 643-646.

Weiskrantz, L. (1986). Blindsight. Oxford University Press. ISBN 0-19-852129-4

Weiskrantz, L. (1987). Residual vision in scotoma; a follow-up study of 'form' discrimination. *Brain,* **110**, 77-92.

Weiskrantz, L. (1990). Outlook for blindsight: Explicit methodologies for implicit processes. *Proceedings of the Royal Society of London B,* **239**, 247-278.

Weiskrantz, L., Barbur J.L. and Sahraie A. (1995). Parameters affecting conscious versus visual discrimination with damage to the visual cortex (V1). *Proceedings of the National Academy of Science, USA,* **92**, 6122-6126.

Weiskrantz, L., Harlow A. and Barbur J.L. (1991). Factors affecting visual sensitivity in hemianopic subjects. *Brain,* **114**, 2269-2282.

Weiskrantz, L., Warrington, E.K., Sanders, M.D. and Marshall, J. (1974). Visual Capacity in the Hemianopic Field Following a Restricted Occipital Ablation. *Brain,* **97**, 709-728.

Werblin, F.S. (1970). Responses of retinal cells to moving spots: intracellular recording in Necturus Maculosus. *Journal of Neurophysiology,* **33**, 342-350.

Werblin, F.S. (1973). The control of sensitivity in the retina. *Scientific American,* **January**, 71-79.

Werblin, F.S. and Dowling J.E. (1969). Organisation of the retina in the mudpuppy, Necturus Maculosus II. Intracellular recording. *Journal of Neurophysiology,* **32**, 339-355.

Werner, A., Menzel, R. and Wehrhahn, C. (1988). Color constancy in the honey bee. *Journal of Neuroscience*, **81**, 156-159.

Werner, J.S. and Walraven, J. (1982). Effect of chromatic adaptation on the chromatic locus: the role of contrast, luminace and background color. *Vision Research*, **22**, 929-943.

Wesner M.F. and Shevell S.K. (1992). Color perception within a chromatic context: Changes in red/green equilibria caused by a noncontiguous light. *Vision Research,* **32**, 1623-1634.

West, G. and Brill, M.H. (1982). Necessary and sufficient conditions for Von Kries chromatic adaption to give color constancy. *Journal of Mathematical Biology*, **15**, 249+.

Westheimer G., Campbell F.W. (1962) Light distribution in the image formed by the living human eye. *Journal of Optical Society of America A,* **52**, 1040-1045.

Wiesel T.N., Hubel D.H. (1966) Spatial and chromatic interactions in the lateral geniculate body of the rhesus monkey. *Journal Neurophysiology*, **29**, 1115-1156.

Wild, H,M., Butler, S.R., Carden, D. and Kulikowski, J.J. (1985). Primate cortical area V4 important for colour constancy but not wavelength discrimination. *Nature*, **313**, 133-135.

Wolin L.R. Massopust L.C. and Meder J. (1966). Differential color responses from the superior colliculus of squirrel monkeys. *Vision Research,* **6**, 637-644.

Wong-Riley M.T.T. (1978). Reciprocal connections between striate and prestriate cortex in squirrel monkey as demonstrated by combined peroxidase histochemistry and autoradiography. *Brain Research,* **147,** 159-164.

Worthey J. A. (1985) Limitations of color constancy. *Journal of the Optical Society of America A*, **2**, 1014-1026

Worthey J. A. and Brill M. H. (1986) Heuristic analysis of von Kries color constancy. *Journal of the Optical Society of America*, **A3**, 1708-1712

Wright, W.D. (1926-27). A trichromatic colorimeter with spectral primaries. *Transactions of the Optical Society of London*, **29**, 225-242.

Wright, W.D. (1927). A trichromatic colorimeter with spectral primaries. *Transactions of the Optical Society of London*, **30**, 141-164.

Wright, W.D. (1946). *Researches on normal and defective colour vision.* London: Henry Kimpton.

Wyszecki G. and Stiles W. S. (1982) Color science: Concepts and methods, Quantitative data and formulae. New York: Wiley.

Yoshioka T., Levitt J.B. and Lund J.S. (1992). Intrinsic lattice connections of macaque monkey visual cortex. *Journal of Neuroscience,* **12,** 2785-2802.

Young R.S. and Fishman G.A. (1980). Loss of color vision and Stiles' mechanism in a patient with cerebral infarction. *Journal of the Optical Society of America,* **70,** 1301-1305.

Young R.A. and Marrocco R.T. (1989). Predictions about chromatic receptive fields assuming random cone connections. *Journal of Theoretical biology,* **141,** 23-40.

Young, T. (1802). On the theory of light and colours. *Philosophical Transactions of the Royal Society of London*, 12-48.

Yukie M., Iwai E. (1981) Direct projection from the dorsal lateral geniculate nucleus to the prestriate cortex in macaque monkey. *Journal of Comparative Neurology,* **201,** 81-97.

Zeki S.M. (1971a) Convergent input from the striate cortex (area 17) to the cortex of the superior temporal sulcus in the rhesus monkey. *Brain Research,* **28,** 338-340.

Zeki S.M. (1971b) Cortical projections from the prestriate areas in the monkey. *Brain Research,* **34,** 19-35.

Zeki S.M. (1974) Cells responding to changing image size and disparity in the cortex of the rhesus monkey. *Journal of Physiology,* **242,** 827-841.

Zeki S.M. (1978a) Functional specialisation in the visual cortex of the rhesus monkey. *Nature,* **274,** 423-328.

Zeki S.M. (1978b) Uniformity and diversity of structure and function in rhesus monkey prestriate visual cortex. *Journal of Physiology,* **277,** 273-290.

Zeki, S. (1980). The representation of colours in the cerebral cortex. *Nature*, **284**, 412-418.

Zeki, S. (1983). Colour coding in the cerebral cortex: The reaction of cells in monkey visual cortex to wavelengths and colours. *Neuroscience,* **9,** 741-765.

Zeki S.M. (1990) A century of cerebral achromatopsia. *Brain,* **113,** 1421-1777.

Zeki S.M. (1990). Colour vision and functional specialisation in the visual cortex. *Discussions in Neuroscience,* **6,** 44-64.

Zeki S., Watson J.D.C., Lueck C.J., Friston K.J., Kennard C. and Frackowiak R.S.J. (1991). A direct demonstration of functional specialisation in the human visual cortex. *Journal of Neuroscience,* **11,** 641-649.

Zeki S.M. (1993). A Vision of the Brain. Oxford: Blackwell Scientific Publishers.

Zrenner, E. (1983) Neurophysiological aspects of colour vision mechanisms in the primate retina. In: *Colour Vision: Physiology and Psychophysics* (Mollon, J.D., Sharpe, L.T., eds.). London: Academic Press.